AFWL-TR-78-184

AFWL-TR-
78-184

TRESTLE WIND TUNNEL STUDY

Calspan Advanced Technology Center
Buffalo, NY 14225

March 1979

Final Report

Approved for public release; distribution unlimited.

AIR FORCE WEAPONS LABORATORY
Air Force Systems Command
Kirtland Air Force Base, NM 87117

This final report was prepared by the Calspan Advanced Technology Center, Buffalo, New York, under Contract F29601-77-C-0093, Job Order ILIR7705 with the Air Force Weapons Laboratory, Kirtland Air Force Base, New Mexico. Major Sherwood A. Richers (TPO) was the Laboratory Project Officer-in-Charge.

When US Government drawings, specifications, or other data are used for any purpose other than a definitely related Government procurement operation, the Government thereby incurs no responsibility nor any obligation whatsoever, and the fact that the Government may have formulated, furnished, or in any way supplied the said drawings, specifications, or other data, is not to be regarded by implication or otherwise, as in any manner licensing the holder or any other person or corporation, or conveying any rights or permission to manufacture, use, or sell any patented invention that may in any way be related thereto.

This report has been reviewed by the Office of Information (OI) and is releasable to the National Technical Information Service (NTIS). At NTIS, it will be available to the general public, including foreign nations.

This report has been authored by a contractor of the United States Government. Accordingly, the United States Government retains a nonexclusive, royalty-free license to publish or reproduce the material contained herein, or allow others to do so, for the United States Government purposes.

This technical report has been reviewed and is approved for publication.

FOR THE COMMANDER

SHERWOOD A. RICHERS
Major, USAF
Project Officer

DOUGLAS H. MERKLE
Lt Colonel, USAF
TRESTLE, Program Officer

DO NOT RETURN THIS COPY. RETAIN OR DESTROY.

UNCLASSIFIED

SECURITY CLASSIFICATION OF THIS PAGE (When Data Entered)

REPORT DOCUMENTATION PAGE

READ INSTRUCTIONS BEFORE COMPLETING FORM

1 REPORT NUMBER: AFWL-TR-78-184	2 GOVT ACCESSION NO. / 3 RECIPIENT'S CATALOG NUMBER
4 TITLE (and Subtitle): TRESTLE WIND TUNNEL STUDY	5 TYPE OF REPORT & PERIOD COVERED: Final Report
	6 PERFORMING ORG. REPORT NUMBER: 6171-A-2
7 AUTHOR(s): Gary R. Ludwig and Joseph P. Nenni	8 CONTRACT OR GRANT NUMBER(s): F29601-77-C-0093
9 PERFORMING ORGANIZATION NAME AND ADDRESS: Calspan Corporation, Advanced Technology Center, P. O. Box 400, Buffalo, New York 14225	10 PROGRAM ELEMENT, PROJECT, TASK AREA & WORK UNIT NUMBERS: ILIP 7705
11 CONTROLLING OFFICE NAME AND ADDRESS: Air Force Weapons Laboratory (TPC), Albuquerque, NM 87117	12 REPORT DATE: March 1979 / 13 NUMBER OF PAGES: 252
14 MONITORING AGENCY NAME & ADDRESS (if different from Controlling Office)	15 SECURITY CLASS. (of this report): UNCLASSIFIED / 15a DECLASSIFICATION/DOWNGRADING SCHEDULE

16 DISTRIBUTION STATEMENT (of this Report)

Aporoved for public release; distribution unlimited

17 DISTRIBUTION STATEMENT (of the abstract entered in Block 20, if different from Report)

18 SUPPLEMENTARY NOTES

19 KEY WORDS (Continue on reverse side if necessary and identify by block number)

Atmospheric Modeling
Wind Flow Around Structures
Wird Forces on Aircraft
Aircraft Ground Handling
Aircraft Safety

20 ABSTRACT (Continue on reverse side if necessary and identify by block number)

This report presents the results of an experimental and analytical study to determine the effects of atmospheric winds on aircraft situated on the ramp and test stand of the TRESTLE facility which is being built at Kirtland Air Force Base, New Mexico. The program included model tests to determine the wind flow patterns around the TRESTLE facility and the use of the wind flow data in an analysis to predict the effects of these winds on various large aircraft. The model tests, which were conducted in the Calspan Atmospheric Simulation Facility,

(over)

DD FORM 1 JAN 73 1473 EDITION OF 1 NOV 65 IS OBSOLETE

UNCLASSIFIED

SECURITY CLASSIFICATION OF THIS PAGE (When Data Entered)

20. ABSTRACT (Cont'd)

included flow visualization studies and quantitative hot-film anemometer measurements of three components of mean velocity. A simplified method of analysis was developed to estimate the forces and moments on aircraft situated in the experimentally determined flow field. The analysis incorporated provisions to account for unconventional wind-aircraft orientations and nonuniform flow fields. Results of the program are presented for twelve wind directions, three different aircraft, and nine positions of each aircraft on the TRESTLE facility ramp and test stand.

PREFACE

This is the final report prepared by Calspan Corporation, Advanced Technology Center on a program sponsored by the Air Force Weapons Laboratory, Kirtland Air Force Base, New Mexico under Contract F29601-77-C-0093 for the period September 1977 to August 1978. The work herein entitled "TRESTLE WIND TUNNEL STUDY" was accomplished with Major Sherwood A. Richers, AFWL/TPO as Project Engineer. Dr. Gary R. Ludwig of the Calspan Corporation was technically responsible for the overall program. Dr. Joseph P. Nenni of Calspan developed the analytical portion of the program. Other Calspan personnel were: Dr. George T. Skinner, Mr. John R. Moselle, and Mr. John Nemeth.

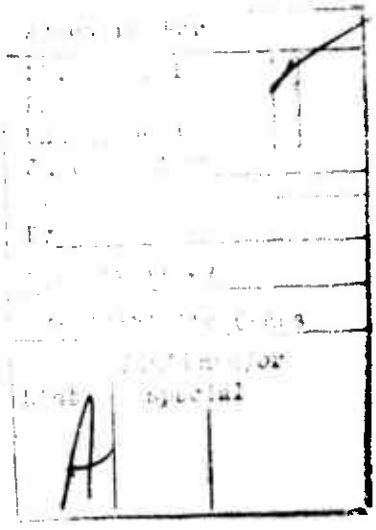

TABLE OF CONTENTS

LIST OF ILLUSTRATIONS

LIST OF ILLUSTRATIONS (CONT'D)

LIST OF TABLES

1. INTRODUCTION

The U.S. Air Force is building a TRESTLE facility to test the effects of electromagnetic pulses on large aircraft. Test aircraft will be situated in flight configuration on the test stand of the facility. The test stand is situated approximately 120 feet above a square bowl-shaped excavation in the ground. Access to the test stand is by a ramp over the excavation. The ramp is 50 feet wide by nearly 400 feet long. Large aircraft being towed over the ramp will be subject to complex wind fields which may cause handling problems leading to aircraft and facility damage. The present program consists of model tests to determine the wind flow patterns around the TRESTLE facility, and the use of the wind flow data in an analysis to determine the effects of these winds on aircraft on the ramp and the test stand.

The model tests were performed in the Calspan Atmospheric Simulation Facility (ASF). This is a specialized wind tunnel designed for the purpose of modeling the wind in the lower atmosphere. In the current program, a scale model of the TRESTLE facility and its surroundings was designed and constructed to fit on one of the large turntables in the ASF. Suitably scaled, randomly distributed terrain roughness elements were used for a long fetch upstream of the turntable model to generate the proper wind characteristics in the wind approaching the turntable. Preliminary flow visualization experiments using smoke were performed to study the general flow patterns near the TRESTLE facility and aid in the selection of locations for making quantitative velocity measurements. Three-component mean velocity measurements were then made with hot-film equipment at sufficient points to define the flow field in the vicinity of the ramp and the test stand. The velocity surveys were performed for every 30 degrees in wind direction.

The experimental velocity measurements were used to estimate the effects of the wind on various large test aircraft while the aircraft are being towed on the facility or are tied down on the facility. Since available methods of estimating the aerodynamic characteristics of aircraft do not apply

to these flow conditions because of a combination of wind shear, ground effects and unconventional wind-aircraft orientation, a simplified method was developed to estimate the forces and moments on the aircraft. It was envisioned that the primary aircraft motions of interest would be overturning, lift-off and sliding in either translation or rotation. The simplified method of aerodynamic analysis was used to estimate the forces on the aircraft for various wind directions and velocities and for various positions on the facility in order to identify wind conditions that might produce any of the above aircraft motions.

It was expected that the wind flow patterns around the model of the TRESTLE facility would show significant variations in velocity over the typical dimension of an aircraft. Therefore, in order to obtain realistic estimates of the forces and moments acting upon the test aircraft, the method of analysis incorporated provisions to account for the nonuniform flow in the vicinity of the aircraft. This necessitated measuring the local wind velocity components at a sufficient number of points so that the data could be interpolated to any point on the aircraft surfaces. Thus, a large number of velocity measurements were required for each wind direction. The acquisition of these data and their incorporation into the analysis essentially determined the scope of the program.

This report presents the results of the model test program and the aircraft force analysis. The scaling criteria for the model tests are presented in Section 2 followed by a description of the ASF and its instrumentation in Section 3. The model design and construction are described in Section 4 and the test program and its results are presented in Section 5. A description of the aircraft force analysis and its results are presented in Section 6. A summary of the results and the conclusions reached are presented in the last section. Details of the hot-film anemometer data analysis, the experimental velocity results, and the aircraft force analysis computer program are presented in Appendices A through D.

2. SCALING CRITERIA

In conducting small-scale modeling of flows in the atmospheric boundary layer, care must be taken to ensure that all important features of the full-scale situation are represented in the model. Broadly speaking, these include the ambient wind environment, including both the mean and turbulent characteristics, as well as the local terrain. Although not relevant here, in the special case of studies of the dispersion of stack emissions, one must also model the relevant features of the exhaust gases, namely, exit momentum, buoyancy and pollutant concentration. The dynamics of such flows involve inertial, viscous and buoyancy forces, as well as turbulent transport. The scaling criteria presented below are mathematical statements of the requirement that each of these forces be present in the same relative degree in the model as in full-scale. They are discussed at some length in References 1 through 4, and here we will only list them, along with a brief description of what they represent.

The most obvious requirement is that of geometric scaling between the full-scale and model flows, with regard to buildings and local topography. This also implies that one should hold the ratio of some characteristic geometric length, say L, to a length characteristic of the local ground roughness, say Z_o, constant between full-scale and the model:

---

1. McVehil, G.E., Ludwig, G.R. and Sundaram, T.R. "On the Feasibility of Modeling Small Scale Atmospheric Motions" Calspan Report No. ZB-2328-P-1 April 1967

2. Ludwig, G.R. and Sundaram, T.R. "On the Laboratory Simulation of Small-Scale Atmospheric Turbulence" Calspan Report No. VC-2740-S-1 December 1969

3. Ludwig, G.R., Sundaram, T.R. and Skinner, G.T. "Laboratory Modeling of the Atmospheric Surface Layer with Emphasis on Diffusion" Calspan Report No. VC-2740-S-2 July 1971

4. Sundaram, T.R., Ludwig, G.R. and Skinner, G.T. "Modeling of the Turbulence Structure of the Atmospheric Surface Layer" AIAA Journal Vol. 10 No. 6 June 1972

$$\frac{(L)}{(Z_o)_m} = \frac{(L)}{(Z_o)_p} \qquad (1)$$

where the subscripts "m" and "p" denote model and prototype (full-scale), respectively. Since Z_o essentially determines the scale of the turbulent eddies near the ground, this ensures that the relative size of the structures and the eddies is maintained.

The majority of flows very near the ground are "aerodynamically rough"; i.e., no laminar sublayer exists, and the flow is fully turbulent. In such cases, molecular diffusion is negligible in comparison with that resulting from turbulent transport. For this reason, holding the usual Reynolds number constant, based on free-stream conditions and a characteristic model length, is generally not required. Experience has shown that the flow will be aerodynamically rough when a Reynolds number based on surface conditions is sufficiently large; i.e.,

$$\frac{u_* Z_o}{\nu} \simeq 3 \qquad (2)$$

where u_*, the friction velocity, is related to the shear stress at the ground, τ, by $u_* = \sqrt{\tau/\rho}$. Here ν is the kinematic viscosity and ρ the air density.

Of the two conditions, (1) and (2), it is more important to satisfy condition (2). In addition to these criteria, it is also necessary to make certain that the turbulence spectra of the tunnel flow are suitably scaled reproductions of the atmospheric flow. When these conditions are met, the wind environment in the tunnel flow is a proper representation of the atmosphere, for neutrally stable conditions.

The problem of actually generating the required flow in a laboratory facility is one that has received a great deal of attention in recent years. A wide variety of approaches is available for the development of the proper flow; these involve the use of various types of roughness elements, fences, spires,

and jets transverse to the flow. At Calspan, the approach that has been used is that of a matched fence/rough-floor combination.[2,3,4] With this technique, the appropriate semi-logarithmic mean velocity profile, as well as a turbulence spectrum representative of that in the neutral atmosphere, is generated.

There are some additional scaling criteria which must be satisfied when modeling buoyant flows such as stack emission or thermally stratified atmospheric flows. A relatively comprehensive summary of these is presented in Reference 5. However, these additional criteria do not apply to the present program. For the neutrally stable atmosphere of the current tests, both the full-scale and model flow patterns will be independent of the magnitude of the wind velocity if the local velocities are normalized by a reference velocity which is representative of the wind approaching the TRESTLE facility. The reference velocity can be that measured at corresponding locations in the model and full scale, say, for example, at 10 meters above a specific ground level location. Thus it is necessary to measure flow patterns at only one reference wind velocity in the model tests. The dimensionless results will be applicable to all reference wind velocities. Furthermore, the forces and moments on a building or aircraft model immersed in the flow may be suitably normalized to be independent of the magnitude of the reference velocity. It should be noted, however, that the flow patterns will change with wind direction and it is necessary to measure the flow field for a variety of wind directions.

As noted in the preceding discussion, Reynolds number does not play as important a role in atmospheric modeling as it does in aeronautical modeling. However, it is necessary to consider Reynolds number effects in the design of some portions of the TRESTLE facility model. Specifically, it is necessary to consider Reynolds number effects when designing the model of the wire

---

5. Ludwig, G.R. and Skinner, G.T. "Wind Tunnel Modeling Study of the Dispersion of Sulfur Dioxide in Southern Allegheny County, Pennsylvania" Environmental Portection Agency Report No. EPA 903/9-75-019 December 1976

mesh structures used to simulate the transmission lines and the central ground plane wedge structure. It is necessary to keep the drag or loss characteristics of these structures the same in the model and in full-scale. Similar considerations are necessary in the design of the support structure heneath the test stand and ramp. This topic is addressed more fully in Section 4.

A final discussion, regarding the comparison of model results with full-scale, relates to the well-known fact that in full-scale, the averaging time has a distinct effect on the measurements. This is not the case in model tests in the ASF. The model results correspond to short-time averaged full-scale measurements, taken over not more than 10 or 15 minutes in most cases. Briefly, what is involved here is the following. The frequency spectrum of wind gusts in full-scale always shows a null, or near null, in the range 1 to 3 cycles per hour.[6] Thus, it is theoretically correct to separate the spectrum into two parts at a frequency in that range, and deal with phenomena associated with each part separately. In the ASF, the high-frequency portion related to the ground-induced turbulence is fully simulated. The low-frequency portion related to meandering of the wind, diurnal fluctuations, passage of weather systems, annual changes, and so on, must be considered separately if they are important to the study. In the current program, these very low frequency effects are not important. Usually, meteorological forecasts will provide estimates of hourly mean velocity and gust maximum velocity. The velocity measurements in the ASF correspond most closely to the hourly mean meteorological forecasts. However, conservative estimates of the wind effects will be obtained if the peak gust velocity instead of the hourly mean velocity is interpreted as the reference velocity in the force analysis.

Since the effective full-scale averaging time is independent of model averaging times, one can choose the model averaging time to provide data which

---

6. Lumley, J.L. and Panofsky, H.A. The Structure of Atmospheric-Turbulence Interscience (John Wiley and Sons) New York pp. 42-43

are repeatable to within a specified accuracy. The model averaging times required to obtain a given accuracy can be estimated from statistical considerations as described in the following paragraphs.

For a statistically stationary process, one can form an average of any quantity by taking N independent samples, adding their values and dividing by N. If one were to do this many times, one would obtain a distribution of average values having some standard deviation from the true mean. The ratio of this standard deviation to the true mean value is approximately $N^{-1/2}$, in most cases. This ratio may be regarded as a typical fractional error in a quantity measured by averaging N independent samples. Thus, to keep this error within 10% of the mean requires about 100 samples; to keep it within 1% requires about 10,000 samples.

We have stressed that the samples must be independent. That means that the system (the air flow around the model in the ASF) must "forget" what it was doing in the time span between samples -- an independent sample can be obtained once the correlation with the last value has essentially vanished. To estimate the time interval required between samples, one can proceed along the following lines. The model is immersed in a boundary layer of thickness, δ, typically about 4 feet. The velocity, U_∞, near the top of the boundary layer may be anything from roughly 1 to 80 feet per second. The biggest eddies in the turbulent flow essentially span the boundary layer, so that we are not assured of an independent turbulence picture until the boundary layer has moved a distance of about δ. We can say that most of the boundary layer moves at a velocity close to U_∞, so we can take "independent" samples at a rate U_∞/δ per second. We can now construct an equation which relates the sampling time, t, required to obtain a given

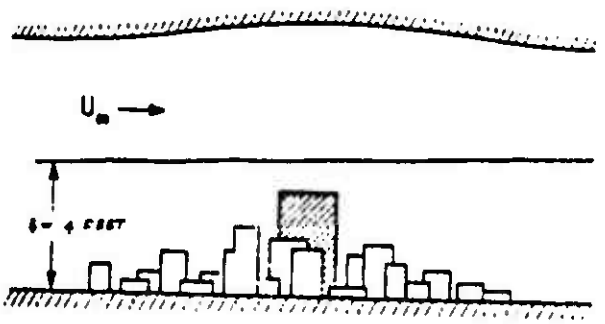

fractional error, σ , to the tunnel reference velocity, U_∞ . From the above discussion,

$$\sigma \approx \frac{1}{\sqrt{N}} \quad , \text{and} \quad \Delta t_s \approx \frac{\delta}{U_\infty}$$

Thus,

$$t_s \approx \frac{N\delta}{U_\infty} = \frac{\delta}{U_\infty \sigma^2} \tag{3}$$

where N = number of independent samples

Δt_s = minimum time interval between samples (seconds)

t_s = model sampling time (seconds)

δ = ASF boundary layer thickness (≈ 4 feet)

U_∞ = ASF reference velocity at top of boundary layer (feet/sec.)

σ = fractional error in measurements (% error/100)

It should be noted that, in the case of turbulence measurements, high frequency components require the same averaging time as discussed above because they are products of the breakdown of the large (low frequency) eddies. Therefore, they are subject to the same statistical considerations.

It is not generally appreciated how long an averaging time is required for ASF data processing. This can be illustrated by application of Equation (3). Typical accuracies expected in pollution studies are about 10% and typical velocities are about 2 ft/sec. Equation (3) indicates a required sampling time of 200 seconds. On the other hand, a typical velocity for the TRESTLE model tests was about 35 ft/sec. In this case, Equation (3) indicates that an accuracy of 5% would require 400 samples taken in a minimum total time of 46 seconds.

In the current program, the total number of samples used was 400 taken over a time interval of 68 seconds. For the 35 ft/sec reference velocity used for the majority of the tests, this time interval is nearly 50 percent larger than the approximate minimum time given by Equation (3). A few tests were performed with a reference velocity of 20 ft/sec. The corresponding minimum averaging time given by Equation (3) is approximately 80 seconds for 400 samples. The 68 second integration time is about 15 percent lower than the value suggested by Equation (3). However, as indicated in the derivation, Equation (3) is only approximate. In practice, it has usually been found that somewhat shorter averaging times provide the required accuracy. To establish a suitable value at the start of any program, a few averages are generally checked as a function of integration period. Varying the integration period was not practical in the current program because of the way in which the on-line minicomputer was programmed for data reduction of the instantaneous samples. Nevertheless, comparison of the non-dimensional velocities measured at the two reference speeds indicated satisfactory agreement.

3. TEST FACILITIES

3.1 THE ATMOSPHERIC SIMULATION FACILITY

The Calspan Atmospheric Simulation Facility (ASF), is designed mainly for studying atmospheric flow phenomena. This wind tunnel differs from the conventional aeronautical wind tunnel in two important respects, namely, the wind shear and the degree of turbulence. Every effort is made in a conventional aeronautical wind tunnel to assure a smooth, uniform flow, free from turbulent gusts. In contrast to this, a wind tunnel for simulating the lower atmospheric flow requires a relatively thick turbulent boundary layer within which the mean and turbulent properties are similar to those in the atmosphere.

In order to simulate these effects properly, a wind tunnel must be constructed in a very unconventional way. The particular method developed at Calspan for this purpose[2-4] is to use a fence, protruding from the floor of the tunnel, followed by a length of floor that is covered with roughness elements. This combination assures both the desired shear, and the associated turbulent gust spectrum as well. Figure 1 shows an exterior view of the facility. The rough floor, consisting of 30 feet of wooden blocks followed by 12 feet of gravel in this case, can be seen upstream of the model in Figure 2. The fence, which is a solid aluminum plate, protruding from the floor at the beginning of the flow development region, is also visible in this figure.

The facility is 119 feet long. The test flow is developed generally over a 80-foot length downwind of the intake, leaving approximately 30 feet available as a test section. The tunnel is 8 feet wide by approximately 7 feet high. The tunnel ceiling is adjustable to allow the axial pressure gradient to be set near zero. The turbulent boundary layer occupies roughly the lower 4 to 5 feet in the ASF depending on the rough ground configuration. A variable-pitch fan powered by a two-speed motor pulls air through the tunnel at speeds from less than 1 mph to 55 mph. Sound attenuators upstream and downstream of the fan system are included in the power package. Even at

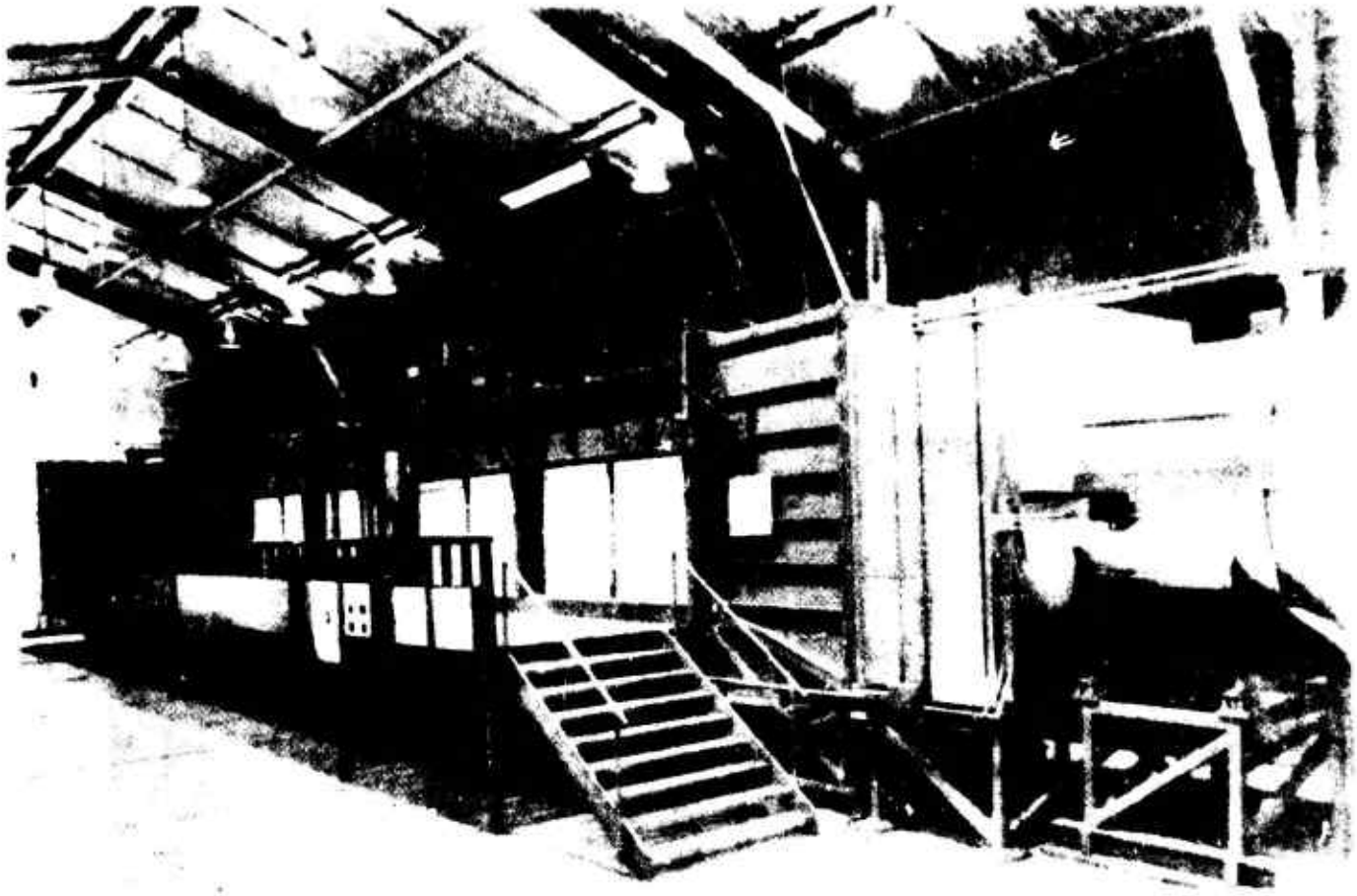

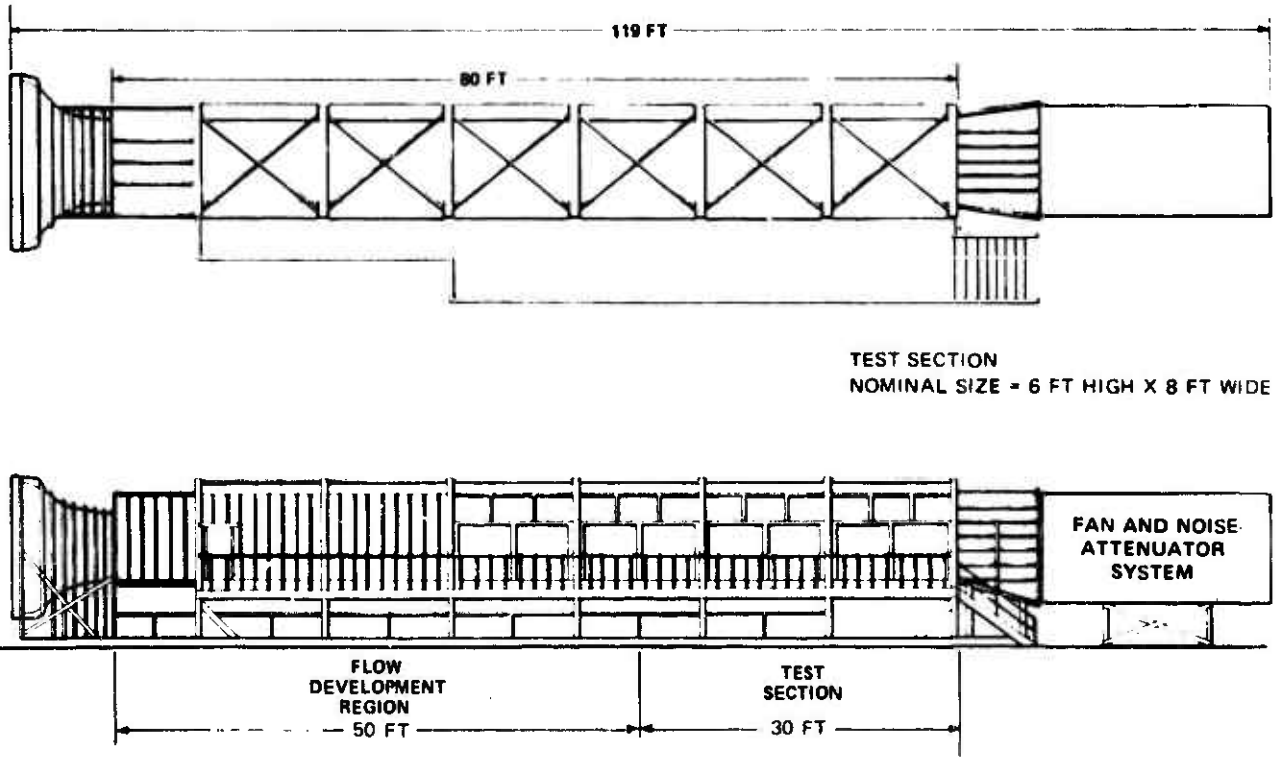

Figure 1 THE CALSPAN ATMOSPHERIC SIMULATION FACILITY (ASF)

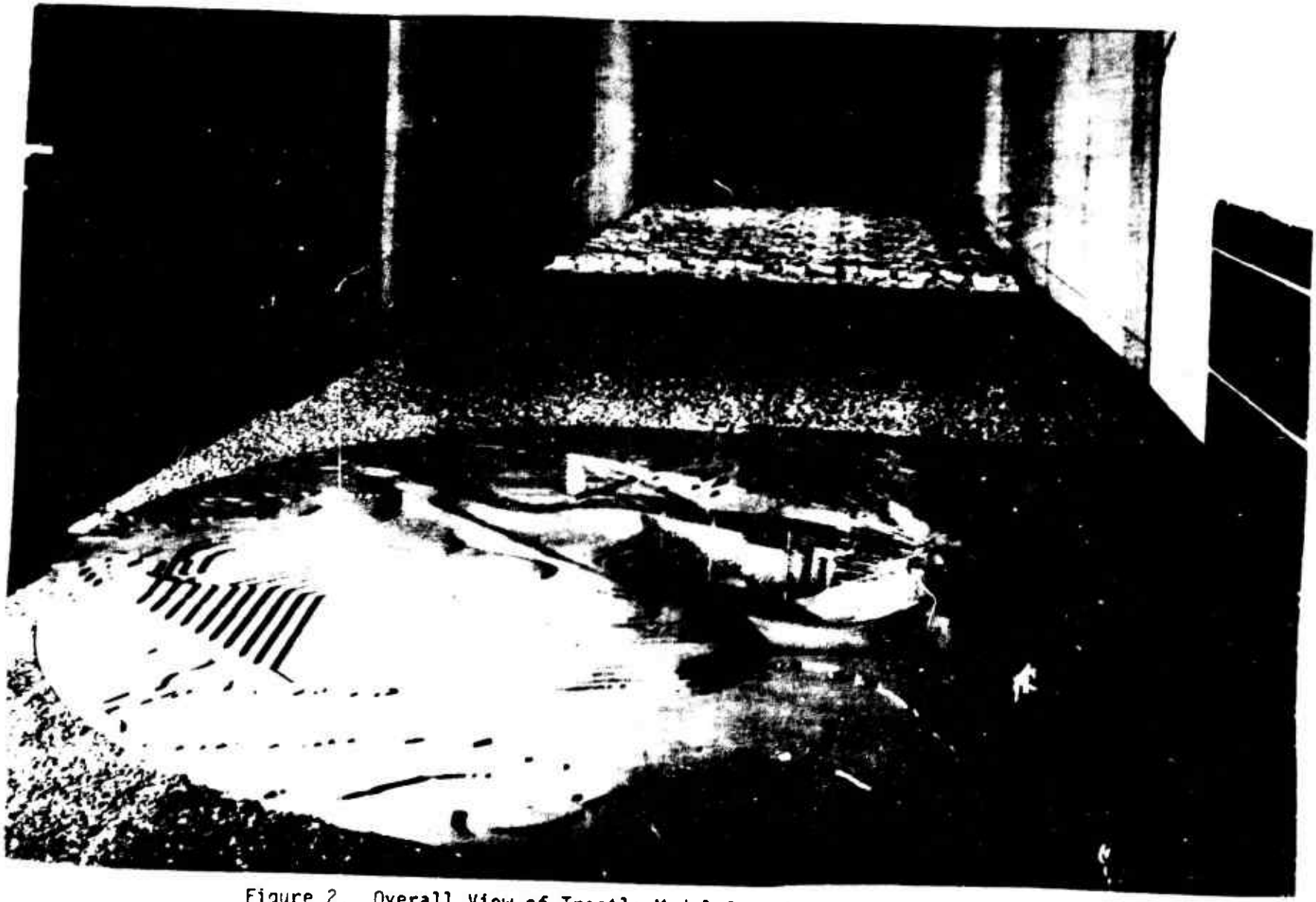

Figure 2. Overall View of Trestle Model Installed in Atmospheric Simulation Facility (Looking Upstream)

very low free-stream velocities, the mean flow in the tunnel is quite steady. The wind tunnel is situated in a very large room which forms the return circuit between the tunnel inlet and exhaust.

Two mechanical turntables are incorporated into the floor of the ASF. Both of them have a diameter of 88 inches. These turntables can be placed at various axial locations, depending on the program requirements. Models to be tested are mounted on one of the turntables. In this way, when upstream details are not sufficiently unique to require specific modeling, the general rough ground can be continued up to the turntable, which can then be rotated to change wind direction. The floor of the ASF can be warped both upstream and downstream of a model placed on either of the turntables in order to match the terrain contours at the edge of the model.

Various rough grounds are used depending on the scale of the model and the upwind terrain. The latter may change as the wind direction is changed; for example, a building located near a shore line will require an over-water approach for on-shore winds and perhaps a suburban approach for other wind directions. Close to the actual model under test, greater detail is incorporated. For example, a city building will be surrounded by several blocks of accurately modeled city.

3.2 INSTRUMENTATION

The primary measurements made in this program were the three components (vertical, longitudinal, and lateral) of the mean velocity at numerous locations above the ramp and test stand of the TRESTLE model. This was accomplished through the use of a specialized three-sensor hot-film probe in conjunction with three Calspan-manufactured constant temperature anemometers and associated electronics. The specialized probe (TSI Model No. 1298CC-20-18) was made by Thermo Systems Inc., St. Paul, Minnesota. The shaft of the probe is vertical with the sensing elements oriented for use with flows which are primarily horizontal. A sketch of the probe configuration is shown in Figure 3. The output voltages from the three anemometers were digitized

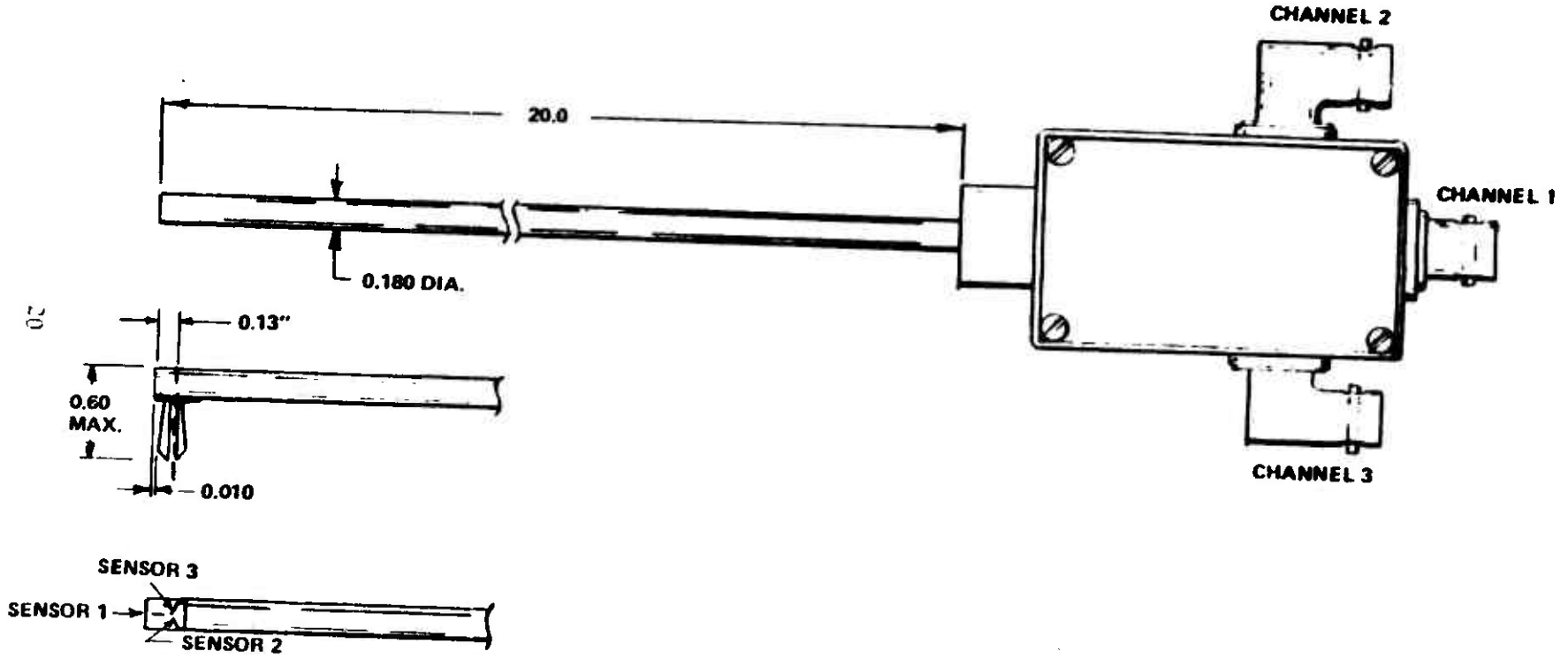

Figure 3. Thermo-System Three-Sensor, Hot-Film Probe (Model 1294-CC-20-18)

simultaneously by three A/D converters and analyzed on-line by a Hewlett-Packard 9825A minicomputer. Four hundred sets of three digitized samples were used for each calculation of velocity components. A Hewlett-Packard 9862A plotter was used to plot the reduced data. Details of the hot-film anemometer calibration and data reduction are presented in Appendix A.

In use, the hot-film probe was mounted in the ASF traverse system to position the probe tip at any desired location. Lateral and vertical locations were indicated by counters on the traverse mechanism. Axial location was indicated by a pointer mounted on the traverse system and a tape measure fixed to the windows of the ASF. Parallax in the tape measure and pointer system was less than 1/32 of an inch (about 1.25 feet in full-scale).

The reference velocity, U_∞, was measured in the approximately uniform flow 4 feet above the ground just upstream of the model. A standard pitot-static probe connected to an inclined micro-manometer was used for this purpose.

Smoke for flow visualization was generated by passing a small amount of nitrogen through a flask containing Titanium Tetrachloride. This produced a dense white smoke which was observed visually and also photographed.

4. MODEL DESIGN AND CONSTRUCTION

In general, it is desirable to select a model to prototype scale ratio which will allow both the TRESTLE facility and the local terrain to fit on the 88-inch turntable in the ASF. The upstream approach over which the flow is developed is then modeled approximately with random roughness elements of the proper mean height. Such a procedure allows variation of the wind direction by rotating the mechanized turntable. The specifications for the model tests required that all significant upwind terrain effects for a distance of not less than 2000 feet from the center of the site be included in the tests. Modeling a radius of 2000 feet would have required a scale ratio of 1:540 or 1-inch equals 45 feet. However, it was possible to model all significant terrain effects by using a scale ratio of 1:480 (1-inch = 40 feet) and designing the model with the turntable center slightly to the west of the center of the TRESTLE site. Coincidence of the site center and the turntable center is not a necessity and we have often used offsets to allow use of the largest possible model. Thus, the model was fabricated at a scale ratio of 1:480. A plan view of the area modeled is presented in Figure 4. The area includes the horizontal simulator which is the focus of this test program, the existing excavation for the vertical simulator, and the major features of the ARES site. The model is shown in Figure 2 installed on the turntable in the ASF.

The terrain model was made from plywood sheets laminated together to provide elevation contours every ten feet except in the immediate vicinity of the TRESTLE horizontal simulator. In this region, the excavation and landscaping were held as close to the drawing dimensions as possible. Contour maps at the proper scale were made by photographically enlarging the appropriate sections of the drawings supplied by the government. The photographic results were then reproduced on Bruning Copiers. The inexpensive Bruning copies were used to lay out the complete terrain model. Moreover, before the model was painted, the copies also provided outlines for accurately locating the elements of the TRESTLE model and other structures in the vicinity.

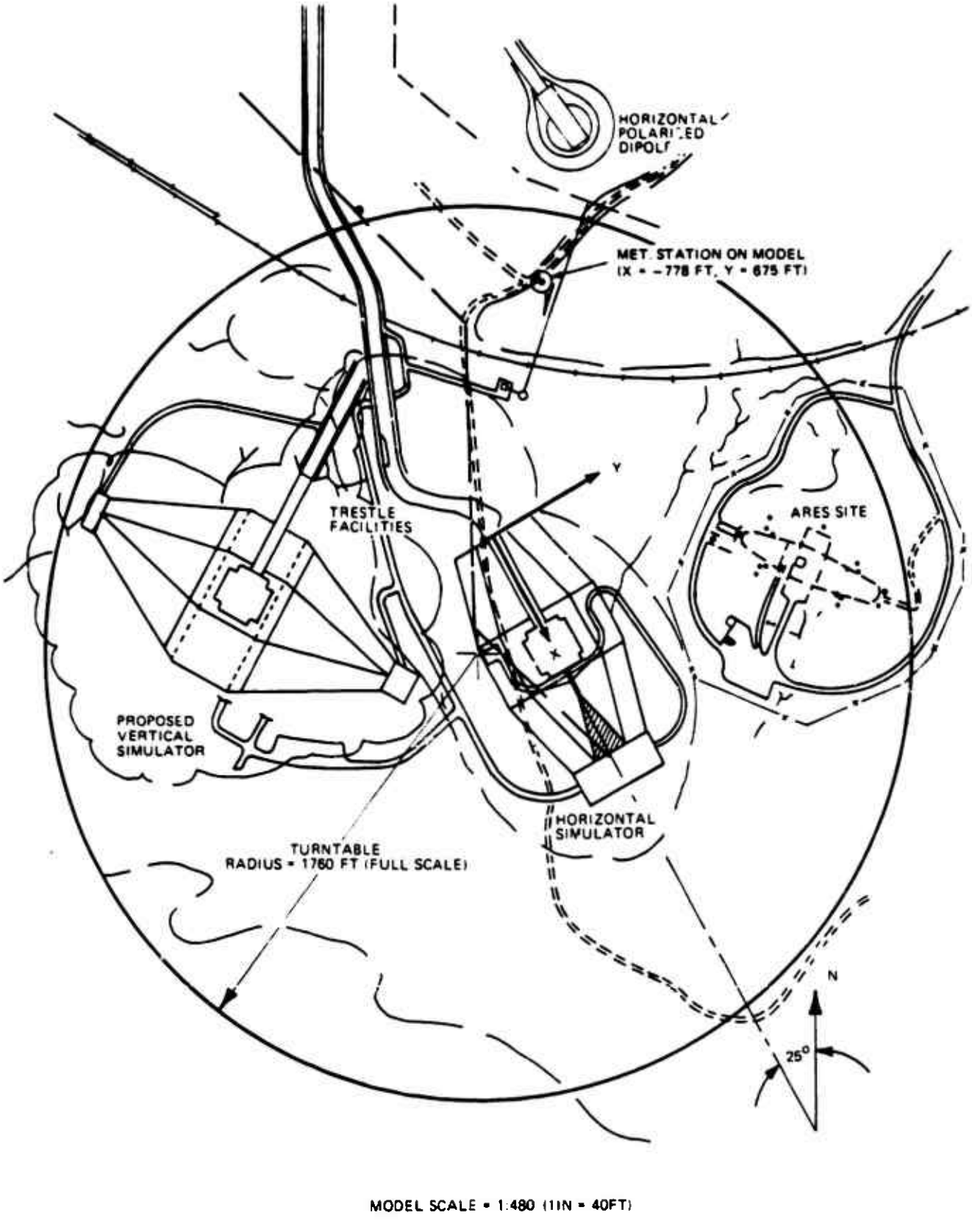

Figure 4. Plan View of Trestle Facility and Surrounding Area Modeled on ASF Turntable

Modeling of the ground elevations incurred changes in height at the edge of the turntable which made it necessary to provide a smooth junction between the upstream edge of the turntable and the ground upstream of the turntable. This was accomplished by mounting the upstream ground on an adjustable ramp frame which can be warped to match the edge of the turntable. An example of this can be seen in Figure 2, where the ramp has been adjusted to provide a good match between the upstream ground and the front edge of the turntable. For other orientations of the turntable, the ramp was readjusted to provide a similar match. It was not necessary to match the downstream edge of the turntable with the ASF flooring since a moderate discontinuity at this location will not affect the flow behavior in the vicinity of the TRESTLE model.

In addition to the excavation in the terrain model, the TRESTLE facility model contains three other major features which were modeled. These are:

1. The test platform and ramp and their support structure.
2. The transmission line support cables and support tower.
3. The central ground plane wedge structure.

The above items are shown in Figure 5. The support structures, the transmission lines, and the ground plane wedge are all porous mesh-type structures. Because of the small scale of the model, it was neither practical nor correct to use exact geometric modeling of these elements. Instead, the geometric outlines of these structures and the loss characteristics of the flow passing through them were modeled. The loss characteristics of the full-scale porous structures were estimated from their mesh geometry (mainly their porosity). The support structure under the ramp and test stand was modeled with expanded aluminum mesh with a porosity very close to the porosity of the full-scale wooden frame support structure (bents). The model mesh was assembled in a three-dimensional array similar to the actual structure. (See Figure 5 and the close-up view in Figure 6.) The full-scale wire mesh structure on the transmission lines has a porosity close to 99 percent. This is completely

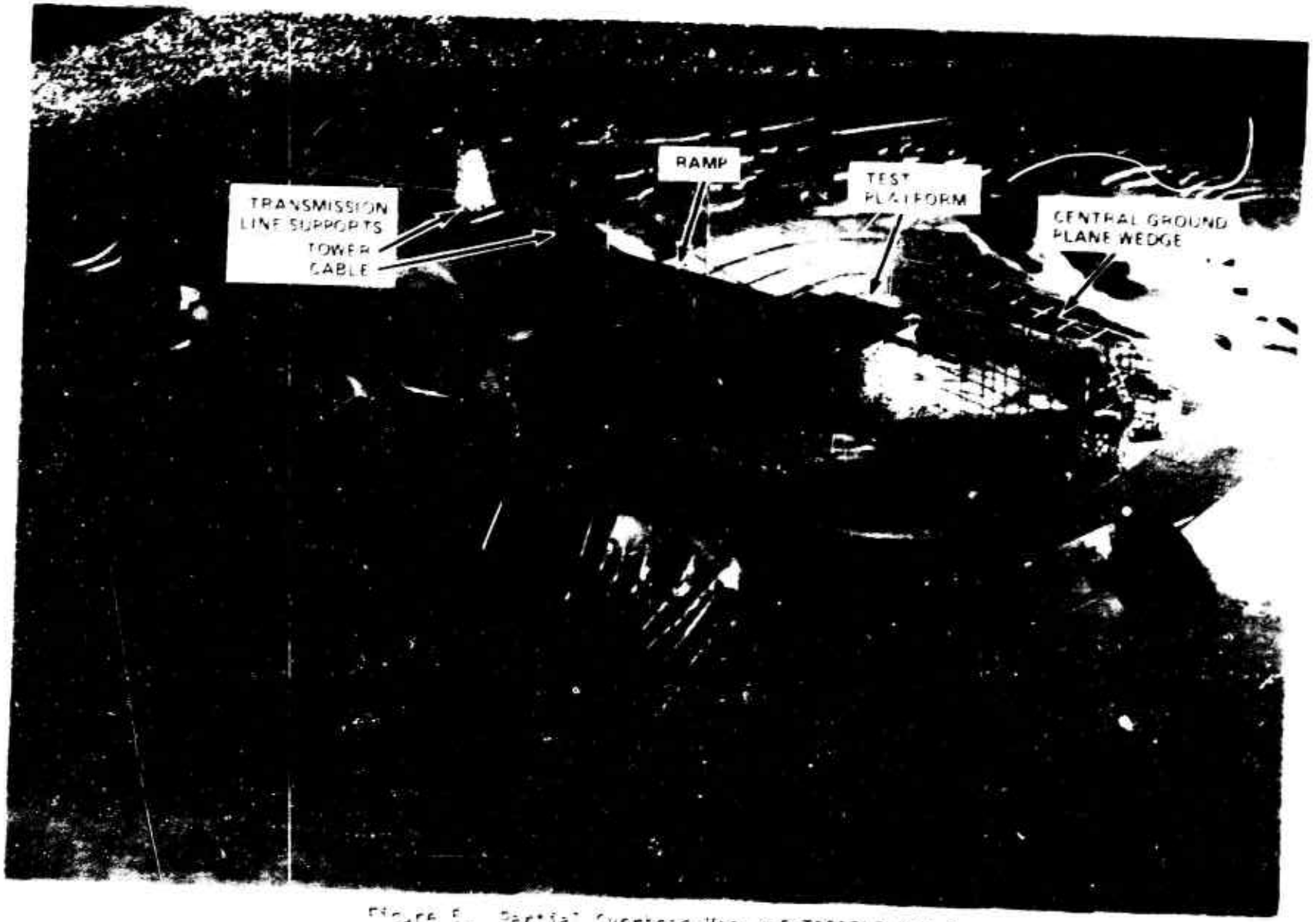

Figure 5. Partial Overhead View of TRESTLE Model

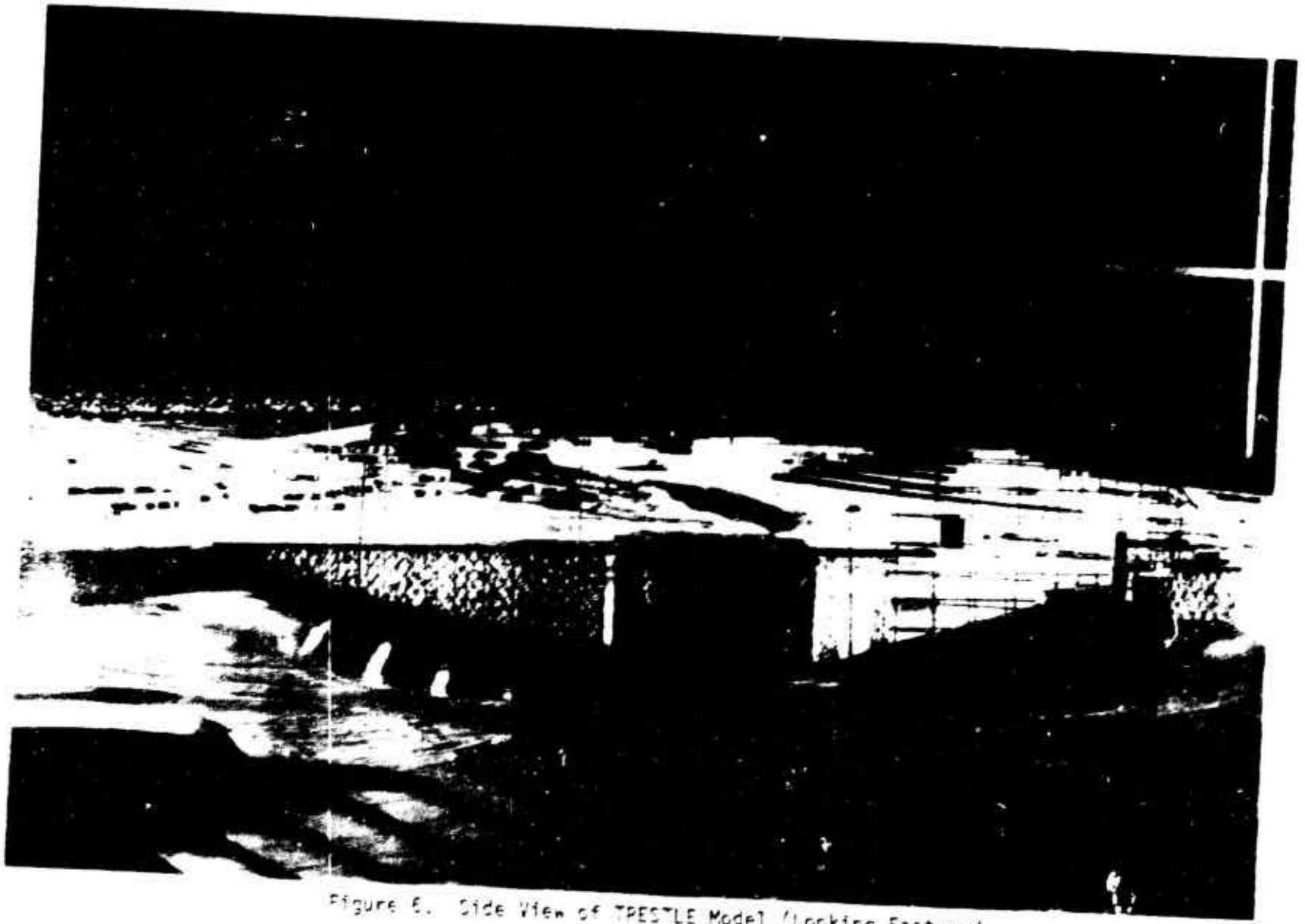

Figure 6. Side View of TRESTLE Model Looking Eastward.

transparent to the wind. Thus, only the support cables on the transmission lines were modeled. Similarly, on the central ground plane wedge the majority of the full-scale wire mesh is about 99 percent porous and was not modeled. Instead, the support structure for the wedge was modeled along with any solid blockages and the lower porosity (4" x 4") sections of full-scale wire mesh.

As described in Section 3.1 and at the start of this section, the flow approaching the turntable model is developed over a length of ground covered with random roughness elements of the proper mean height. The full-scale approach to the TRESTLE facility is relatively flat and unobstructed for a mile or more in all wind directions. The city of Albuquerque lies farther away to the North, with mountains even farther away to the East, running North-South. The local wind characteristics in the immediate vicinity of the TRESTLE facility will not be measurably affected by the mountains. Moreover, Albuquerque should have a negligible effect on the local flow characteristics since the low altitude winds adjust rapidly to changes in the terrain roughness. In the model, the approaching flow was generated by allowing it to develop over a 36 foot length of randomly distributed wooden blocks followed by 12 feet of gravel. Mean velocity profiles for each of these roughness distributions when used alone are shown in Figure 7. The combination of the two rough grounds provided a mean velocity profile similar to that obtained with the gravel alone (Figure 7). Such a profile is typical of relatively flat open country.

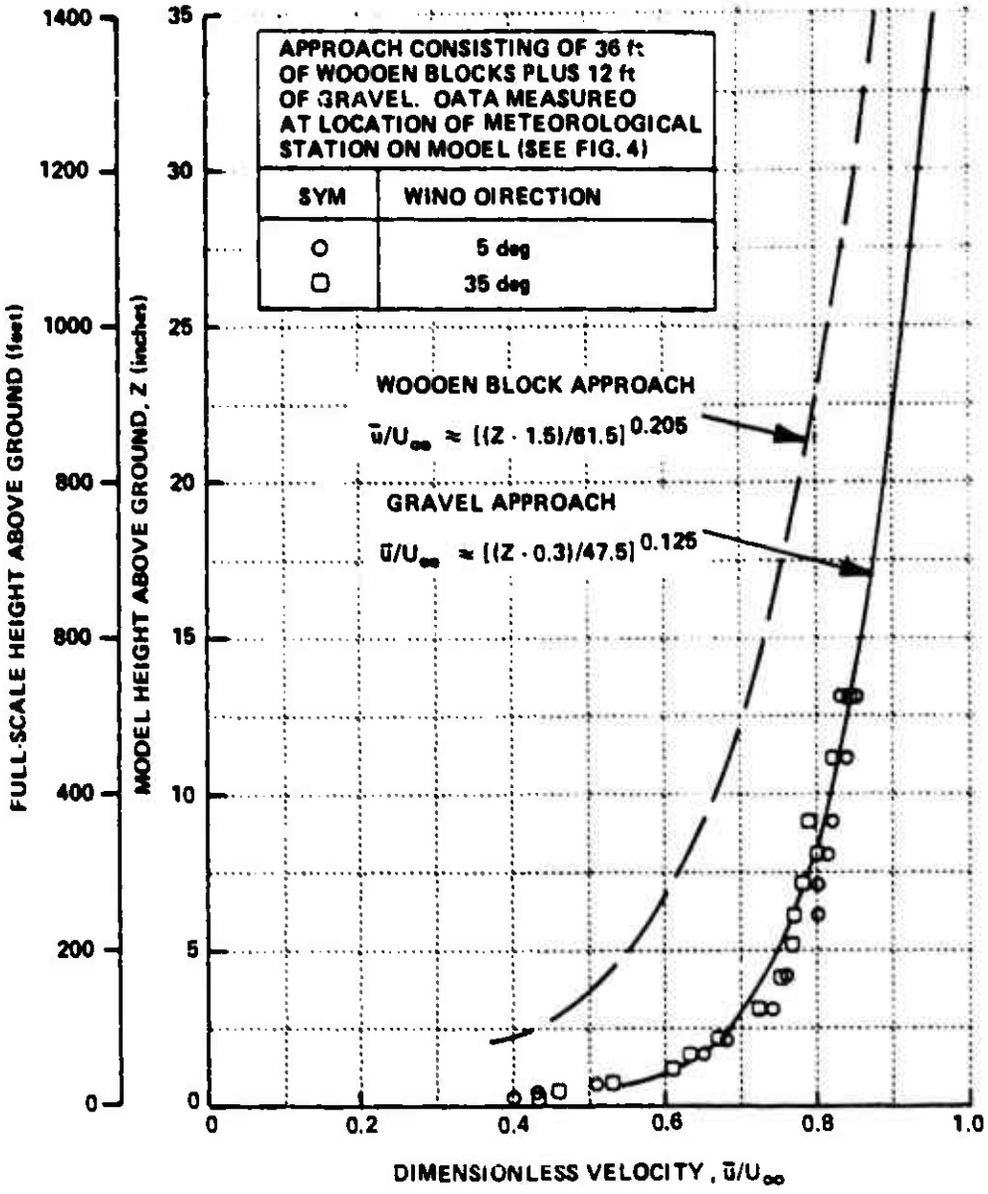

Figure 7. Mean Velocity Profiles in Approaching Flow

5. WIND TUNNEL TESTS

The wind tunnel tests are presented in five parts. Mean velocity profiles measured at the location of the meteorological station on the model are presented in 5.1. Flow visualization studies are discussed in 5.2. Section 5.3 presents the results of a study to investigate the effect of the transmission line support cables on the flow over the ramp and test stand. A comparison of dimensionless velocity profiles measured with two different reference wind velocities is presented in 5.4. Finally, the wind velocities measured above the TRESTLE model test stand and ramp are presented in 5.5.

5.1 WIND CONDITIONS AT METEOROLOGICAL TOWER

One of the problems encountered in interpreting model test data, or for that matter full scale data, is the selection of a location for measuring the mean wind velocity. In full scale these are usually measured at meteorological stations which may be remote from the area of interest. Moreover, the anemometers are located at low altitudes, typically about 100 feet or less above local ground level. The measured wind velocities can be influenced by the local terrain as well as the height above ground. In the ASF, the possibility of local terrain influences on the reference wind velocity is avoided by selecting a measuring location well above the terrain, in this case at a model height of 4 feet or an effective full scale height of 1920 feet above the ground. However, this reference velocity is still required to have a known relationship with some full-scale meteorological station. Such a relationship can be found from mean velocity profiles measured above the model.

A full-scale meteorological tower for monitoring winds near the TRESTLE facility will be located in a relatively flat area almost due north of the facility test stand. The winds will be measured at a height of 10 meters above local ground level. In the model tests, velocity profiles were measured at the approximate location of this tower. The location on the model is shown in Figure 4. Velocity profiles were measured for six different wind directions, three with the meteorological station located upwind of the test

stand (335, 005, and 035 degrees) and three with the station located downwind (155, 185, and 215 degrees). The results of these measurements are shown in Figures 8 and 9. The velocities shown in these figures have been made dimensionless by dividing by the reference velocity, U_∞, measured at a model height of four feet.

With the meteorological station upwind (Figure 8), the velocity profiles are similar for wind directions of 5 degrees and 35 degrees. The velocities measured for a wind direction of 335 degrees are slightly lower at all heights. The latter result may be caused by proximity of the wind tunnel wall because in this case the meteorological station was closer to the tunnel rear side wall than for any of the other wind directions. With the meteorological station downwind of the TRESTLE model (Figure 9), the three velocity profiles are similar at model heights above about 3 inches. Below this height, the three profiles differ because of direction sensitive terrain differences just upwind of the measuring station. The highest velocities near the ground were obtained for a wind direction of 155 degrees. With this wind direction, the ARES Site (Figure 4) is just upwind of the measuring station and the terrain is very rough before it levels out. Apparently this rough local terrains distorts the velocity profile near the ground.

A full-scale height of 10 meters is shown on Figures 8 and 9. As mentioned previously, this is the height at which it is planned to monitor the full-scale wind velocities. For wind directions of 005, 035, and 185 degrees the velocity at this height is 0.55 times the tunnel reference velocity, U_∞. For wind directions of 155, 215 and 335 degrees the velocity ratios at 10 meters full-scale are approximately 0.62, 0.60, and 0.51 respectively. It was not possible to measure the velocity ratios at 10 meters for other wind directions because the location of the meteorological station was too close to the wind tunnel walls. However, it is believed that the observed range of values 0.55 to 0.62 (the measured value 0.51 is discounted because of possible wall proximity effects) is representative of the full-scale wind velocity that

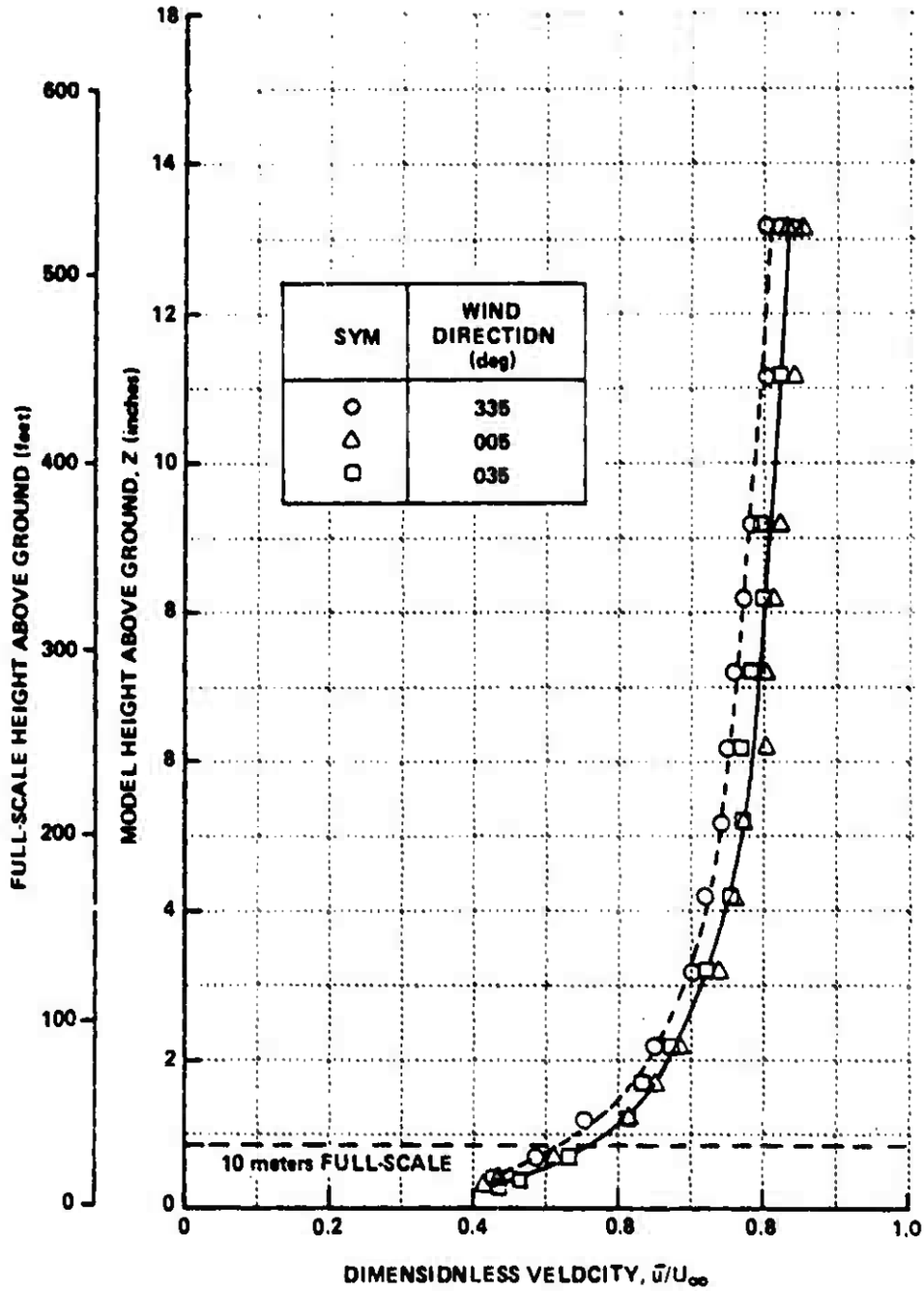

Figure 8. Mean Velocity Profiles at Meteorological Station With Station Upwind of TRESTLE Model

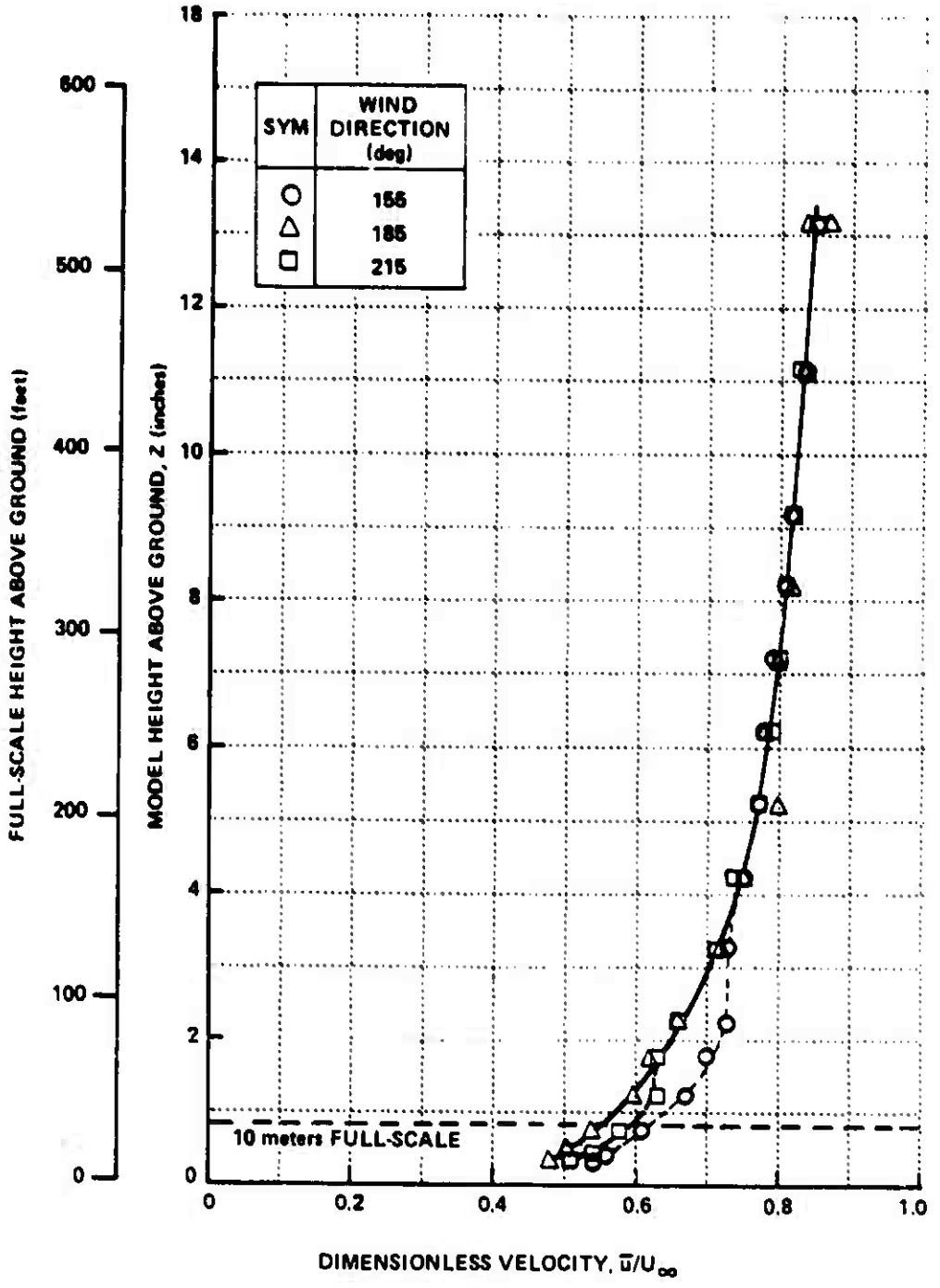

Figure 9. Mean Velocity Profiles at Meteorological Station With Station Downwind of TRESTLE Model

will be measured at a height of 10 meters for all wind directions. In view of this, it was decided to choose a single value of $\bar{u}/U_\infty$ at the 10 meter height which would provide a conservative representation of the full-scale winds from any direction. The value selected for this quantity was 0.55, thus the velocity data measured for use in the subsequent aircraft force analysis were nondimensionalized by a reference velocity U_{REF} given by

$$U_{REF} = 0.55\, U_\infty$$

where U_∞ is the velocity calculated from the pitot-static pressure measured at a height of 4 feet above the model. Selecting the lowest reliable value for for $\bar{u}/U_\infty$ at 10 meters has the effect of making the measured velocities about the TRESTLE platform appear slightly larger than they really are for those wind directions where $\bar{u}/U_\infty$ at 10 meters is larger than 0.55. Thus for these wind directions, the force estimates will indicate unsafe handling at a lower reference velocity than the 10 meter value at which it will actually occur.

5.2 FLOW VISUALIZATION STUDIES

A flow visualization study was made at the start of the model tests. As noted in Section 3.2, the smoke was generated by passing nitrogen through flasks containing small amounts of Titanium Tetrachloride. The mixtures were then piped to various locations on the model and the resulting smoke plumes were observed visually and also photographed. Although some visual observations of the smoke from a single hand-held wand were made, the majority of the study was performed with an arrangement of twelve small diameter tubes inserted through the base of the model and outlining the model ramp and test stand. The tubes could be moved up or down to place their exits above or below the top surface of the ramp and test stand. Side view and overhead view photographs of the smoke plumes were taken for twelve wind directions with the tubes at several heights for each wind direction. In all, more than 300 photographs were taken.

Since the flow in the ASF is turbulent as in full-scale winds, the smoke plumes do not behave in the same fashion as in aeronautical tunnels where the plumes provide a good picture of the general flow pattern. Instead, the plumes fluctuate in time and diffuse rapidly after they leave the tube exits. Photographing such plumes requires very good lighting and a relatively fast shutter speed. Typical results are shown in Figures 10, and 11 where enlarged photographs are presented for the smoke plumes obtained with the wind approaching from 35 degrees and 65 degrees respectively. In Figure 10 the smoke tube exits are level with the top of the TRESTLE platform and in Figure 11 they are 1/2 inch (20 feet in full scale) above the top of the platform. The lack of definition in the smoke plumes is the result of a compromise between shutter speed and available lighting.

Photographic results from the smoke flow visualization studies are presented in Figures 12 through 23 for all wind directions. In these photographs the smoke tube exits were level with the upper surface of the TRESTLE model platform. Each figure has two photographs, an overhead view and a side view. The wind is approaching from the left in all photographs. In most cases, an array of 6 smoke tubes on the upwind side of the TRESTLE ramp and platform was used in the photographs. In these cases only one set of photographs (overhead and side views) is presented for each wind direction. For two wind directions, 155 and 335 degrees (Figures 17 (a, b, c) and 23 (a, b, c)), the wind was parallel to the TRESTLE model ramp. In these cases, three sets of photographs are presented; one with the two upstream smoke tubes operating (Figures 17(a) and 23(a)), one with two of the midstream tubes operating (Figures 17(b) and 23(b)), and one with the two downstream tubes operating (Figures 17(c) and 23(c)).

In all of the smoke pictures, the nitrogen flow in the smoke tubes was adjusted to the lowest level which would still give a satisfactory amount of smoke. This was done to minimize the effect of the initial vertical momentum at the smoke tube exits. It is believed that initial momentum effects are negligible in most of the photographs. For example, see the enlarged

Figure 10. Smoke Visualization of Flow over TRESTLE Platform For Wind Direction of 35 Degrees

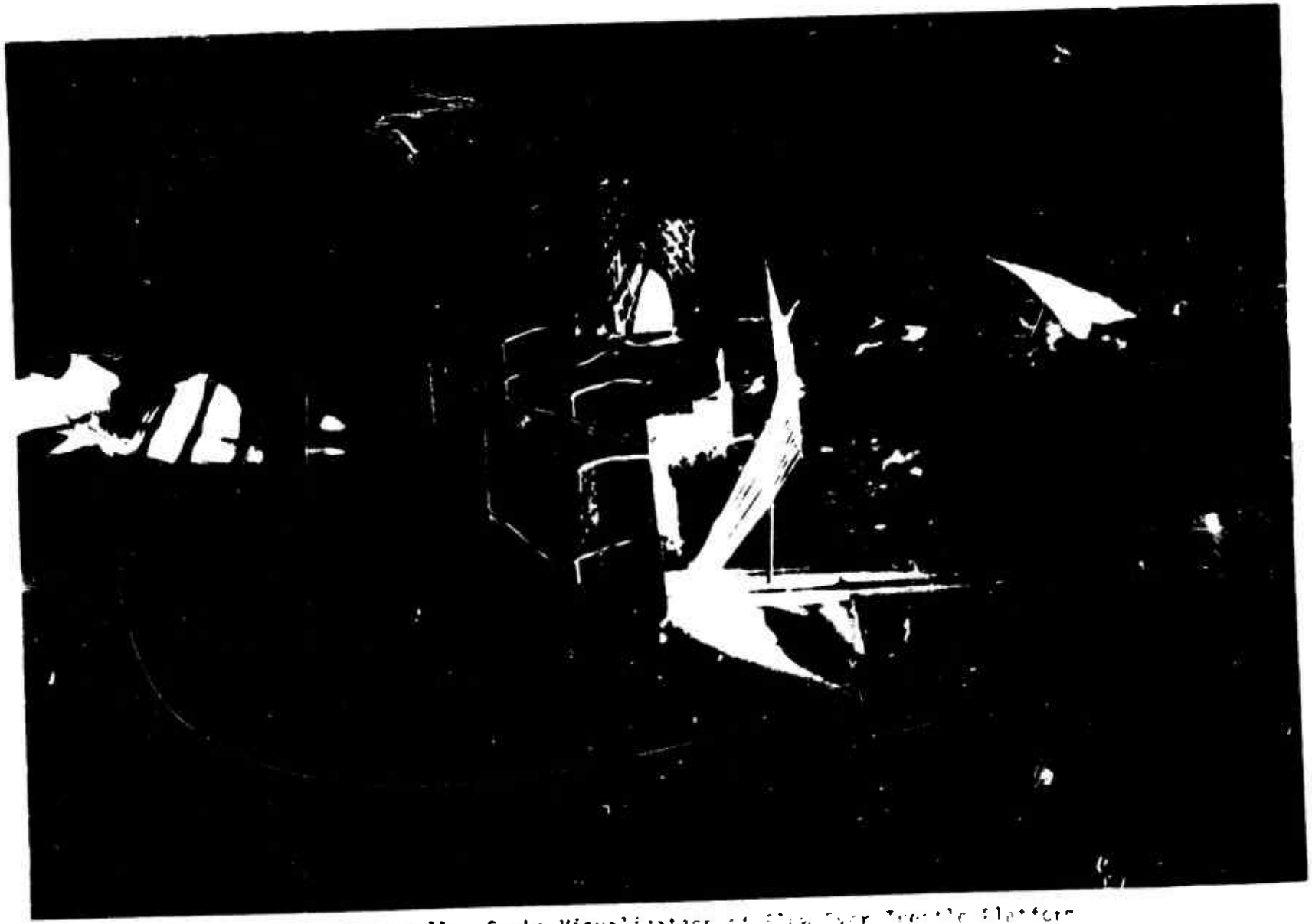

Figure 11. Smoke Visualization [illegible] Platform
For Wind Direction [illegible] Degrees

Figure 12. TRESTLE Model Smoke Studies, 5 Degrees Wind

Figure 13. [illegible] Model Smoke Studies, 35 Degrees Wind

Figure 14. [illegible] Model Smoke Studies, 60 Degrees Wind

Figure 15. TRESTLE Model Smoke Studies, 95 Degrees Wind

Figure 16. IBFSHI Model Smoke Studies, 135 Degrees Wind

(a) UPSTREAM SMOKE TUBES

Figure 17. TRESTLE Model Smoke Studies, 155 Degrees Wind

(b) MIDSTREAM SMOKE TUBES

Figure 17 (Cont.) TRESTLE Model Smoke Studies, 155 Degrees Wind

(c) DOWNSTREAM SMOKE TUBES

Figure 17 (Cont.) TRESTLE Model Smoke Studies, 155 Degrees Wind

Figure 18. TRESTLE Model Smoke Studies, 185 Degrees Wind

Figure 19. TRESTLE Model Smoke Studies, 215 Degrees Wind

Figure 20. TRESTLE Model Smoke Studies, 245 Degrees Wind

Figure 21. TRESTLE Model Smoke Studies, 275 Degrees Wind

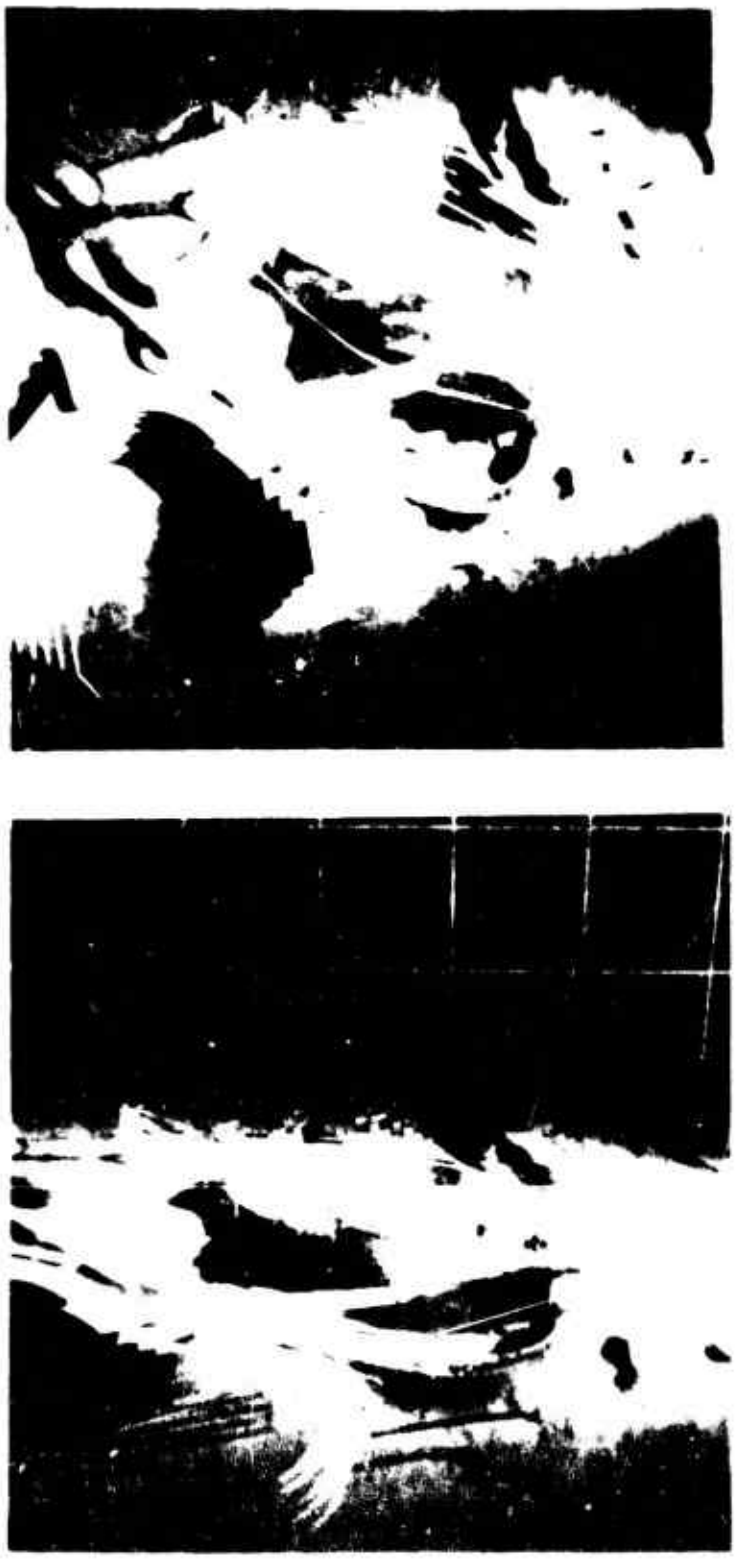

Figure 22. TFE-TL Model Smoke Flow, 45 Degree Wire

(a) UPSTREAM SMOKE TUBES

Figure 23. TRESTLE Model Smoke Studies, 335 Degrees Wind

(b) MIDSTREAM SMOKE TUBES

Figure [illegible] degrees wind

(c) DOWNSTREAM SMOKE TUBES

Figure 23 (Cont.) TRESTLE Model Smoke Studies, 335 Degrees Wind

photograph in Figure 10 where the smoke tube exits were raised above the level of the TRESTLE platform. There appears to be a negligible amount of vertical rise at the tube exits. Thus those photographs which show a substantial vertical component at the tube exits indicate the true flow direction at the instant that the photograph was taken. It is worth noting that the smoke plumes were quite unsteady in time and the instantaneous photographs provide only a rough idea of the average flow direction whereas the long time intervals used in the quantitative velocity measurements provide true averages of the velocity components.

Overall inspection of the photographic results presented in Figures 12 through 23 allow a few general observations to be made. The overhead views show that lateral deviations from the mean flow direction are relatively small in all cases. The side views show that there is frequently a substantial upwash just upwind of the TRESTLE ramp and test stand and a downwash which begins after the flow has partially crossed the ramp or test stand. Relatively large values of upwash and downwash are evident in the side view of Figure 21. The smoke tube in the foreground shows a large upwash component while the tube at the juncture between the ramp and test stand shows an initial upwash followed by a large downwash partway across the ramp. Visual observations for this wind direction (275 degrees) and for a wind direction of 35 degrees showed there was an intermittent vortex which formed close to the platform surface in the region near the juncture between the ramp and test stand. Since this condition occurred only occasionally it was very difficult to photograph. Figure 21 is the closest we came to capturing this phenomenon on film. With the flow parallel to the ramp (155 and 335 degrees), there was very little evidence of consistent directional changes from the mean wind. There did appear to be a fairly steady upwash near the juncture between the ramp and downstream edge of the excavation for a wind direction of 155 degrees. This can be seen in the side view of Figure 17(c). The apparent upwash in Figure 17(b) is an instantaneous result generated in the turbulent wake from the ground plane edge structure. The flow in this region was generally quite turbulent and the average velocity was low. The high level of turbulence is indicated by the rapid diffusion of the smoke plumes, especially apparent

in the overhead view of Figure 17(b). In contrast, the overhead view in Figure 17(c) shows much less diffusion of the smoke plumes.

The smoke visualization study showed that there was considerable variation in the flow over the TRESTLE platform with the largest deviations from the mean flow occurring near the upstream edges of the ramp and test stand and additional deviations occurring near the juncture between the ramp and excavation for southerly winds. A grid of test points for the velocity surveys was selected with these flow features in mind. The grid arrangement is presented in Figure 24 superimposed on an outline of the TRESTLE platform. In selecting the grid pattern there were two other requirements to consider in addition to the smoke visualization results. First, a regularly spaced grid pattern was required to facilitate rapid location changes of the hot-film probe and ease of interpolating the test results. Second, the number of grid points should be minimized to keep the test program within reasonable limits. The final pattern selected contained 58 points at which vertical surveys of the velocity were made. The survey points are identified in the following discussions in terms of their full-scale coordinates in the TRESTLE coordinate system. The coordinate system is indicated in Figure 24.

5.3 EFFECT OF TRANSMISSION LINE SUPPORT CABLES

After selecting the grid pattern to be used in the velocity surveys above the TRESTLE platform, it was determined that the transmission line support cables would interfere with the hot-film probe at a number of the test points on the grid. Thus it was decided to perform a brief study to see if the support cables had a significant influence on the flow in the region of the planned measurements. The study consisted of measuring velocity profiles at several locations downwind of the support cables and then removing the cables and repeating the velocity surveys. A wind direction of 305 degrees was used for this study and the velocity surveys were made at three locations on the test grid shown in Figure 24. The (X, Y) coordinates of these locations were (-64, 0), (22, -50), and (280, -100). It is believed that the wind direction and test locations chosen for this study represent a worst case for flow distortion from the support cables.

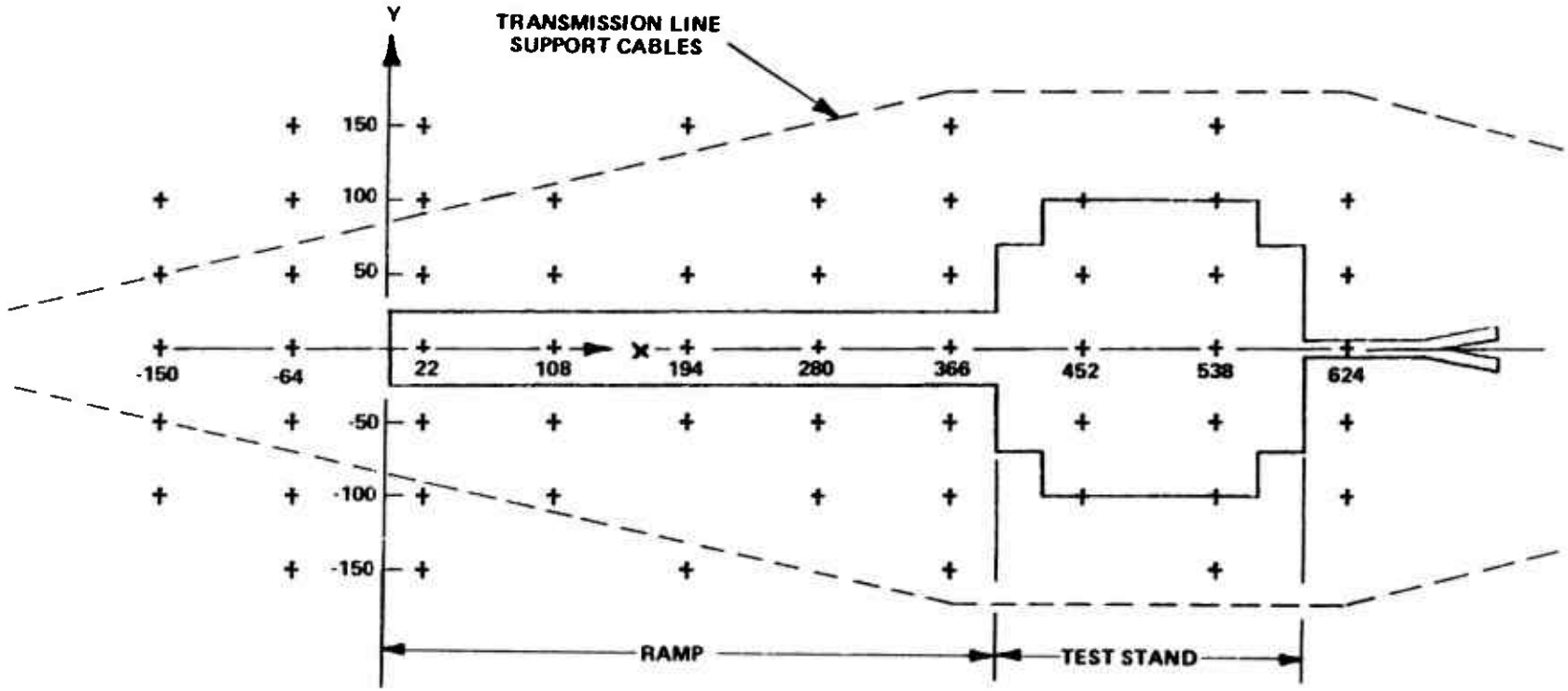

NOTES: GRID DIMENSIONS SHOWN ARE IN FULL-SCALE FEET
+ INDICATES LOCATION OF GRID TEST POINT
VERTICAL AXIS, Z, IS POSITIVE UPWARDS

Figure 24. Test Grid Used for Vertical Surveys of Velocity above Trestle Platform

The results of the study are shown in Figures 25, 26 and 27. Each figure shows two velocity profiles, one measured with the support cables present and one with the cables removed for a given grid location. The measured velocities have been nondimensionalized by dividing by the wind tunnel reference velocity, U_∞. The figures also show a dashed line to indicate a full-scale height of 66 feet above the TRESTLE platform. This is the maximum height of interest for the subsequent flow surveys to determine the forces on aircraft.

Inspection of Figures 25 and 26 shows that there is a measurable velocity defect in the wake from the support cables. As expected, the largest defect is in the region where the cables are closest together (Figure 25). However, in these two figures the defect occurs at or above the 66 foot level. The data in Figure 27 indicate a slightly lower velocity with the cables present over a height range from 0 to above 400 feet full-scale. It is unlikely that the apparent velocity defect is due solely to the transmission line support cables since they have a high porosity in this region and only extend to a maximum full-scale height of about 140 feet above the platform. Some of the apparent velocity defect may be due to experimental accuracy which is expected to be within approximately 5 percent for the hot-film measurements. In any event, the data in Figures 25 through 27 show that the effect of the support cables is not large and in all cases creates a defect in velocity. Thus, it was decided to remove the support cables for the remainder of the tests so that the velocity surveys could be made at all of the selected grid points.

5.4 TESTS WITH DIFFERENT WIND VELOCITIES

As stated in Section 2, it is only necessary to measure the flow field for one value of the reference velocity, U_{REF}. The dimensionless velocity profiles will be independent of the magnitude of the reference velocity. The independence of the dimensionless velocity profiles is illustrated in Figures 28 and 29. Figure 28 compares dimensionless axial velocity profiles for two values of U_{REF} (10.0 and 19.4 ft/sec) at a location upstream

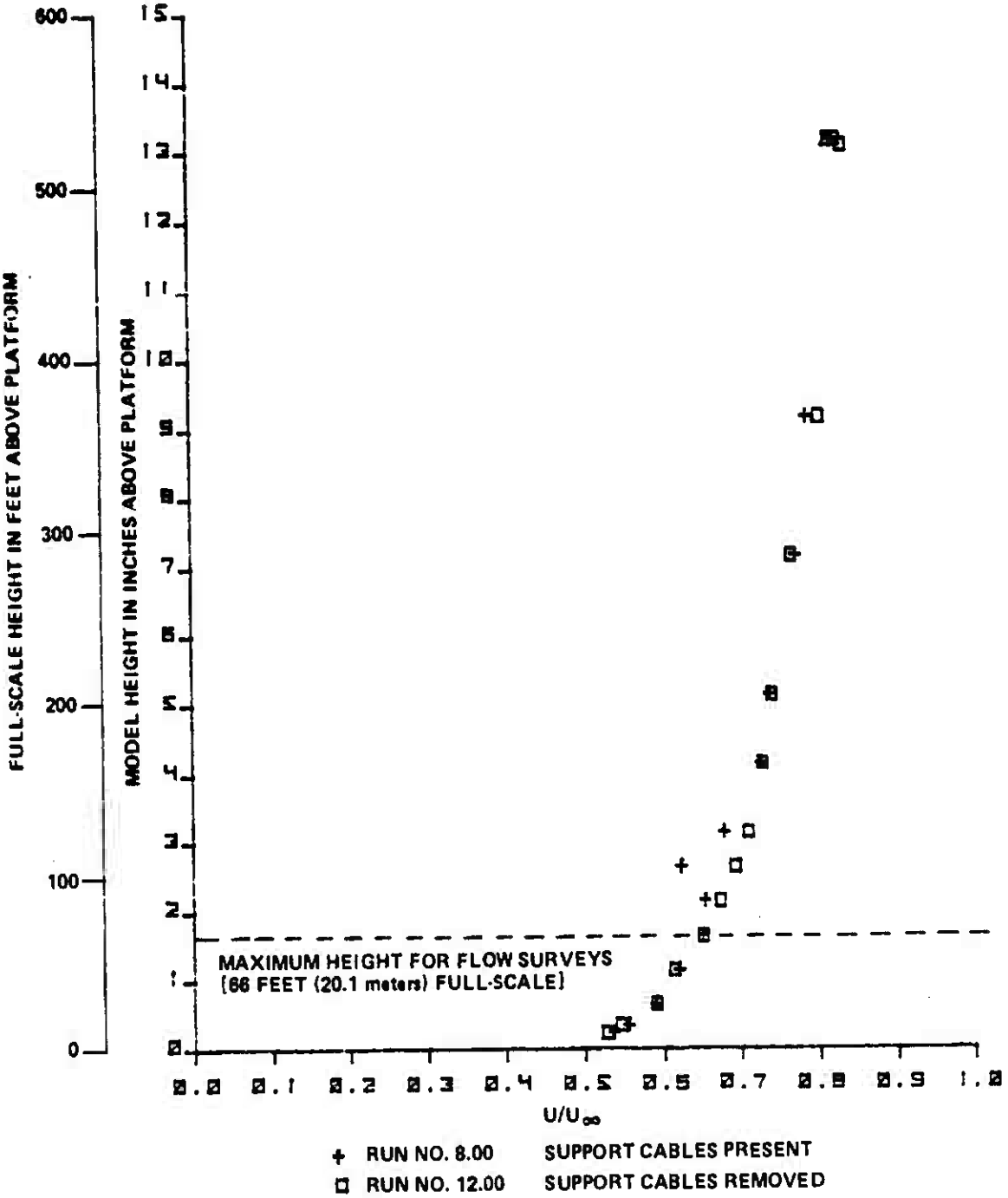

Figure 25: Effect of Transmission Line Support Cables, 305 Degrees Wind Angle, Test Location; X = - 64 ft, Y = 0 ft.

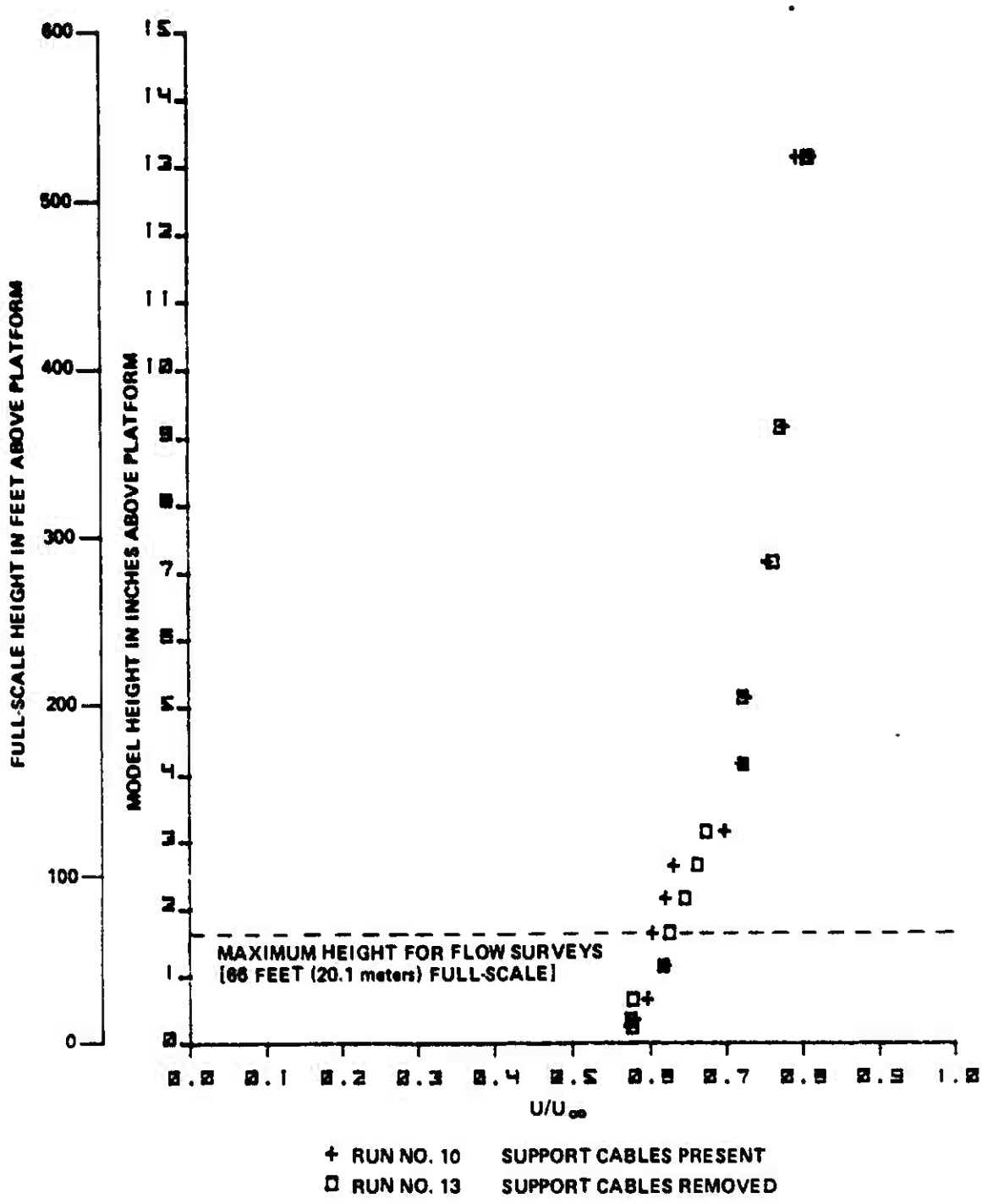

Figure 26. Effect of Transmission Line Support Cables, 305 Degrees Wind Angle, Test Location; X = 22 ft, Y = - 50 ft.

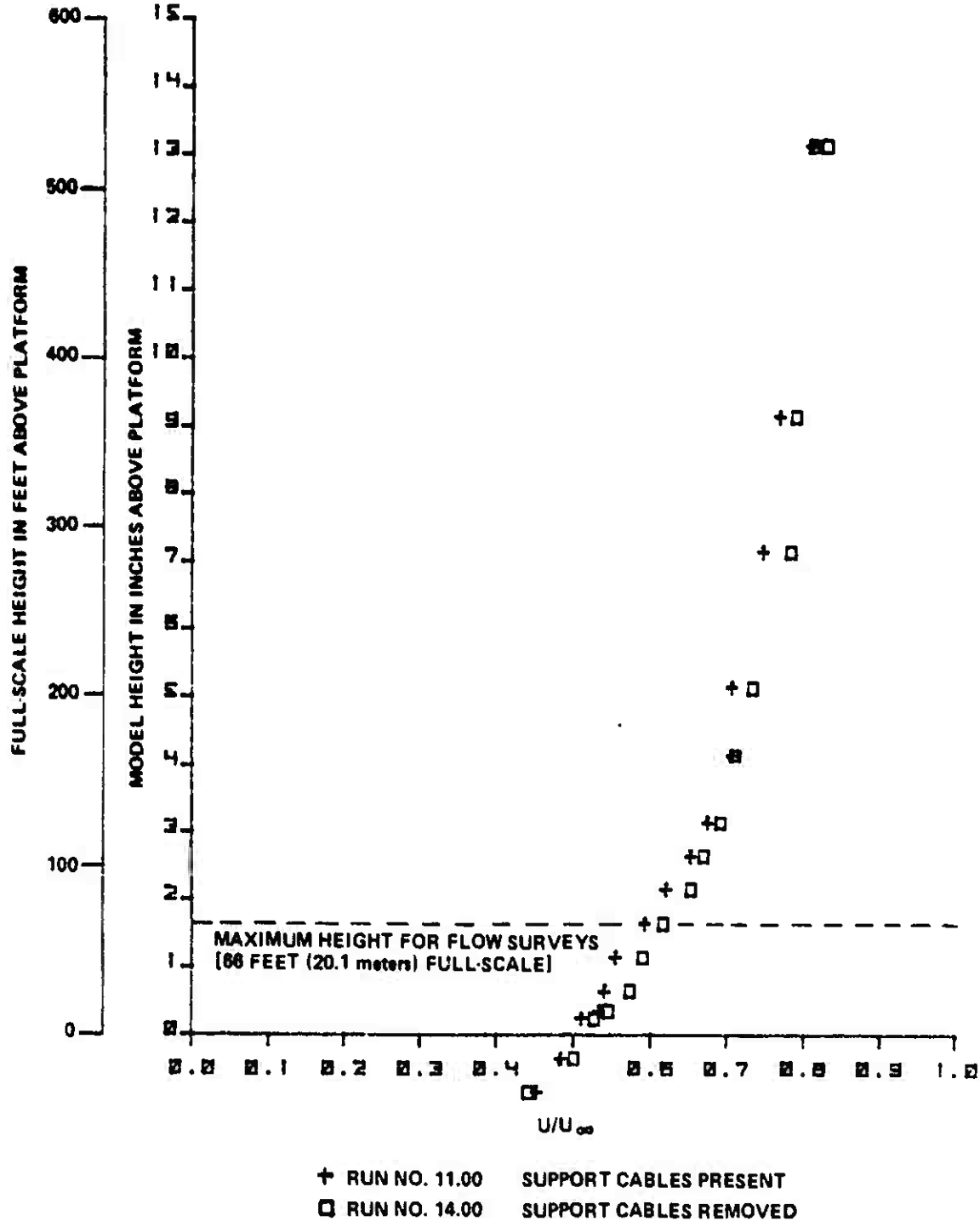

Figure 27. Effect of Transmission Line Support Cables, 305 Degrees Wind Angle, Test Location; X = 280 ft, Y = - 100 ft.

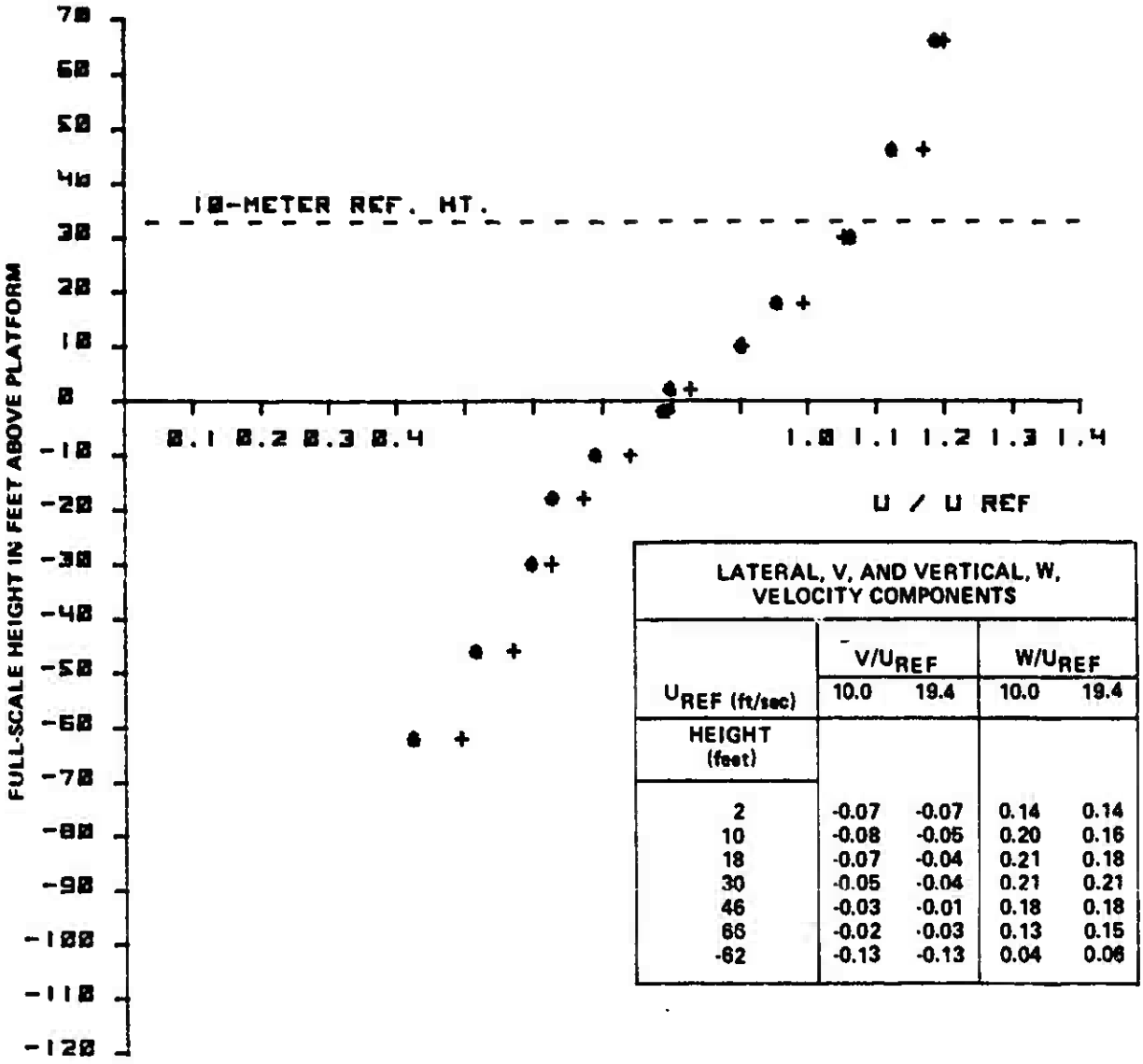

LATERAL, V, AND VERTICAL, W, VELOCITY COMPONENTS				
	$\bar{V}/U_{REF}$		W/U_{REF}	
U_{REF} (ft/sec)	10.0	19.4	10.0	19.4
HEIGHT (feet)				
2	-0.07	-0.07	0.14	0.14
10	-0.08	-0.05	0.20	0.16
18	-0.07	-0.04	0.21	0.18
30	-0.05	-0.04	0.21	0.21
46	-0.03	-0.01	0.18	0.18
66	-0.02	-0.03	0.13	0.15
-62	-0.13	-0.13	0.04	0.06

+ RUN NO. 15 X = 194 FT Y = 50 FT U REF = 19.4 FT/SEC
● RUN NO. 28 X = 194 FT Y = 50 FT U REF = 10.0 FT/SEC

Figure 28. Effect of Different Wind Velocities, Wind Angle 65 Degrees, Survey Upstream of Ramp

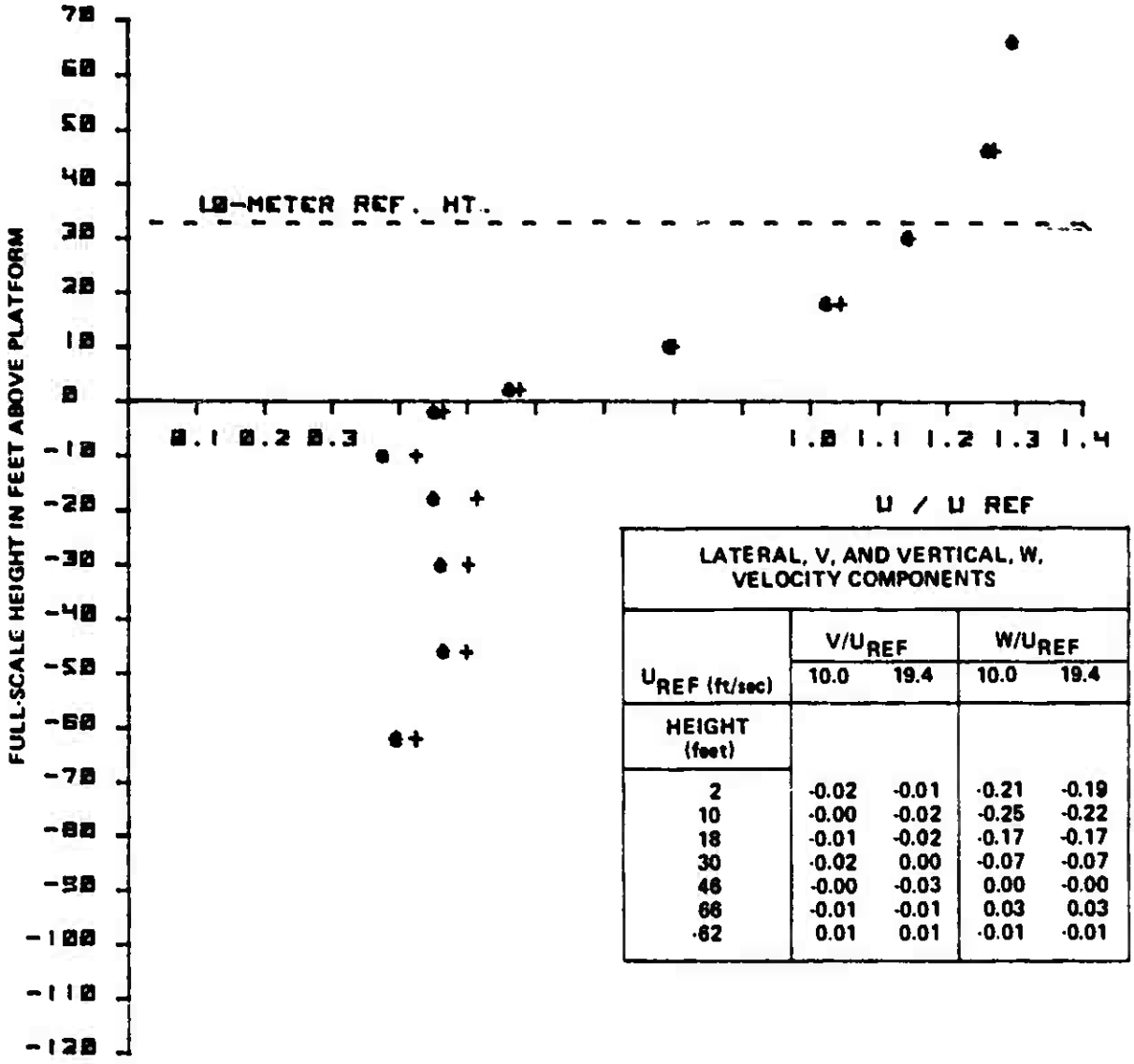

LATERAL, V, AND VERTICAL, W, VELOCITY COMPONENTS				
	V/U_{REF}		W/U_{REF}	
U_{REF} (ft/sec)	10.0	19.4	10.0	19.4
HEIGHT (feet)				
2	-0.02	-0.01	-0.21	-0.19
10	-0.00	-0.02	-0.25	-0.22
18	-0.01	-0.02	-0.17	-0.17
30	-0.02	0.00	-0.07	-0.07
46	-0.00	-0.03	0.00	-0.00
66	-0.01	-0.01	0.03	0.03
82	0.01	0.01	-0.01	-0.01

+ RUN NO. 16 X = 194 FT Y = -50 FT U REF = 19.4 FT/SEC
♦ RUN NO. 30 X = 194 FT Y = -50 FT U REF = 10.0 FT/SEC

Figure 29. Effect of Different Wind Velocities, Wind Angle 65 Degree, Survey Downstream of Ramp.

of the ramp with the wind approaching perpendicular to the ramp centerline. Figure 29 compares similar axial velocity profiles measured just downstream of the ramp. Both figures also contain a short table of dimensionless lateral and vertical velocity components measured at the same time as the axial components.

The portion of the axial velocity profiles above the platform surface show excellent agreement (to within 5 percent or better). Below the platform surface, the axial velocity profiles display a small but consistent difference. In this region, the profiles measured with U_{REF} = 19.4 feet per second show dimensionless velocities which are about 10 percent higher than those measured with U_{REF} = 10.0 feet per second. This may be evidence of a small Reynolds number effect on the flow through the porous understructure of the ramp. At low velocities, the drag coefficient of the porous structure will increase as the velocity decreases. Thus one would expect the dimensionless profiles to display the trend which is shown by the data. However, the effect is not large and does not appear to influence the data in the region of interest, namely the velocity profiles measured above the ramp surface. The tabulated results for the lateral and vertical velocity components show that these components are also independent of the value of U_{REF}. The largest difference observed in either V/U_{REF} or W/U_{REF} was 0.04 and most of the data agreed to within better than this value. Such results are within the accuracy of the hot-film measurements. Thus it is concluded that velocity surveys measured at a single value of U_{REF} will be representative of all wind velocities. The value of U_{REF} selected to be used for the major portion of the flow field surveys was approximately 19.5 feet per second or a tunnel reference velocity U_∞ = 35.5 feet per second (See Section 5.1).

5.5 WIND PATTERNS ABOVE TRESTLE TEST STAND AND RAMP

Following the flow visualization studies and preliminary velocity surveys, quantitative measurements of the mean velocity components were made for each of twelve wind directions. Since the major axis of the ramp on the TRESTLE facility lies parallel to a direction 25 degrees from north (i.e.,

335 degrees), the twelve wind directions tested were 335, 005, 035, 065, 095, 125, 155, 185, 215, 245, 275, and 305 degrees. For each wind direction, vertical traverses were made at the 58 grid points shown in Figure 24. Each traverse consisted of measuring the longitudinal, U, lateral, V, and vertical, W, mean velocity components at five different heights. The heights used for each traverse were 0.25, 0.45, 0.75, 1.15, and 1.65 inches above the surface of the TRESTLE model platform. This corresponds to full-scale heights of 10, 18,30, 46, and 66 feet. The lowest height was governed by the minimum safe distance that the hot-film probe could approach the TRESTLE model platform. The maximum height (66 feet or 20.1 meters full-scale) was chosen to correspond to the 20 meter height called for in the specifications for this program.

The mean velocity components were measured in a wind-axis or tunnel axis coordinate system. A sample of the results is shown in Figure 30, a through e, for a wind direction of 275 degrees. Each part of this figure (a through e) shows the velocities measured at a different height, Z, above the test stand and ramp surface. The wind direction is listed numerically and also shown by an arrow at the bottom of the page. The mean velocities at each station are listed in a vertical column with three numbers. The numbers are in order from the top, the mean horizontal component, U, in the wind direction (positive in the direction of the arrow), the mean horizontal component, V, perpendicular to the wind direction (positive to the left when looking in the direction of the arrow), and the mean vertical component, W, (positive upwards). Each component has been normalized by the mean wind velocity, U_{REF}, at the meteorological station at a height 10 meters above local ground level. A complete set of data for all wind directions is presented in Appendix B.

The velocity components shown in Figure 30 can be compared to the flow visualization results presented in Section 5.2 and Figure 21 for this wind direction. The flow visualization study indicated that there was an upwash just upwind of the TRESTLE ramp and test stand and a downwash after the flow has partially crossed the ramp or test stand. The downwash was most evident

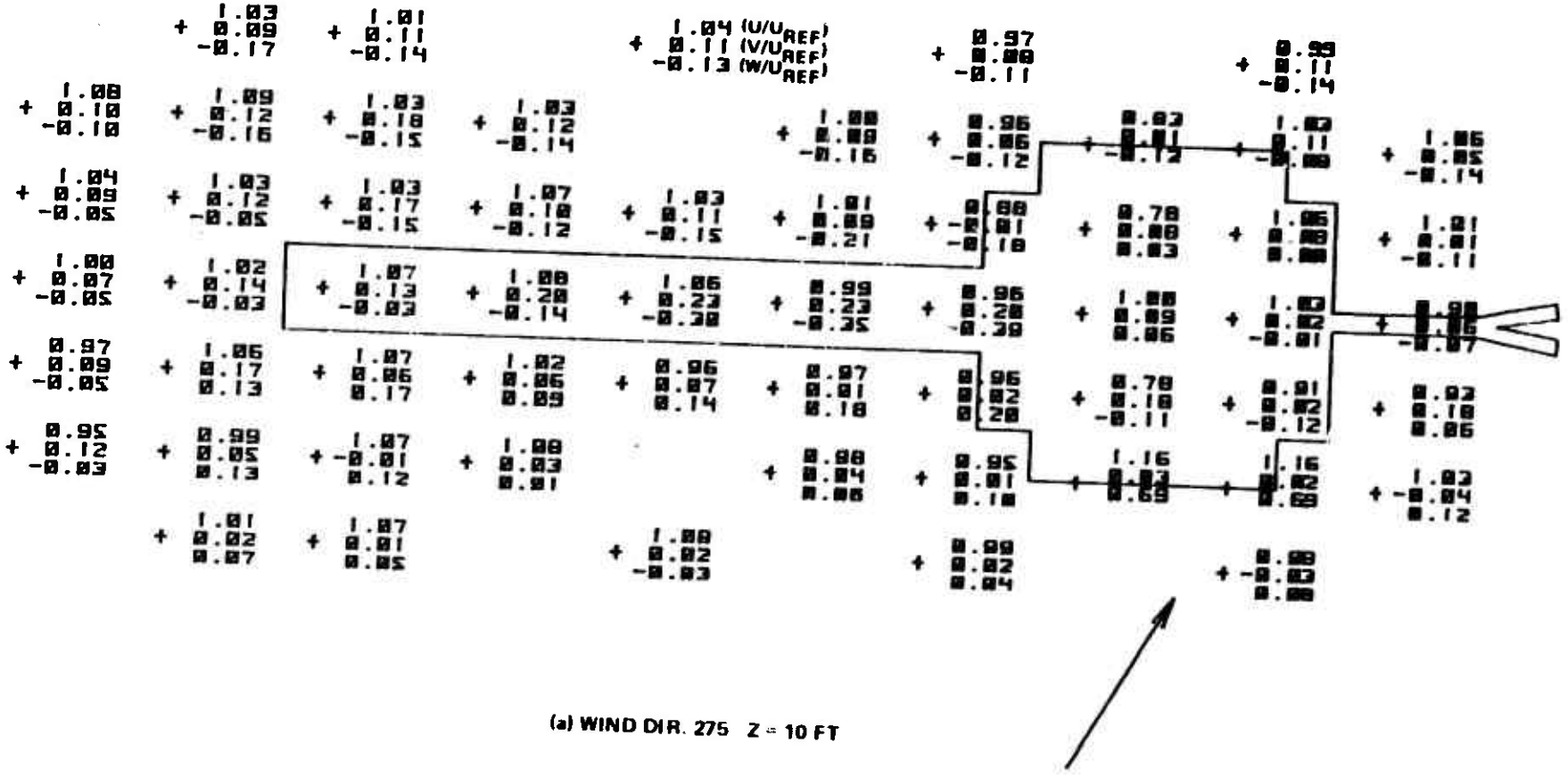

(a) WIND DIR. 275 Z = 10 FT

Figure 30. Mean Velocity Components Above TRESTLE Program (Wind Axis Coordinates)

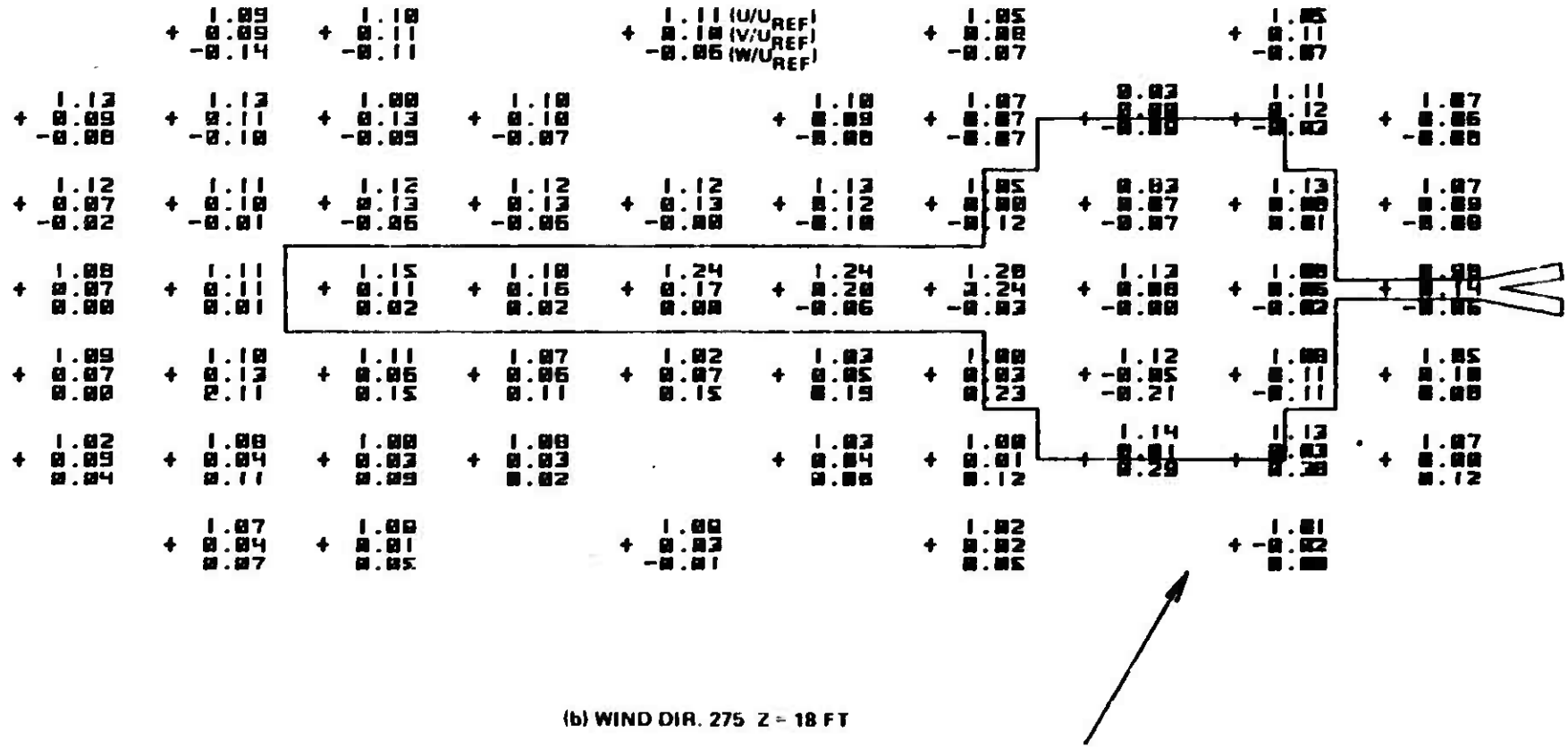

(b) WIND DIR. 275 Z = 18 FT

Figure 30. (Cont.) Mean Velocity Components Above TRESTLE Platform (Wind Axis Coordinates)

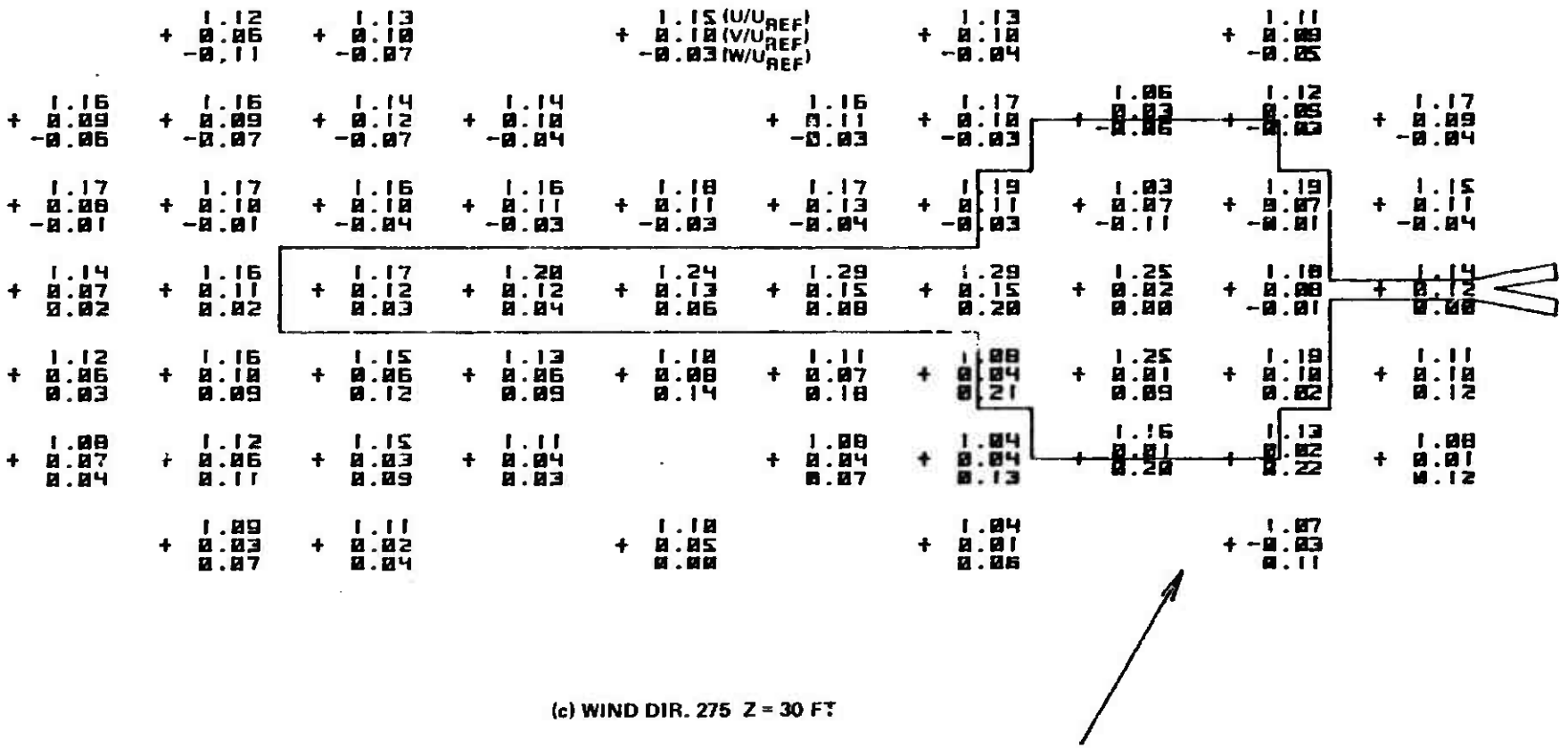

(c) WIND DIR. 275 Z = 30 FT

Figure 30. (Cont.) Mean Velocity Components Above TRESTLE Platform (Wind Axis Coordinates)

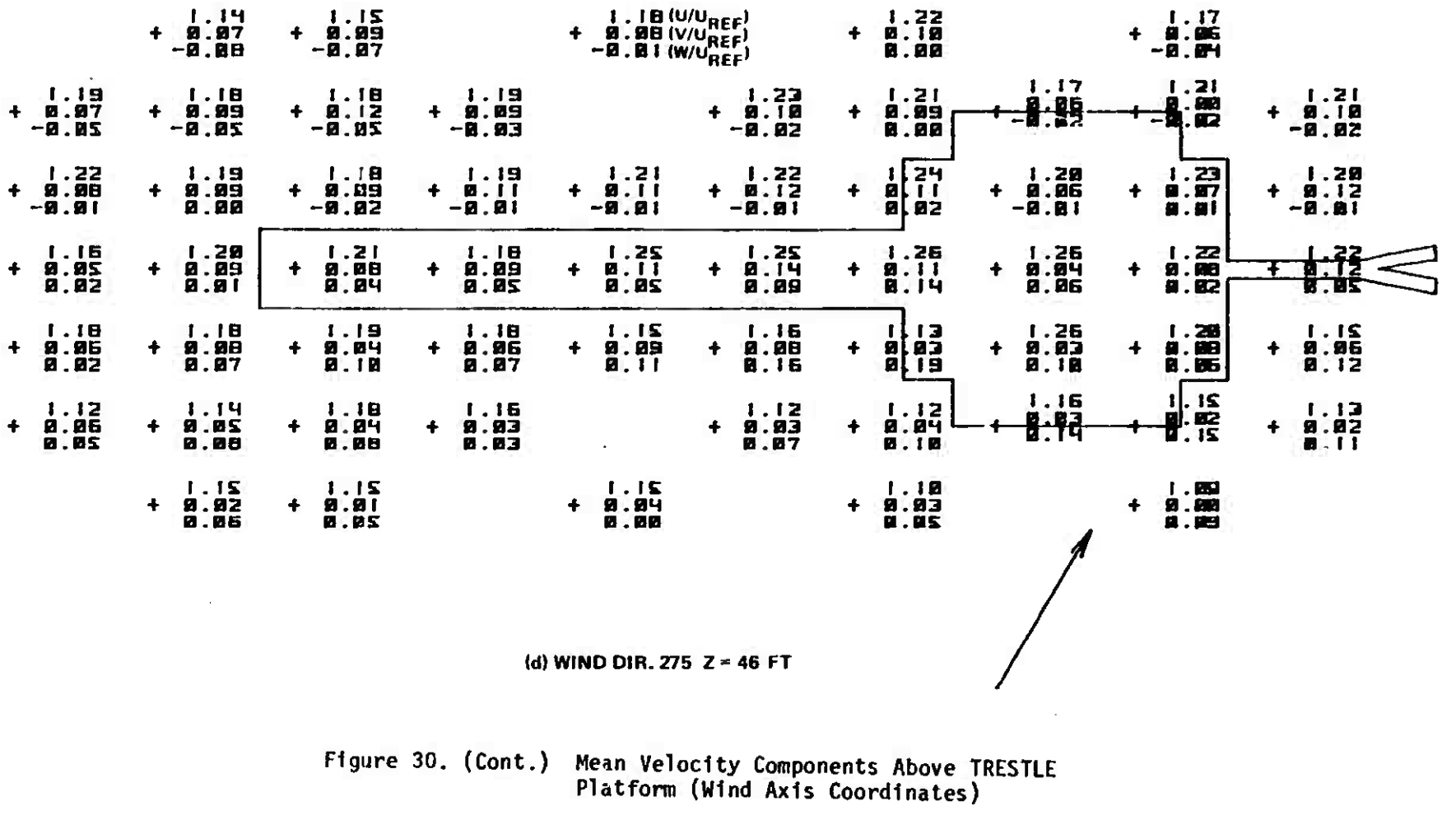

(d) WIND DIR. 275 Z = 46 FT

Figure 30. (Cont.) Mean Velocity Components Above TRESTLE Platform (Wind Axis Coordinates)

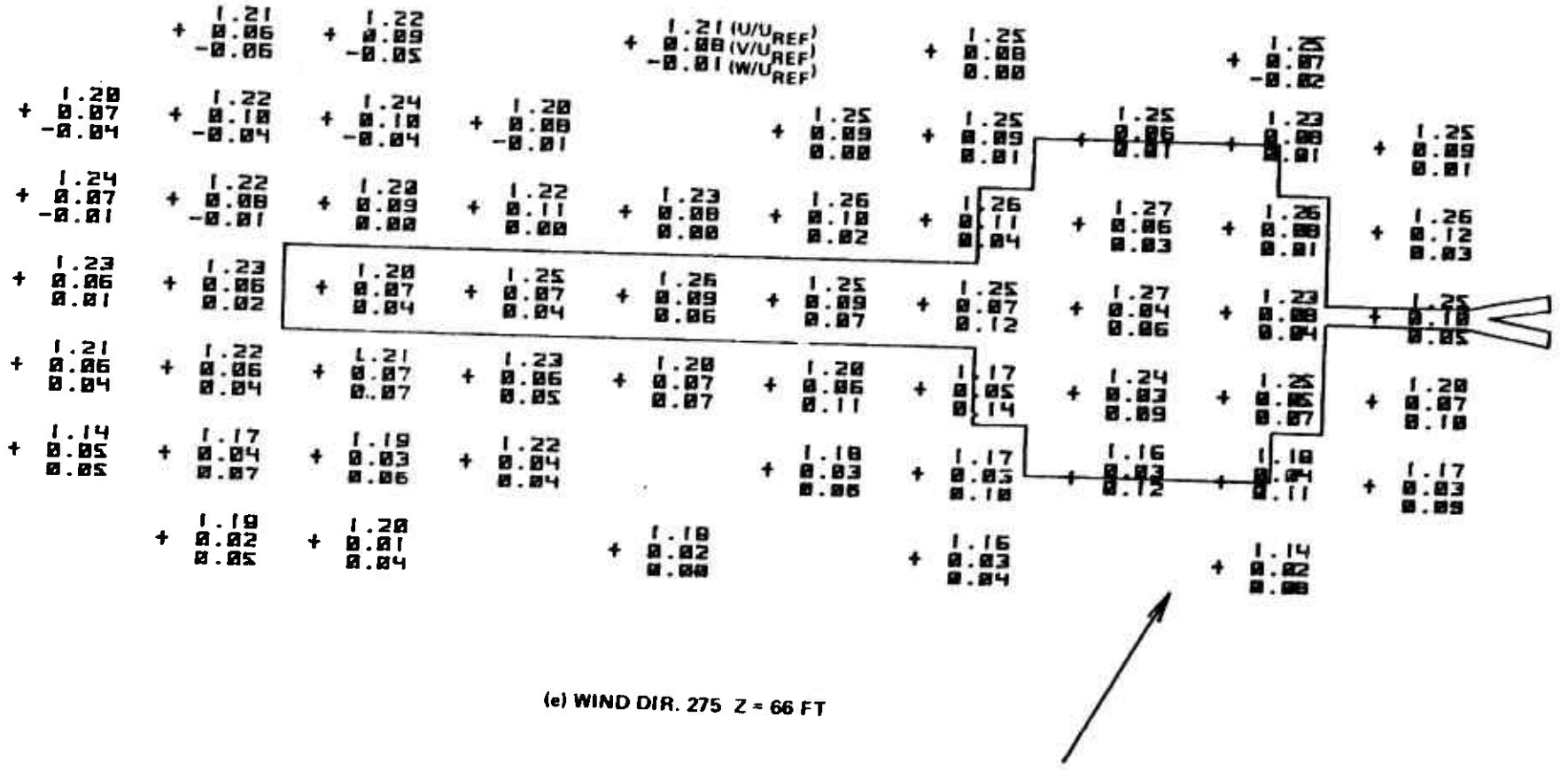

(e) WIND DIR. 275 Z = 66 FT

Figure 30. (Cont.) Mean Velocity Components Above TRESTLE Platform (Wind Axis Coordinates)

at low heights near the juncture between the ramp and test stand. Inspection of Figure 30 provides similar results on a numerical basis. There is a general upwash field upwind of the ramp and test stand which intensifies as the ramp or test stand is approached. Moreover, there is a downwash field at low heights after the upstream edge of the platform has been traversed by the flow. The largest downwash occurs at a height of 10 feet (Figure 30(a)) in the vicinity of the juncture between the ramp and test stand. There were other similarities between the smoke pictures and the numerical results. For instance, with a wind direction of 155 degrees, the numerical data confirmed the presence of an upwash near the juncture between the ramp and downstream edge of the excavation.

In addition to similarities between the smoke and quantitative results, the latter provided information not apparent from the smoke studies. One such result is the acceleration of the flow as it crosses the ramp and test stand. This is most apparent in Figures 30, b through e where the normalized longitudinal, U, component of velocity increased by as much as 20 percent as it crossed the ramp centerline. Similar accelerations were observed for other wind directions with the flow approaching from either side of the ramp centerline. Such accelerations are important in determining the side forces on the tail and fuselage of aircraft situated on the ramp and test stand. Moreover, the unsymmetrical upwash and downwash fields play a major role in determining rolling moments on the aircraft.

As noted in the next section, the mean velocity components measured in the wind axis coordinate system were converted to components (U_x, U_y, U_z) parallel to the TRESTLE axis system (X, Y, Z) shown in Figure 24. A set of crossflow velocity vectors, $U_{y,z}$, were prepared to aid in visualizing the flow field above the TRESTLE platform. A sample of computer plots of these vectors is presented in Figure 31 for a wind direction of 275 degrees. A complete set of crossflow plots for all wind directions is presented in Appendix C.

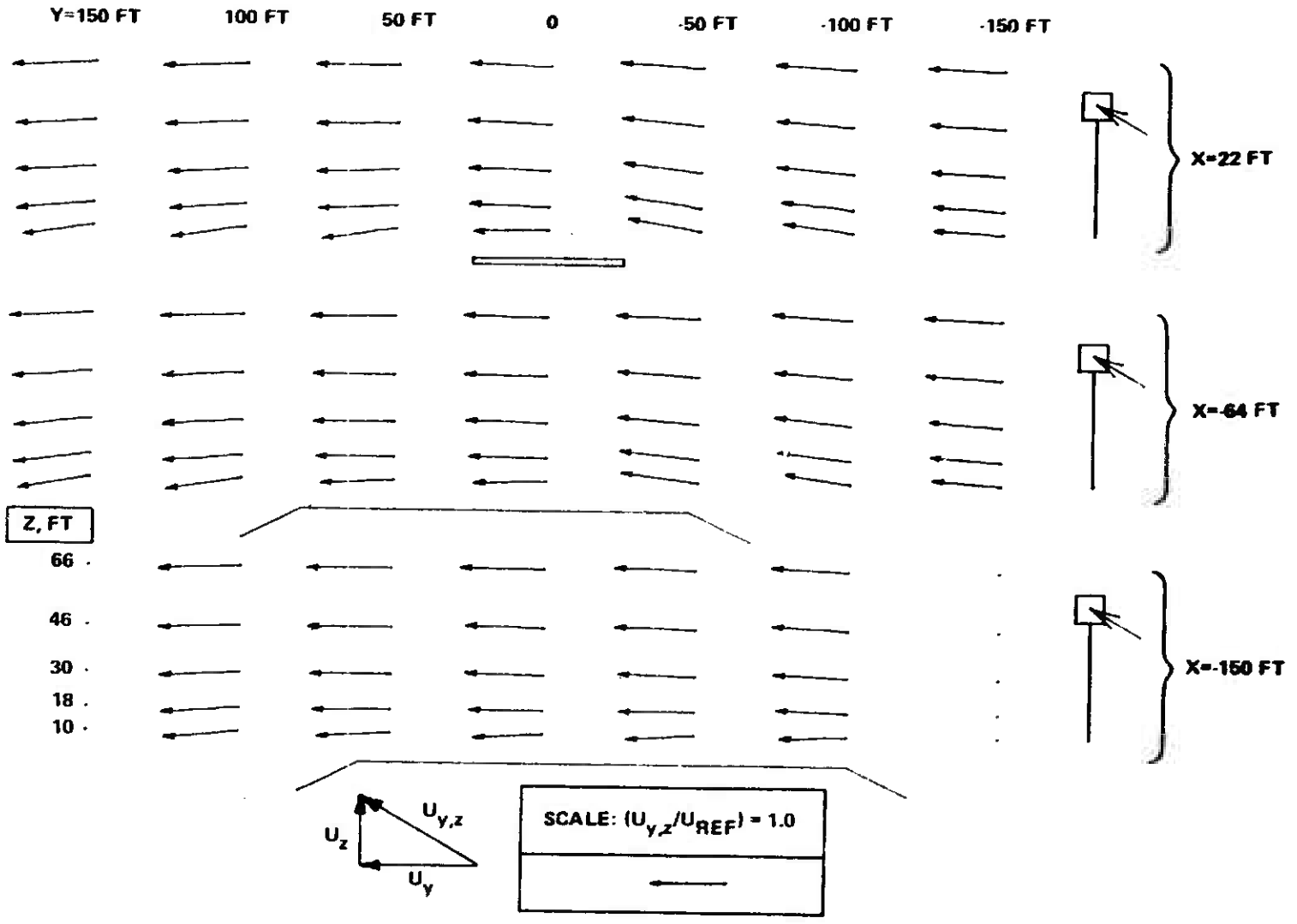

Figure 31. Mean Crossflow Velocity Vectors, $U_{y,z}$, in Vertical Planes Above TRESTLE Platform, 275 Degrees Wind.

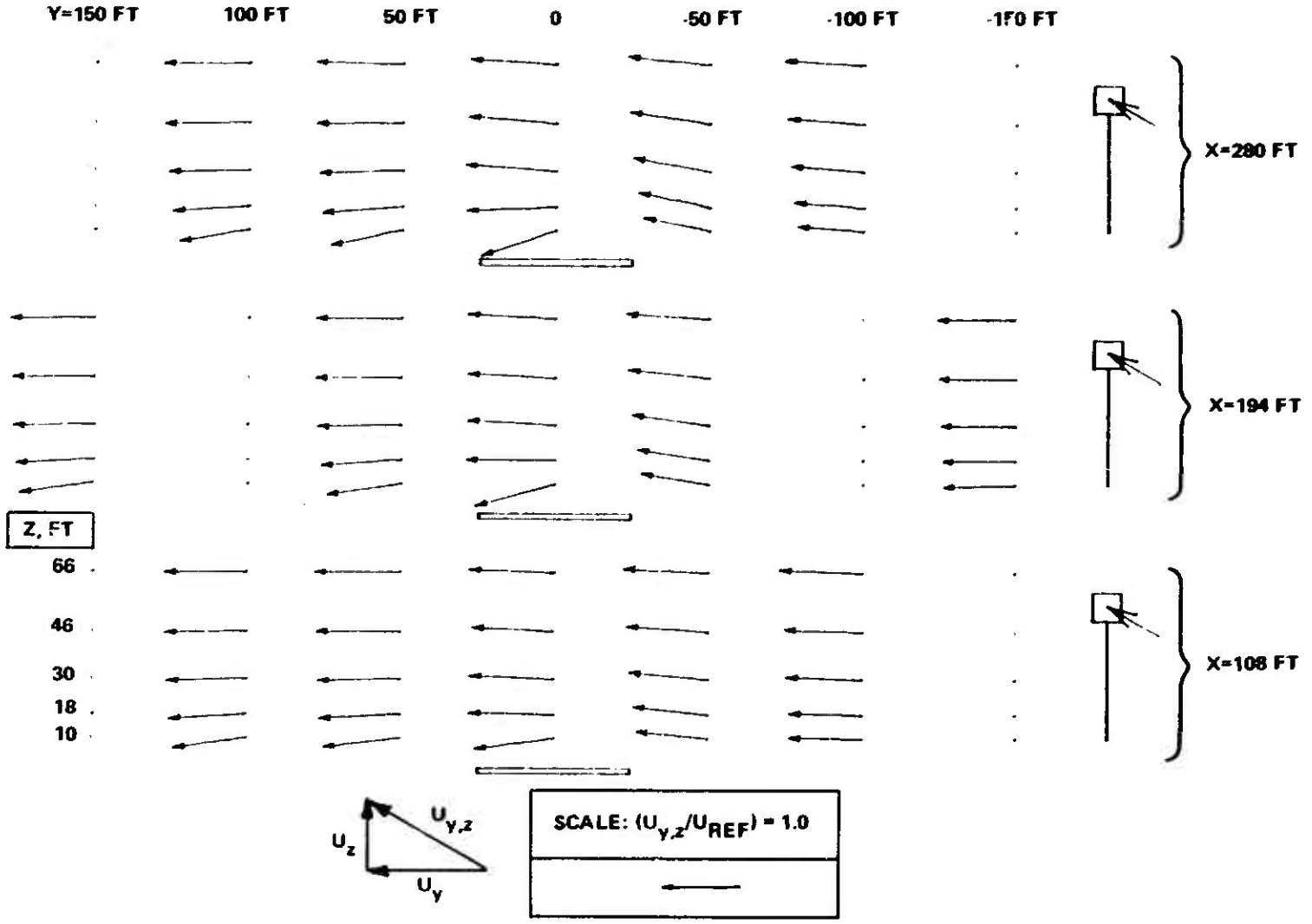

Figure 31. (Cont) Mean Crossflow Velocity Vectors, $U_{y,z}$, in Vertical Planes Above TRESTLE Platform, 275 Degree Wind

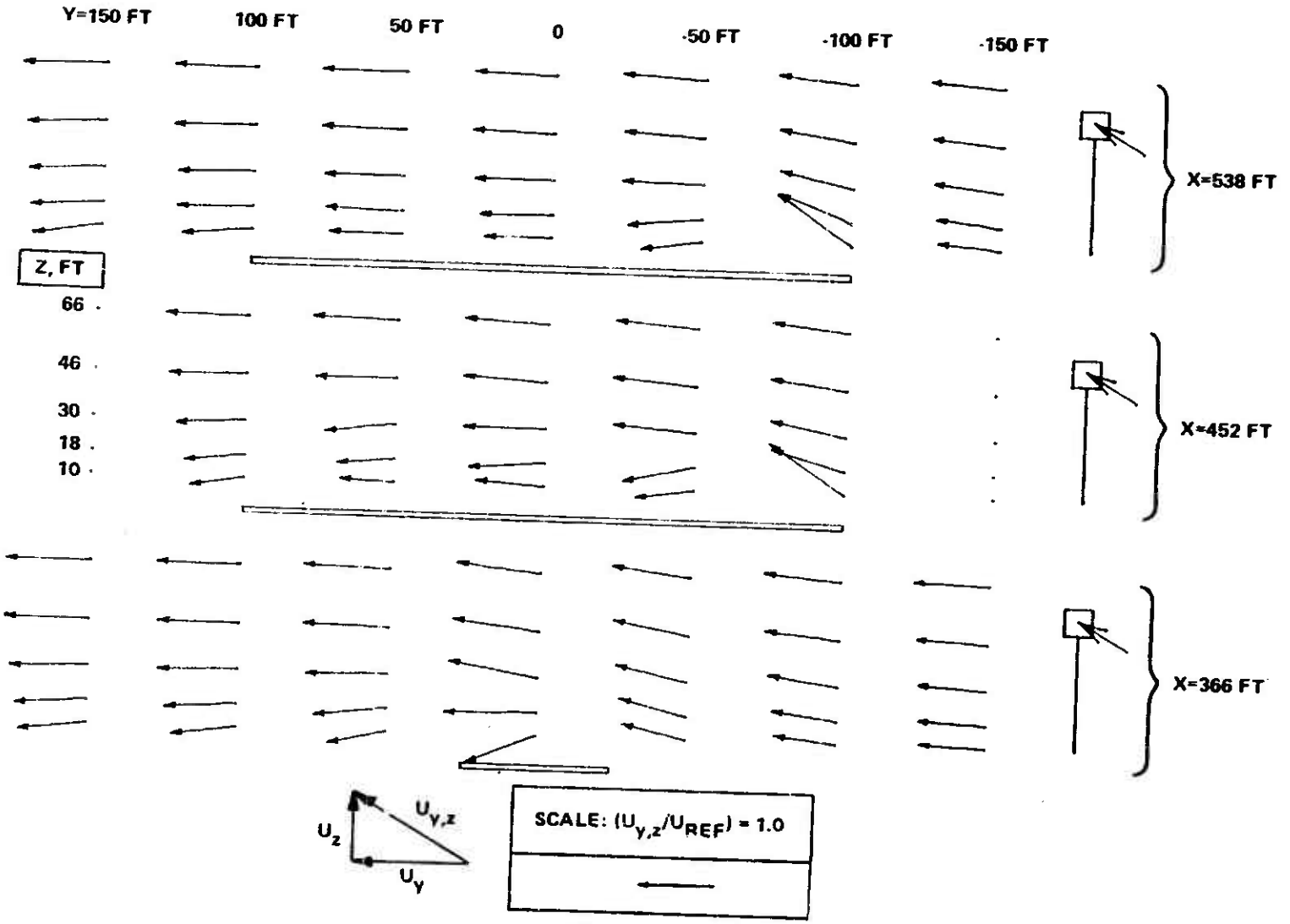

Figure 31. (Cont.) Mean Crossflow Velocity Vectors, $U_{y,z}$, in Vertical Planes Above TRESTLE Platform, 275 Degrees Wind.

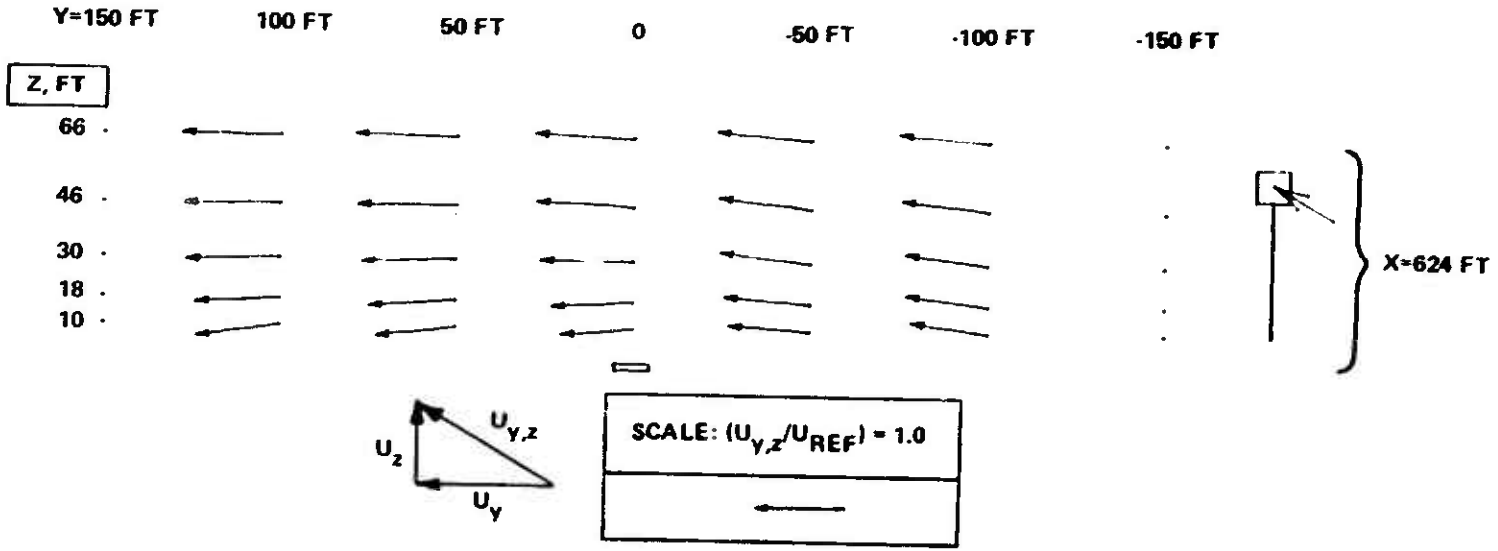

Figure 31. (Cont.) Mean Crossflow Velocity Vectors, $U_{y,z}$, in Vertical Planes Above TRESTLE Platform, 275 Degree Wind.

In Figure 31 (and Appendix C), each vector $U_{y,z}$ is composed of the lateral wind velocity, U_y, and the vertical wind velocity, U_z. The axial wind component, U_x, along the TRESTLE axis is not shown in these plots. Figure 31 contains 10 different plots showing the velocity vectors in vertical planes at the ten axial, (X), locations which were tested. The appropriate vertical cross-section of the test stand, ramp, or local ground contour is shown schematically below each plot. The wind direction (275 degrees) is listed on each page of Figure 31 and is also shown schematically beside each of the ten vertical planes. All velocity vectors have been normalized by the 10 meter reference velocity, U_{REF}. A velocity scale showing $U_{y,z}/U_{REF} = 1$ is provided on each page of Figure 31.

Figure 31 displays visually the upwash and downwash fields noted in the discussion of Figure 30. The vector plot for X = 366 feet is at the measuring location closest to the juncture between the ramp and test stand. For this value of X, note the gradually increasing upwash at low levels as the wind approaches the ramp followed by a relatively large downwash over the ramp centerline at Z = 10 feet. There is also a small downwash at Z = 10 feet after the flow has crossed the ramp. At the upstream edge of the test stand (X = 452 and 558 feet, Y = -100 feet) there is a very large upwash right at the test stand edge followed by a downwash at Y = -50 feet. It is believed that the results obtained at the upstream edge of the test stand indicate the presence of a bubble of separated flow at the edge of the ramp which reattaches a short distance downwind. Similar results were obtained for most of the other cross-wind vector plots (See Appendix C) when the wind was not parallel to the ramp centerline.

A general inspection of all the cross-wind vector plots showed that the cross-wind flows were highly nonuniform for wind directions which were not parallel to the ramp centerline. These nonuniform flow results were used in the computer program to predict the forces on aircraft situated on the ramp and test stand of the TRESTLE facility. In addition, the velocity data indicated the presence of nonuniform flows over the access road at the entry end of the TRESTLE ramp. Thus the forces on aircraft situated on this access road

were included in the computer force analysis. The aircraft force analysis and its results are presented in the next section.

6. AIRCRAFT FORCE ANALYSIS

6.1 GENERAL DESCRIPTION

Aircraft being towed onto and tested on the TRESTLE facility are subject to a variety of unconventional wind loads. It was considered unlikely that lift-off would occur since this would require wind velocities approaching take-off speed of the aircraft (generally in excess of 100 knots). However it was considered possible that the wind might produce forces that could not be completely reacted by the aircraft landing gear or towing vehicle. This situation could cause sliding, tilting or weather-vaning motions of the aircraft and result in damage to either the aircraft or TRESTLE facility.

A computer program was developed to determine the reactions between the aircraft landing gear and the TRESTLE facility for various wind conditions and various aircraft positions on the facility. The aircraft are considered stationary on the facility and the analysis used is steady state in the sense that dynamic effects that might be imposed by runway roughness or high frequency wind turbulence have not been considered. The program is essentially broken into two parts. The first part of the program takes the wind velocity field as measured in the wind tunnel tests and uses a strip theory approach to estimate the aerodynamic forces and moments acting upon the aircraft. In the second portion of the program these aerodynamic forces and moments are used as inputs to a statics problem and the required reactions between the landing gear and the facility are determined. The computer program was designed to handle the three aircraft of primary interest in this study; namely the E-3, E-4 and B-52. However, the computer program is sufficiently general that it will handle a number of other aircraft that are of the same generic shape as those mentioned. (Only the appropriate aircraft geometry is needed as input).

The minimum wind speed at which a gear slips or tends to lift at any position on the ramp has been taken as the maximum safe wind speed for

operating the aircraft on the ramp for a given wind direction. It was found that under the conditions investigated the axial force on the aircraft never exceeded the capabilities of the towing tugs. It may be possible for one gear to slide or lift and no motion of the aircraft result because the remaining gears can take up the load without sliding or lifting. However these possibilities have not been analyzed. It was felt that basing the safe criteria on the lifting or slipping of a single gear provides a conservative estimate of the safe operating speed.

The remainder of this section will describe the two portions of this program in more detail.

6.2 AERODYNAMIC FORCES AND MOMENTS

An aerodynamic strip theory approach was chosen as the most practical approach to handle the non-uniform flow and large angles of side slip and angles of attack that are presented to an aircraft sitting on the TRESTLE facility. The analysis is refined to the extent that the major geometrical features of the aircraft such as wing planform area and sweep may be distinguished, but minor geometrical features such as the specific airfoil section of the wing are not distinguishable. A quasi-two-dimensional strip theory was used wherein the flow over an aircraft geometrical component was broken into components normal to and parallel to the major axis of each component. For the flow normal to each component, the aerodynamic forces upon an elemental strip or slice of the component is assumed to be that force that acts upon an infinite cylinder of the same cross-sectional shape as the slice, and which is immersed in a stream with the local properties as measured in the wind tunnel tests. These slices are taken perpendicular to the major axis of each component such as the fuselage longitudinal axis or the wing quarter chord line. The sectional forces were taken from two-dimensional experimental data. For the flow along the major axis of each component, slender-wing or slender-body theory was used, as appropriate, to estimate the forces. The forces on a component were then due to both the flow normal to and parallel to its major

axis. Integration of these forces over all the aircraft components and proper resolution of these forces lead to an estimate of the total forces and moments on each aircraft.

The major components of the aircraft considered in this analysis were the fuselage, wings, vertical tail, horizontal tail and the radome pod and its supporting strut for the E-3 aircraft. The engines and their nacelles were not considered in the analysis. Each of the major aircraft components will be discussed in more detail subsequently, but first the various axis systems used in the analysis will be discussed.

There are two axis systems employed in the analysis. The first axis system used is the wind tunnel axis system. All of the wind velocity data measured in the wind tunnel were recorded in this system. This system has been discussed previously in this report. The second axis system used is the TRESTLE axis system. This axis system is fixed to the facility and is depicted in the following sketch:

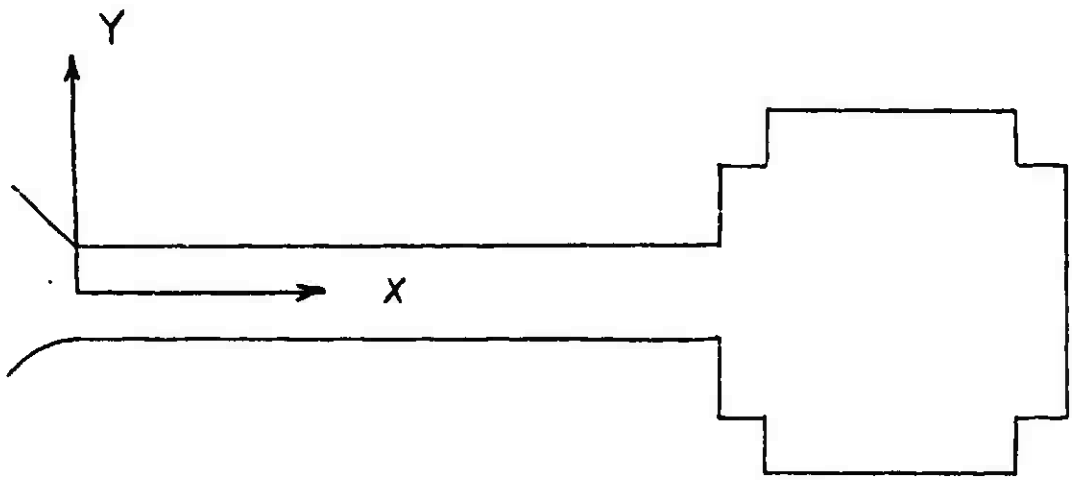

The Z axis is positive in the upward direction. The forces on the aircraft are resolved parallel to these X,Y,Z axes. The rolling moments on the aircraft are calculated with respect to the fuselage center line. The pitching and yawing moments are calculated with respect to the nose of the aircraft. The sign convention for forces and moments on the aircraft are, however, chosen with respect to the aircraft according to the following rules:

- A positive axial force points towards the nose of the aircraft.
- A positive normal force points upwards.
- A positive side force points out the left wing.
- A positive rolling moment tends to depress the right wing.
- A positive yawing moment tends to move the right wing back.
- A positive pitching moment tends to raise the tail.

The velocity measurements in the wind tunnel axis system are normalized by the reference velocity taken at the 10 meter height on the meteorological tower. The data at the five heights and fifty-eight stations are then resolved into the TRESTLE axis system and stored in the program once and for all. Linear interpolation is used to obtain the velocity at the local stations required on the aircraft.

For ease of analysis the fuselage was broken into three segments. It was assumed that the fuselage could be divided into a nose section, a cylindrical mid section and an afterbody section. Each section is assumed to be circular in cross sectional shape and the nose and afterbody are also assumed to be half an ellipsoid of revolution. The length of each fuselage section for a particular airplane is chosen by inspecting the three view drawings of the aircraft. Each portion of the fuselage is assumed to see a uniform flow under the conditions that exist at the centroid of each portion.

The normal force and side force on the nose and afterbody are assumed to be composed of two components. The first is a potential flow part that is estimated from slender body theory as $2 \sin\alpha \cos\alpha S_q$ where S is the cross-sectional area of the body, α the local angle of attack and q is the dynamic pressure. The values used for q and α are those that exist at the centroid of each component. This force is only applied when the component sees a head wind. That is for the conventional case when the fuselage nose is pointed into the wind, the nose would experience this force but the afterbody would not. The second component of force experienced by each fuselage component is the cross flow drag force and is equal to $C_{D_c} q_n A_n$. Here A_n is the side area of the component in the direction under consideration, q_n is the dynamic pressure based upon the velocity normal to the component and C_{D_C} is the cross flow drag coefficient taken to be equal to 1.2 for the present calculations. This is essentially the drag coefficient for a circular cylinder. For purposes of calculating moments the forces are assumed to act at the centroid of each fuselage component. The fuselage also experiences an axial force due to the component of flow along the axis. This force has been estimated using an empirical expression given in Reference 7

$$F_A = C_F \left\{ 3\frac{\ell}{d} + \frac{4.5}{(\ell/d)^{1/2}} + \frac{21}{(\ell/d)^2} \right\} q_A A_F$$

Where F_A is the axial force, ℓ is the fuselage length, d the fuselage diameter, q_A the dynamic pressure based upon the axial velocity component, A_F is the maximum cross section area of the fuselage and C_F is the skin friction coefficient taken as .003 for the present work.

Each wing is divided into three panels. The velocity at the centroid of each panel is resolved into components perpendicular and parallel to the quarter chord of the wing. For the two inboard panels on each wing the flow normal to the quarter chord is assumed to be two dimensional. The angle of

---

7. Hoerner, S.F. Fluid Dynamic Drag Published by the author 1965

attack of each panel is calculated from the velocity normal to the leading edge and the Z component of velocity at the centroid of each panel. The lift coefficient and drag coefficient of each panel is then taken to be that of an NACA 0012 airfoil as given in Reference 8. This airfoil section was used since it is the only section that has been tested through the complete angle of attack range and this airfoil is not too different from those used on the actual aircraft. The lift coefficient and drag coefficient as a function of angle of attack for this airfoil have been built into the computer program. The angle of attack for the wing tip panels is calculated in the same fashion as the other two panels, however the tip panel is assumed to have an elliptic load variation falling to no load at the tip. In addition to these quasi-two dimensional forces the flow normal to the quarter chord line is assumed to produce an induced drag. The induced drag is generated by the trailing vortex system produced by the wing. In the model used the wing trails a discrete vortex at the juncture of the wing panels and a continuous sheet from the elliptically loaded tips. The induced drag contribution appropriate for this model has been added to the forces on the wing. The forces produced by the flow normal to the quarter chord are assumed to act at the quarter chord of the wing when the normal flow is from leading edge to trailing edge. When the flow is from trailing edge to leading edge the forces are assumed to act at the half chord. This assumption appears consistent with the moment data of Reference 8. When the wing tip is pointing into the wind the wing will appear to have a very low aspect ratio and a semi empirical slender wing theory has been used to estimate the normal force on the wing due to the spanwise flow. An average angle of attack for the wing in the spanwise direction is calculated from the spanwise flow component and Z component of velocity at the centroid of each wing panel. The normal force due to the spanwise flow is estimated as

$$\frac{\pi AR_s}{2} \sin\alpha\,(1+2\sin\alpha)\,q_s A_w$$ where AR_s is the wing aspect

---

8. Critzos, C, Heyson, H. and Boswinkle, R "Aerodynamic Characteristics of NACA 0012 Airfoil Section At Angles of Attack From 0° to 180°" NACA TN 3361, January 1955

ratio viewed from the spanwise direction, α is the average angle of attack, q_s is the dynamic pressure based upon the spanwise velocity component and A_W is the wing area. The lift from the spanwise flow is neglected when the fuselage is upstream of the wing under consideration as this would effectively block the spanwise flow along the wing.

Each side of the horizontal tail is treated as a single panel. The flow over each panel is broken into components normal to and parallel to the quarter chord line of each panel. The spanwise flow on each panel is treated as in the case for the wing. For the normal component of flow over each panel the angle of attack is also computed as in the case for the wing and the data for the NACA 0012 airfoil built into the program are used at this angle of attack. However a finite aspect ratio correction as given in Reference 9 was applied to the lift and drag coefficients and is given by the following expression

$$C_\ell = \frac{C_{\ell_o}}{1 + \frac{2}{AR_T}}$$

$$C_{D_i} = C_{D_o} + \frac{C_\ell^2}{\pi AR_T}$$

Here C_{ℓ_o} is the two dimensional lift coefficient, AR_T is the aspect ratio as viewed from normal to the quarter chord, and C_{D_o} is the two dimensional drag coefficient.

The vertical tail was treated as a half wing mounted on a reflection plane. The wind tunnel tests showed that there was generally a very small W component of velocity at the vertical tail centroid. Therefore this component was neglected. The lift coefficient on the tail is calculated according to following formula taken from Nicolai[9]

---

9. Nicolai, L.M. Fundamentals of Aircraft Design METS Inc. Xenia, Ohio, 1975

$$C_L = \frac{C_{l_o}}{1 + \frac{2}{ARVT}} \sqrt{\cos \Lambda_{VT}}$$

where C_{l_o} is the two dimensional lift coefficient (taken from NACA 0012 data), ARVT is the aspect ratio of the vertical tail and Λ_{VT} is the sweep of the quarter chord line. The drag coefficient is

$$C_D = C_{D_o} + \frac{C_L^2}{\pi\, ARVT}$$

where C_{D_o} is the two dimensional value.

The E-3 aircraft has a large circular radome attached to the fuselage by a pair of struts. For ease of analysis only a single strut on the fuselage centerline is considered. This strut is treated as one of the wing panels and is assumed to act in a strictly two dimensional fashion since it is end plated by the fuselage and the radome. The radome is treated as a circular planform wing. The local velocities for computing the forces on the radome are taken as those at its center. The following expressions for lift and drag coefficient for the pod were used:

$$C_l = 1.8 \sin\alpha \,(1 + 2\,|\sin\alpha|)\cos\alpha$$

$$C_d = 2\,C_F + C_l \tan\alpha$$

Here α is the angle calculated from the local velocities, and C_F is the skin friction coefficient. In the expression for C_l the constant 1.8 factor is the theoretical lift curve slope for the potential flow about a circular planform wing as given in Reference 10.

---

10. Thwaites, B. Editor Incompressible Aerodynamics Oxford Press 1960

A compilation of the required geometrical data, the aerodynamic force and moment quantities calculated by the computer program and the symbol used for each quantity are given in Appendix D.

6.3 STATICS PROBLEM

The aerodynamic forces and moments on the aircraft are used as inputs to a statics problem. The statics problems for all of the aircraft are statically indeterminate with different degrees of redundancies dependent upon the number of landing gear. This fact has necessitated a separate analysis for each aircraft depending upon the number of landing gears. The principle of consistent deflections has been used to make the statics problems determinate. In general it has been assumed that the landing gear can supply a normal or vertical force and a side force parallel to the axle of each gear up to the frictional limit between the wheels and the ramp. A coefficient of friction of 1.0 has been assumed. Since the aircraft will generally be towed, only the gear which has a tug affixed can supply an axial force. This gives a total of 7 unknowns in the problem for the E-3, 9 unknowns in the problem for the B-S2 and 11 unknowns in the problem for the E-4. Since there are only six equations available from requiring equilibrium of the total forces and moments on the aircraft each problem is statically indeterminate. The equations required to make the problem determinate in each case are obtained by considering the elastic deflections of the aircraft and equating these deflections to zero at the appropriate landing gear locations. In order to calculate these elastic deflections the aircraft structure has been idealized to consist of beams with uniform structural properties. This assumption allows the problem to be solved without detailed knowledge of the structural stiffness of each aircraft. The analysis for each aircraft will be discussed separately.

For the case of the E-3 aircraft it is sufficient to consider the fuselage as a beam supported by the landing gear. The main gear can supply a vertical force, a lateral horizontal force and a resistance to rolling moments. The nose gear can supply a vertical force , a lateral horizontal

force and an axial horizontal force since the tug will be affixed to it. The nose gear also supplies a rolling moment proportional to its side force. The beam with its reactive forces is depicted in the following sketch.

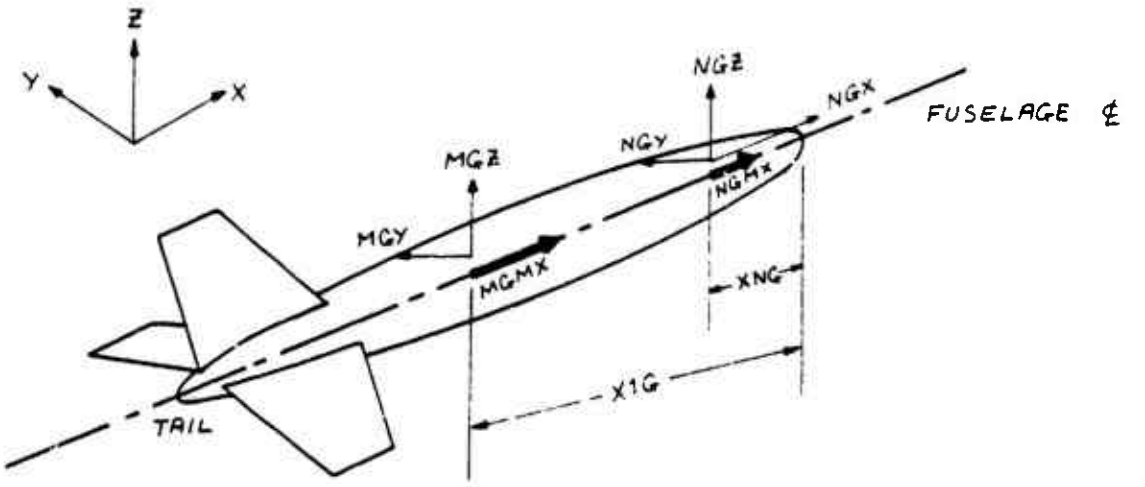

The aerodynamic forces applied in the X, Y and Z directions are designated as FXA, FYA and FZA respectively. The applied aerodynamic rolling moment about the fuselage centerline is designated as MXA, the applied aerodynamic yawing moment about the nose is designated as MZA and the applied aerodynamic pitching moment about the nose is designated as MYA.

Requiring the equilibrumm of forces in the X, Y and Z directions respectively results in the following relations

$$FXA + NGX = 0 \tag{4}$$

$$FYA + MGY + NGY = 0 \tag{5}$$

$$FZA - W + MGZ + NGZ = 0 \tag{6}$$

where W is the aircraft weight.

Equilibrating the rolling moments about the fuselage centerline results in

$$MXA + MGMX + NGMX = 0 \tag{7}$$

where

$$NGMX = (NGY)(ZF)$$

and ZF is the height of the fuselage centerline above the ramp.

Equilibrium of pitching moments about the aircraft nose results in

$$MYA + MGZ \cdot X1G + NGZ \cdot XNG - W \cdot Xcg - NGX \cdot ZF = 0 \tag{8}$$

Equilibrium of yawing moments about the aircraft nose results in

$$MZA + NGY \cdot XNG + MGY \cdot X1G = 0 \tag{9}$$

This system of six equations may be solved directly for the six unknowns NGX, NGY, NGZ, MGZ, MGY and MGMX. This group contains the desired three components of force between the nose gear and the ramp i.e., NGX, NGY and NGZ but the forces between the main gear and the ramp are still undetermined.

The forces between the main gear and ramp have been determined by idealizing the landing gear, wing and fuselage carry through structure as the bent problem shown in the following sketch.

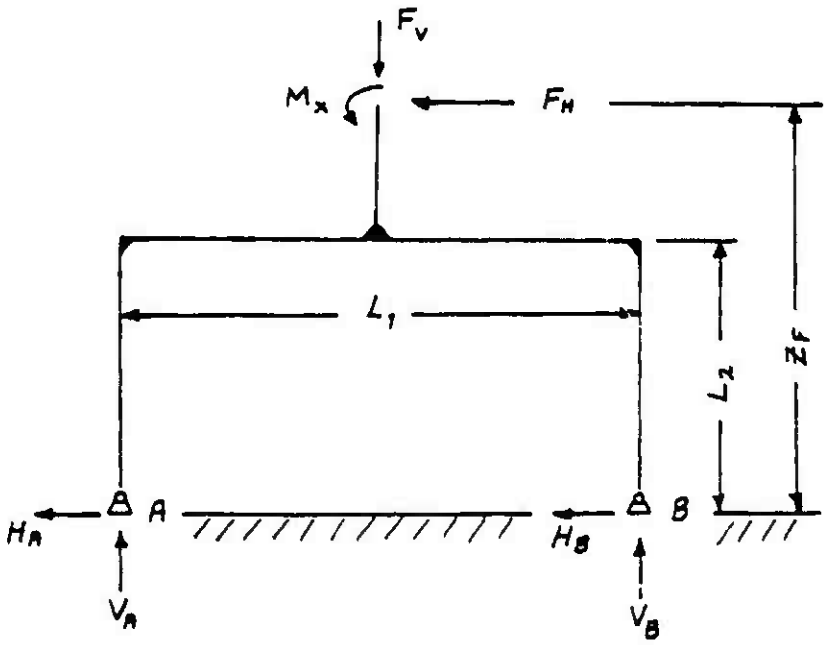

Here A represents the left gear and B the right gear. The quantities H_A and H_B are the horizontal reactions at the left and right gear respectively; V_A and V_B are the vertical reactions at the left gear and right gear respectively. The quantities F_V, F_H and M_X are related to the previously found quantities by

$$M_x = MGMX$$

$$F_v = MGZ$$

$$F_H = -MGY$$

and

$$L_1 = 2Y1G \qquad L_2 = L1G$$

The supports at A and B are assumed pinned and all other joints of the bent are assumed rigid. The members of the bent are all assumed to have the same value of EI where E is the modulus of elasticity and I is the

moment of inertia of the cross section of the beams. The horizontal and vertical reactions at A and B may be solved by requiring equilibrium of the total forces and moments on the bent and by requiring no deflection of point A relative to point B. The results are

$$V_B = \frac{1}{L_1}\left\{F_V \frac{L_1}{2} - \left[M_x + F_H (zF - L_2)\right] - F_H \cdot L_2\right\} \tag{10}$$

$$V_A = F_V - V_B \tag{11}$$

$$H_A = \frac{1}{\frac{2}{3}L_2^3 + L_1 L_2^2}\left\{L_2\left[\frac{L_1}{2}\left[M_x + F_H(zF - L_2)\right] - \frac{1}{2}V_A L_1^2 + F_V \frac{L_1^2}{8}\right]\right.$$
$$\left. + L_2^2\left[\frac{F_H L_2}{6} + \frac{F_V L_1}{4} - \frac{V_A L_1}{2} + \frac{1}{2}\left[M_x + F_H(zF - L_2)\right]\right]\right\} \tag{12}$$

$$H_B = -H_A - F_H \tag{13}$$

A gear lifts when the vertical reaction becomes negative and a gear slides when

$$\frac{|H_A|}{V_A}, \frac{|H_B|}{V_B} > 1$$

Now all of the required gear reactions for the E-3 can be calculated from the foregoing equations.

For the case of the B-52 the overall procedure for solving the problem is similar with the exception that one more relation must be developed by considering the elastic deformation of the aircraft. The fuselage supported by the landing gear is again considered first. The beam representing the fuselage with the reaction forces applied is shown in the following sketch

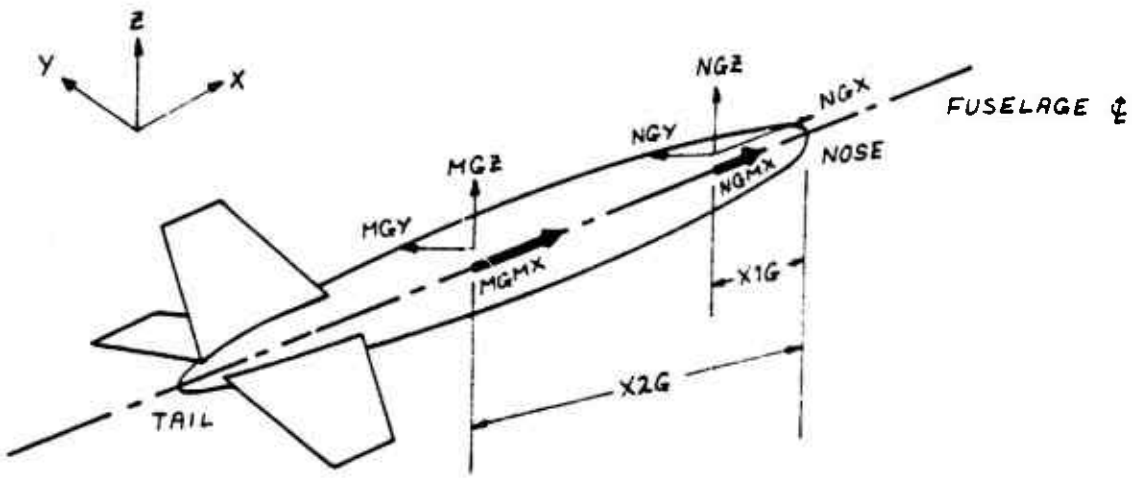

However now NGMX, the reactive moment supplied by the front pair of landing gear, is an unknown. This unknown is determined by considering the torsional deflection of the fuselage. It is assumed that both sets of landing gear will not allow torsional rotation of the beam (fuselage). The torsional loads on the fuselage are shown in the following sketch.

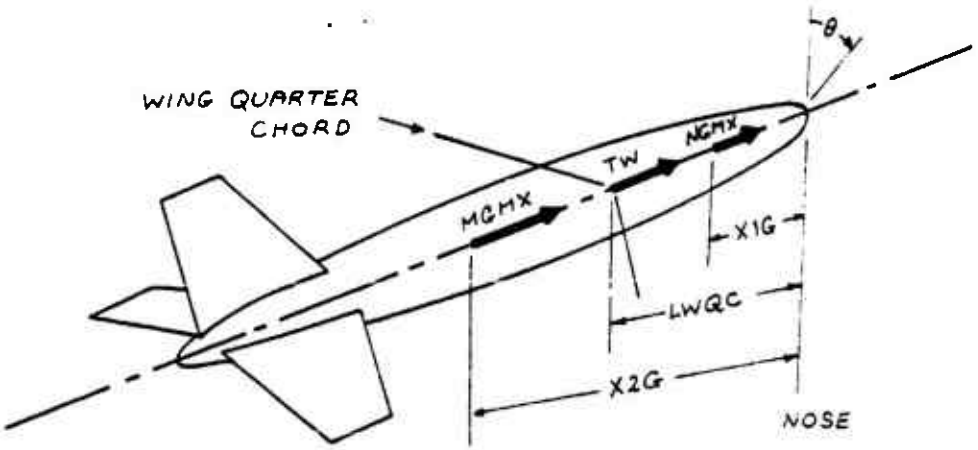

Here LWQC is the distance of the wing quarter chord line at the wing root from the nose and TW is the rolling moment applied to the fuselage by the wing (known from the aerodynamic portion of the analysis). The torsional moments applied by the tail are not shown in this sketch since they are not

required for the present purposes. Assuming that the second pair of main gear does not allow torsional rotation and the fuselage has uniform structural properties the angular rotation at the first set of gear θ_{x1G} may be expressed as

$$\theta_{x1G} = \frac{1}{JG}\left\{TW\,(X2G - LWQC) + NGMX\,(X2G - X1G)\right\}$$

where G is the shearing modulus and J is the polar moment of inertia of the fuselage. Then if no rotation is alloweu at X1G we have

$$NGMX = -TW\,\frac{(X2G - LWQC)}{(X2G - X1G)} \tag{14}$$

Equilibrium of overall forces and moments on the fuselage result in a set of six equations similar to the case for the E-3 namely:

$$FXA + NGX = 0 \tag{15}$$

$$FYA + MGY + NGY = 0 \tag{16}$$

$$FZA - W + MGZ + NGZ = 0 \tag{17}$$

$$MXA + MGMX + NGMX = 0 \tag{18}$$

$$MYA + MGZ \cdot X2G + NGZ \cdot X1G - W \cdot XCG - NGX \cdot ZF = 0 \tag{19}$$

$$MZA + NGY \cdot X1G + MGY \cdot X2G = 0 \tag{20}$$

Equations (14) through (20) are solved for the seven unknowns NGMX, MGMX, NGX, MGY, NGY, MGZ, and NGZ. The reactions between the gear and the ramp for each set of gears are found by idealizing the gear and carry through structure as a bent, similar to the case for the E-3 problem. The reactions on the front two gear are found from Equations (10) through (13) with the substitutions

$$F_v = NGZ$$

$$M_x = NGMX$$

$$F_H = -NGY$$

The reactions on the rear two gears are found from Equations (10) through (15) with the substitutions

$$F_v = MGZ$$

$$M_x = MGMX$$

$$F_H = -MGY$$

Now all of the required reactions on the B-52 gear are determined.

The statics problem for the E-4 is considerably more complicated than those for the other two aircraft. The E-4 statics problem was initially formulated along lines similar to the other two aircraft. However, this analysis led to unreasonably low predictions for the maximum safe handling speed. The reasons for this failure of the analysis were traced to the peculiar geometry of the E-4 gear and the method in which the structure was idealized. The minimum safe handling speeds on the E-4 were subsequently determined by replacing the actual 5 landing gear configuration of the aircraft with an equivalent 3 gear configuration. For the sake of completeness the original analysis will be developed along with its reasons for failing.

The E-4 statics problem requires that two more relations be developed from considerations of the elastic deformation of the aircraft than were necessary for the B-52 case. These relations were developed by considering the bending of the fuselage in the horizontal and vertical planes. The reactive forces and moments on the beam representing the fuselage are shown in the following sketch.

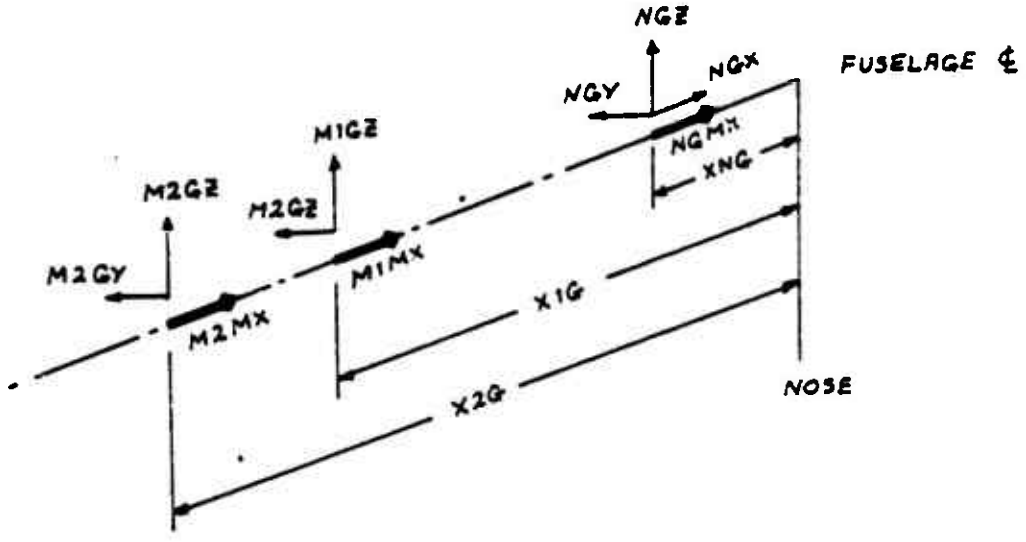

Requiring equilibrium of the overall forces and moments results in the following relations

$$FXA + NGX = 0 \tag{21}$$

$$FYA + M2GY + M1GY + NGY = 0 \tag{22}$$

$$FZA + M2GZ + M1GZ + NGZ - W = 0 \tag{23}$$

$$MXA + M2MX + M1MX + NGMX = 0 \tag{24}$$

where

$$NGMX = NGY \cdot ZF$$

$$MYA + M2GZ \cdot X2G + M1GZ \cdot X1G + NGZ \cdot XNG$$

$$- NGX \cdot ZF - W \cdot XCG = 0 \tag{25}$$

$$MZA + M2GY \cdot X2G + M1GY \cdot X1G + NGY \cdot XNG = 0 \tag{26}$$

Thus far there are nine unknowns M1GZ, M2GZ, NGZ, MZGY, M1GY, NGY, NGX, M1MX and M2MX. Consideration of fuselage torsional deflection similar

to that for the B-52 case gives the following expression for M1MX.

$$M1MX = -TW - NGY \cdot ZF \tag{27}$$

The preceding equations may now be solved directly for M2MX and NGX; also, M1GZ and M2GZ may be found in terms of NGZ, and M1GY and NGY may be found in terms of M2GY. NGZ is found by considering the bending of the fuselage in the vertical plane. The bending has been calculated by an application of Castigliano's Theorem. First the strain energy, U_v, due to vertical bending is calculated along the length of the fuselage according to

$$U_v = \frac{1}{2EI} \int_0^{LF} (M_{BV}(s))^2 \, ds$$

where M_{B_V} is the vertical bending moment. Calculation of this integral requires the distribution of the aerodynamic normal forces on the fuselage plus the wing pitching moment and normal force transmitted to the fuselage which are available from the aerodynamic analysis. Also the entire weight of the aircraft is considered concentrated at the location of the center of gravity. Since as previously noted M1GZ, and M2GZ may be expressed in terms of NGZ the strain energy, U_v, is functionally

$$U_v = U_v(NGZ)$$

Now the vertical deflection of the fuselage, δ_v, at the nose gear is

$$\delta_v = \frac{\partial U_v}{\partial (NGZ)}$$

and for no deflection, $\delta_v = 0$ gives one of the required relations.

This deflection constraint results in the following expression

$$NGZ = \frac{-N}{TD}$$

where

$$N = N_1 + N_2 + N_3 + N_4 + N_5 + N_6 + N_7 + N_8$$

$$TD = TD_1 + TD_2 + TD_3 + TD_4 + TD_5 + TD_6$$

$$TD_1 = \frac{1}{3}(s_5 - s_2)^3$$

$$TD_2 = (1 + K_2)\,[FACSK(7,2,5) - FACSK(5,2,5)]$$

$$TD_3 = \frac{-K_6}{2}\left[(s_9 - s_2)^2 - (s_7 - s_2)^2\right]$$

$$TD_4 = K_2(1 + K_2)\,FACSK(7,5,5)$$

$$TD_5 = \frac{-K_2 K_6}{2}\left[(s_9 - s_5)^2 - (s_7 - s_5)^2\right]$$

$$TD_6 = \frac{-K_4 K_6}{2}(s_9 - s_7)^2$$

$$N_1 = NL\left\{FACSS(5,1,2) + (1+K_2)\left[FACSK(7,1,5) - FACSK(5,1,5)\right] - \frac{K_6}{2}\left[(s_9 - s_1)^2 - (s_7 - s_1)^2\right]\right\}$$

$$N_2 = -FXA \cdot \frac{\Sigma F}{2}(s_3 - s_2)^2 - \frac{1}{2}(FXA \cdot \Sigma F + WPM)\left\{(s_5 - s_2)^2 - (s_3 - s_2)^2 + (1+K_2)\left[(s_7 - K_5)^2 - (s_5 - K_5)^2\right] - 2K_6(s_9 - s_7)\right\}$$

$$N_3 = NFW\left\{FACSS(5,2,3) + (1+K_2)\left[FACSK(7,3,5) - FACSK(5,3,5)\right] - \frac{K_6}{2}\left[(s_9 - s_3)^2 - (s_7 - s_3)^2\right]\right\}$$

$$N_4 = CCNF\left\{FACSS(5,2,4) + (1+K_2)\left[FACSK(7,4,5) - FACSK(5,4,5)\right] - \frac{K_6}{2}\left[(s_9 - s_4)^2 - (s_7 - s_4)^2\right]\right\}$$

$$N_5 = \frac{K_1}{K_2}\,TD_4$$

$$N_6 = -W\left\{(1+K_2)\,FACKS(7,5,6) - \frac{K_6}{2}\left[(s_9 - s_6)^2 - (s_7 - s_6)^2\right]\right\}$$

$$N_7 = \frac{K_3}{K_4} TD_6$$

$$N_8 = -ANF \cdot \frac{K_6}{2} (s_9 - s_8)^2$$

$s_1 = XNL$

$s_2 = XNG$

$s_3 = LWQC$

$s_4 = XCCNF$

$s_5 = X1G$

$s_6 = XCG$

$s_7 = X2G$

$s_8 = XANF$

$s_9 = LQCT$

$s_{10} = LQCV$

$$FACSS(I,J,L) = \frac{1}{2}\left\{s_I - s_J - \frac{1}{3}(s_I - s_L)\right\}(s_I - s_L)^2$$

$$FACSK(I,J,L) = \frac{1}{2}\left\{s_I - s_J - \frac{1}{3}(s_I - K_L)\right\}(s_I - K_L)^2$$

$$FACKS(I,J,L) = \frac{1}{2}\left\{s_I - K_J - \frac{1}{3}(s_I - s_L)\right\}(s_I - s_L)^2$$

$$K_1 = \frac{W \cdot s_6 - FXA \cdot ZF - MYA - s_7(W - FZA)}{s_5 - s_7}$$

$$K_2 = \frac{s_7 - s_2}{s_5 - s_7}$$

$$K_3 = \frac{W \cdot s_6 - FXA \cdot ZF - MYA - s_5(W - FZA)}{s_7 - s_5}$$

$$K_4 = \frac{\Delta_5 - \Delta_6}{\Delta_7 - \Delta_5}$$

$$K_5 = \frac{\Delta_2 + \Delta_5 K_2}{1 + K_2}$$

$$K_6 = (1 + K_2) K_5 + K_4 \Delta_7$$

and where NL, WPM, NFW, CCNF and ANF are aerodynamic forces or moments acting upon the aircraft components and are defined in Appendix D.

Then after NGZ is known M1GZ and M2GZ are determined by

$$M1GZ = K_1 + K_2 NGZ$$

$$M2GZ = K_3 + K_4 NGZ$$

The process for solving for M2GY is similar to that for NGZ. The bending of the fuselage in the horizontal plane is considered. The strain energy due to bending in the horizontal plane, U_H, is calculated according to

$$U_H = \frac{1}{2EI} \int_0^{LF} (M_{B_H}(s))^2 \, ds$$

where M_{B_H} is the horizontal bending moment. This is essentially an expression of the form

$$U_H = U_H(M2GY)$$

and the horizontal deflection of the fuselage at X2G is

$$\delta_H = \frac{\partial U_H}{\partial (M2GY)}$$

Requiring δ_H to be zero results in

$$M2GY = \frac{-T}{B}$$

where

$$T = T_1 + T_2 + T_3 + T_4 + T_5 + T_6 + T_7$$

$$B = B_1 + B_2 + B_3$$

$$T_1 = SF\left\{K_{10}\ FACSS(5,1,2) - FACSK(7,1,11) + FACSK(5,1,11) - \frac{K_{12}}{2}\left[(s_{10}-s_1)^2-(s_7-s_1)^2\right]\right\}$$

$$T_2 = \frac{K_9}{K_{10}}\ B_1$$

$$T_3 = -WYM\left\{\frac{K_{10}}{2}\left[(s_5-s_2)^2-(s_3-s_2)^2\right]-\frac{1}{2}\left[(s_7-K_{11})^2-(s_5-K_{11})^2\right]-K_{12}(s_{10}-s_7)\right\}$$

$$T_4 = WSF\left\{K_{10}\ FACSS(5,2,3) - FACSK(7,3,11) + FACSK(5,3,11) - \frac{K_{12}}{2}\left[(s_{10}-s_3)^2-(s_7-s_3)^2\right]\right\}$$

$$T_5 = CCSF\left\{K_{10}\ FACSS(5,2,4) - FACSK(7,4,11) + FACSK(5,4,11) - \frac{K_{12}}{2}\left[(s_{10}-s_4)^2-(s_7-s_4)^2\right]\right\}$$

$$T_6 = \frac{K_7}{K_8}\ B_2$$

$$T_7 = -ASF \cdot \frac{K_{12}}{2}\ (s_{10}-s_8)^2$$

$$B_1 = K_{10}\left\{\frac{K_{10}}{3}\ (s_5-s_2)^3 - FACSK(7,2,11) + FACSK(5,2,11) - \frac{K_{12}}{2}\left[(s_{10}-s_2)^2-(s_7-s_2)^2\right]\right\}$$

$$B_2 = -K_8\ FACKS(7,11,5) - \frac{K_8 K_{12}}{2}\left[(\Delta_{10}-\Delta_5)^2-(\Delta_7-\Delta_5)^2\right]$$

$$B_3 = -\frac{K_{12}}{2}(\Delta_{10}-\Delta_7)^2$$

$$K_7 = \frac{FYA\cdot\Delta_2 - MZA}{\Delta_5-\Delta_2}$$

$$K_8 = \frac{\Delta_2-\Delta_7}{\Delta_5-\Delta_2}$$

$$K_9 = \frac{\Delta_5\cdot FYA - MZA}{\Delta_2-\Delta_5}$$

$$K_{10} = \frac{\Delta_5-\Delta_7}{\Delta_2-\Delta_5}$$

$$K_{11} = -(\Delta_2 K_{10} + \Delta_5 K_8)$$

$$K_{12} = \Delta_7 - K_{11}$$

Here SF, WYM, WSF, CCSF and ASF are aerodynamic forces or moments acting upon the aircraft components and are defined in Appendix D. Then after M2GY is known M1GY and NGY may be determined as

$$M1GY = K_7 + K_8\cdot M2GY$$

$$NGY = K_9 + K_{10}\cdot M2GY$$

Thus far the reactions at the nose gear NGX, NGY and NGZ have been determined. The reactions on the two sets of main gear are again calculated by idealizing the gear and carry through structure as a bent problem. The horizontal reactions on the front set of main gear, H1A and H1B, and the vertical reactions, V1A and V1B, are found from Equations (10) through (13) with the substitutions

$$F_V = M1GZ \quad , \quad L_1 = 2 \cdot Y1G$$

$$M_X = M1MX \quad , \quad L_2 = L1G$$

$$F_H = -M1GY$$

The horizontal reactions on the rear set of main gear, H2A and H2B, and the vertical reactions, V2A and V2B, are found from Equations (10) through (13) with the following substitutions

$$F_V = M2GZ \quad , \quad L_1 = 2 \cdot Y2G$$

$$M_X = M2MX \quad , \quad L_2 = L2G$$

$$F_H = -M2GY$$

The preceding analysis supply sufficient relations to calculate all of the unknown reactions at the landing gear. However, these calculations, as previously mentioned, lead to unreasonably low estimates of the safe handling speeds for the E-4. The minimum speed predicted by this analysis can be discerned by inspection of Table 1. In this table L indicates when the rear main upwind gear is lifting, L-S incidates when the rear main upwind gear is lifting and the nose wheel is sliding and S indicates when one of the main gear is sliding. It is seen that trouble occurs at as low a wind speed as 15 knots. This value was judged to be unrealistically low. Analysis of the numerical results indicated that the problem arose because of the method used to analyze the side load and yawing moment on the fuselage and the peculiar geometry of the undercarriage wherein the main gear have a close axial spacing. The source of the large side force reactions can be seen by considering the following simplified version of the horizontal bending problem for the fuselage. In this simplified problem we only consider one aerodynamic side force applied to the fuselage at the center of pressure for the side forces, and the fuselage is restrained by the gear located at three axial stations along the fuselage. The problem is shown in the following sketch.

Table 1

AIRCRAFT FORCE ANALYSIS SUMMARY SHEET; AIRCRAFT E-4 (5 GEAR) GOING ONTO RAMP

WIND DIRECTION (degrees)	WIND SPEED (knots) 15	20	25	WIND SPEED (knots) 15	20	25
	AIRCRAFT NOSE POSITION, XN = 75'			AIRCRAFT NOSE POSITION, XN = 390'		
335	X	X	X	X	X	X
005	X	X	S	X	X	S
035	X	L	L	S	L	L-S
065	L	L-S	L-S	L	L-S	L-S
095	X	L	L-S	L	L	L-S
125	X	X	X	X	L	L
155	X	X	X	X	X	X
185	X	X	X	X	S	L
215	X	L	L-S	L	L	L-S
245	L	L-S	L-S	L	L-S	L-S
275	S	L	L-S	L	L	L-S
305	X	X	S	X	X	L
	AIRCRAFT NOSE POSITION, XN = 175'			AIRCRAFT NOSE POSITION, XN = 485'		
335	X	X	X	X	X	X
005	X	X	X	X	X	S
035	X	L	L-S	L	L	L
065	L	L-S	L-S	L	L	L-S
095	X	L-S	L-S	L	L	L-S
125	X	X	S	X	S	L
155	X	X	X	X	X	X
185	X	X	L-S	X	X	L
215	S	L-S	L-S	L	L	L-S
245	L	L-S	L-S	L	L-S	L-S
275	S	L	L-S	L	L	L-S
305	X	X	X	X	X	L

LEGEND: X - AIRCRAFT SAFE; S - GEAR SLIPPING; L - GEAR LIFTING

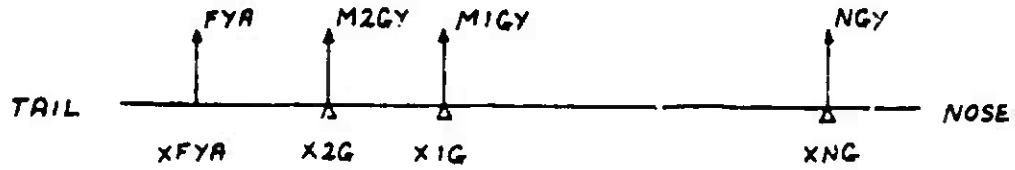

Here FYA is the applied aerodynamic side load applied at the center of pressure which is aft of the second main gear because of the vertical tail. Also M2GY, M1GY and NGY are the side force reactions supplied by the landing gear. If we let X2G = XMG + ϵ and X1G = XMG - ϵ (for the E-4, XMG = 109.45 ft. and ϵ = 5.05 ft) and require no lateral deflection at X2G to resolve the indeterminacy, then the reactions may be expressed by the following relations

$$M1GY = K_3 + K_4\, M2GY$$

$$NGY = K_1 + K_2\, M2GY$$

$$M2GY = \left\{ \frac{K_1 K_2}{3}(XMG - \epsilon - XNG) + K_1\left[2(XMG - \epsilon - XNG)\epsilon^2 + \frac{4}{3}\epsilon^3\right] + \frac{4K_3}{3}\epsilon^3 \right\} \Big/ \left\{ \frac{K_2^2}{3}(XMG - \epsilon - XNG)^3 + 2K_2\epsilon^2[XMG - \epsilon - XNG] + \frac{4K_4}{3}\epsilon^3 \right\}$$

where

$$K_1 = \frac{FYA(XMG - \epsilon - XFYA)}{XNG - XMG + \epsilon}$$

$$K_2 = \frac{-2\epsilon}{XNG - XMG + \epsilon}$$

$$K_3 = \frac{FYA(XNG - XFYA)}{XMG - \epsilon - XNG}$$

$$K_4 = \frac{XNG - XMG - \epsilon}{XMG - \epsilon - XNG}$$

The following limiting behavior with respect to ϵ may be deduced from the above formulae

$$\lim_{\epsilon \to 0} M2GY \to \infty$$

$$\lim_{\epsilon \to 0} M1GY \to -\infty$$

but

$$\lim_{\epsilon \to 0} (M2GY + M1GY) \to FYA \frac{(XFYA - XNG)}{XMG - XNG} < \infty$$

so it is seen that for small axial spacing between the main gear that M2GY becomes large and positive while M1GY becomes large and negative. As a sample case that corresponds to uniform wind conditions at 35.35 knots approaching from 45° from the left the following results are obtained

$$FYA = 1.5041 \times 10^4 \text{ pounds}$$

$$XFYA = 139.6 \text{ ft.}$$

$$M2GY = 5.4504 \times 10^4 \text{ pounds}$$

$$M1GY = -3.9734 \times 10^4 \text{ pounds}$$

$$NGY = 2.32 \times 10^2 \text{ pounds}$$

These large lateral reactions result in lifting of the upwind gear located at X2G at low wind speeds.

This difficiency in the analysis could probably be corrected by treating the four main gear as a space frame unit. However, this would have required a more detailed knowledge of the aircraft structure and was beyond the scope of the present program. As an approximation, to fill the needs of the present program, the actual 5 gear undercarriage of the aircraft was replaced with an equivalent 3 gear undercarriage. The four main gear of the E-4 were replaced with two gears. The original two main gears on each side of the aircraft were replaced with a single gear located at the mean axial

station and mean lateral position of the original gear. It was felt that this was a reasonable approximation considering the relatively close axial spacing of the actual main gears. The approximate three gear configuration does not have as wide a track as the actual aircraft gear and therefore can supply less resistance to overturning moments than the actual gears. It is, therefore, thought that the approximate three gear results for safe handling speed should be conservative.

6.4 RESULTS

The foregoing analysis was applied to each aircraft for five positions going onto the facility and four positions coming off. The wind speeds ranged from 20 to 80 knots. The positions of the aircraft going onto and off the facility were selected as those most likely to cause trouble on the basis of inspection of the smoke flow studies and velocity surveys. The results for safe handling speeds are shown in Tables 2-4. In these tables XN is the coordinate of the aircraft nose in the TRESTLE axis system. The fuselage centerline is always parallel to the X axis of the TRESTLE. The last XN position for going onto the ramp in each case corresponds to the test position for the aircraft on the test stand. For the first XN location going onto the ramp the aircraft is mainly located on the approach area. This location was selected on the basis of the smoke flow studies and quite often provides the minimum safe handling speed. For the case of the B-52 (Table 2) an unsafe condition first appears at a wind speed of 35 knots. Initial trouble with this aircraft always entails the slipping of the upwind front gear. The wind directions which are thirty degrees off alignment with the fuselage axis give the minimum safe speeds. For the cases of the E-3 and E-4 (Tables 3 and 4) aircraft unsafe conditions first appear at 35 knots. Initial trouble with these aircraft always entails slipping of the nose gear. The cross wind cases of 65 degrees and 245 degrees give the minimum safe handling speeds. A composite graph has been made for each aircraft which gives the safe handling speeds as a function of wind direction considering all positions on the facility. These plots are shown in Figures 32, 33, 34. The dashed line with

Table 2

AIRCRAFT FORCE ANALYSIS SUMMARY SHEET; AIRCRAFT: B-52 GOING ONTO RAMP

WIND DIRECTION (degrees)	WIND SPEED (knots) 25	30	35	40	45	50	60
	AIRCRAFT NOSE POSITION, XN = 10'						
335	X	X	X	X	X	X	S
005	X	X	X	X	X	S	L
035	X	X	X	X	S	L	L
065	X	X	X	X	S	L	L
095	X	X	X	X	S	L	L
125	X	X	X	X	S	L	L
155	X	X	X	X	X	L	L
185	X	X	S	S	S	L	L
215	X	X	S	S	S	L	L
245	X	X	X	S	S	L	L
275	X	X	X	X	S	L	L
305	X	X	X	X	X	X	S
	AIRCRAFT NOSE POSITION, XN = 113'						
335	X	X	X	X	X	X	X
005	X	X	X	X	X	S	L
035	X	X	X	X	X	L	L
065	X	X	X	X	X	L	L
095	X	X	X	S	S	L	L
125	X	X	X	L	L	L	L
155	X	X	X	X	X	X	X
185	X	X	S	S	S	L	L
215	X	X	X	S	S	L	L
245	X	X	X	X	X	L	L
275	X	X	X	X	S	L	L
305	X	X	X	X	X	S	L

WIND DIRECTION (degrees)	WIND SPEED (knots) 25	30	35	40	45	50	60
	AIRCRAFT NOSE POSITION, XN = 325'						
335	X	X	X	X	X	X	X
005	X	X	X	X	X	S	L
035	X	X	X	X	X	S	L
065	X	X	X	X	X	L	L
095	X	X	X	X	X	L	L
125	X	X	S	S	L	L	L
155	X	X	X	X	X	X	X
185	X	X	S	S	L	L	L
215	X	X	X	X	X	L	L
245	X	X	X	X	X	L	L
275	X	X	X	X	X	L	L
305	X	X	X	X	S	L	L
	AIRCRAFT NOSE POSITION, XN = 430'						
335	X	X	X	X	X	X	X
005	X	X	X	X	S	L	L
035	X	X	X	X	X	S	L
065	X	X	X	X	X	L	L
095	X	X	X	X	X	L	L
125	X	X	X	X	S	L	L
155	X	X	X	X	X	X	X
185	X	X	X	X	S	L	L
215	X	X	X	X	S	L	L
245	X	X	X	X	X	L	L
275	X	X	X	X	X	L	L
305	X	X	X	S	S	L	L

WIND DIRECTION (degrees)	WIND SPEED (knots) 25	30	35	40	45	50	60
	AIRCRAFT NOSE POSITION, XN = 578'						
335	X	X	X	X	X	X	X
005	X	X	X	X	X	S	L
035	X	X	X	X	X	S	L
065	X	X	X	X	X	S	L
095	X	X	X	X	X	X	L
125	X	X	X	X	X	S	L
155	X	X	X	X	X	X	X
185	X	X	X	X	X	L	L
215	X	X	X	X	X	S	L
245	X	X	X	X	X	L	L
275	X	X	X	X	X	S	L
305	X	X	X	X	X	S	L

LEGEND: X - AIRCRAFT SAFE; S - GEAR SLIPPING; L - GEAR LIFTING

Table 2 (Cont.)

AIRCRAFT FORCE ANALYSIS SUMMARY SHEET; AIRCRAFT: I-52 GOING OFF RAMP

WIND DIRECTION (degrees)	WIND SPEED (knots) 25	30	35	40	45	60	80	WIND SPEED (knots) 25	30	35	40	45	60	80
	AIRCRAFT NOSE POSITION, XN = -10'							AIRCRAFT NOSE POSITION, XN = 325'						
335		X	X	X	X				X	X	X	X		
005		X	X	X	X				X	X	X	S		
035		X	X	X	X				X	X	X	X		
065		X	X	X	X				X	X	X	X		
095		X	X	X	S				X	X	X	X		
125		X	S	S	L				X	X	X	X		
155		X	X	X	X				X	X	X	X		
185		X	S	S	L				X	X	X	X		
215		X	X	X	S				X	X	X	S		
245		X	X	X	X				X	X	X	X		
275		X	X	S	S				X	X	X	X		
305		X	X	X	X				X	X	S	S		
	AIRCRAFT NOSE POSITION, XN = 113'							AIRCRAFT NOSE POSITION, XN = 422'						
335		X	X	X	X				X	X	X	X		
005		X	X	X	X				X	X	X	X		
035		X	X	X	X				X	X	X	X		
065		X	X	X	X				X	X	X	X		
095		X	X	X	X				X	X	X	X		
125		X	X	S	L				X	X	X	X		
155		X	X	X	X				X	X	X	X		
185		X	X	S	S				X	X	X	X		
215		X	X	X	X				X	X	X	X		
245		X	X	X	X				X	X	X	X		
275		X	X	X	S				X	X	X	X		
305		X	X	X	X				X	X	X	X		

LEGEND: X - AIRCRAFT SAFE; S - GEAR SLIPPING; L - GEAR LIFTING

Table 3

AIRCRAFT FORCE ANALYSIS SUMMARY SHEET; AIRCRAFT: E-3 GOING ONTO RAMP

WIND DIRECTION (degrees)	WIND SPEED (knots) 25	30	35	40	45	50	60	WIND SPEED (knots) 25	30	35	40	45	50	60	WIND SPEED (knots) 25	30	35	40	45	50	60
	AIRCRAFT NOSE POSITION, XN = 0'							AIRCRAFT NOSE POSITION, XN = 325'							AIRCRAFT NOSE POSITION, XN = 573'						
335	X	X	X	X	X	X		X	X	X	X	X	X		X	X	X	X	X	X	
005	X	X	X	X	X	S		X	X	X	X	X	S		X	X	X	X	X	S	
035	X	X	X	X	S	S		X	X	X	S	S	S		X	X	X	S	S	S	
065	X	X	S	S	S	S		X	S	S	S	S	L		X	X	X	S	S	S	
095	X	X	X	X	S	S		X	X	X	S	S	S		X	X	X	X	S	S	
125	X	X	X	X	X	X		X	X	X	X	S	S		X	X	X	X	X	S	
155	X	X	X	X	X	S		X	X	X	X	X	X		X	X	X	X	X	X	
185	X	X	X	X	S	S		X	X	X	X	S	S		X	X	X	X	X	S	
215	X	X	X	S	S	L		X	X	X	S	S	L		X	X	X	X	S	S	
245	X	X	S	S	S	L		X	S	S	S	S	S		X	X	S	S	S	S	
275	X	X	X	S	S	S		X	X	S	S	S	S		X	X	S	S	S	S	
305	X	X	X	X	X	S		X	X	X	X	X	S		X	X	X	X	X	S	
	AIRCRAFT NOSE POSITION, XN = 95'							AIRCRAFT NOSE POSITION, XN = 455'													
335	X	X	X	X	X	X		X	X	X	X	X	X								
005	X	X	X	X	X	S		X	X	X	X	X	S								
035	X	X	X	X	S	S		X	X	S	S	S	S								
065	X	X	S	S	S	L		X	X	S	S	S	S								
095	X	X	X	X	S	S		X	X	X	X	S	S								
125	X	X	X	X	S	S		X	X	X	X	X	S								
155	X	X	X	X	X	X		X	X	X	X	X	X								
185	X	X	X	X	S	S		X	X	X	X	X	S								
215	X	X	X	X	S	S		X	X	X	S	S	S								
245	X	X	X	S	S	L		X	X	S	S	S	S								
275	X	X	X	X	S	S		X	X	S	S	S	S								
305	X	X	X	X	X	S		X	X	X	X	S	S								

LEGEND: X - AIRCRAFT SAFE; S - GEAR SLIPPING; L - GEAR LIFTING

Table 3 (Cont.)

AIRCRAFT FORCE ANALYSIS SUMMARY SHEET; AIRCRAFT: E-3 GOING OFF RAMP

WIND DIRECTION (degrees)	WIND SPEED (knots) 25	30	35	40	45	50	60	WIND SPEED (knots) 25	30	35	40	45	50	60
	AIRCRAFT NOSE POSITION; XN = -10'							AIRCRAFT NOSE POSITION, XN = 319'						
335		X	X	X					X	X	X			
005		X	X	X					X	X	X			
035		X	X	X					X	X	X			
065		X	S	S					X	X	X			
095		X	X	S					X	X	X			
125		X	X	X					X	X	X			
155		X	X	X					X	X	X			
185		X	X	X					X	X	X			
215		X	X	S					X	X	X			
245		X	S	S					X	X	S			
275		X	X	S					X	X	X			
305		X	X	X					X	X	X			
	AIRCRAFT NOSE POSITION, XN = 130'							AIRCRAFT NOSE POSITION, XN = 427'						
335		X	X	X					X	X	X			
005		X	X	X					X	X	X			
035		X	X	S					X	X	X			
065		X	X	S					X	X	S			
095		X	X	X					X	X	X			
125		X	X	X					X	X	X			
155		X	X	X					X	X	X			
185		X	X	X					X	X	X			
215		X	X	X					X	X	X			
245		X	X	S					X	S	S			
275		X	X	X					X	X	X			
305		X	X	X					X	X	X			

LEGEND: X - AIRCRAFT SAFE; S- GEAR SLIPPING; L - GEAR LIFTING

Table 4

AIRCRAFT FORCE ANALYSIS SUMMARY SHEET; AIRCRAFT: E-4 (3 GEARS) GOING ONTO RAMP

WIND DIRECTION (degrees)	WIND SPEED (knots) 25	30	35	40	45	60	80	WIND SPEED (knots) 25	30	35	40	45	60	80	WIND SPEED (knots) 25	30	35	40	45	60	80
	AIRCRAFT NOSE POSITION, XN = 75'							AIRCRAFT NOSE POSITION, XN = 280'							AIRCRAFT NOSE POSITION, XN = 612'						
335	X	X	X	X	X	X		X	X	X	X	X	X		X	X	X	X	X	X	
005	X	X	X	X	X	S		X	X	X	X	X	S		X	X	X	X	X	S	
035	X	X	X	X	S	L		X	X	X	S	S	L		X	X	S	S	S	S	
065	X	X	S	S	S	L		X	S	S	S	S	L		X	X	S	S	S	L	
095	X	X	X	X	S	L		X	X	S	S	S	L		X	X	X	X	S	L	
125	X	X	X	X	S	L		X	X	X	X	S	L		X	X	X	X	X	S	
155	X	X	X	X	X	X		X	X	X	X	X	X		X	X	X	X	X	X	
185	X	X	X	X	X	S		X	X	X	X	X	S		X	X	X	X	X	S	
215	X	X	X	X	S	L		X	X	X	S	S	L		X	X	X	S	S	L	
245	X	X	X	S	S	L		X	X	S	S	S	L		X	S	S	S	S	L	
275	X	X	X	S	S	L		X	X	S	S	S	L		X	S	S	S	S	L	
305	X	X	X	X	X	S		X	X	X	X	X	S		X	X	X	X	S	S	
	AIRCRAFT NOSE POSITION, XN = 175'							AIRCRAFT NOSE POSITION, XN = 485'													
335	X	X	X	X	X	X		X	X	X	X	X	X								
005	X	X	X	X	X	S		X	X	X	X	X	S								
035	X	X	X	S	S	L		X	X	S	S	S	L								
065	X	X	S	S	S	L		X	S	S	S	S	L								
095	X	X	X	X	S	L		X	X	S	S	S	L								
125	X	X	X	X	S	L		X	X	X	X	X	S								
155	X	X	X	X	X	X		X	X	X	X	X	X								
185	X	X	X	X	S	L		X	X	X	X	X	S								
215	X	X	X	X	S	L		X	X	S	S	S	L								
245	X	X	X	S	S	L		X	S	S	S	S	L								
275	X	X	X	S	S	L		X	X	S	S	S	L								
305	X	X	X	X	X	S		X	X	X	X	X	S								

LEGEND: X - AIRCRAFT SAFE; S- GEAR SLIPPING; L - GEAR LIFTING

Table 4 (Cont.)

AIRCRAFT FORCE ANALYSIS SUMMARY SHEET; AIRCRAFT: E-4 (3 GEARS) GOING OFF RAMP

WIND DIRECTION (degrees)	WIND SPEED (knots) 25	30	35	40	45	50	60	WIND SPEED (knots) 25	30	35	40	45	50	60
	AIRCRAFT NOSE POSITION, XN = -63'							AIRCRAFT NOSE POSITION, XN = 263'						
336		X	X	X	X				X	X	X	X		
005		X	X	X	X				X	X	X	X		
035		X	X	X	S				X	X	X	X		
065		X	S	S	S				X	X	S	S		
095		X	X	S	S				X	X	X	X		
125		X	X	X	X				X	X	X	X		
155		X	X	X	X				X	X	X	X		
185		X	X	X	X				X	X	X	X		
215		X	X	S	S				X	X	X	X		
245		X	S	S	S				X	X	S	S		
275		X	X	X	S				X	X	X	S		
305		X	X	X	X				X	X	X	X		
	AIRCRAFT NOSE POSITIDN, XN = 200'							AIRCRAFT NOSE POSITION, XN = 386'						
335		X	X	X	X				X	X	X	X		
005		X	X	X	X				X	X	X	X		
035		X	X	X	S				X	X	X	X		
065		X	S	S	S				X	X	X	S		
095		X	X	S	S				X	X	X	X		
125		X	X	X	X				X	X	X	X		
155		X	X	X	X				X	X	X	X		
185		X	X	X	X				X	X	X	X		
215		X	X	S	S				X	X	X	X		
245		X	X	S	S				X	X	X	S		
275		X	X	S	S				X	X	X	X		
305		X	X	X	X				X	X	X	X		

LEGEND: X - AIRCRAFT SAFE; S - GEAR SLIPPING; L - GEAR LIFTING

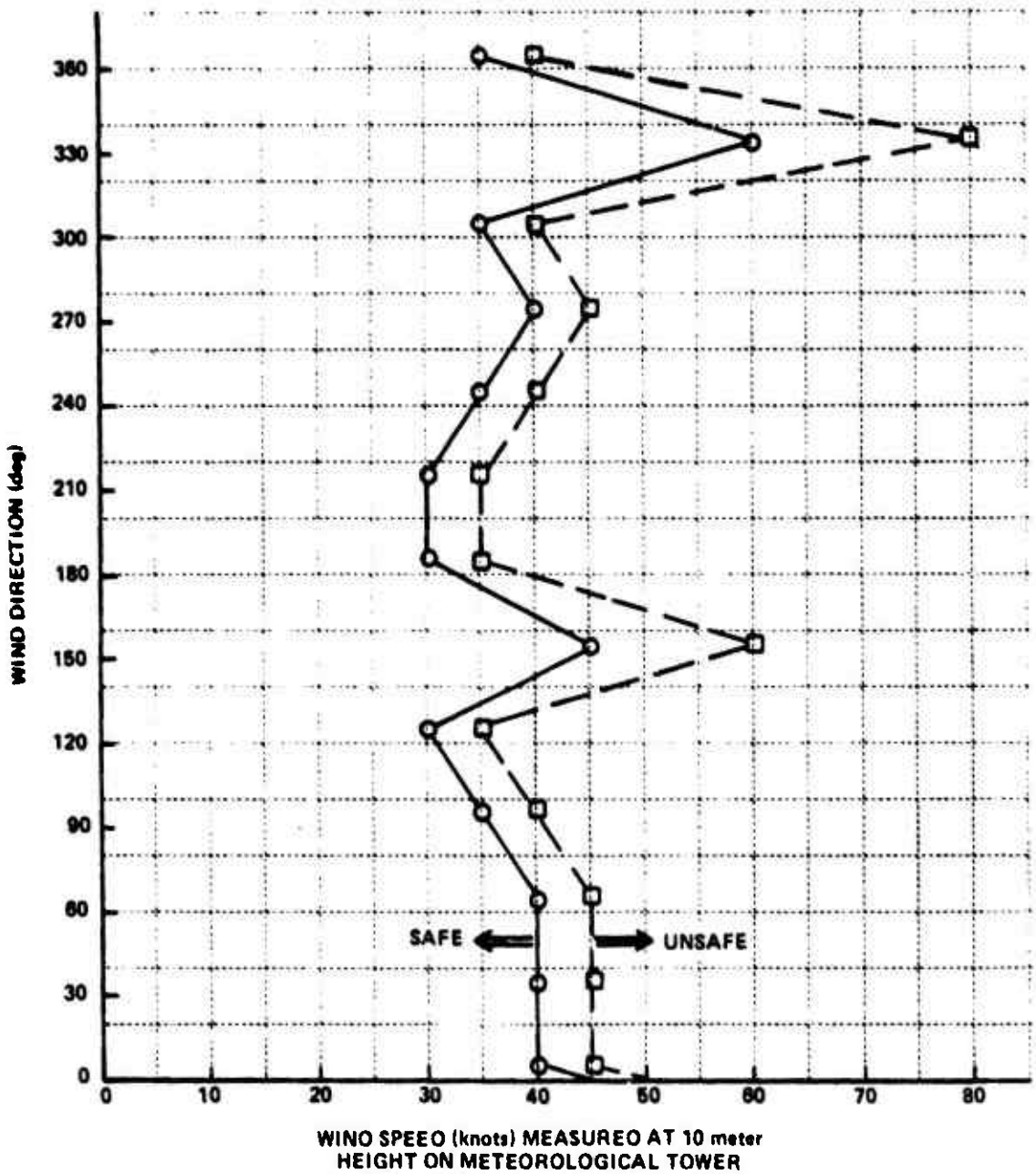

Figure 32. Summary of Results from Force Analysis of B-52 Aircraft For All Positions on Ramp and Test Stand of TRESTLE Facility.

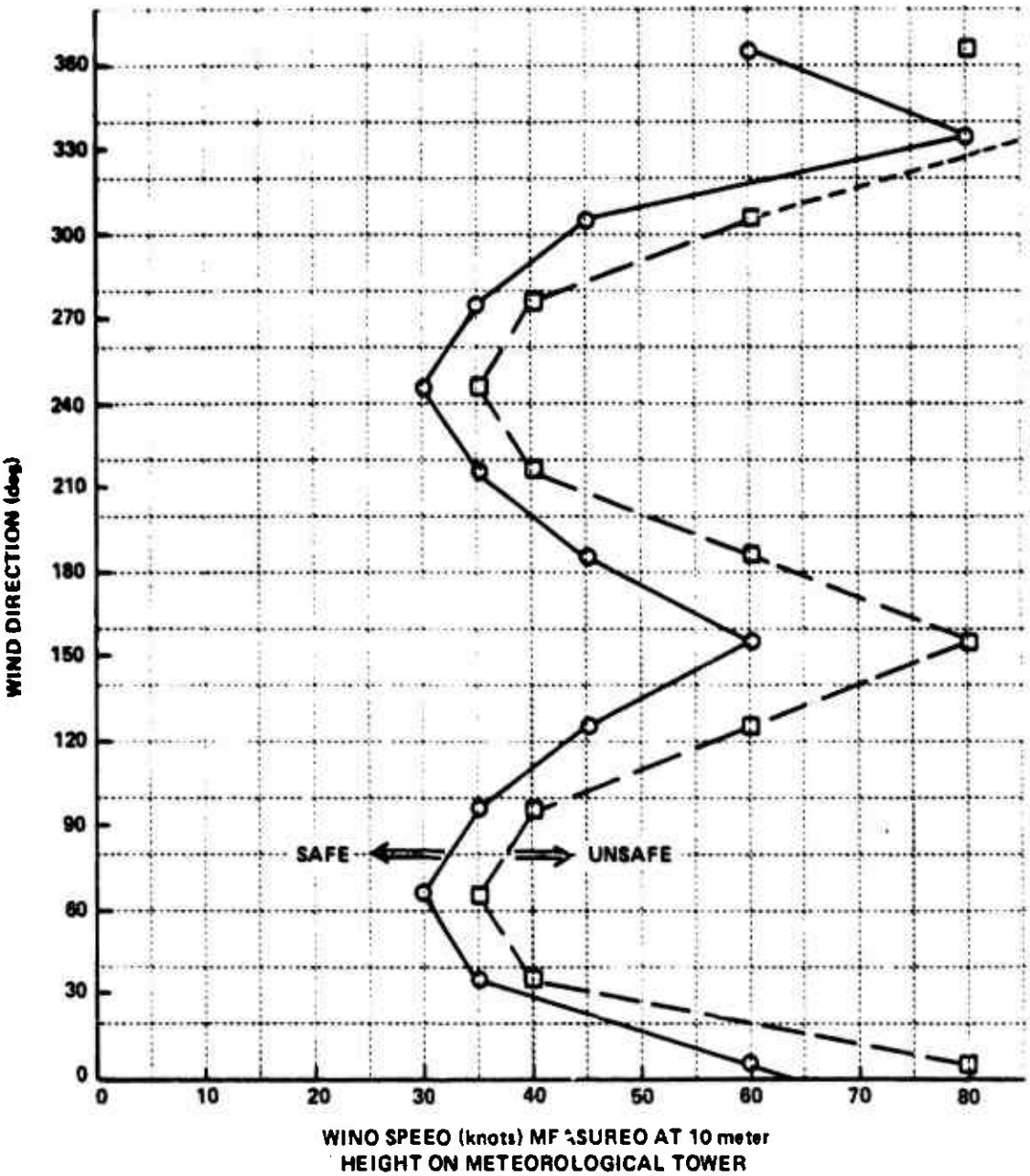

Figure 33. Summary of Results from Force Analysis of E-3 Aircraft For All Positions on Ramp and Test Stand of TRESTLE Facility.

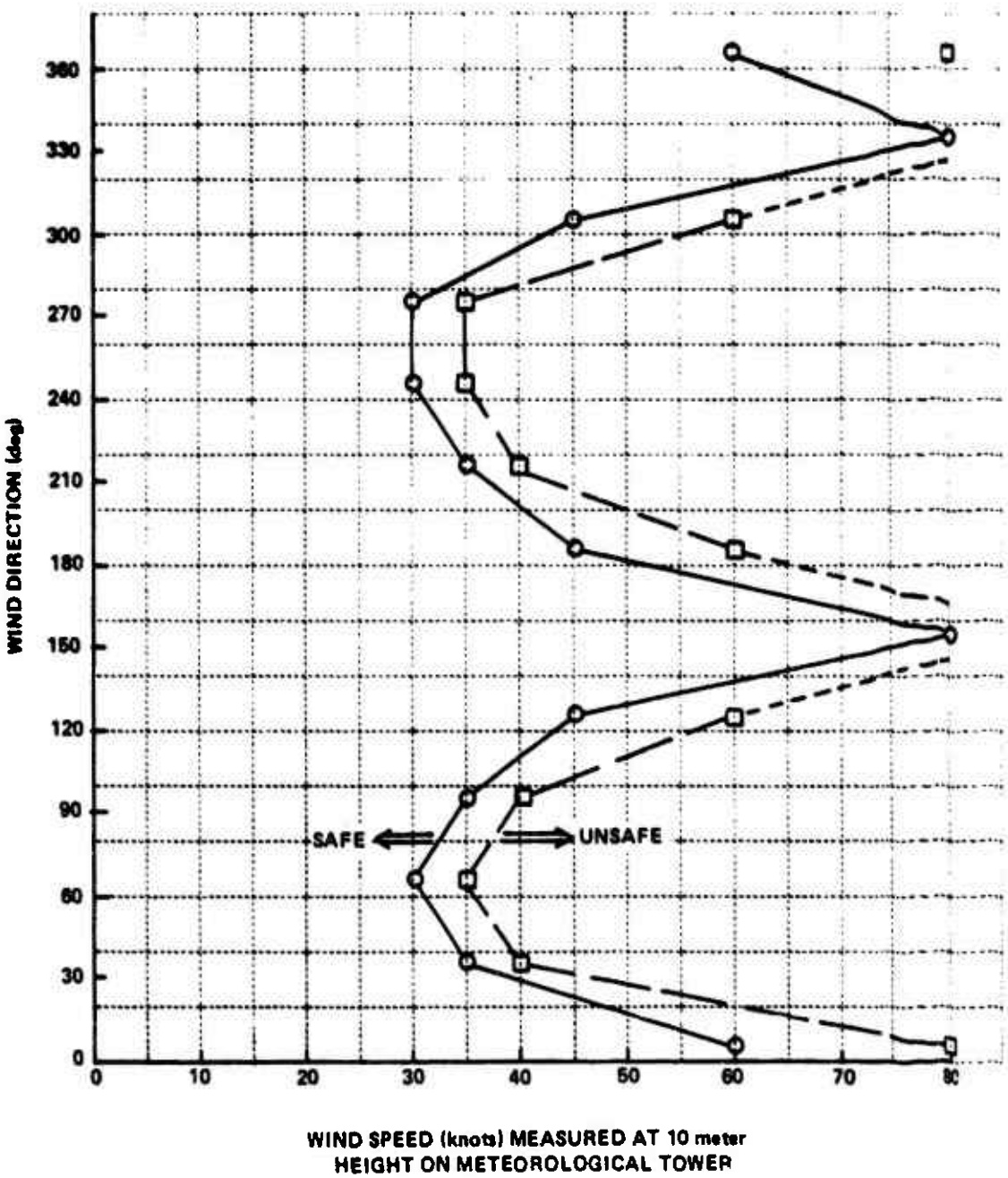

Figure 34. Summary of Results from Force Analysis of E-4 Aircraft (Tricycle Gear Approximation) For All Positions on Ramp and Test Stand of TRESTLE Facility.

the square symbols indicate the lowest speed points where the calculations indicated trouble exists. The solid line with circular symbols indicate the next lowest speed increment where a calculation was made and no unsafe conditions were found. This solid curve is recommended as the boundary for safe ground handling.

The reactions between the aircraft gears and the test platform are given in Tables 5, 6, 7 and 8. In these tables are listed the gear reaction (in pounds) for the nose position on the test platform XN, the wind direction, PHI and the wind speed, UN1F, in knots.

For the case of the B-52 (Table 5) the reaction quantities are defined according to the following list

H1A - Horizontal reaction at the front left gear
H1B - Horizontal reaction at the front right gear
H2A - Horizontal reaction at the rear left gear
H2B - Horizontal reaction at the rear right gear
V1A - Vertical reaction at the front left gear
V1B - Vertical reaction at the front right gear
V2A - Vertical reaction at the rear left gear
V2B - Vertical reaction at the rear right gear
NGX - Axial force reaction at front gears

For the case of the C-5 (Table 6) the following definitions apply

NGX - Axial force reaction at nose gear
NGY - Horizontal reaction at nose gear
NGZ - Vertical reaction at nose gear
HA - Horizontal reaction at left main gear
HB - Horizontal reaction at right main gear
VA - Vertical reaction at left main gear
VB - Vertical reaction at right main gear

Table 5
LANDING GEAR REACTIONS FOR B-52 AIRCRAFT ON TEST STAND

AIRCRAFT: B-52 AIRCRAFT GOING ONTO RAMP

XN=578.0	PHI= 5.0	UINF= 25.0		
H1A=-2.2906E+04 H2A=-2.6985E+04	H1B= 2.2694E+04 H2B= 2.8810E+04	V1A= 5.2650E+04 V2A= 7.0080E+04	V1B= 6.9356E+04 V2B= 7.8707E+04	NGX=-9.6034E+02
XN=578.0	PHI= 5.0	UINF= 30.0		
H1A=-2.3003E+04 H2A=-2.6948E+04	H1B= 2.2916E+04 H2B= 2.9277E+04	V1A= 4.9197E+04 V2A= 6.8354E+04	V1B= 7.3253E+04 V2B= 8.0777E+04	NGX=-6.6288E+02
XN=578.0	PHI= 5.0	UINF= 35.0		
H1A=-2.3117E+04 H2A=-2.6299E+04	H1B= 2.2999E+04 H2B= 2.9828E+04	V1A= 4.5114E+04 V2A= 6.6314E+04	V1B= 7.7859E+04 V2B= 8.3228E+04	NGX=-9.0224E+02
XN=578.0	PHI= 5.0	UINF= 40.0		
H1A=-2.3248E+04 H2A=-2.5790E+04	H1B= 2.3095E+04 H2B= 3.0463E+04	V1A= 4.0408E+04 V2A= 6.3941E+04	V1B= 8.3174E+04 V2B= 8.4047E+04	NGX=-1.1785E+03
XN=578.0	PHI= 5.0	UINF= 45.0		
H1A=-2.3398E+04 H2A=-2.5269E+04	H1B= 2.3203E+04 H2B= 3.1189E+04	V1A= 3.5071E+04 V2A= 6.1299E+04	V1B= 8.9197E+04 V2B= 8.9246E+04	NGX=-1.4915E+03
XN=578.0	PHI= 5.0	UINF= 50.0		
H1A=-2.3951E+04 H2A=-2.3338E+04	H1B= 2.3605E+04 H2B= 3.3859E+04	V1A= 1.5295E+04 V2A= 5.1410E+04	V1B= 1.1152E+05 V2B= 1.0110E+05	NGX=-2.4515E+03
XN=578.0	PHI= 5.0	UINF= 80.0		
H1A=-2.4933E+04 H2A=-1.9907E+04	H1B= 2.4319E+04 H2B= 3.8401E+04	V1A=-1.9863E+04 V2A= 3.3838E+04	V1B= 1.5120E+05 V2B= 1.2218E+05	NGX=-4.7134E+03
XN=578.0	PHI= 35.0	UINF= 25.0		
H1A=-2.3141E+04 H2A=-2.5141E+04	H1B= 2.2572E+04 H2B= 3.0520E+04	V1A= 5.5403E+04 V2A= 6.3259E+04	V1B= 6.6498E+04 V2B= 8.5225E+04	NGX=-5.1434E+02
XN=578.0	PHI= 35.0	UINF= 30.0		
H1A=-2.3341E+04 H2A=-2.4022E+04	H1B= 2.2521E+04 H2B= 3.1738E+04	V1A= 5.3162E+04 V2A= 5.8532E+04	V1B= 6.9138E+04 V2B= 9.0163E+04	NGX=-7.4072E+02
XN=578.0	PHI= 35.0	UINF= 35.0		
H1A=-2.3577E+04 H2A=-2.2476E+04	H1B= 2.2462E+04 H2B= 3.3178E+04	V1A= 5.0512E+04 V2A= 5.2946E+04	V1B= 7.2259E+04 V2B= 9.5998E+04	NGX=-1.0082E+03
XN=578.0	PHI= 35.0	UINF= 40.0		
H1A=-2.3850E+04 H2A=-2.1122E+04	H1B= 2.2393E+04 H2B= 3.4840E+04	V1A= 4.7455E+04 V2A= 4.6500E+04	V1B= 7.5859E+04 V2B= 1.0273E+05	NGX=-1.3158E+03

Table 5 (Cont.)

LANDING GEAR REACTIONS FOR B-52 AIRCRAFT ON TEST STAND

XN=578.0	PHI= 35.0	UINF= 95.0		
H1A=-2.4159E+04	H1B= 2.2315E+04	V1A= 4.3991E+04	V1B= 7.5939E+04	
H2A=-1.9361E+04	H2B= 3.6723E+04	V2A= 3.9195E+04	V2B= 1.1036E+05	NGX=-1.6666E+03
XN=578.0	PHI= 35.0	UINF= 60.0		
H1A=-2.5304E+04	H1B= 2.2025E+04	V1A= 3.1152E+04	V1B= 9.5060E+04	
H2A=-1.2836E+04	H2B= 4.3702E+04	V2A= 1.2122E+04	V2B= 1.3864E+05	NGX=-2.9629E+03
XN=578.0	PHI= 35.0	UINF= 80.0		
H1A=-2.7340E+04	H1B= 2.1510E+04	V1A= 8.3277E+03	V1B= 1.2194E+05	
H2A=-1.2354E+03	H2B= 5.6168E+04	V2A=-3.6007E+04	V2B= 1.8892E+05	NGX=-5.2673E+03
XN=578.0	PHI= 65.0	UINF= 25.0		
H1A=-2.3166E+04	H1B= 2.2467E+04	V1A= 6.2664E+04	V1B= 5.9084E+04	
H2A=-2.4729E+04	H2B= 3.1371E+04	V2A= 6.1749E+04	V2B= 8.7850E+04	NGX=-2.2099E+02
XN=578.0	PHI= 65.0	UINF= 30.0		
H1A=-2.3377E+04	H1B= 2.2370E+04	V1A= 6.3531E+04	V1B= 5.8462E+04	
H2A=-2.3399E+04	H2B= 3.2963E+04	V2A= 5.6357E+04	V2B= 9.3993E+04	NGX=-3.1814E+02
XN=578.0	PHI= 65.0	UINF= 35.0		
H1A=-2.3626E+04	H1B= 2.2256E+04	V1A= 6.4626E+04	V1B= 5.7726E+04	
H2A=-2.1628E+04	H2B= 3.4846E+04	V2A= 4.9986E+04	V2B= 1.0114E+05	NGX=-4.3306E+02
XN=578.0	PHI= 65.0	UINF= 40.0		
H1A=-2.3914E+04	H1B= 2.2124E+04	V1A= 6.5869E+04	V1B= 5.6878E+04	
H2A=-2.0014E+04	H2B= 3.7018E+04	V2A= 4.2634E+04	V2B= 1.0945E+05	NGX=-5.6562E+02
XN=578.0	PHI= 65.0	UINF= 45.0		
H1A=-2.4239E+04	H1B= 2.1975E+04	V1A= 6.7321E+04	V1B= 5.5916E+04	
H2A=-1.7959E+04	H2B= 3.9479E+04	V2A= 3.4301E+04	V2B= 1.1887E+05	NGX=-7.1587E+02
XN=578.0	PHI= 65.0	UINF= 60.0		
H1A=-2.5447E+04	H1B= 2.1721E+04	V1A= 7.2620E+04	V1B= 5.2333E+04	
H2A=-1.0344E+04	H2B= 4.8602E+04	V2A= 5.4229E+03	V2B= 1.5376E+05	NGX=-1.2727E+03
XN=578.0	PHI= 65.0	UINF= 80.0		
H1A=-2.7594E+04	H1B= 2.0436E+04	V1A= 8.2063E+04	V1B= 4.6017E+04	
H2A= 3.1952E+03	H2B= 6.4819E+04	V2A=-5.1472E+04	V2B= 2.1580E+05	NGX=-2.2625E+03
XN=578.0	PHI= 95.0	UINF= 25.0		
H1A=-2.2697E+04	H1B= 2.2415E+04	V1A= 5.7279E+04	V1B= 6.3019E+04	
H2A=-2.5376E+04	H2B= 3.0043E+04	V2A= 6.4398E+04	V2B= 8.3388E+04	NGX= 3.0315E+02

Table 5 (Cont.)

LANDING GEAR REACTIONS FOR B-52 AIRCRAFT ON TEST STAND

XN=578.0	PHI= 95.0	U1NF= 30.0		
H1A=-2.2701E+04	H1B= 2.2295E+04	V1A= 5.5862E+04	V1B= 6.6128E+04	
H2A=-2.4332E+04	H2B= 3.1052E+04	V2A= 6.0172E+04	V2B= 8.7517E+04	NGX= 4.3653E+02
XN=578.0	PHI= 95.0	U1NF= 35.0		
H1A=-2.2706E+04	H1B= 2.2154E+04	V1A= 5.4188E+04	V1B= 6.5439E+04	
H2A=-2.3097E+04	H2B= 3.2249E+04	V2A= 5.5177E+04	V2B= 9.2398E+04	NGX= 5.9617E+02
XN=578.0	PHI= 95.0	U1NF= 40.0		
H1A=-2.2712E+04	H1B= 2.1991E+04	V1A= 5.2257E+04	V1B= 6.6951E+04	
H2A=-2.1672E+04	H2B= 3.3619E+04	V2A= 4.9419E+04	V2B= 9.8029E+04	NGX= 7.7606E+02
XN=578.0	PHI= 95.0	U1NF= 45.0		
H1A=-2.2719E+04	H1B= 2.1806E+04	V1A= 5.0066E+04	V1B= 6.8665E+04	
H2A=-2.0058E+04	H2B= 3.5178E+04	V2A= 4.2883E+04	V2B= 1.0491E+05	NGX= 9.8220E+02
XN=578.0	PHI= 95.0	U1NF= 60.0		
H1A=-2.2744E+04	H1B= 2.1120E+04	V1A= 4.1955E+04	V1B= 7.5017E+04	
H2A=-1.4074E+04	H2B= 4.0955E+04	V2A= 1.8680E+04	V2B= 1.2806E+05	NGX= 1.7461E+03
XN=578.0	PHI= 95.0	U1NF= 80.0		
H1A=-2.2769E+04	H1B= 1.9902E+04	V1A= 3.7533E+04	V1B= 8.6310E+04	
H2A=-3.4366E+03	H2B= 5.1225E+04	V2A=-2.4348E+04	V2B= 1.7011E+05	NGX= 3.1042E+03
XN=578.0	PHI= 125.0	U1NF= 25.0		
H1A=-2.2634E+04	H1B= 2.2535E+04	V1A= 5.0202E+04	V1B= 7.0241E+04	
H2A=-2.6134E+04	H2B= 2.8614E+04	V2A= 6.7432E+04	V2B= 7.9176E+04	NGX= 2.9794E+02
XN=578.0	PHI= 125.0	U1NF= 30.0		
H1A=-2.2610E+04	H1B= 2.2465E+04	V1A= 4.9672E+04	V1B= 7.4528E+04	
H2A=-2.5465E+04	H2B= 2.9282E+04	V2A= 6.4542E+04	V2B= 8.1452E+04	NGX= 4.2904E+02
XN=578.0	PHI= 125.0	U1NF= 35.0		
H1A=-2.2582E+04	H1B= 2.2385E+04	V1A= 4.8318E+04	V1B= 7.9595E+04	
H2A=-2.4640E+04	H2B= 2.9634E+04	V2A= 6.1126E+04	V2B= 8.4143E+04	NGX= 5.8404E+02
XN=578.0	PHI= 125.0	U1NF= 40.0		
H1A=-2.2551E+04	H1B= 2.2292E+04	V1A= 4.6140E+04	V1B= 8.5441E+04	
H2A=-2.3688E+04	H2B= 3.0479E+04	V2A= 5.7184E+04	V2B= 8.7247E+04	NGX= 7.6283E+02
XN=578.0	PHI= 125.0	U1NF= 45.0		
H1A=-2.2514E+04	H1B= 2.2188E+04	V1A= 4.3139E+04	V1B= 9.2066E+04	
H2A=-2.2609E+04	H2B= 3.1197E+04	V2A= 5.2716E+04	V2B= 9.0766E+04	NGX= 9.6545E+02

Table 5 (Cont.)

LANDING GEAR REACTIONS FOR B-52 AIRCRAFT ON TEST STAND

XN=578.0	PHI= 125.0	UINF= 60.0		
M1A=-2.2560E+04	M1B= 2.1800E+04	V1A= 1.1935E+03	V1B= 1.1662E+05	
M2A=-1.6609E+04	M2B= 3.3877E+04	V2A= 3.6161E+04	V2B= 1.0380E+05	NGX= 1.7164E+03
XN=578.0	PHI= 125.0	UINF= 80.0		
M1A=-2.2142E+04	M1B= 2.1110E+04	V1A=-4.4932E+04	V1B= 1.6027E+05	
M2A=-1.1499E+04	M2B= 3.8643E+04	V2A= 6.7285E+03	V2B= 1.2658E+05	NGX= 3.0513E+03
XN=578.0	PHI= 155.0	UINF= 25.0		
M1A=-2.2635E+04	M1B= 2.2596E+04	V1A= 6.0625E+04	V1B= 5.9993E+04	
M2A=-2.7590E+04	M2B= 2.7682E+04	V2A= 7.3491E+04	V2B= 7.3900E+04	NGX= 1.0724E+01
XN=578.0	PHI= 155.0	UINF= 30.0		
M1A=-2.2612E+04	M1B= 2.2557E+04	V1A= 6.0681E+04	V1B= 5.5770E+04	
M2A=-2.7520E+04	M2B= 2.7691E+04	V2A= 7.3267E+04	V2B= 7.3856E+04	NGX= 1.5443E+01
XN=578.0	PHI= 155.0	UINF= 35.0		
M1A=-2.2586E+04	M1B= 2.2510E+04	V1A= 6.0746E+04	V1B= 5.5508E+04	
M2A=-2.7436E+04	M2B= 2.7615E+04	V2A= 7.3001E+04	V2B= 7.3603E+04	NGX= 2.1019E+01
XN=578.0	PHI= 155.0	UINF= 40.0		
M1A=-2.2555E+04	M1B= 2.2456E+04	V1A= 6.0823E+04	V1B= 5.5205E+04	
M2A=-2.7340E+04	M2B= 2.7574E+04	V2A= 7.2695E+04	V2B= 7.3742E+04	NGX= 2.7454E+01
XN=578.0	PHI= 155.0	UINF= 45.0		
M1A=-2.2519E+04	M1B= 2.2394E+04	V1A= 6.0905E+04	V1B= 5.8861E+04	
M2A=-2.7231E+04	M2B= 2.7526E+04	V2A= 7.2347E+04	V2B= 7.3673E+04	NGX= 3.4746E+01
XN=578.0	PHI= 155.0	UINF= 60.0		
M1A=-2.2589E+04	M1B= 2.2167E+04	V1A= 6.1228E+04	V1B= 5.7588E+04	
M2A=-2.6827E+04	M2B= 2.7552E+04	V2A= 7.1060E+04	V2B= 7.3416E+04	NGX= 6.1771E+01
XN=578.0	PHI= 155.0	UINF= 80.0		
M1A=-2.2158E+04	M1B= 2.1762E+04	V1A= 6.1756E+04	V1B= 5.5324E+04	
M2A=-2.6108E+04	M2B= 2.7042E+04	V2A= 6.8772E+04	V2B= 7.2961E+04	NGX= 1.0981E+02
XN=578.0	PHI= 185.0	UINF= 25.0		
M1A=-2.2763E+04	M1B= 2.2405E+04	V1A= 7.0510E+04	V1B= 4.9953E+04	
M2A=-2.8604E+04	M2B= 2.6351E+04	V2A= 7.8619E+04	V2B= 6.7873E+04	NGX= 5.5573E+02
XN=578.0	PHI= 185.0	UINF= 30.0		
M1A=-2.2797E+04	M1B= 2.2275E+04	V1A= 7.4916E+04	V1B= 4.5285E+04	
M2A=-2.8575E+04	M2B= 2.5706E+04	V2A= 8.0651E+04	V2B= 6.5176E+04	NGX= 5.6986E+02

Table 5 (Cont.)

LANDING GEAR REACTIONS FOR B-52 AIRCRAFT ON TEST STAND

XN=378.0	PHI= 185.0	UINF= 35.0		
H1A=-2.2836E+04 H2A=-2.9422E+04	H1B= 2.2131E+04 H2B= 2.4968E+04	V1A= 8.0122E+04 V2A= 8.3052E+04	V1B= 3.9791E+04 V2B= 6.1989E+04	NGX= 7.7562E+02
XN=378.0	PHI= 185.0	UINF= 40.0		
H1A=-2.2882E+04 H2A=-2.9934E+04	H1B= 2.1961E+04 H2B= 2.4116E+04	V1A= 8.6129E+04 V2A= 8.5822E+04	V1B= 3.3453E+04 V2B= 5.8311E+04	NGX= 1.0131E+03
XN=378.0	PHI= 185.0	UINF= 45.0		
H1A=-2.2934E+04 H2A=-3.0314E+04	H1B= 2.1769E+04 H2B= 2.3150E+04	V1A= 9.2938E+04 V2A= 8.8962E+04	V1B= 2.6269E+04 V2B= 5.4143E+04	NGX= 1.2821E+03
XN=378.0	PHI= 185.0	UINF= 50.0		
H1A=-2.3126E+04 H2A=-3.2663E+04	H1B= 2.1034E+04 H2B= 1.9572E+04	V1A= 1.1817E+03 V2A= 1.0060E+05	V1B=-3.5422E+02 V2B= 3.8697E+04	NGX= 2.2794E+03
XN=378.0	PHI= 185.0	UINF= 00.0		
H1A=-2.3468E+04 H2A=-3.6484E+04	H1B= 1.9785E+04 H2B= 1.3211E+04	V1A= 1.6302E+03 V2A= 1.2128E+03	V1B=-4.7684E+04 V2A= 1.1238E+04	NGX= 4.0322E+03
XN=378.0	PHI= 215.0	UINF= 25.0		
H1A=-2.2641E+04 H2A=-2.9786E+04	H1B= 2.2474E+04 H2B= 2.3420E+04	V1A= 6.8779E+04 V2A= 8.2938E+04	V1B= 5.1527E+04 V2B= 6.4257E+04	NGX= 4.3268E+02
XN=378.0	PHI= 213.0	UINF= 30.0		
H1A=-2.2621E+04 H2A=-3.0681E+04	H1B= 2.2380E+04 H2B= 2.4394E+04	V1A= 7.2423E+04 V2A= 8.6898E+04	V1B= 4.7580E+04 V2B= 3.9970E+04	NGX= 6.5186E+02
XN=378.0	PHI= 213.0	UINF= 33.0		
H1A=-2.2397E+04 H2A=-3.1740E+04	H1B= 2.2270E+04 H2B= 2.3182E+04	V1A= 7.6729E+04 V2A= 9.1555E+04	V1B= 4.2913E+04 V2B= 5.4902E+04	NGX= 8.8726E+02
XN=378.0	PHI= 213.0	UINF= 40.0		
H1A=-2.2569E+04 H2A=-3.2961E+04	H1B= 2.2142E+04 H2B= 2.1703E+04	V1A= 8.1698E+04 V2A= 9.6928E+04	V1B= 3.7332E+04 V2B= 4.9055E+04	NGX= 1.1389E+03
XN=378.0	PHI= 215.0	UINF= 43.0		
H1A=-2.2338E+04 H2A=-3.4344E+04	H1B= 2.1997E+04 H2B= 2.0198E+04	V1A= 8.7330E+04 V2A= 1.0302E+05	V1B= 3.1432E+04 V2B= 4.2429E+04	NGX= 1.4667E+03
XN=378.0	PHI= 215.0	UINF= 60.0		
H1A=-2.2423E+04 H2A=-3.9473E+04	H1B= 2.1461E+04 H2B= 1.4324E+04	V1A= 1.0820E+05 V2A= 1.2339E+05	V1B= 8.8248E+03 V2B= 1.7872E+04	NGX= 2.6074E+03

Table 5 (Cont.)

LANDING GEAR REACTIONS FOR B-52 AIRCRAFT ON TEST STAND

XN=570.0	PHI= 215.0	UINF= 80.0		
H1A=-2.2218E+04	H1B= 2.6907E+04	V1A= 1.4538E+05	V1B=-3.1369E+04	
H2A=-4.8590E+04	H2B= 3.4813E+03	V2A= 1.4571E+05	V2B=-2.5784E+04	NGX= 4.6395E+03
XN=570.0	PHI= 245.0	UINF= 25.0		
H1A=-2.2447E+04	H1B= 2.3212E+04	V1A= 6.1378E+04	V1B= 6.0380E+04	
H2A=-3.1943E+04	H2B= 2.4000E+04	V2A= 9.0292E+04	V2B= 5.8888E+04	NGX=-2.0092E+02
XN=570.0	PHI= 245.0	UINF= 30.0		
H1A=-2.2342E+04	H1B= 2.3443E+04	V1A= 6.1765E+04	V1B= 6.0329E+04	
H2A=-3.3788E+04	H2B= 2.2349E+04	V2A= 9.7460E+04	V2B= 5.2238E+04	NGX=-2.8932E+02
XN=570.0	PHI= 245.0	UINF= 35.0		
H1A=-2.2217E+04	H1B= 2.3716E+04	V1A= 6.2223E+04	V1B= 6.0248E+04	
H2A=-3.5968E+04	H2B= 2.0398E+04	V2A= 1.0593E+05	V2B= 4.4379E+04	NGX=-3.9380E+02
XN=570.0	PHI= 245.0	UINF= 40.0		
H1A=-2.2079E+04	H1B= 2.4032E+04	V1A= 6.2750E+04	V1B= 6.0197E+04	
H2A=-3.8469E+04	H2B= 1.8148E+04	V2A= 1.1571E+05	V2B= 3.5311E+04	NGX=-5.1434E+02
XN=570.0	PHI= 245.0	UINF= 45.0		
H1A=-2.1911E+04	H1B= 2.4389E+04	V1A= 6.3349E+04	V1B= 6.0117E+04	
H2A=-4.1335E+04	H2B= 1.5597E+04	V2A= 1.2678E+05	V2B= 2.5034E+04	NGX=-6.9097E+02
XN=570.0	PHI= 245.0	UINF= 50.0		
H1A=-2.1307E+04	H1B= 2.5713E+04	V1A= 6.9566E+04	V1B= 5.9821E+04	
H2A=-5.1900E+04	H2B= 6.1436E+03	V2A= 1.4784E+05	V2B=-1.3052E+04	NGX=-1.1573E+03
XN=570.0	PHI= 245.0	UINF= 80.0		
H1A=-2.0239E+04	H1B= 2.8066E+04	V1A= 6.9508E+04	V1B= 5.9295E+04	
H2A=-7.0603E+04	H2B=-1.0662E+04	V2A= 2.4082E+05	V2B=-8.0761E+04	NGX=-2.0974E+03
XN=570.0	PHI= 275.0	UINF= 25.0		
H1A=-2.2415E+04	H1B= 2.3249E+04	V1A= 6.6247E+04	V1B= 5.5529E+04	
H2A=-3.0967E+04	H2B= 2.4662E+04	V2A= 8.7158E+04	V2B= 6.1240E+04	NGX=-5.3719E+02
XN=570.0	PHI= 275.0	UINF= 30.0		
H1A=-2.2299E+04	H1B= 2.3497E+04	V1A= 6.8776E+04	V1B= 5.3335E+04	
H2A=-3.2412E+04	H2B= 2.3303E+04	V2A= 9.2947E+04	V2B= 5.9624E+04	NGX=-7.7349E+02
XN=570.0	PHI= 275.0	UINF= 35.0		
H1A=-2.2134E+04	H1B= 2.3789E+04	V1A= 7.1765E+04	V1B= 5.0748E+04	
H2A=-3.4095E+04	H2B= 2.1697E+04	V2A= 9.9789E+04	V2B= 4.8988E+04	NGX=-1.0528E+03

Table 5 (Cont.)

LANDING GEAR REACTIONS FOR B-52 AIRCRAFT ON TEST STAND

XN=578.0	PHI= 275.0	UINF= 40.0		
H1A=-2.1990E+04	H1B= 2.4127E+04	V1A= 7.5214E+04	V1B= 4.7764E+04	
H2A=-3.6037E+04	H2B= 1.9843E+04	V2A= 1.0768E+05	V2B= 4.1331E+04	NGX=-1.3751E+03
XN=578.0	PHI= 275.0	UINF= 45.0		
H1A=-2.1805E+04	H1B= 2.4509E+04	V1A= 7.9123E+04	V1B= 4.4381E+04	
H2A=-3.8237E+04	H2B= 1.7743E+04	V2A= 1.1663E+05	V2B= 3.2652E+04	NGX=-1.7404E+03
XN=578.0	PHI= 275.0	UINF= 50.0		
H1A=-2.1120E+04	H1B= 2.5926E+04	V1A= 9.3609E+04	V1B= 3.1846E+04	
H2A=-4.0394E+04	H2B= 9.9592E+03	V2A= 1.4978E+05	V2B= 4.9132E+02	NGX=-3.0940E+03
XN=578.0	PHI= 275.0	UINF= 80.0		
H1A=-1.9901E+04	H1B= 2.8446E+04	V1A= 1.1936E+05	V1B= 9.5617E+03	
H2A=-6.0894E+04	H2B=-3.8786E+03	V2A= 2.0872E+05	V2B=-5.6684E+04	NGX=-5.5004E+03
XN=578.0	PHI= 305.0	UINF= 25.0		
H1A=-2.2842E+04	H1B= 2.2909E+04	V1A= 6.8949E+04	V1B= 5.3055E+04	
H2A=-2.8884E+04	H2B= 2.6821E+04	V2A= 7.8979E+04	V2B= 6.9568E+04	NGX=-4.9622E+02
XN=578.0	PHI= 305.0	UINF= 30.0		
H1A=-2.2910E+04	H1B= 2.3008E+04	V1A= 7.2668E+04	V1B= 4.9780E+04	
H2A=-2.9382E+04	H2B= 2.6413E+04	V2A= 8.1169E+04	V2B= 6.7616E+04	NGX=-7.1456E+02
XN=578.0	PHI= 305.0	UINF= 35.0		
H1A=-2.2991E+04	H1B= 2.3123E+04	V1A= 7.7063E+04	V1B= 4.5910E+04	
H2A=-2.9971E+04	H2B= 2.5929E+04	V2A= 8.3757E+04	V2B= 6.5310E+04	NGX=-9.7259E+02
XN=578.0	PHI= 305.0	UINF= 40.0		
H1A=-2.3085E+04	H1B= 2.3257E+04	V1A= 8.2133E+04	V1B= 4.1444E+04	
H2A=-3.0651E+04	H2B= 2.5372E+04	V2A= 8.6744E+04	V2B= 6.2650E+04	NGX=-1.2703E+03
XN=578.0	PHI= 305.0	UINF= 45.0		
H1A=-2.3190E+04	H1B= 2.3408E+04	V1A= 8.7880E+04	V1B= 3.6383E+04	
H2A=-3.1421E+04	H2B= 2.4740E+04	V2A= 9.0128E+04	V2B= 5.9634E+04	NGX=-1.6078E+03
XN=578.0	PHI= 305.0	UINF= 60.0		
H1A=-2.3582E+04	H1B= 2.3970E+04	V1A= 1.0918E+05	V1B= 1.7626E+04	
H2A=-3.4276E+04	H2B= 2.2398E+04	V2A= 1.0267E+05	V2B= 4.8459E+04	NGX=-2.8582E+03
XN=578.0	PHI= 305.0	UINF= 80.0		
H1A=-2.4278E+04	H1B= 2.4968E+04	V1A= 1.4704E+05	V1B=-1.5718E+04	
H2A=-3.9351E+04	H2B= 1.8235E+04	V2A= 1.2497E+05	V2B= 2.8593E+04	NGX=-5.0813E+03

Table 5 (Cont.)

LANDING GEAR REACTIONS FOR B-52 AIRCRAFT ON TEST STAND

XN=578.0	PH1= 355.0	U1NF= 23.0		
H1A=-2.2830E+04	H1B= 2.2917E+04	V1A= 6.1328E+04	V1B= 6.0519E+04	
H2A=-2.8100E+04	H2B= 2.7926E+04	V2A= 7.5151E+04	V2B= 7.4251E+04	NGX=-2.0974E+02
XN=378.0	PH1= 333.0	U1NF= 50.0		
H1A=-2.2925E+04	H1B= 2.3018E+04	V1A= 6.1981E+04	V1B= 6.0328E+04	
H2A=-2.8255E+04	H2B= 2.8003E+04	V2A= 7.3637E+04	V2B= 7.4560E+04	NGX=-3.0202E+02
XN=378.0	PH1= 533.0	U1NF= 35.0		
H1A=-2.3008E+04	H1B= 2.3158E+04	V1A= 6.2316E+04	V1B= 6.0339E+04	
H2A=-2.8453E+04	H2B= 2.8093E+04	V2A= 7.6253E+04	V2B= 7.4489E+04	NGX=-4.1104E+02
XN=378.0	PH1= 553.0	U1NF= 40.0		
H1A=-2.3106E+04	H1B= 2.3276E+04	V1A= 6.3154E+04	V1B= 6.0532E+04	
H2A=-2.8644E+04	H2B= 2.8200E+04	V2A= 7.6944E+04	V2B= 7.4639E+04	NGX=-3.5693E+02
XN=578.0	PH1= 355.0	U1NF= 45.0		
H1A=-2.3217E+04	H1B= 2.3433E+04	V1A= 6.3835E+04	V1B= 6.0566E+04	
H2A=-2.8881E+04	H2B= 2.8319E+04	V2A= 7.7726E+04	V2B= 7.4808E+04	NGX=-6.7935E+02
XN=378.0	PH1= 355.0	U1NF= 60.0		
H1A=-2.3630E+04	H1B= 2.4014E+04	V1A= 6.6430E+04	V1B= 6.0620E+04	
H2A=-2.9760E+04	H2B= 2.8761E+04	V2A= 8.0622E+04	V2B= 7.5434E+04	NGX=-1.2081E+03
XN=578.0	PH1= 333.0	U1NF= 80.0		
H1A=-2.4364E+04	H1B= 2.3046E+04	V1A= 7.1043E+04	V1B= 6.0714E+04	
H2A=-3.1323E+04	H2B= 2.9347E+04	V2A= 8.3772E+04	V2B= 7.6548E+04	NGX=-2.1477E+03

Table 6
LANDING GEAR REACTIONS FOR E-3 AIRCRAFT ON TEST STAND

AIRCRAFT E-3	AIRCRAFT BOEING 0610 RAMP		
XN=573.0	PHI= 5.0	GINF= 45.0	
NGXS=5.4[illegible]E+02	NGYS=4.5[illegible]E+02	NGZ= 0.5124[illegible]E+05	
HAS=6.[illegible]E+04	HPS= 7.2[illegible]E+04	VAS= 9.[illegible]E+04	VHS= 1.0463E+05
XN=573.0	PHI= 5.0	GINF= 30.0	
NGXS=7.[illegible]E+02	NGYS=1.3807E+03	NGZ= 0.5538E+05	
HAS=6.9034E+04	HPS= 7.3917E+04	VAS= 9.4174E+04	VHS= 1.0649E+05
XN=573.0	PHI= 5.0	GINF= 35.0	
NGXS=1.05[illegible]E+03	NGYS=1.0793E+03	NGZ= 0.5018E+05	
HAS=6.8405E+04	HPS= 7.5124E+04	VAS= 9.2535E+04	VHS= 1.0476E+05
XN=573.0	PHI= 5.0	GINF= 40.0	
NGXS=1.3[illegible]E+03	NGYS=2.4[illegible]E+03	NGZ= 0.4573E+05	
HAS=6.7[illegible]E+04	HPS= 7.6527E+04	VAS= 9.0209E+04	VHS= 1.1[illegible]E+05
XN=573.0	PHI= 5.0	GINF= 45.0	
NGXS=1.71[illegible]E+03	NGYS=3.10[illegible]E+03	NGZ= 0.4203E+05	
HAS=6.713[illegible]E+04	HPS= 7.8111E+04	VAS= 8.7790E+04	VHS= 1.1[illegible]E+05
XN=573.0	PHI= 5.0	GINF= 50.0	
NGXS=2.04[illegible]E+03	NGYS=3.[illegible]E+03	NGZ= 0.[illegible]E+05	
HAS=6.[illegible]E+04	HPS= 8.3489E+04	VAS= 7.8849E+04	VHS= 1.3005E+05
XN=573.0	PHI= 5.0	GINF= 80.0	
NGXS=3.41[illegible]E+03	NGYS=4.81[illegible]E+03	NGZ= 0.3[illegible]E+05	
HAS=5.97[illegible]E+04	HPS= 9.4424E+04	VAS= 6.2[illegible]E+04	VHS= 1.[illegible]E+05
XN=573.0	PHI= 35.0	GINF= 25.0	
NGXS=5.[illegible]E+02	NGYS=2.[illegible]E+03	NGZ= 0.5147E+05	
HAS=6.[illegible]E+04	HPS= 7.5502E+04	VAS= 9.3038E+04	VHS= 1.0658E+05
XN=573.0	PHI= 35.0	GINF= 30.0	
NGXS=8.0754E+02	NGYS=4.[illegible]E+03	NGZ= 0.5[illegible]E+05	
HAS=6.[illegible]E+04	HPS= 7.7791E+04	VAS= 9.0238E+04	VHS= 1.0978E+05

Table 6 (Cont.)
LANDING GEAR REACTIONS FOR E-3 AIRCRAFT ON TEST STAND

XN=573.0	PHI= 35.0	DINF= 35.0	
NGX=-1.0992E+03	NGY=-5.5382E+03	NG = 8.6150E+03	
HA=-8.2163E+04	HB= 6.0402E+04	VA= 8.7037E+04	VB= 1.1357E+05
XN=573.0	PHI= 35.0	DINF= 40.0	
NGX=-1.4356E+03	NGY=-7.2355E+03	NGZ= 8.6746E+03	
HA=-5.9593E+04	HB= 8.3415E+04	VA= 8.5266E+04	VB= 1.1795E+05
XN=573.0	PHI= 35.0	DINF= 45.0	
NGX=-1.8170E+03	NGY=-9.1549E+03	NGZ= 8.7422E+03	
HA=-5.8679E+04	HB= 8.6829E+04	VA= 7.9035E+04	VB= 1.2290E+05
XN=573.0	PHI= 35.0	DINF= 60.0	
NGX=-3.2302E+03	NGY=-1.6275E+04	NGZ= 8.9925E+03	
HA=-4.5602E+04	HB= 9.9462E+04	VA= 6.5251E+04	VB= 1.4127E+05
XN=573.0	PHI= 35.0	DINF= 80.0	
NGX=-5.7465E+03	NGY=-2.8934E+04	NGZ= 9.4376E+03	
HA=-2.6608E+04	HB= 1.2198E+05	VA= 3.5275E+04	VB= 1.7392E+05
XN=573.0	PHI= 65.0	DINF= 25.0	
NGX=-2.3075E+02	NGY=-3.1486E+03	NGZ= 8.3669E+03	
HA=-6.5446E+04	HB= 7.6522E+04	VA= 9.3905E+04	VB= 1.0587E+05
XN=573.0	PHI= 65.0	DINF= 30.0	
NGX=-5.3226E+02	NGY=-4.5340E+03	NGZ= 8.3433E+03	
HA=-6.3196E+04	HB= 7.9145E+04	VA= 9.1535E+04	VB= 1.0876E+05
XN=573.0	PHI= 65.0	DINF= 35.0	
NGX=-4.5224E+02	NGY=-6.1713E+03	NGZ= 8.3155E+03	
HA=-6.0537E+04	HB= 8.2245E+04	VA= 8.8735E+04	VB= 1.1218E+05
XN=573.0	PHI= 65.0	DINF= 40.0	
NGX=-5.9073E+02	NGY=-8.0604E+03	NGZ= 8.2835E+03	
HA=-5.7468E+04	HB= 8.5822E+04	VA= 8.5504E+04	VB= 1.1613E+05
XN=573.0	PHI= 65.0	DINF= 45.0	
NGX=-7.4764E+02	NGY=-1.0201E+04	NGZ= 8.2471E+03	
HA=-5.3990E+04	HB= 8.9876E+04	VA= 8.1842E+04	VB= 1.2060E+05

Table 6 (Cont.)

LANDING GEAR REACTIONS FOR E-3 AIRCRAFT ON TEST STAND

XN=573.0	PHI= 65.0	GINF= 60.0	
NGX=-1.3291E+03	NGY=-1.8136E+04	NGZ= 8.1124E+03	
HA=-4.1102E+04	HB= 1.0490E+05	VA= 8.8272E+04	VB= 1.3717E+05
XN=573.0	PHI= 65.0	GINF= 60.0	
NGX=-2.3629E+03	NGY=-3.2242E+04	NGZ= 7.8729E+03	
HA=-1.8109E+04	HB= 1.3161E+05	VA= 9.4148E+04	VB= 1.6664E+05
XN=573.0	PHI= 95.0	GINF= 25.0	
NGX= 2.5604E+02	NGY=-2.1246E+03	NGZ= 8.5342E+03	
HA=-6.6084E+04	HB= 7.4070E+04	VA= 9.3004E+04	VB= 1.0418E+05
XN=573.0	PHI= 95.0	GINF= 30.0	
NGX= 5.6985E+02	NGY=-3.0577E+03	NGZ= 8.5843E+03	
HA=-6.4068E+04	HB= 7.3613E+04	VA= 9.0244E+04	VB= 1.0634E+05
XN=573.0	PHI= 95.0	GINF= 35.0	
NGX= 5.0340E+02	NGY=-4.1646E+03	NGZ= 8.6435E+03	
HA=-6.1730E+04	HB= 7.7438E+04	VA= 8.6978E+04	VB= 1.0888E+05
XN=573.0	PHI= 95.0	GINF= 40.0	
NGX= 6.5751E+02	NGY=-5.4395E+03	NGZ= 8.7119E+03	
HA=-5.9053E+04	HB= 7.9543E+04	VA= 8.3209E+04	VB= 1.1182E+05
XN=573.0	PHI= 95.0	GINF= 45.0	
NGX= 8.3216E+02	NGY=-6.8844E+03	NGZ= 8.7893E+03	
HA=-5.5497E+04	HB= 8.1929E+04	VA= 7.8938E+04	VB= 1.1515E+05
XN=573.0	PHI= 95.0	GINF= 60.0	
NGX= 1.4794E+03	NGY=-1.2239E+04	NGZ= 9.0763E+03	
HA=-4.4664E+04	HB= 9.0771E+04	VA= 6.3108E+04	VB= 1.2748E+05
XN=573.0	PHI= 95.0	GINF= 80.0	
NGX= 2.6300E+03	NGY=-2.1758E+04	NGZ= 9.5864E+03	
HA=-2.4531E+04	HB= 1.0649E+05	VA= 3.4966E+04	VB= 1.4940E+05
XN=573.0	PHI= 125.0	GINF= 25.0	
NGX= 5.3595E+02	NGY=-1.0315E+04	NGZ= 8.6272E+03	
HA=-6.7379E+04	HB= 7.1918E+04	VA= 9.3067E+04	VB= 1.0294E+05

Table 6 (Cont.)
LANDING GEAR REACTIONS FOR E-3 AIRCRAFT ON TEST STAND

XN=573.0	PHI= 125.0	UINF= 30.0	
NGX= 4.6827E+02	NGY=-1.4854E+03	NGZ= 9.0062E+03	
HA=-6.5979E+04	HB= 7.2515E+04	VA= 9.0329E+04	VB= 1.0455E+05
XN=573.0	PHI= 125.0	UINF= 35.0	
NGX= 6.6513E+02	NGY=-2.0217E+03	NGZ= 9.2177E+03	
HA=-6.4324E+04	HB= 7.3221E+04	VA= 8.7094E+04	VB= 1.0645E+05
XN=573.0	PHI= 125.0	UINF= 40.0	
NGX= 8.0874E+02	NGY=-2.6406E+03	NGZ= 9.4618E+03	
HA=-6.2415E+04	HB= 7.4035E+04	VA= 8.5360E+04	VB= 1.0865E+05
XN=573.0	PHI= 125.0	UINF= 45.0	
NGX= 1.0995E+03	NGY=-3.3421E+03	NGZ= 9.7584E+03	
HA=-6.0201E+04	HB= 7.4958E+04	VA= 7.9129E+04	VB= 1.1113E+05
XN=573.0	PHI= 125.0	UINF= 60.0	
NGX= 1.9547E+03	NGY=-5.9415E+03	NGZ= 1.0764E+04	
HA=-5.2253E+04	HB= 7.6377E+04	VA= 6.3448E+04	VB= 1.2034E+05
XN=573.0	PHI= 125.0	UINF= 80.0	
NGX= 3.4750E+03	NGY=-1.0563E+04	NGZ= 1.2586E+04	
HA=-3.7978E+04	HB= 8.4457E+04	VA= 3.5570E+04	VB= 1.3671E+05
XN=573.0	PHI= 155.0	UINF= 25.0	
NGX= 5.2539E+01	NGY=-5.1991E+01	NGZ= 8.8029E+03	
HA=-7.0011E+04	HB= 7.0133E+04	VA= 9.8573E+04	VB= 9.8631E+04
XN=573.0	PHI= 155.0	UINF= 30.0	
NGX= 4.6857E+01	NGY=-7.4868E+01	NGZ= 8.6833E+03	
HA=-6.9709E+04	HB= 6.9945E+04	VA= 9.8258E+04	VB= 9.8341E+04
XN=573.0	PHI= 155.0	UINF= 35.0	
NGX= 6.3777E+01	NGY=-1.0190E+02	NGZ= 8.7782E+03	
HA=-6.9483E+04	HB= 6.9723E+04	VA= 9.7885E+04	VB= 9.7998E+04
XN=573.0	PHI= 155.0	UINF= 40.0	
NGX= 8.3301E+01	NGY=-1.3310E+02	NGZ= 8.8878E+03	
HA=-6.9153E+04	HB= 6.9466E+04	VA= 9.7455E+04	VB= 9.7602E+04

Table 6 (Cont.)
LANDING GEAR REACTIONS FOR E-3 AIRCRAFT ON TEST STAND

XN=573.0	PHI= 155.0	GINF= 45.0	
NGX= 1.0543E+02	NGY=-1.6845E+02	NGZ= 9.0119E+03	
HA=-6.6779E+04	HB= 6.9178E+04	VA= 9.6908E+04	VB= 9.7154E+04
XN=573.0	PHI= 155.0	GINF= 60.0	
NGX= 1.6743E+02	NGY=-2.9947E+02	NGZ= 9.4720E+03	
HA=-6.7392E+04	HB= 6.8098E+04	VA= 9.5163E+04	VB= 9.5493E+04
XN=573.0	PHI= 155.0	GINF= 80.0	
NGX= 3.5742E+02	NGY=-3.5239E+02	NGZ= 1.0290E+04	
HA=-6.6952E+04	HB= 6.8102E+04	VA= 9.1932E+04	VB= 9.2540E+04
XN=573.0	PHI= 165.0	GINF= 25.0	
NGX= 2.7377E+02	NGY= 4.0097E+03	NGZ= 9.0440E+03	
HA=-7.1539E+04	HB= 6.7066E+04	VA= 1.0338E+05	VB= 9.1685E+04
XN=573.0	PHI= 165.0	GINF= 50.0	
NGX= 5.9943E+02	NGY= 1.4594E+03	NGZ= 9.5134E+03	
HA=-7.1569E+04	HB= 6.5560E+04	VA= 1.0519E+05	VB= 8.8339E+04
XN=573.0	PHI= 165.0	GINF= 55.0	
NGX= 5.3659E+02	NGY= 1.9791E+03	NGZ= 9.6927E+03	
HA=-7.2478E+04	HB= 6.3754E+04	VA= 1.0752E+05	VB= 8.4384E+04
XN=573.0	PHI= 165.0	GINF= 40.0	
NGX= 7.0085E+02	NGY= 2.5850E+03	NGZ= 1.0017E+04	
HA=-7.3065E+04	HB= 6.1671E+04	VA= 1.0977E+05	VB= 7.9821E+04
XN=573.0	PHI= 165.0	GINF= 45.0	
NGX= 8.6701E+02	NGY= 3.2716E+03	NGZ= 1.0341E+04	
HA=-7.3730E+04	HB= 5.9409E+04	VA= 1.1256E+05	VB= 7.4650E+04
XN=573.0	PHI= 165.0	GINF= 60.0	
NGX= 1.5769E+03	NGY= 5.8162E+03	NGZ= 1.2013E+04	
HA=-7.6194E+04	HB= 5.0558E+04	VA= 1.2287E+05	VB= 5.5486E+04
XN=573.0	PHI= 165.0	GINF= 80.0	
NGX= 2.6034E+03	NGY= 1.0340E+04	NGZ= 1.4807E+04	
HA=-8.0576E+04	HB= 5.5001E+04	VA= 1.4122E+05	VB= 2.1416E+04

Table 6 (Cont.)
LANDING GEAR REACTIONS FOR E-3 AIRCRAFT ON TEST STAND

XN=573.0	PHI= 215.0	DINF= 25.0	
NGX= 2.7090E+02	NGY= 2.2094E+03	NGZ= 6.5377E+03	
HA=-7.4156E+04	HB= 6.5985E+04	VA= 1.0477E+05	VB= 9.2427E+04
XN=573.0	PHI= 215.0	DINF= 30.0	
NGX= 5.4009E+02	NGY= 3.1815E+03	NGZ= 8.5893E+03	
HA=-7.5736E+04	HB= 6.5907E+04	VA= 1.0718E+05	VB= 8.9402E+04
XN=573.0	PHI= 215.0	DINF= 35.0	
NGX= 5.3596E+02	NGY= 4.3304E+03	NGZ= 8.6503E+03	
HA=-7.7606E+04	HB= 6.1548E+04	VA= 1.1033E+05	VB= 8.5840E+04
XN=573.0	PHI= 215.0	DINF= 40.0	
NGX= 6.9349E+02	NGY= 5.6560E+03	NGZ= 8.7207E+03	
HA=-7.9765E+04	HB= 5.8841E+04	VA= 1.1332E+05	VB= 8.1722E+04
XN=573.0	PHI= 215.0	DINF= 45.0	
NGX= 8.7770E+02	NGY= 7.1564E+03	NGZ= 8.8005E+03	
HA=-8.2216E+04	HB= 5.5728E+04	VA= 1.1704E+05	VB= 7.7036E+04
XN=573.0	PHI= 215.0	DINF= 60.0	
NGX= 1.5604E+03	NGY= 1.2726E+04	NGZ= 9.0962E+03	
HA=-9.1271E+04	HB= 4.4192E+04	VA= 1.3085E+05	VB= 5.9762E+04
XN=573.0	PHI= 215.0	DINF= 80.0	
NGX= 2.7740E+03	NGY= 2.2624E+04	NGZ= 9.6219E+03	
HA=-1.0736E+05	HB= 2.3683E+04	VA= 1.5540E+05	VB= 2.9019E+04
XN=573.0	PHI= 245.0	DINF= 25.0	
NGX=-2.1495E+02	NGY= 5.8376E+03	NGZ= 8.3948E+03	
HA=-7.7623E+04	HB= 6.4214E+04	VA= 1.0743E+05	VB= 9.2160E+04
XN=573.0	PHI= 245.0	DINF= 30.0	
NGX=-3.0949E+02	NGY= 5.5261E+03	NGZ= 8.3855E+03	
HA=-8.0730E+04	HB= 6.1422E+04	VA= 1.1101E+05	VB= 8.9024E+04
XN=573.0	PHI= 245.0	DINF= 35.0	
NGX=-4.2126E+02	NGY= 7.5216E+03	NGZ= 8.3702E+03	
HA=-8.4402E+04	HB= 5.8122E+04	VA= 1.1524E+05	VB= 8.5316E+04

Table 6 (Cont.)
LANDING GEAR REACTIONS FOR E-3 AIRCRAFT ON TEST STAND

XN=573.0	PHI= 245.0	DINF= 40.0	
NGX=-5.5021E+02	NGY= 9.8242E+03	NGZ= 8.3549E+03	
HA=-8.8639E+04	HB= 5.4314E+04	VA= 1.2012E+05	VB= 8.1039E+04
XN=573.0	PHI= 245.0	DINF= 45.0	
NGX=-6.9636E+02	NGY= 1.2434E+04	NGZ= 8.3375E+03	
HA=-9.3442E+04	HB= 4.9998E+04	VA= 1.2565E+05	VB= 7.6191E+04
XN=573.0	PHI= 245.0	DINF= 50.0	
NGX=-1.2366E+03	NGY= 2.2104E+04	NGZ= 8.2730E+03	
HA=-1.1164E+05	HB= 3.4005E+04	VA= 1.4615E+05	VB= 5.8225E+04
XN=573.0	PHI= 245.0	DINF= 80.0	
NGX=-2.2605E+03	NGY= 3.9297E+04	NGZ= 8.1564E+03	
HA=-1.4267E+05	HB= 5.5729E+03	VA= 1.8260E+05	VB= 2.6285E+04
XN=573.0	PHI= 275.0	DINF= 25.0	
NGX=-5.4602E+02	NGY= 5.4329E+03	NGZ= 8.4400E+03	
HA=-7.6368E+04	HB= 6.5531E+04	VA= 1.0699E+05	VB= 9.2709E+04
XN=573.0	PHI= 275.0	DINF= 30.0	
NGX=-7.6667E+02	NGY= 4.9434E+03	NGZ= 8.4487E+03	
HA=-7.8952E+04	HB= 6.3319E+04	VA= 1.1038E+05	VB= 8.9413E+04
XN=573.0	PHI= 275.0	DINF= 35.0	
NGX=-1.0702E+03	NGY= 6.7265E+03	NGZ= 8.4589E+03	
HA=-8.1902E+04	HB= 6.0703E+04	VA= 1.1439E+05	VB= 8.6391E+04
XN=573.0	PHI= 275.0	DINF= 40.0	
NGX=-1.3978E+03	NGY= 8.7882E+03	NGZ= 8.4708E+03	
HA=-8.5479E+04	HB= 5.7686E+04	VA= 1.1901E+05	VB= 8.2442E+04
XN=573.0	PHI= 275.0	DINF= 45.0	
NGX=-1.7691E+03	NGY= 1.1123E+04	NGZ= 8.4841E+03	
HA=-8.9441E+04	HB= 5.4266E+04	VA= 1.2425E+05	VB= 7.7567E+04
XN=573.0	PHI= 275.0	DINF= 60.0	
NGX=-3.1451E+03	NGY= 1.9774E+04	NGZ= 8.5338E+03	
HA=-1.0413E+05	HB= 4.1591E+04	VA= 1.4366E+05	VB= 6.1383E+04

Table 6 (Cont.)
LANDING GEAR REACTIONS FOR E-3 AIRCRAFT ON TEST STAND

XA=573.0	PHI= 475.0	GIAF= 60.0	
NGX=-5.5912E+03	NGY= 5.5153E+04	NGZ= 8.6226E+03	
HA=-1.3023E+05	HB= 1.4086E+04	VA= 1.7818E+05	VB= 3.1900E+04
XN=573.0	PHI= 305.0	GIAF= 25.0	
NGX=-5.6451E+02	NGY= 1.0961E+03	NGZ= 8.5444E+03	
HA=-7.3067E+04	HB= 6.9235E+04	VA= 1.0457E+05	VB= 9.5671E+04
XN=573.0	PHI= 305.0	GIAF= 30.0	
NGX=-8.1269E+02	NGY= 1.5784E+03	NGZ= 8.5962E+03	
HA=-7.4169E+04	HB= 6.8652E+04	VA= 1.0669E+05	VB= 9.4079E+04
XN=573.0	PHI= 305.0	GIAF= 35.0	
NGX=-1.1084E+03	NGY= 2.1484E+03	NGZ= 8.6597E+03	
HA=-7.5472E+04	HB= 6.7582E+04	VA= 1.0964E+05	VB= 9.2197E+04
XN=573.0	PHI= 305.0	GIAF= 40.0	
NGX=-1.4451E+03	NGY= 2.8066E+03	NGZ= 8.7329E+03	
HA=-7.6976E+04	HB= 6.7167E+04	VA= 1.1260E+05	VB= 9.0026E+04
XN=573.0	PHI= 305.0	GIAF= 45.0	
NGX=-1.8290E+03	NGY= 3.5514E+03	NGZ= 8.8160E+03	
HA=-7.8480E+04	HB= 6.6265E+04	VA= 1.1639E+05	VB= 8.7565E+04
XN=573.0	PHI= 305.0	GIAF= 60.0	
NGX=-3.2516E+03	NGY= 6.3136E+03	NGZ= 9.1237E+03	
HA=-8.4994E+04	HB= 6.2924E+04	VA= 1.2970E+05	VB= 7.8446E+04
XN=573.0	PHI= 305.0	GIAF= 80.0	
NGX=-5.7806E+03	NGY= 1.1224E+04	NGZ= 9.6707E+03	
HA=-9.6220E+04	HB= 5.8965E+04	VA= 1.5335E+05	VB= 6.2234E+04
XN=573.0	PHI= 335.0	GIAF= 25.0	
NGX=-5.1805E+02	NGY= 1.0398E+04	NGZ= 8.4015E+03	
HA=-7.1434E+04	HB= 7.1194E+04	VA= 1.0070E+05	VB= 1.0000E+05
XN=573.0	PHI= 335.0	GIAF= 30.0	
NGX=-4.5800E+02	NGY= 1.4973E+04	NGZ= 8.3932E+03	
HA=-7.1819E+04	HB= 7.1473E+04	VA= 1.0132E+05	VB= 1.0032E+05

Table 6 (Cont.)
LANDING GEAR REACTIONS FOR E-3 AIRCRAFT ON TEST STAND

XN=573.0	PHI= 335.0	DINF= 35.0	
NGX=-6.2359E+02	NGY= 2.0379E+02	NGZ= 6.3834E+03	
MA=-7.2275E+04	MH= 7.1803E+04	VA= 1.0205E+05	VH= 1.0069E+05
XN=573.0	PHI= 335.0	DINF= 40.0	
NGX=-6.1428E+02	NGY= 2.0618E+02	NGZ= 6.3721E+03	
MA=-7.2757E+04	MH= 7.2163E+04	VA= 1.0259E+05	VH= 1.0112E+05
XN=573.0	PHI= 335.0	DINF= 45.0	
NGX=-1.0305E+03	NGY= 3.3688E+02	NGZ= 6.3593E+03	
MA=-7.3391E+04	MH= 7.2614E+04	VA= 1.0385E+05	VH= 1.0160E+05
XN=573.0	PHI= 335.0	DINF= 60.0	
NGX=-1.6320E+03	NGY= 5.9890E+02	NGZ= 6.3118E+03	
MA=-7.5552E+04	MH= 7.4210E+04	VA= 1.0740E+05	VH= 1.0340E+05
XN=573.0	PHI= 335.0	DINF= 80.0	
NGX=-3.2589E+03	NGY= 1.0647E+03	NGZ= 6.2273E+03	
MA=-7.[illegible]5E+04	MH= 7.7049E+04	VA= 1.1370E+05	VH= 1.0659E+05

Table 7

LANDING GEAR REACTIONS FOR E-4 AIRCRAFT ON TEST STAND

XN=612.0	PHI= 5.0	GINF= 25.0	
NGX=-1.8295E+03	NGY= 7.3938E+02	NGZ= 2.0117E+03	
M1A=-1.7574E+04	M1B= 1.4470E+05	V1A= 2.2419E+05	V1B= 2.0488E+05
M2A=-5.8599E+03	M2B= 9.1334E+04	V2A= 2.4745E+03	V2B= 1.2031E+05
XN=612.0	PHI= 5.0	GINF= 30.0	
NGX=-2.3465E+03	NGY= 1.0647E+03	NGZ= 2.0149E+03	
M1A=-1.6017E+03	M1B= 1.3836E+05	V1A= 2.2350E+05	V1B= 2.0070E+05
M2A= 1.9044E+03	M2B= 9.9495E+04	V2A=-2.2695E+04	V2B= 1.4704E+05
XN=612.0	PHI= 5.0	GINF= 35.0	
NGX=-3.1539E+03	NGY= 1.4442E+03	NGZ= 2.0187E+03	
M1A=-1.0776E+05	M1B= 1.3087E+05	V1A= 2.3359E+05	V1B= 1.9576E+05
M2A= 1.0821E+04	M2B= 9.9140E+04	V2A=-5.2331E+04	V2B= 1.7863E+05
XN=612.0	PHI= 5.0	GINF= 40.0	
NGX=-4.1716E+03	NGY= 1.8928E+03	NGZ= 2.0231E+03	
M1A=-1.9055E+05	M1B= 1.2222E+05	V1A= 2.3947E+05	V1B= 1.9005E+05
M2A= 2.1110E+04	M2B= 7.0206E+04	V2A=-8.8585E+04	V2B= 2.1504E+05
XN=612.0	PHI= 5.0	GINF= 45.0	
NGX=-5.2797E+03	NGY= 2.3956E+03	NGZ= 2.0281E+03	
M1A=-2.0649E+05	M1B= 1.1242E+05	V1A= 2.4613E+05	V1B= 1.8358E+05
M2A= 3.2770E+04	M2B= 8.2800E+04	V2A=-1.2541E+05	V2B= 2.5639E+05
XN=612.0	PHI= 5.0	GINF= 50.0	
NGX=-9.3892E+03	NGY= 4.2588E+03	NGZ= 2.0466E+03	
M1A=-2.4334E+05	M1B= 7.6107E+04	V1A= 2.7081E+05	V1B= 1.5962E+05
M2A= 7.5981E+04	M2B= 1.2962E+05	V2A=-2.6927E+05	V2B= 4.0944E+05
XN=612.0	PHI= 5.0	GINF= 55.0	
NGX=-1.6687E+04	NGY= 7.5712E+03	NGZ= 2.0794E+03	
M1A=-3.0886E+05	M1B= 1.1545E+04	V1A= 3.1469E+05	V1B= 1.1702E+05
M2A= 1.5200E+05	M2B= 2.1271E+05	V2A=-5.2503E+05	V2B= 6.8163E+05
XN=612.0	PHI= 35.0	GINF= 25.0	
NGX=-1.8222E+03	NGY= 2.2526E+03	NGZ= 2.2209E+03	
M1A=-2.0053E+05	M1B= 1.1807E+05	V1A= 2.5250E+05	V1B= 1.7679E+05
M2A= 2.0575E+04	M2B= 7.2974E+04	V2A=-9.9882E+04	V2B= 2.2115E+05

Table 7 (Cont.)
LANDING GEAR REACTIONS FOR E-4 AIRCRAFT ON TEST STAND

XW=612.0	PHI= 35.0	GINF= 30.0	
NGX=-2.6240E+03	NGY= 3.2437E+03	NGZ= 2.3182E+03	
M1A=-2.1677E+05 M2A= 4.4560E+04	M1B= 1.0000E+05 M2B= 9.5058E+04	V1A= 2.6926E+05 V2A=-1.7004E+05	V1B= 1.6024E+05 V2B= 2.9225E+05
XW=612.0	PHI= 35.0	GINF= 35.0	
NGX=-3.5745E+04	NGY= 4.4150E+03	NGZ= 3.4268E+03	
M1A=-2.4545E+05 M2A= 7.3970E+04	M1B= 7.0657E+04 M2B= 1.2115E+05	V1A= 2.8907E+05 V2A=-2.5295E+05	V1B= 1.4068E+05 V2B= 3.7628E+05
XW=612.0	PHI= 35.0	GINF= 40.0	
NGX=-4.8[illegible]E+03	NGY= 5.7665E+03	NGZ= 2.5567E+03	
M1A=-2.6514E+05 M2A= 1.0856E+05	M1B= 3.4027E+04 M2B= 1.5126E+05	V1A= 3.1193E+05 V2A=-3.4862E+05	V1B= 1.1612E+05 V2B= 4.7324E+05
XW=612.0	PHI= 35.0	GINF= 45.0	
NGX=-5.9640E+03	NGY= 7.2963E+03	NGZ= 2.7059E+03	
M1A=-2.9331E+05 M2A= 1.3716E+05	M1B= 2.6113E+04 M2B= 1.8539E+05	V1A= 3.3784E+05 V2A=-4.3704E+05	V1B= 9.2547E+04 V2B= 5.8512E+05
XW=612.0	PHI= 35.0	GINF= 60.0	
NGX=-1.0496E+04	NGY= 1.2975E+04	NGZ= 3.2516E+03	
M1A=-3.4700E+05 M2A= 2.6135E+05	M1B=-7.7334E+04 M2B= 3.1186E+05	V1A= 4.3386E+05 V2A=-6.3084E+05	V1B=-2.2223E+03 V2B= 9.6033E+05
XW=612.0	PHI= 35.0	GINF= 80.0	
NGX=-1.6[illegible]E+04	NGY= 2.3066E+04	NGZ= 4.2216E+03	
M1A=-5.8[illegible]E+05 M2A= 4.0[illegible]E+05	M1B=-2.6124E+05 M2B= 5.3670E+05	V1A= 5.6456E+05 V2A=-1.5732E+06	V1B=-1.7070E+05 V2B= 1.7143E+06
XW=612.0	PHI= 65.0	GINF= 25.0	
NGX=-5.2045E+03	NGY= 5.3019E+03	NGZ= 1.5079E+03	
M1A=-2.0699E+05 M2A= 5.6910E+04	M1B= 1.1072E+05 M2B= 9.2453E+04	V1A= 2.6243E+05 V2A=-1.5305E+05	V1B= 1.6835E+05 V2B= 2.5210E+05
XW=612.0	PHI= 65.0	GINF= 30.0	
NGX=-7.4944E+02	NGY= 4.7547E+03	NGZ= 1.7215E+03	
M1A=-2.3093E+05 M2A= 6.3176E+04	M1B= 8.9425E+04 M2B= 1.0871E+05	V1A= 2.6557E+05 V2A=-2.1780E+05	V1B= 1.4809E+05 V2B= 3.3681E+05

Table 7 (Cont.)

LANDING GEAR REACTIONS FOR E-4 AIRCRAFT ON TEST STAND

RN=612.0	PHI= 65.0	GIMP= 35.0	
NGX=-1.0201E+03	NGY= 6.9717E+03	NGZ= 1.6193E+03	
M1A=-2.5600E+05	M1B= 6.9259E+04	V1A= 3.0854E+05	V1B= 1.2414E+05
M2A= 9.9215E+04	M2B= 1.5973E+05	V2A=-5.1796E+05	V2B= 9.3695E+05
RN=612.0	PHI= 65.0	GIMP= 40.0	
NGX=-1.3523E+03	NGY= 8.9528E+03	NGZ= 1.5015E+03	
M1A=-2.8879E+05	M1B= 5.9221E+04	V1A= 3.3737E+05	V1B= 9.6513E+04
M2A= 1.3[illegible]E+05	M2B= 1.7553E+05	V2A=-4.3353E+05	V2B= 5.5295E+05
RN=612.0	PHI= 65.0	GIMP= 45.0	
NGX=-1.6[illegible]E+03	NGY= 1.0698E+04	NGZ= 1.3679E+03	
M1A=-3.2070E+05	M1B= 4.9120E+03	V1A= 3.7303E+05	V1B= 6.5200E+04
M2A= 1.7063E+05	M2B= 2.1610E+05	V2A=-5.6451E+05	V2B= 6.8337E+05
RN=612.0	PHI= 65.0	GIMP= 50.0	
NGX=-2.9476E+03	NGY= 1.9019E+04	NGZ= 8.7253E+02	
M1A=-4.4[illegible]E+05	M1B=-1.1965E+05	V1A= 4.9108E+05	V1B=-5.0039E+04
M2A= 3.2167E+05	M2B= 3.0646E+05	V2A=-1.0499E+06	V2B= 1.1688E+06
RN=612.0	PHI= 65.0	GIMP= 60.0	
NGX=-5.3[illegible]E+03	NGY= 3.3811E+04	NGZ=-7.[illegible]E+00	
M1A=-6.0501E+05	M1B=-3.3649E+05	V1A= 7.0629E+05	V1B=-2.5713E+05
M2A= 5.8851E+05	M2B= 6.5376E+05	V2A=-1.9128E+06	V2B= 2.0511E+06
RN=612.0	PHI= 95.0	GIMP= 25.0	
NGX= 1.0733E+03	NGY= 5.1709E+03	NGZ= 1.7212E+03	
M1A=-1.9106E+05	M1B= 1.2578E+05	V1A= 2.4203E+05	V1B= 1.8512E+05
M2A= 1.7615E+04	M2B= 8.2294E+04	V2A=-7.0549E+04	V2B= 1.8736E+05
RN=612.0	PHI= 95.0	GIMP= 30.0	
NGX= 1.5455E+03	NGY= 4.5776E+03	NGZ= 1.5966E+03	
M1A=-2.0401E+05	M1B= 1.1112E+05	V1A= 2.5506E+05	V1B= 1.7224E+05
M2A= 3.5537E+04	M2B= 7.9678E+04	V2A=-1.2780E+05	V2B= 2.4360E+05
RN=612.0	PHI= 95.0	GIMP= 35.0	
NGX= 2.1036E+03	NGY= 6.2307E+03	NGZ= 1.4494E+03	
M1A=-2.2295E+05	M1B= 9.3784E+04	V1A= 2.6974E+05	V1B= 1.5702E+05
M2A= 5.0382E+04	M2B= 1.0022E+05	V2A=-1.9546E+05	V2B= 3.1005E+05

Table 7 (Cont.)

LANDING GEAR REACTIONS FOR E-4 AIRCRAFT ON TEST STAND

XN=612.0	PHI= 95.0	UINF= 40.0	
NGX= 2.7476E+03	NGY= 8.1380E+03	NGZ= 1.2795E+03	
H1A=-2.4249E+05	H1B= 7.3785E+04	V1A= 2.8669E+05	V1B= 1.3946E+05
H2A= 8.0817E+04	H2B= 1.2393E+05	V2A=-2.7353E+05	V2B= 3.8673E+05
XN=612.0	PHI= 95.0	UINF= 45.0	
NGX= 3.4774E+03	NGY= 1.0300E+04	NGZ= 1.0870E+03	
H1A=-2.e4e5E+05	H1B= 5.1119E+04	V1A= 3.0889E+05	V1B= 1.1956E+05
H2A= 1.0808E+05	H2B= 1.5079E+05	V2A=-3.e200E+05	V2B= 4.7364E+05
XN=612.0	PHI= 95.0	UINF= 60.0	
NGX= 6.1826E+03	NGY= 1.8314E+04	NGZ= 3.7345E+02	
H1A=-3.4670E+05	H1B=-3.2879E+04	V1A= 3.7705E+05	V1B= 4.5796E+04
H2A= 2.0907E+05	H2B= 2.5035E+05	V2A=-e.e989E+05	V2B= 7.9569E+05
XN=612.0	PHI= 95.0	UINF= 80.0	
NGX= 1.0590E+04	NGY= 3.2552E+04	NGZ=-e.9503E+02	
H1A=-4.9261E+05	H1B=-1.e221E+05	V1A= 5.0357E+05	V1B=-6.5336E+04
H2A= 3.9063E+05	H2B= 4.2734E+05	V2A=-1.e728E+06	V2B= 1.3682E+06
XN=612.0	PHI= 125.0	UINF= 25.0	
NGX= 1.1557E+03	NGY= 2.1600E+03	NGZ= 2.0621E+03	
H1A=-1.7698E+03	H1B= 1.4281E+05	V1A= 2.2734E+05	V1B= 2.0355E+05
H2A=-1.0902E+03	H2B= 4.1860E+04	V2A=-1.0290E+04	V2B= 1.2261E+05
XN=612.0	PHI= 125.0	UINF= 30.0	
NGX= 1.6642E+03	NGY= 3.1104E+03	NGZ= 2.0876E+03	
H1A=-1.84e4E+05	H1B= 1.35e4E+05	V1A= 2.3304E+05	V1B= 1.9878E+05
H2A= 8.4565E+03	H2B= 5.0280E+04	V2A=-4.1025E+04	V2B= 1.5035E+05
XN=612.0	PHI= 125.0	UINF= 35.0	
NGX= 2.2651E+03	NGY= 4.2335E+03	NGZ= 2.1176E+03	
H1A=-1.9414E+05	H1B= 1.2716E+05	V1A= 2.3977E+05	V1B= 1.9314E+05
H2A= 1.9759E+04	H2B= e.0208E+04	V2A=-7.7349E+04	V2B= 1.8319E+05
XN=612.0	PHI= 125.0	UINF= 40.0	
NGX= 2.95e5E+03	NGY= 5.5295E+03	NGZ= 2.1523E+03	
H1A=-2.0486E+05	H1B= 1.1737E+05	V1A= 2.4754E+05	V1B= 1.8663E+05
H2A= 3.2757E+04	H2B= 7.1664E+04	V2A=-1.1926E+05	V2B= 2.2096E+05

Table 7 (Cont.)
LANDING GEAR REACTIONS FOR E-4 AIRCRAFT ON TEST STAND

WN=12.0	PHI= 125.0	GINF= 45.0	
N0X= 3.7444E+01	N0Y= 6.9983E+03	N0Z= 2.1916E+03	
M1A=-2.1701E+05	M1H= 1.0628E+05	V1A= 2.5635E+05	V1H= 1.7925E+05
M2A= 9.7511E+04	M2H= 8.4847E+04	V2A=-1.8878E+05	V2H= 2.0383E+05
WN=12.0	PHI= 125.0	GINF= 60.0	
N0X= 6.0587E+03	N0Y= 1.2441E+04	N0Z= 2.3372E+03	
M1A=-2.8203E+04	M1H= 8.5194E+04	V1A= 2.0898E+05	V1H= 1.5192E+05
M2A= 1.0219E+05	M2H= 1.3278E+05	V2A=-3.4279E+05	V2H= 4.2271E+05
WN=12.0	PHI= 125.0	GINF= 80.0	
N0X= 1.1634E+04	N0Y= 2.2116E+04	N0Z= 2.5960E+03	
M1A=-3.4260E+03	M1H=-7.8580E+03	V1A= 3.4700E+05	V1H= 1.0333E+05
M2A= 1.9454E+05	M2H= 2.1829E+05	V2A=-6.5579E+05	V2H= 7.0515E+05
WN=12.0	PHI= 155.0	GINF= 25.0	
N0X= 6.1510E+01	N0Y= 2.9631E+01	N0Z= 2.3359E+03	
M1A=-1.5485E+05	M1H= 1.5904E+05	V1A= 2.1531E+05	V1H= 2.1435E+05
M2A=-2.1639E+04	M2H= 2.2543E+04	V2A= 5.0102E+04	V2H= 5.9328E+04
WN=12.0	PHI= 155.0	GINF= 30.0	
N0X= 8.8826E+01	N0Y= 4.2838E+01	N0Z= 2.4018E+03	
M1A=-1.8017E+05	M1H= 1.5901E+05	V1A= 2.1572E+05	V1H= 2.1434E+05
M2A=-2.1134E+04	M2H= 2.2438E+04	V2A= 5.0075E+04	V2H= 5.9224E+04
WN=12.0	PHI= 155.0	GINF= 35.0	
N0X= 1.2017E+02	N0Y= 5.8079E+01	N0Z= 2.0542E+03	
M1A=-1.6055E+05	M1H= 1.5897E+05	V1A= 2.1620E+05	V1H= 2.1432E+05
M2A=-2.0537E+04	M2H= 2.2310E+04	V2A= 5.0496E+04	V2H= 5.9102E+04
WN=12.0	PHI= 155.0	GINF= 40.0	
N0X= 1.5095E+02	N0Y= 7.5854E+01	N0Z= 2.8532E+03	
M1A=-1.4094E+05	M1H= 1.5892E+05	V1A= 2.1675E+05	V1H= 2.1429E+05
M2A=-1.9848E+04	M2H= 2.2163E+04	V2A= 5.0854E+04	V2H= 5.8961E+04
WN=12.0	PHI= 155.0	GINF= 45.0	
N0X= 1.9004E+02	N0Y= 9.6003E+01	N0Z= 3.0788E+03	
M1A=-1.2140E+05	M1H= 1.5887E+05	V1A= 2.1737E+05	V1H= 2.1427E+05
M2A=-1.9087E+04	M2H= 2.1998E+04	V2A= 5.0541E+04	V2H= 5.8800E+04

Table 7 (Cont.)
LANDING GEAR REACTIONS FOR E-4 AIRCRAFT ON TEST STAND

XN=612.0	PHI= 155.0	UINF= 60.0	
NGX= 5.5515E+02	NGY= 1.7087E+02	NGZ= 5.9142E+03	
M1A=-1.6332E+05	M1B= 1.5868E+05	V1A= 2.1969E+05	V1B= 2.1417E+05
M2A=-1.6174E+04	M2B= 2.1584E+04	V2A= 5.9968E+04	V2B= 5.8206E+04
XN=612.0	PHI= 155.0	UINF= 80.0	
NGX= 6.2701E+02	NGY= 5.0342E+02	NGZ= 5.5996E+03	
M1A=-1.6459E+05	M1B= 1.5833E+05	V1A= 2.2581E+05	V1B= 2.1399E+05
M2A=-1.1031E+04	M2B= 2.0292E+04	V2A= 6.4726E+04	V2B= 5.7151E+04
XN=612.0	PHI= 185.0	UINF= 25.0	
NGX= 1.0984E+03	NGY=-2.0518E+03	NGZ= 1.9883E+03	
M1A=-1.4579E+05	M1B= 1.7455E+05	V1A= 2.0657E+05	V1B= 2.2476E+05
M2A=-5.6865E+04	M2B= 4.0753E+03	V2A= 1.1226E+05	V2B=-6.4136E+02
XN=612.0	PHI= 185.0	UINF= 50.0	
NGX= 1.5736E+03	NGY=-2.9546E+03	NGZ= 1.9524E+03	
M1A=-1.3995E+05	M1B= 1.8102E+05	V1A= 2.0313E+05	V1B= 2.2935E+05
M2A=-4.5293E+04	M2B=-4.1579E+03	V2A= 1.0594E+05	V2B=-2.7132E+04
XN=612.0	PHI= 185.0	UINF= 35.0	
NGX= 2.1422E+03	NGY=-4.0216E+03	NGZ= 1.9536E+03	
M1A=-1.3501E+05	M1B= 1.8095E+05	V1A= 1.9906E+05	V1B= 2.3472E+05
M2A=-5.5624E+04	M2B=-1.3088E+04	V2A= 1.0204E+05	V2B=-5.8438E+04
XN=612.0	PHI= 185.0	UINF= 40.0	
NGX= 2.7579E+03	NGY=-5.2527E+03	NGZ= 1.9120E+03	
M1A=-1.2501E+05	M1B= 1.9806E+05	V1A= 1.9457E+05	V1B= 2.4094E+05
M2A=-6.5531E+04	M2B=-2.5115E+04	V2A= 1.0445E+05	V2B=-9.4561E+04
XN=612.0	PHI= 185.0	UINF= 45.0	
NGX= 3.5411E+03	NGY=-6.6479E+03	NGZ= 1.9874E+03	
M1A=-1.1596E+05	M1B= 2.0840E+05	V1A= 1.8905E+05	V1B= 2.4800E+05
M2A=-7.4100E+04	M2B=-3.7839E+04	V2A= 2.3028E+05	V2B=-1.3550E+05
XN=612.0	PHI= 185.0	UINF= 60.0	
NGX= 6.2954E+03	NGY=-1.1819E+04	NGZ= 1.7965E+03	
M1A=-8.2307E+04	M1B= 2.4674E+05	V1A= 1.6933E+05	V1B= 2.7415E+05
M2A=-1.1401E+05	M2B=-6.4993E+04	V2A= 3.6307E+05	V2B=-2.8722E+05

Table 7 (Cont.)
LANDING GEAR REACTIONS FOR E-4 AIRCRAFT ON TEST STAND

XN=612.0	PHI= 185.0	GINF= 80.0	
NGX= 1.1192E+04	NGY=-2.1011E+04	NGZ= 1.6348E+03	
H1A=-2.2710E+04 H2A=-1.6496E+05	H1B= 3.1488E+05 H2B=-1.6882E+05	V1A= 1.3428E+05 V2A= 5.9913E+05	V1B= 3.2060E+05 V2B=-5.5694E+05
XN=612.0	PHI= 215.0	GINF= 25.0	"
NGX= 1.2961E+03	NGY=-3.1624E+03	NGZ= 1.6086E+03	
H1A=-1.2257E+05 H2A=-6.5930E+04	H1B= 1.9532E+05 H2B=-2.1571E+04	V1A= 1.6196E+05 V2A= 1.9960E+05	V1B= 2.4636E+05 V2B=-8.3599E+04
XN=612.0	PHI= 215.0	GINF= 30.0	
NGX= 1.8117E+03	NGY=-4.5539E+03	NGZ= 1.4315E+03	
H1A=-1.0649E+05 H2A=-8.4941E+04	H1B= 2.1125E+05 H2B=-4.1089E+04	V1A= 1.8769E+05 V2A= 2.8122E+05	V1B= 2.8045E+05 V2B=-1.4659E+05
XN=612.0	PHI= 215.0	GINF= 35.0	
NGX= 2.4659E+03	NGY=-6.1984E+03	NGZ= 1.2247E+03	
H1A=-8.7490E+04 H2A=-1.0739E+05	H1B= 2.3007E+05 H2B=-6.4155E+04	V1A= 1.9033E+05 V2A= 3.3404E+05	V1B= 2.7704E+05 V2B=-2.2104E+05
XN=612.0	PHI= 215.0	GINF= 40.0	
NGX= 3.2208E+03	NGY=-8.0959E+03	NGZ= 9.8601E+02	
H1A=-6.5504E+04 H2A=-1.3548E+05	H1B= 2.5180E+05 H2B=-9.0770E+04	V1A= 1.9157E+05 V2A= 4.1806E+05	V1B= 2.9424E+05 V2B=-3.0693E+05
XN=612.0	PHI= 215.0	GINF= 45.0	
NGX= 4.0763E+03	NGY=-1.0246E+04	NGZ= 7.1551E+02	
H1A=-4.0715E+04 H2A=-1.6203E+05	H1B= 2.7641E+05 H2B=-1.2093E+05	V1A= 1.0932E+05 V2A= 5.1329E+05	V1B= 3.1798E+05 V2B=-4.0428E+05
XN=612.0	PHI= 215.0	GINF= 60.0	
NGX= 7.2468E+03	NGY=-1.8216E+04	NGZ=-4.8691E+02	
H1A= 5.1375E+04 H2A=-2.7140E+05	H1B= 3.0765E+05 H2B=-2.3272E+05	V1A= 2.7598E+04 V2A= 8.8618E+05	V1B= 3.4355E+05 V2B=-7.6506E+05
XN=612.0	PHI= 215.0	GINF= 80.0	
NGX= 1.2803E+04	NGY=-3.2383E+04	NGZ=-2.0690E+03	
H1A= 2.1509E+05 H2A=-9.6477E+05	H1B= 5.2984E+05 H2B=-4.3144E+05	V1A=-1.1769E+05 V2A= 1.4956E+06	V1B= 5.4178E+05 V2B=-1.4064E+06

Table 7 (Cont.)
LANDING GEAR REACTIONS FOR E-4 AIRCRAFT ON TEST STAND

XN=612.0		PHI= 245.0	DINF= 25.0	
NGX=-5.7639E+02	NGY=-5.7036E+03		NGZ= 1.6751E+03	
M1A=-1.0603E+05 M2A=-8.9404E+04	M1B= 2.1748E+05 M2B=-4.6040E+04		V1A= 1.6400E+05 V2A= 2.7488E+05	V1B= 2.7189E+05 V2B=-1.6132E+05
XN=612.0		PHI= 245.0	DINF= 30.0	
NGX=-5.4229E+02	NGY=-5.3332E+03		NGZ= 1.5302E+03	
M1A=-8.2606E+04 M2A=-1.1883E+05	M1B= 2.4316E+05 M2B=-7.6325E+04		V1A= 1.4163E+05 V2A= 3.6961E+05	V1B= 2.9719E+05 V2B=-2.5851E+05
XN=612.0		PHI= 245.0	DINF= 35.0	
NGX=-7.3812E+02	NGY=-7.2590E+03		NGZ= 1.3589E+03	
M1A=-5.5060E+04 M2A=-1.9351E+05	M1B= 2.7351E+05 M2B=-1.1211E+05		V1A= 1.1503E+05 V2A= 4.6158E+05	V1B= 3.2709E+05 V2B=-3.7337E+05
XN=612.0		PHI= 245.0	DINF= 40.0	
NGX=-9.6402E+02	NGY=-9.4812E+03		NGZ= 1.1814E+03	
M1A=-2.3206E+04 M2A=-1.9353E+05	M1B= 3.0853E+05 M2B=-1.5341E+05		V1A= 8.5397E+04 V2A= 5.1076E+05	V1B= 3.6159E+05 V2B=-5.0590E+05
XN=612.0		PHI= 245.0	DINF= 45.0	
NGX=-1.2202E+03	NGY=-1.2000E+04		NGZ= 9.5745E+02	
M1A= 1.2895E+04 M2A=-2.5488E+05	M1B= 3.4822E+05 M2B=-2.0021E+05		V1A= 5.1132E+04 V2A= 7.5718E+05	V1B= 4.0069E+05 V2B=-6.5610E+05
XN=612.0		PHI= 245.0	DINF= 60.0	
NGX=-2.1692E+03	NGY=-2.1333E+04		NGZ= 1.0763E+02	
M1A= 1.4666E+05 M2A=-4.0896E+05	M1B= 4.9531E+05 M2B=-3.7366E+05		V1A=-7.5849E+04 V2A= 1.2998E+06	V1B= 5.4559E+05 V2B=-1.2127E+06
XN=612.0		PHI= 245.0	DINF= 80.0	
NGX=-3.8563E+03	NGY=-3.7925E+04		NGZ=-1.5676E+03	
M1A= 3.6452E+05 M2A=-7.0576E+05	M1B= 7.5679E+05 M2B=-5.8201E+05		V1A=-3.0159E+05 V2A= 2.2644E+06	V1B= 8.0319E+05 V2B=-2.2023E+06
XN=612.0		PHI= 275.0	DINF= 25.0	
NGX=-1.9160E+03	NGY=-2.5174E+03		NGZ= 2.2838E+03	
M1A=-1.0944E+05 M2A=-8.2704E+04	M1B= 2.0876E+05 M2B=-3.6223E+04		V1A= 1.6718E+05 V2A= 2.5196E+05	V1B= 2.6157E+05 V2B=-1.3030E+05

Table 7 (Cont.)

LANDING GEAR REACTIONS FOR E-4 AIRCRAFT ON TEST STAND

XN=612.0	PHI= 275.0	GINF= 30.0	
NGX=-2.8211E+03	NGY=-3.3370E+03	NGZ= 2.4067E+03	
M1A=-8.7589E+04	M1B= 2.3060E+05	V1A= 1.4640E+05	V1B= 2.8232E+05
M2A=-1.0915E+05	M2B=-8.2168E+04	V2A= 3.3661E+05	V2B=-2.1385E+05
XN=612.0	PHI= 275.0	GINF= 35.0	
NGX=-3.0534E+03	NGY=-4.5421E+03	NGZ= 2.8520E+03	
M1A=-6.1759E+04	M1B= 2.5641E+05	V1A= 1.2105E+05	V1B= 3.0685E+05
M2A=-1.4034E+05	M2B=-9.2873E+04	V2A= 4.3666E+05	V2B=-3.1258E+05
XN=612.0	PHI= 275.0	GINF= 40.0	
NGX=-3.0350E+03	NGY=-5.9325E+03	NGZ= 2.7197E+03	
M1A=-3.1457E+04	M1B= 2.8619E+05	V1A= 9.3523E+04	V1B= 3.3515E+05
M2A=-1.7833E+05	M2B=-1.2826E+05	V2A= 5.5209E+05	V2B=-4.2650E+05
XN=612.0	PHI= 275.0	GINF= 45.0	
NGX=-6.3699E+03	NGY=-7.5084E+03	NGZ= 2.9097E+03	
M1A= 1.6200E+05	M1B= 3.1995E+05	V1A= 6.1417E+04	V1B= 3.6723E+05
M2A=-2.1711E+05	M2B=-1.6841E+05	V2A= 6.8292E+05	V2B=-5.5561E+05
XN=612.0	PHI= 275.0	GINF= 50.0	
NGX=-1.1344E+04	NGY=-1.3348E+04	NGZ= 3.6139E+03	
M1A= 1.2699E+05	M1B= 4.4504E+05	V1A=-5.7565E+04	V1B= 4.8610E+05
M2A=-3.0[illegible]E+05	M2B=-3.1711E+05	V2A= 1.1678E+06	V2B=-1.0341E+06
XN=612.0	PHI= 275.0	GINF= 60.0	
NGX=-2.0132E+04	NGY=-2.3730E+04	NGZ= 4.8657E+03	
M1A= 3.4952E+05	M1B= 6.6742E+05	V1A=-2.6909E+05	V1B= 6.9745E+05
M2A=-6.3[illegible]E+05	M2B=-5.8148E+05	V2A= 2.0297E+06	V2B=-1.8847E+06
XN=612.0	PHI= 305.0	GINF= 25.0	
NGX=-1.6314E+04	NGY=-8.8740E+03	NGZ= 2.1206E+03	
M1A=-1.4096E+05	M1B= 1.7695E+05	V1A= 2.0104E+05	V1B= 2.2734E+05
M2A=-4.5375E+04	M2B= 1.7285E+03	V2A= 1.3341E+05	V2B=-1.0284E+04
XN=612.0	PHI= 305.0	GINF= 30.0	
NGX=-2.6373E+03	NGY=-1.2778E+03	NGZ= 2.1717E+03	
M1A=-1.5300E+05	M1B= 1.8480E+05	V1A= 1.9516E+05	V1B= 2.3304E+05
M2A=-5.5313E+04	M2B=-7.5375E+03	V2A= 1.6590E+05	V2B=-4.1017E+04

Table 7 (Cont.)
LANDING GEAR REACTIONS FOR E-4 AIRCRAFT ON TEST STAND

XN=612.0	PHI= 305.0	GINF= 35.0	
NGX=-3.5696E+03	NGY=-1.7395E+03	NGZ= 2.2322E+03	
M1A=-1.2357E+05 M2A=-6.7059E+04	M1R= 1.9407E+05 M2R=-1.0468E+04	V1A= 1.6622E+05 V2A= 2.0430E+05	V1R= 2.3977E+05 V2R=-7.7358E+04
XN=612.0	PHI= 305.0	GINF= 40.0	
NGX=-4.6705E+03	NGY=-2.2717E+03	NGZ= 2.3019E+03	
M1A=-1.1269E+05 M2A=-8.0811E+04	M1R= 2.0477E+05 M2R=-5.1163E+04	V1A= 1.6062E+05 V2A= 2.4860E+05	V1R= 2.4754E+05 V2R=-1.1425E+05
XN=612.0	PHI= 305.0	GINF= 45.0	
NGX=-5.9339E+03	NGY=-2.8752E+03	NGZ= 2.3810E+03	
M1A=-1.0036E+05 M2A=-9.5070E+04	M1R= 2.1650E+05 M2R=-4.5443E+04	V1A= 1.7113E+05 V2A= 2.9802E+05	V1R= 2.5835E+05 V2R=-1.6674E+05
XN=612.0	PHI= 305.0	GINF= 60.0	
NGX=-1.0294E+04	NGY=-5.1114E+03	NGZ= 2.6739E+03	
M1A=-5.4653E+04 M2A=-1.5209E+05	M1R= 2.6184E+05 M2R=-9.0511E+04	V1A= 1.9747E+05 V2A= 4.4491E+05	V1R= 2.8898E+05 V2R=-3.4276E+05
XN=612.0	PHI= 305.0	GINF= 80.0	
NGX=-1.4734E+04	NGY=-7.0889E+03	NGZ= 3.1947E+03	
M1A= 2.8590E+04 M2A=-2.5408E+05	M1R= 3.4175E+05 M2R=-1.9265E+05	V1A= 7.7644E+04 V2A= 6.1573E+05	V1R= 3.4700E+05 V2R=-6.5568E+05
XN=612.0	PHI= 305.0	GINF= 25.0	
NGX=-6.2681E+03	NGY=-1.1121E+01	NGZ= 1.6300E+03	
M1A=-1.5912E+05 M2A=-2.4376E+04	M1R= 1.6156E+05 M2R= 2.1592E+04	V1A= 2.1507E+05 V2A= 6.4901E+04	V1R= 2.1702E+05 V2R= 5.5256E+04
XN=612.0	PHI= 305.0	GINF= 30.0	
NGX=-4.0109E+02	NGY=-1.5670E+01	NGZ= 1.4769E+03	
M1A=-1.5912E+05 M2A=-2.5076E+04	M1R= 1.6264E+05 M2R= 2.1066E+04	V1A= 2.1536E+05 V2A= 6.7250E+04	V1R= 2.1818E+05 V2R= 5.3360E+04
XN=612.0	PHI= 305.0	GINF= 35.0	
NGX=-1.2276E+03	NGY=-2.1601E+01	NGZ= 1.2664E+03	
M1A=-1.5912E+05 M2A=-2.5902E+04	M1R= 1.6391E+05 M2R= 2.0444E+04	V1A= 2.1571E+05 V2A= 7.0025E+04	V1R= 2.1955E+05 V2R= 5.1120E+04

Table 7 (Cont.)

LANDING GEAR REACTIONS FOR E-4 AIRCRAFT ON TEST STAND

XN=612.0	YMI= 335.0	GINF= 40.0	
NGX=-1.6034E+03	NGY=-2.8213E+01	NGZ= 1.0666E+03	
M1A=-1.5913E+05	M1B= 1.6538E+05	V1A= 2.1612E+05	V1B= 2.2112E+05
M2A=-2.8820E+04	M2B= 1.9726E+04	V2A= 7.3227E+04	V2B= 9.8535E+04
XN=612.0	YMI= 335.0	GINF= 45.0	
NGX=-2.0293E+03	NGY=-3.5707E+01	NGZ= 8.1750E+02	
M1A=-1.5913E+05	M1B= 1.6704E+05	V1A= 2.1657E+05	V1B= 2.2291E+05
M2A=-2.7936E+04	M2B= 1.8914E+04	V2A= 7.6857E+04	V2B= 9.5605E+04
XN=612.0	YMI= 335.0	GINF= 50.0	
NGX=-3.0807E+03	NGY=-5.5479E+01	NGZ=-1.0560E+02	
M1A=-1.5914E+05	M1B= 1.7021E+05	V1A= 2.1827E+05	V1B= 2.2954E+05
M2A=-2.1941E+04	M2B= 1.5901E+04	V2A= 9.0307E+04	V2B= 3.4798E+04
XN=612.0	YMI= 335.0	GINF= 60.0	
NGX=-6.4105E+03	NGY=-1.1285E+02	NGZ=-1.7467E+03	
M1A=-1.5916E+05	M1B= 1.8417E+05	V1A= 2.2128E+05	V1B= 2.4131E+05
M2A=-3.4066E+04	M2B= 1.0545E+04	V2A= 1.1422E+05	V2B= 1.5447E+04

Table 8

LANDING GEAR REACTIONS FOR E-4 AIRCRAFT (3 GEAR APPROXIMATION) ON TEST STAND

XN=612.0	PHI= 5.0	GIMP= 25.0	
NGX=-1.6295E+03	NGY=-3.1497E+03	NGZ= 2.0419E+04	
MA=-1.5604E+05	MB= 1.6659E+05	VA= 2.5048E+05	VB= 2.8298E+05
XN=612.0	PHI= 5.0	GIMP= 30.0	
NGX=-2.3465E+03	NGY=-4.5356E+03	NGZ= 2.0328E+04	
MA=-1.5447E+05	MB= 1.6494E+05	VA= 2.4424E+05	VB= 2.9104E+05
XN=612.0	PHI= 5.0	GIMP= 35.0	
NGX=-3.1939E+03	NGY=-6.1735E+03	NGZ= 2.0247E+04	
MA=-1.5216E+05	MB= 1.7206E+05	VA= 2.3667E+05	VB= 3.0057E+05
XN=612.0	PHI= 5.0	GIMP= 40.0	
NGX=-4.1716E+03	NGY=-8.0653E+03	NGZ= 2.0110E+04	
MA=-1.4877E+05	MB= 1.7678E+05	VA= 2.2836E+05	VB= 3.1157E+05
XN=612.0	PHI= 5.0	GIMP= 45.0	
NGX=-5.2797E+03	NGY=-1.0205E+04	NGZ= 1.9977E+04	
MA=-1.4704E+05	MB= 1.8122E+05	VA= 2.1872E+05	VB= 3.2403E+05
XN=612.0	PHI= 5.0	GIMP= 50.0	
NGX=-6.3862E+03	NGY=-1.2342E+04	NGZ= 1.9844E+04	
MA=-1.3690E+05	MB= 1.8767E+05	VA= 2.0879E+05	VB= 3.3021E+05
XN=612.0	PHI= 5.0	GIMP= 60.0	
NGX=-1.0667E+04	NGY=-2.2253E+04	NGZ= 1.8609E+04	
MA=-1.1809E+05	MB= 2.0692E+05	VA= 1.1947E+05	VB= 4.5231E+05
XN=612.0	PHI= 35.0	GIMP= 25.0	
NGX=-1.8222E+03	NGY=-3.2838E+03	NGZ= 2.0727E+04	
MA=-1.4608E+05	MB= 1.7490E+05	VA= 2.3067E+05	VB= 2.9318E+05
XN=612.0	PHI= 35.0	GIMP= 30.0	
NGX=-2.6240E+03	NGY=-1.2505E+04	NGZ= 2.0774E+04	
MA=-1.4108E+05	MB= 1.8143E+05	VA= 2.2753E+05	VB= 3.0572E+05
XN=612.0	PHI= 35.0	GIMP= 35.0	
NGX=-3.5715E+03	NGY=-1.7020E+04	NGZ= 2.0840E+04	
MA=-1.3422E+05	MB= 1.8919E+05	VA= 2.1412E+05	VB= 3.2056E+05
XN=612.0	PHI= 35.0	GIMP= 40.0	
NGX=-4.6649E+03	NGY=-2.2231E+04	NGZ= 2.0910E+04	
MA=-1.2832E+05	MB= 1.9805E+05	VA= 1.9865E+05	VB= 3.3767E+05
XN=612.0	PHI= 35.0	GIMP= 45.0	
NGX=-5.9040E+03	NGY=-2.8136E+04	NGZ= 2.0990E+04	
MA=-1.1735E+05	MB= 2.0814E+05	VA= 1.8112E+05	VB= 3.5706E+05

Table 8 (Cont.)

LANDING GEAR REACTIONS FOR E-4 AIRCRAFT (3 GEAR APPROXIMATION) ON TEST STAND

XN=612.0	PHI= 35.0	CLP= 30.0	
NGX= -1.0496E+04	NGY= -5.0019E+04	NGZ= 2.1206E+04	
HA= -8.4132E+04	MX= 2.4553E+05	VA= 1.1019E+05	VH= 4.2493E+05
XN=612.0	PHI= 35.0	CLP= 30.0	
NGX= -1.0660E+04	NGY= -5.0543E+04	NGZ= 2.1812E+04	
HA= -2.3079E+04	MX= 3.1201E+05	VA= 8.5194E+02	VH= 5.8671E+05
XN=612.0	PHI= 65.0	CLP= 25.0	
NGX= -5.2045E+02	NGY= -9.7741E+03	NGZ= 2.0538E+04	
HA= -1.4352E+05	MX= 1.7709E+05	VA= 2.3538E+04	VH= 2.9971E+05
XN=612.0	PHI= 65.0	CLP= 30.0	
NGX= -7.4446E+02	NGY= -1.4075E+04	NGZ= 2.0500E+04	
HA= -1.3624E+05	MX= 1.6544E+05	VA= 2.2292E+04	VH= 3.0437E+05
XN=612.0	PHI= 65.0	CLP= 35.0	
NGX= -1.0201E+03	NGY= -1.9157E+04	NGZ= 2.0040E+04	
HA= -1.2763E+05	MX= 1.9461E+05	VA= 2.0726E+04	VH= 3.2552E+05
XN=612.0	PHI= 65.0	CLP= 40.0	
NGX= -1.3363E+03	NGY= -2.5062E+04	NGZ= 2.0042E+04	
HA= -1.1770E+05	MX= 2.0518E+05	VA= 1.8972E+04	VH= 3.4419E+05
XN=612.0	PHI= 65.0	CLP= 45.0	
NGX= -1.6862E+03	NGY= -3.1696E+04	NGZ= 2.0376E+04	
HA= -1.0645E+05	MX= 2.1717E+05	VA= 1.8902E+04	VH= 3.6527E+05
XN=612.0	PHI= 65.0	CLP= 50.0	
NGX= -2.9978E+03	NGY= -5.6299E+04	NGZ= 2.0174E+04	
HA= -6.4750E+04	MX= 2.6158E+05	VA= 9.6059E+04	VH= 4.4352E+05
XN=612.0	PHI= 65.0	CLP= 55.0	
NGX= -5.3294E+03	NGY= -1.0009E+05	NGZ= 1.9871E+04	
HA= 9.3681E+03	MX= 3.4054E+05	VA= -5.5072E+04	VH= 5.8264E+05
XN=612.0	PHI= 95.0	CLP= 25.0	
NGX= 1.0753E+03	NGY= -5.5812E+03	NGZ= 2.0409E+04	
HA= -1.4705E+05	MX= 1.7041E+05	VA= 2.3868E+05	VH= 2.8721E+05
XN=612.0	PHI= 95.0	CLP= 30.0	
NGX= 1.5455E+03	NGY= -8.0369E+03	NGZ= 2.0315E+04	
HA= -1.4219E+05	MX= 1.7496E+05	VA= 2.2745E+05	VH= 2.9714E+05

Table 8 (Cont.)

LANDING GEAR REACTIONS FOR E-4 AIRCRAFT (3 GEAR APPROXIMATION) ON TEST STAND

XN=612.0	PHI= 95.0	ULNF= 35.0	
NGX= 2.1036E+03	NGY=-1.0939E+04	NGZ= 2.0206E+04	
HA=-1.3573E+05	HB= 1.8034E+05	VA= 2.1374E+05	VB= 5.0886E+05
XN=612.0	PHI= 95.0	ULNF= 40.0	
NGX= 2.7476E+03	NGY=-1.4288E+04	NGZ= 2.0002E+04	
HA=-1.8248E+05	HB= 1.8635E+05	VA= 1.9015E+05	VB= 3.2240E+05
XN=612.0	PHI= 95.0	ULNF= 45.0	
NGX= 3.4774E+03	NGY=-1.8083E+04	NGZ= 1.9442E+04	
HA=-1.1504E+05	HB= 1.9358E+05	VA= 1.8049E+05	VB= 3.3774E+05
XN=612.0	PHI= 95.0	ULNF= 50.0	
NGX= 4.1240E+03	NGY=-2.2148E+04	NGZ= 1.9423E+04	
HA=-8.0535E+04	HB= 2.1965E+05	VA= 1.1503E+05	VB= 3.9458E+05
XN=612.0	PHI= 95.0	ULNF= 80.0	
NGX= 1.0990E+04	NGY=-3.7151E+04	NGZ= 1.0499E+04	
HA=-3.2634E+04	HB= 2.8600E+05	VA=-1.3469E+03	VB= 4.9563E+05
XN=612.0	PHI= 125.0	ULNF= 25.0	
NGX= 1.1557E+03	NGY=-2.3440E+03	NGZ= 2.1203E+04	
HA=-1.5292E+05	HB= 1.6404E+05	VA= 2.4534E+05	VB= 2.7486E+05
XN=612.0	PHI= 125.0	ULNF= 30.0	
NGX= 1.0642E+03	NGY=-3.3754E+03	NGZ= 2.1484E+04	
HA=-1.4977E+05	HB= 1.6579E+05	VA= 2.3663E+05	VB= 2.8512E+05
XN=612.0	PHI= 125.0	ULNF= 35.0	
NGX= 2.2651E+03	NGY=-4.5943E+03	NGZ= 2.1772E+04	
HA=-1.4606E+05	HB= 1.6785E+05	VA= 2.2655E+05	VB= 2.9251E+05
XN=612.0	PHI= 125.0	ULNF= 40.0	
NGX= 2.9585E+03	NGY=-6.0007E+03	NGZ= 2.2128E+04	
HA=-1.4177E+05	HB= 1.7024E+05	VA= 2.1487E+05	VB= 3.0103E+05
XN=612.0	PHI= 125.0	ULNF= 45.0	
NGX= 3.7444E+03	NGY=-7.5946E+03	NGZ= 2.2532E+04	
HA=-1.3691E+05	HB= 1.7294E+05	VA= 2.0184E+05	VB= 3.1069E+05

Table 8 (Cont.)

LANDING GEAR REACTIONS FOR E-4 AIRCRAFT (3 GEAR APPROXIMATION) ON TEST STAND

XN=612.0	PHI= 125.0	DINF= 60.0	
NGX= 6.6567E+03	NGY=-1.3592E+04	NGZ= 2.4027E+04	
MG=-1.1891E+05	MB= 1.8296E+05	VA= 1.5283E+05	VB= 3.4650E+05
XN=612.0	PHI= 125.0	DINF= 80.0	
NGX= 1.1639E+04	NGY=-2.4093E+04	NGZ= 2.4864E+04	
MA=-8.6941E+04	MB= 2.0077E+05	VA= 6.3497E+04	VB= 4.1016E+05
XN=612.0	PHI= 155.0	DINF= 25.0	
NGX= 6.1310E+01	NGY=-7.5135E+01	NGZ= 2.1215E+04	
MG=-1.5905E+05	MB= 1.5925E+05	VA= 2.8303E+05	VB= 2.6525E+05
XN=612.0	PHI= 155.0	DINF= 30.0	
NGX= 8.8208E+01	NGY=-1.0539E+02	NGZ= 2.1478E+04	
MG=-1.5760E+05	MB= 1.5869E+05	VA= 2.8231E+05	VB= 2.6263E+05
XN=612.0	PHI= 155.0	DINF= 35.0	
NGX= 1.2017E+02	NGY=-1.4536E+02	NGZ= 2.1792E+04	
MG=-1.5707E+05	MB= 1.5846E+05	VA= 2.8147E+05	VB= 2.6190E+05
XN=612.0	PHI= 155.0	DINF= 40.0	
NGX= 1.5695E+02	NGY=-1.8728E+02	NGZ= 2.2153E+04	
MG=-1.5746E+05	MB= 1.5797E+05	VA= 2.8049E+05	VB= 2.6106E+05
XN=612.0	PHI= 155.0	DINF= 45.0	
NGX= 1.9688E+02	NGY=-2.3702E+02	NGZ= 2.2569E+04	
MG=-1.5677E+05	MB= 1.5742E+05	VA= 2.5939E+05	VB= 2.6011E+05
XN=612.0	PHI= 155.0	DINF= 50.0	
NGX= 3.5315E+02	NGY=-4.2137E+02	NGZ= 2.4083E+04	
MA=-1.5421E+05	MB= 1.5537E+05	VA= 2.5529E+05	VB= 2.5657E+05
XN=612.0	PHI= 155.0	DINF= 80.0	
NGX= 6.2781E+02	NGY=-7.4910E+02	NGZ= 2.6785E+04	
MG=-1.4965E+05	MB= 1.5171E+05	VA= 2.4801E+05	VB= 2.5028E+05
XN=612.0	PHI= 185.0	DINF= 25.0	
NGX= 1.0929E+03	NGY= 1.7383E+03	NGZ= 2.1178E+04	
MG=-1.6528E+05	MB= 1.5347E+05	VA= 2.7766E+05	VB= 2.4608E+05

Table 8 (Cont.)

LANDING GEAR REACTIONS FOR E-4 AIRCRAFT (3 GEAR APPROXIMATION) ON TEST STAND

AN=612.0	PHI= 185.0	GINF= 30.0	
NGX= 1.573AE+03	NGY= 2.3032E+03	NGZ= 2.1402E+04	
HA=-1.2470E+05	HB= 1.3058E+05	VA= 2.2338E+05	VB= 2.3790E+05
XN=612.0	PHI= 185.0	GINF= 35.0	
NGX= 2.1482E+03	NGY= 3.4071E+03	NGZ= 2.1724E+04	
HA=-1.0637E+05	HB= 1.4719E+05	VA= 2.3015E+05	VB= 2.2824E+05
XN=612.0	PHI= 185.0	GINF= 40.0	
NGX= 2.7979E+03	NGY= 4.4501E+03	NGZ= 2.2205E+04	
HA=-1.0650E+05	HB= 1.4320E+05	VA= 2.2795E+05	VB= 2.1710E+05
XN=612.0	PHI= 185.0	GINF= 45.0	
NGX= 3.5911E+03	NGY= 5.8132E+03	NGZ= 2.2451E+04	
HA=-1.7049E+05	HB= 1.3072E+05	VA= 2.2694E+05	VB= 2.0447E+05
XN=612.0	PHI= 185.0	GINF= 50.0	
NGX= 6.2454E+03	NGY= 1.0013E+04	NGZ= 2.3884E+04	
HA=-1.7842E+05	HB= 1.2212E+05	VA= 2.3937E+05	VB= 1.8765E+05
XN=612.0	PHI= 185.0	GINF= 00.0	
NGX= 1.1192E+04	NGY= 1.7800E+04	NGZ= 2.2430E+04	
HA=-1.9302E+05	HB= 9.2602E+04	VA= 3.9784E+05	VB= 7.4427E+04
XN=612.0	PHI= 215.0	GINF= 25.0	
NGX= 1.2531E+03	NGY= 2.4670E+03	NGZ= 2.0372E+04	
HA=-1.7113E+05	HB= 1.4673E+05	VA= 2.0650E+05	VB= 2.2706E+05
AN=612.0	PHI= 215.0	GINF= 30.0	
NGX= 1.8117E+03	NGY= 3.3124E+03	NGZ= 2.0260E+04	
HA=-1.7600E+05	HB= 1.4086E+05	VA= 2.9899E+05	VB= 2.2492E+05
AN=612.0	PHI= 215.0	GINF= 35.0	
NGX= 2.4659E+03	NGY= 1.2675E+04	NGZ= 2.0199E+04	
HA=-1.8176E+05	HB= 1.3393E+05	VA= 3.1139E+05	VB= 2.1058E+05
XN=612.0	PHI= 215.0	GINF= 40.0	
NGX= 3.2200E+03	NGY= 1.6555E+04	NGZ= 2.0002E+04	
HA=-1.8840E+05	HB= 1.2598E+05	VA= 3.2570E+05	VB= 1.9402E+05

Table 8 (Cont.)

LANDING GEAR REACTIONS FOR E-4 AIRCRAFT (3 GEAR APPROXIMATION) ON TEST STAND

XN=612.0	PHI= 215.0	UINF= 45.0	
NGX= 4.07e3E+03	NGY= 2.0953E+04	NGZ= 1.9640E+04	
HA=-1.9593E+05	HB= 1.1666E+05	VA= 3.4192E+05	VB= 1.7526E+05
XN=612.0	PHI= 215.0	UINF= 60.0	
NGX= 7.2468E+03	NGY= 3.7250E+04	NGZ= 1.9241E+04	
HA=-2.23e2E+05	HB= 8.3258E+04	VA= 4.0201E+05	VB= 1.0574E+05
XN=612.0	PHI= 215.0	UINF= 80.0	
NGX= 1.2e83E+04	NGY= 6.6242E+04	NGZ= 1.8177E+04	
HA=-2.7541E+05	HB= 2.3521E+04	VA= 5.0689E+05	VB=-1.7868E+04
XN=612.0	PHI= 245.0	UINF= 25.0	
NGX=-3.7e39E+02	NGY= 1.1136E+04	NGZ= 2.1042E+04	
HA=-1.7975E+05	HB= 1.4084E+05	VA= 2.9621E+05	VB= 2.3187E+05
XN=612.0	PHI= 245.0	UINF= 30.0	
NGX=-5.4229E+02	NGY= 1.6036E+04	NGZ= 2.1253E+04	
HA=-1.e841E+05	HB= 1.3239E+05	VA= 3.1296E+05	VB= 2.1745E+05
XN=612.0	PHI= 245.0	UINF= 35.0	
NGX=-7.5e12E+02	NGY= 2.1926E+04	NGZ= 2.1455E+04	
HA=-1.9e69E+05	HB= 1.2239E+05	VA= 3.3043E+05	VB= 2.0040E+05
XN=612.0	PHI= 245.0	UINF= 40.0	
NGX=-9.e406E+02	NGY= 2.8508E+04	NGZ= 2.1717E+04	
HA=-2.1047E+05	HB= 1.1086E+05	VA= 3.5056E+05	VB= 1.8074E+05
XN=612.0	PHI= 245.0	UINF= 45.0	
NGX=-1.2202E+03	NGY= 3.6060E+04	NGZ= 2.2011E+04	
HA=-2.2365E+05	HB= 9.7795E+04	VA= 3.7538E+05	VB= 1.5645E+05
XN=612.0	PHI= 245.0	UINF= 60.0	
NGX=-2.1692E+03	NGY= 6.4142E+04	NGZ= 2.3102E+04	
HA=-2.7347E+05	HB= 4.9565E+04	VA= 4.5795E+05	VB= 7.5839E+04
XN=612.0	PHI= 245.0	UINF= 80.0	
NGX=-3.85e3E+03	NGY= 1.1403E+05	NGZ= 2.5040E+04	
HA=-3.61e7E+05	HB=-3.e732E+04	VA= 6.0829E+05	VB=-7.1017E+04

Table 8 (Cont.)

LANDING GEAR REACTIONS FOR E-4 AIRCRAFT (3 GEAR APPROXIMATION) ON TEST STAND

X[illegible] 12.0	PHI= 275.0	DINR= 25.0	
NGX=-1.9460E+03	NGY= 1.0799E+04	NGZ= 2.0735E+04	
HA=-1.7726E+05	HB= 1.9446E+05	VA= [illegible].9516E+05	VB= 2.3678E+05
XN=612.0	PHI= 275.0	DINR= 30.0	
NGX=-2.6311E+03	NGY= 1.0550E+04	NGZ= 2.0740E+04	
HA=-1.6486E+05	HB= 1.8760E+05	VA= 5.0359E+05	VB= 2.2452E+05
XN=612.0	PHI= 275.0	DINR= 35.0	
NGX=-3.0534E+03	NGY= 2.1165E+04	NGZ= 2.0855E+04	
HA=-1.4576E+05	HB= 1.2944E+05	VA= 5.2445E+05	VB= 2.1003E+05
XN=612.0	PHI= 275.0	DINR= 40.0	
NGX=-5.0330E+03	NGY= 2.7645E+04	NGZ= 2.0930E+04	
HA=-2.0400E+05	HB= 1.2013E+05	VA= 5.4275E+05	VB= 1.9331E+05
XN=612.0	PHI= 275.0	DINR= 45.0	
NGX=-6.3699E+03	NGY= 3.4986E+04	NGZ= 2.1015E+04	
HA=-2.1577E+05	HB= 1.0952E+05	VA= 5.6350E+05	VB= 1.7436E+05
XN=612.0	PHI= 275.0	DINR= 50.0	
NGX=-1.1524E+04	NGY= 6.2200E+04	NGZ= 2.1530E+04	
HA=-2.5910E+05	HB= 7.0214E+04	VA= 6.4058E+05	VB= 1.0412E+05
XN=612.0	PHI= 275.0	DINR= 80.0	
NGX=-2.0132E+04	NGY= 1.1039E+05	NGZ= 2.1890E+04	
HA=-3.5613E+05	HB= 3.5191E+02	VA= 5.7705E+05	VB=-2.0733E+04
XN=612.0	PHI= 305.0	DINR= 25.0	
NGX=-1.6514E+03	NGY= 3.6962E+03	NGZ= 2.0462E+04	
HA=-1.6744E+05	HB= 1.5500E+05	VA= 2.8435E+05	VB= 2.4881E+05
XN=612.0	PHI= 305.0	DINR= 30.0	
NGX=-2.6573E+03	NGY= 5.6106E+03	NGZ= 2.0396E+04	
HA=-1.7071E+05	HB= 1.5277E+05	VA= 2.9302E+05	VB= 2.4184E+05
XN=612.0	PHI= 305.0	DINR= 35.0	
NGX=-3.5096E+03	NGY= 7.6366E+03	NGZ= 2.0319E+04	
HA=-1.7456E+05	HB= 1.5014E+05	VA= 3.0326E+05	VB= 2.3561E+05

Table 8 (Cont.)

LANDING GEAR REACTIONS FOR E-4 AIRCRAFT (3 GEAR APPROXIMATION) ON TEST STAND

XN=612.0	PHI= 305.0	DINF= 90.0	
NGX=-4.6805E+03	NGY= 9.9743E+03	NGZ= 2.0230E+04	
HA=-1.7899E+05	HB= 1.4710E+05	VA= 3.1508E+05	VB= 2.2410E+05
XN=612.0	PHI= 305.0	DINF= 45.0	
NGX=-5.9339E+03	NGY= 1.2624E+04	NGZ= 2.0130E+04	
HA=-1.8402E+05	HB= 1.4366E+05	VA= 3.2847E+05	VB= 2.1533E+05
XN=612.0	PHI= 305.0	DINF= 60.0	
NGX=-1.0549E+04	NGY= 2.2442E+04	NGZ= 1.9756E+04	
HA=-2.0206E+05	HB= 1.3009E+05	VA= 3.7811E+05	VB= 1.7341E+05
XN=612.0	PHI= 305.0	DINF= 80.0	
NGX=-1.6754E+04	NGY= 3.9897E+04	NGZ= 1.9092E+04	
HA=-2.3579E+05	HB= 1.0841E+05	VA= 4.4635E+05	VB= 1.0244E+05
XN=612.0	PHI= 335.0	DINF= 45.0	
NGX=-6.2631E+03	NGY= 5.0303E+03	NGZ= 2.0340E+04	
HA=-1.8106E+05	HB= 1.6100E+05	VA= 2.8760E+05	VB= 2.6570E+05
XN=612.0	PHI= 335.0	DINF= 50.0	
NGX=-9.0109E+02	NGY= 4.3636E+02	NGZ= 2.0279 +04	
HA=-1.8236E+05	HB= 1.6142E+05	VA= 2.8419E+05	VB= 2.6616E+05
XN=612.0	PHI= 335.0	DINF= 55.0	
NGX=-1.2276E+03	NGY= 5.9393E+02	NGZ= 2.0159E+04	
HA=-1.8319E+05	HB= 1.6190E+05	VA= 2.7083E+05	VB= 2.6670E+05
XN=612.0	PHI= 335.0	DINF= 40.0	
NGX=-1.6034E+03	NGY= 7.7575E+02	NGZ= 2.0032E+04	
HA=-1.8415E+05	HB= 1.6247E+05	VA= 2.7272E+05	VB= 2.6733E+05
XN=612.0	PHI= 335.0	DINF= 45.0	
NGX=-2.0293E+03	NGY= 9.8181E+02	NGZ= 1.9865E+04	
HA=-1.8524E+05	HB= 1.6311E+05	VA= 2.7406E+05	VB= 2.6804E+05
XN=612.0	PHI= 335.0	DINF= 60.0	
NGX=-3.6076E+03	NGY= 1.7454E+03	NGZ= 1.9286E+04	
HA=-1.8926E+05	HB= 1.6548E+05	VA= 2.6279E+05	VB= 2.7068E+05
XN=612.0	PHI= 335.0	DINF= 80.0	
NGX=-6.4135E+03	NGY= 3.1050E+03	NGZ= 1.8257E+04	
HA=-1.7641E+05	HB= 1.6969E+05	VA= 2.4690E+05	VB= 2.7536E+05

The gear reactions for both the 5 gear E-4 aircraft (Table 7) and the 3-gear approximation (Table 8) are given. In Table 7 the nomenclature is similar to that for the B-52 (Table 5) with the addition of the nomenclature for the nose gear as in the case of the E-3. In Table 8 the nomenclature is similar to that for the E-3 (Table 6). It is recommended that Table 7 be used for tie down loads if each gear is to be tied down individually. This should give conservative results. If the two main gear on one side of the aircraft are to be lashed together then Table 8 is recommended for tie down loads.

The maximum axial force reactions on all the aircraft occurred at a wind speed of 80 knots. The reactions and the wind direction and position on the facility at which they occurred are given in the following table.

TABLE 9

MAXIMUM AXIAL FORCE REACTIONS

Aircraft	Force (lb), Wind Angle (ϕ)		Nose Position XN (ft)
E-3	-1.1375×10^4	275°	455
	$+3.475 \times 10^3$	125°	455
B-52	-9.0519×10^3	275°	325
	$+7.0046 \times 10^3$	215°	113
E-4	-2.3469×10^4	35°	75
	$+2.0641 \times 10^4$	125°	175

The negative sign means that the aerodynamic forces will tend to push the tug. These axial reactions are well within the nominal draw bar pull limits of the tugs recommended for use with each aircraft.

7. SUMMARY AND CONCLUSIONS

A combined experimental and analytical study was performed to determine the effects of atmospheric winds on aircraft being towed onto and tested on the TRESTLE facility which is being built at Kirtland Air Force Base, New Mexico. The ultimate results of the study were criteria for maximum wind speeds for safe handling of aircraft on the facility and tie down loads for aircraft being tested on the facility. The experimental phase of the program consisted of model tests to determine wind flow patterns and mean velocity components in the flow around the TRESTLE facility. The analytical phase of the program developed a method, using the wind velocity measurements, to estimate the forces and moments acting on aircraft positioned on the facility and to estimate the reaction at the landing gears.

Model tests were conducted in the Calspan Atmospheric Simulation Facility on a 1:480 (1 in. = 40 ft) scale model of the TRESTLE facility and its surrounding terrain. The tests consisted of smoke flow visualization studies and hot-film anemometer measurements of the three components of mean velocity in the flow about the model. The velocity surveys were performed for twelve different approaching wind directions (every thirty degrees for angles between 5° and 335°). The velocity measurements in the flow about the TRESTLE were related to the velocity measured at the 10 meter level of a meteorological tower that is located near the facility. The velocity measured at the meteorological station was used as the reference velocity for all wind directions. In general it was found that the highest velocities in the flow field occurred on the ramp leading to the test stand. These velocities could be as much as thirty percent higher than the reference velocity. The velocity measurements in the ASF correspond most closely to the hourly mean meteorological forecasts. However, conservative estimates of the wind effects will be obtained if the peak gust velocity instead of the hourly mean velocity is interpreted as the reference velocity in the force analysis.

The analytical phase of the program consisted of developing an aerodynamic strip theory that used the velocity measurements in the flow about the TRESTLE model to estimate the forces and moments acting on aircraft positioned at various places on the full-scale facility. The aerodynamic forces and moments were then used as inputs to a statics problem in order to determine the reaction between the aircraft landing gear and ramp. The analysis was embodied in a computer program. Three specific aircraft were considered in the study, namely the E-3, E-4, and B-52. However, the analysis and computer program are not limited to these three aircraft, but should be applicable to aircraft of the same generic class.

The statics problems for the three aircraft considered were all indeterminate with different degrees of redundancies depending on the number of landing gears on each aircraft. These redundancies were overcome by idealizing the aircraft structure as being composed of beams with uniform structural properties and applying the principle of consistent deflections. In this fashion the statics problems could be solved without detailed knowledge of the structural characteristics of each aircraft. The analysis worked well for the E-3 aircraft (3 landing gears) and the B-52 aircraft (4 landing gears) but gave unrealisticly low values for the safe handling speed of the E-4 (5 landing gears). The E-4 was subsequently analyzed by replacing the actual 5 gear undercarriage with an equivalent 3 gear undercarriage and this analysis appears to give reasonable results.

The maximum wind velocity for safe handling was set by the occurrence of lifting or sliding of any one of the aircraft landing gears. Using this criterion and considering all wind directions and aircraft positions, the maximum wind speed for safe handling of all three of the aircraft considered was 30 knots measured at a height of 10 meters on the meteorological tower. The B-52 was most sensitive to wind directions which were 30 degrees off the fuselage centerline and the E-3 and E-4 were most sensitive to crosswinds perpendicular to the fuselage centerline. At wind speeds up to 80 knots, the calculated draw bar loads were well within the draw bar pull limits of the tugs recommended for use with each aircraft.

APPENDIX A
HOT-FILM ANEMOMETER DATA ANALYSIS

The three components of flow velocity in the model test program were measured with a three-sensor hot film probe (TSI Model No. 1294CC-20-18) in conjunction with three channels of Calspan fabricated constant temperature hot-wire anemometer bridges. Each of the three channels was calibrated in a flow velocity calibration apparatus (TSI Calibrator Model No. 1125) to determine the output voltage as a function of flow velocity perpendicular to the sensor elements. The results indicated that all three sensors were extremely well matched and that a single calibration equation could be used to calculate the velocity component perpendicular to each sensor. The final calibration equation is:

$$\frac{\rho}{\rho_o} U = \left(\frac{E^2 - 1.44}{0.3909}\right)^2 \qquad \text{(A-1)}$$

where E = anemometer output voltage (volts)

U = velocity perpendicular to hot-film sensor (FT/SEC)

ρ = air density (slugs/ft^3)

ρ_o = air density under standard conditions (2.38×10^{-3} slugs/ft^3)

The density terms are included in the calibration because the hot-film sensors respond to density times velocity rather than to velocity alone. The calibration equation was obtained at air temperatures ranging between 67 and 72 degrees Fahrenheit. There would be small corrections involved in the constants in Equation (A-1) if the air temperature exceeds this temperature range. However, in the test program the air temperature in the wind tunnel was maintained within this range by proper setting of the heater thermostats in the large room which houses the tunnel.

The percentage accuracy of the hot-film calibrations is shown in Figure A-1 where it is plotted as a function of the flow velocity term, $\frac{\rho}{\rho_o} U_{MEASURED}$, perpendicular to each sensor. As can be seen, the calibration

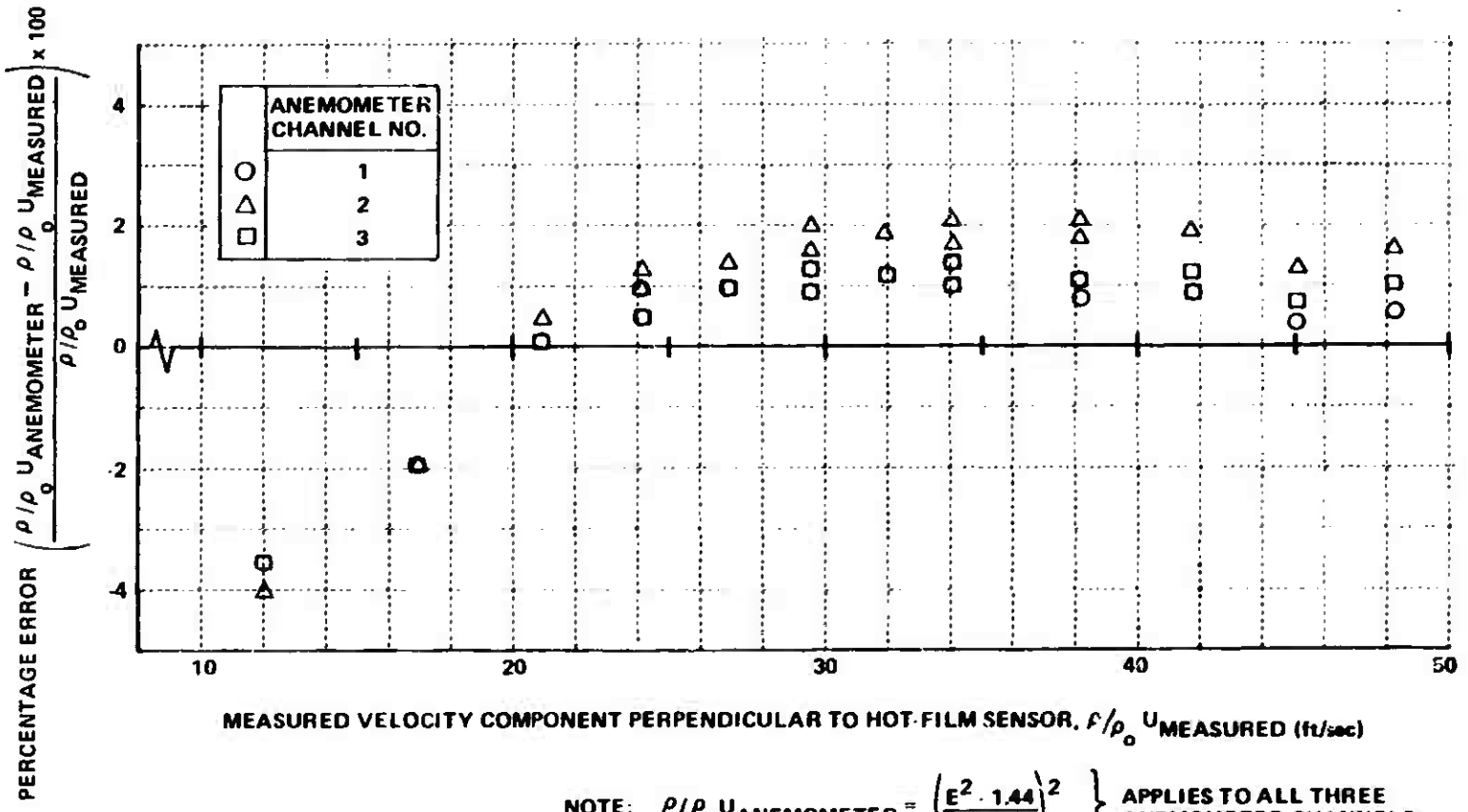

NOTE: $\rho/\rho_o U_{ANEMOMETER} = \left(\frac{E^2 \cdot 1.44}{0.3909}\right)^2$ } APPLIES TO ALL THREE ANEMOMETER CHANNELS

WHERE E = ANEMOMETER VOLTAGE OUTPUT
ρ = AIR DENSITY (slugs/ft^3)
ρ_o = AIR DENSITY AT STANDARD CONDITIONS (2.38×10^{-3} slugs/ft^3)

Figure A-1. Percentage Errors in Calibration of Hot-Film Anemometer Channels.

is within approximately plus or minus two percent except at the lowest test velocity where it approaches four percent. The apparent increase in percentage error at the lowest flow velocities may not be real since it is very difficult to obtain an accurate independent measurement of the flow velocity at low speeds. The independent measurement was obtained from an inclined micromanometer in these calibrations and the measured pressure difference from which $\frac{\rho}{\rho_s} U_{MEASURED}$ is calculated became very small (less than 0.05 inches of water at the lowest calibration velocity). In any event the four percent error (if real) is very small in terms of absolute velocity and since it occurs at low velocities is not significant in terms of calculating the forces on aircraft.

The calibration equation provides a relation from which the effective cooling velocity component normal to each sensor can be calculated. One then uses these cooling velocities to calculate the velocity components in a wind axis or wind tunnel coordinate system. The equations required for calculating velocity components in the tunnel coordinate system can be developed as follows.

The hot-film probe was mounted on the traversing system in the tunnel so that the three mutually perpendicular hot-film sensors each formed an equal angle, θ, with the wind tunnel axis. If one designates the wind tunnel coordinates as x', y', z' and a coordinate system parallel to the three sensors as x, y, z then the resulting geometry is illustrated in the sketch on the following page.

The channel number designations shown in the sketch correspond to the channel numbers marked on the probe purchased from TSI (See Figure 3 in main text). If one uses the calibration Equation A-1 to calculate the effective cooling velocity components to each sensor channel and calls these velocities U_1, U_2 and U_3 to correspond to the channel numbers, then a simple algebraic relationship exists between the cooling velocities U_1, U_2, U_3 and the actual velocity components V_x, V_y, V_z parallel to each sensor. For the TSI probe,

SKETCH OF HOT-FILM SENSOR GEOMETRY

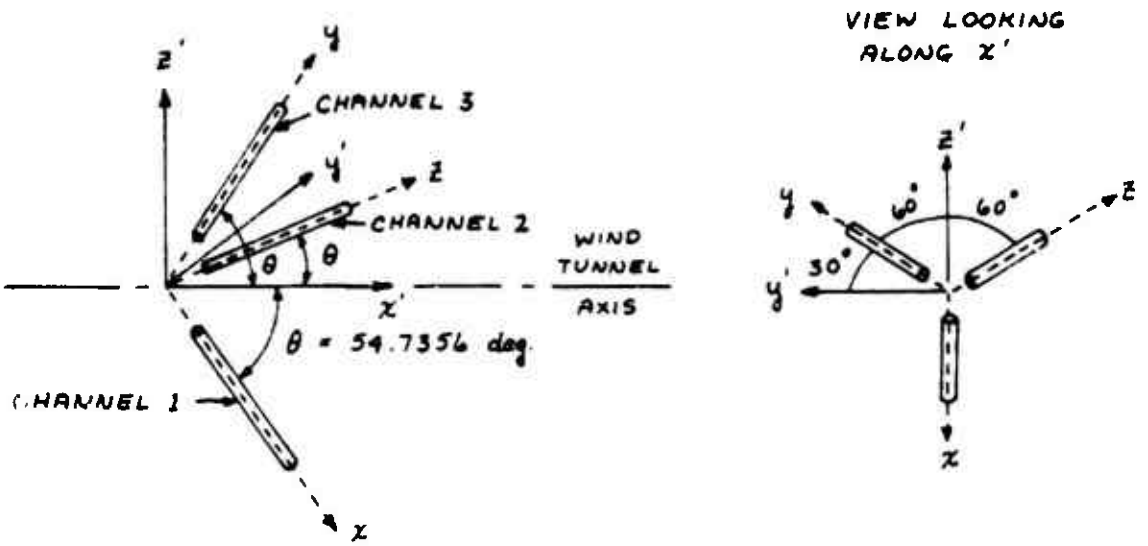

SENSOR COORDINATE SYSTEM IS x, y, z

WIND TUNNEL COORDINATE SYSTEM IS x', y', z'

these relationships are,

$$U_1^2 = V_y^2 + V_z^2 + k^2 V_x^2$$

$$U_2^2 = V_x^2 + V_y^2 + k^2 V_z^2 \qquad \text{(A-2)}$$

$$U_3^2 = V_x^2 + V_z^2 + k^2 V_y^2$$

The information bulletin[A-1] for data reduction on the TSI probe suggests a relation which can be reduced to the form of Equations (A-2). The

---

A-1 "Data Reduction Method for Model 1294 - 3 D Probes Orthogonal Sensors", TSI Technical Bulletin TB8

terms which contain the constant k compensate for sensitivity of the sensor to flow components parallel to it. The value of the constant was found to be k = 0.2 from calibration tests with the flow parallel to the sensors.

Equations (A-2) relate the effective cooling velocities (U_1, U_2, U_3) which are found from the calibration Equation (A-1) to the actual velocity components (V_x, V_y, V_z) parallel to each sensor. If the probe is immersed in a flow with velocity V whose components are V_x, V_y, V_z then

$$V^2 = V_x^2 + V_y^2 + V_z^2$$

and using Equations (A-2)

$$U_1^2 + U_2^2 + U_3^2 = V^2 (2 + k^2)$$

Further algebraic manipulation gives

$$V_x^2 = \frac{V^2 - U_1^2}{(1 - k^2)} = \frac{U_2^2 + U_3^2 - (1 + k^2) U_1^2}{(2 + k^2)(1 - k^2)}$$

$$V_y^2 = \frac{V^2 - U_3^2}{(1 - k^2)} = \frac{U_1^2 + U_2^2 - (1 + k^2) U_3^2}{(2 + k^2)(1 - k^2)} \qquad \text{(A-3)}$$

$$V_z^2 = \frac{V^2 - U_2^2}{(1 - k^2)} = \frac{U_1^2 + U_3^2 - (1 + k^2) U_2^2}{(2 + k^2)(1 - k^2)}$$

Equations (A-3) are explicit relationships which allow calculation of the velocity components V_x, V_y, V_z given the effective cooling velocities U_1, U_2, U_3 calculated from the calibration Equation (A-1).

One final set of equations is required to transform the velocity components V_x, V_y, V_z in the sensor coordinate system to components V_x', V_y', V_z' in the wind tunnel coordinate system. Referring to the sketch of the sensor geometry and noting the following trigonometric values,

$$\sin\theta = \sqrt{\frac{2}{3}} \; ; \quad \cos\theta = \frac{1}{\sqrt{3}} \; ; \quad \sin 60^\circ = \frac{\sqrt{3}}{2} \; ; \quad \cos 60^\circ = \frac{1}{2}$$

then one can show

$$V_{x'} = V_x \cos\theta + V_y \cos\theta + V_z \cos\theta = \frac{1}{\sqrt{3}} (V_x + V_y + V_z)$$

$$V_{y'} = V_y \sin\theta \sin 60^\circ - V_z \sin\theta \sin 60^\circ = \frac{1}{\sqrt{2}} (V_y - V_z) \qquad \text{(A-4)}$$

$$V_{z'} = -V_x \sin\theta + V_z \sin\theta \cos 60^\circ + V_y \sin\theta \cos 60^\circ$$

$$= \sqrt{\frac{2}{3}} \left(-V_x + \frac{1}{2} V_y + \frac{1}{2} V_z \right)$$

Equations (A-1), (A-3) with k = 0.2 , and (A-4) were programmed into the minicomputer (HP 9825A) to provide on-line solutions for the instantaneous velocity components V_x', V_y', V_z'. Four hundred samples of each of these components were then averaged to provide the mean velocity components $\overline{V_x}'$, $\overline{V_y}'$, and $\overline{V_z}'$. In addition, rms values of the fluctuating velocity components v_x', v_y', v_z', were also obtained by using the relations

$$(\overline{v_{x'}^2})^{1/2} = \left[\overline{V_{x'}^2} - \overline{V_{x'}}^2 \right]^{1/2} \; ; \quad (\overline{v_{y'}^2})^{1/2} = \left[\overline{V_{y'}^2} - \overline{V_{y'}}^2 \right]^{1/2} \; ; \quad (\overline{v_{z'}^2})^{1/2} = \left[\overline{V_{z'}^2} - \overline{V_{z'}}^2 \right]^{1/2}$$

where the bar denotes averages taken over the 400 samples.

Obtaining the rms values involved no additional time during the test program. However they were not required for the purposes of this program and are not reported herein. The mean and rms velocity data are stored magnetically on tape cassettes and can be recalled for further data reduction on the minicomputer if desired.

APPENDIX B

MEAN WIND COMPONENTS ABOVE TRESTLE TEST STAND AND RAMP

This appendix presents the mean velocity components (U, V, W) measured with the hot-film sensor above the TRESTLE model test stand and ramp. The data are presented in twelve figures (B-1 through B-12), with each figure presenting the results for a single wind direction. There are five parts (a through e) to each figure. Each part is for a different height, Z, above the test stand and ramp. The wind direction and height are listed numerically at the bottom of each figure. In addition, the wind direction is shown by an arrow at the bottom of each page. The mean velocities at each station are listed in a vertical column with three numbers. The numbers are in order from the top, the mean horizontal component, U, in the wind direction (positive in the direction of the arrow), the mean horizontal component, V, perpendicular to the wind direction (positive to the left when looking in the direction of the arrow), and the mean vertical component, W, (positive upwards). Each component has been normalized by the mean wind velocity, U_{REF}, at the meteorological station at a height 10 meters above local ground level.

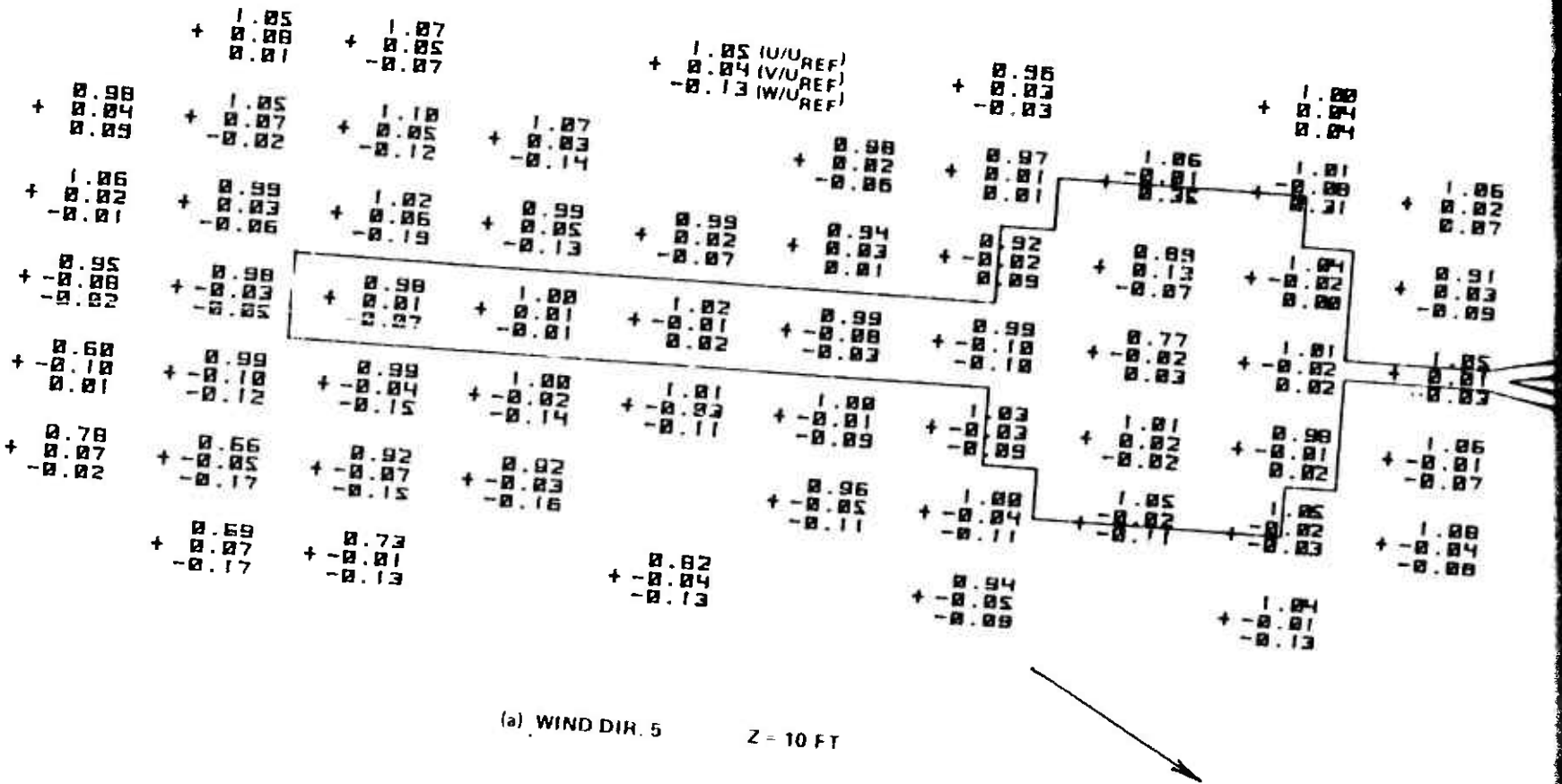

Figure B-1. Mean Velocity Components Above TRESTLE Platform (Wind Axis Coordinates)

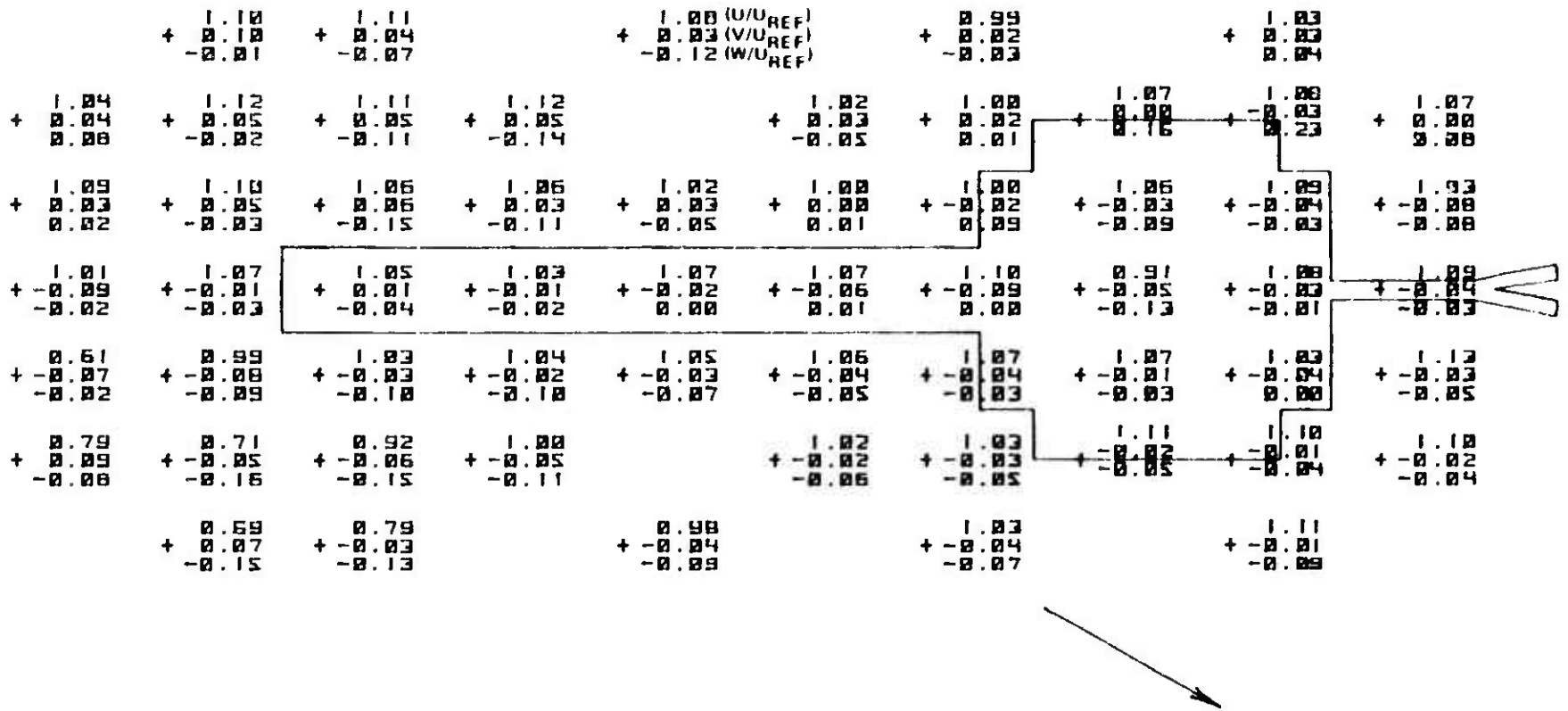

Figure B-1. (Cont.) Mean Velocity Components Above TRESTLE Platform (Wind Axis Coordinates)

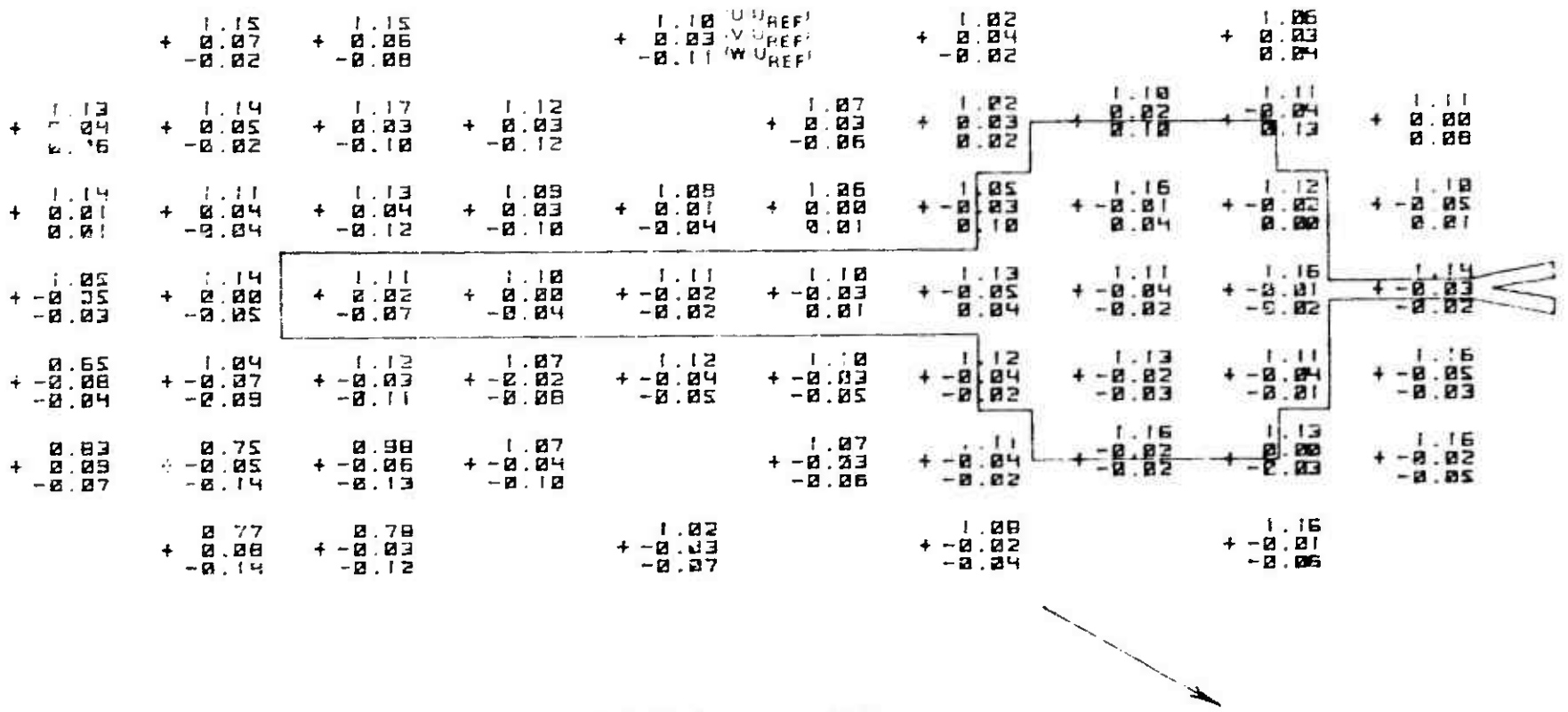

Figure B-1 (Cont.) Mean Velocity Components Above TRESTLE Platform (Wind Axis Coordinates)

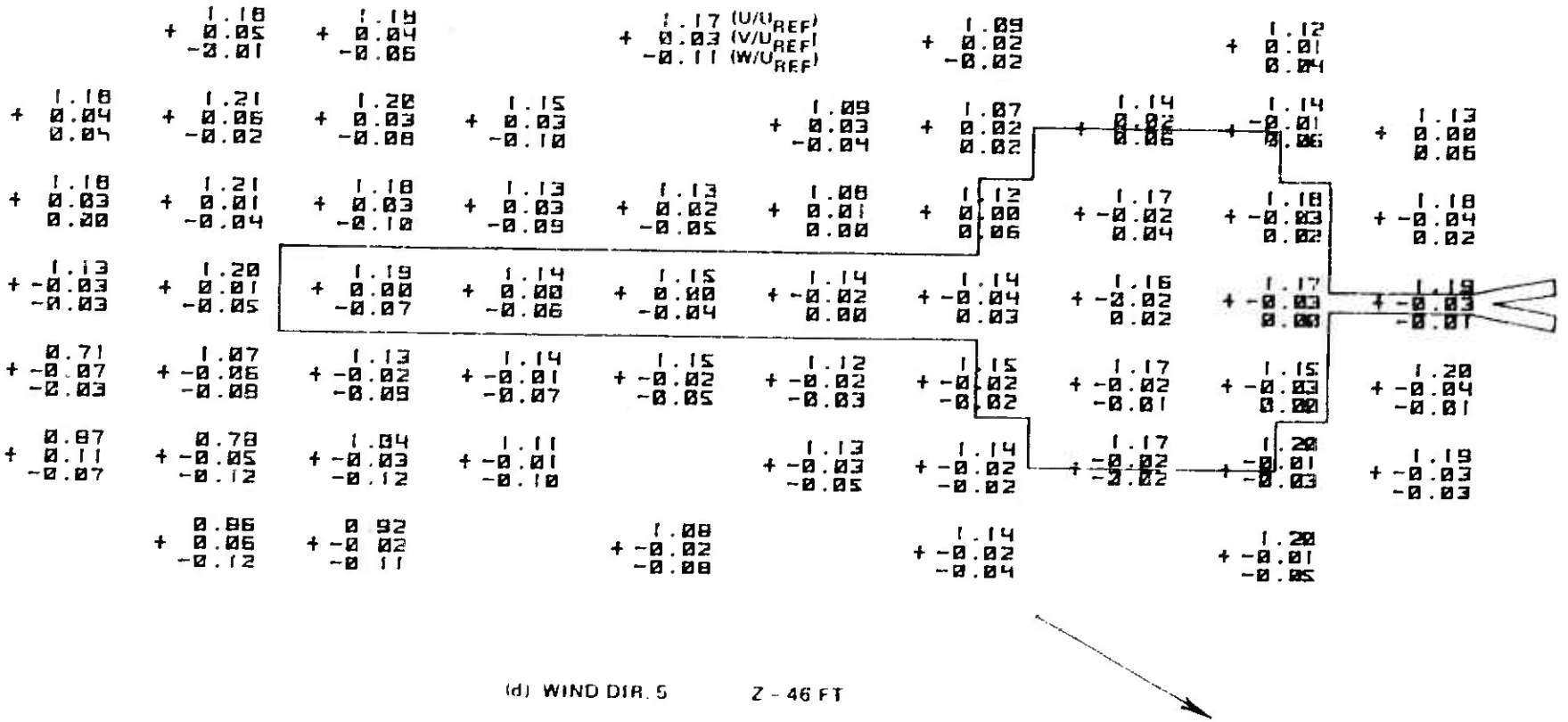

Figure B-1 (Cont.) Mean Velocity Components Above TRESTLE Platform (Wind Axis Coordinates)

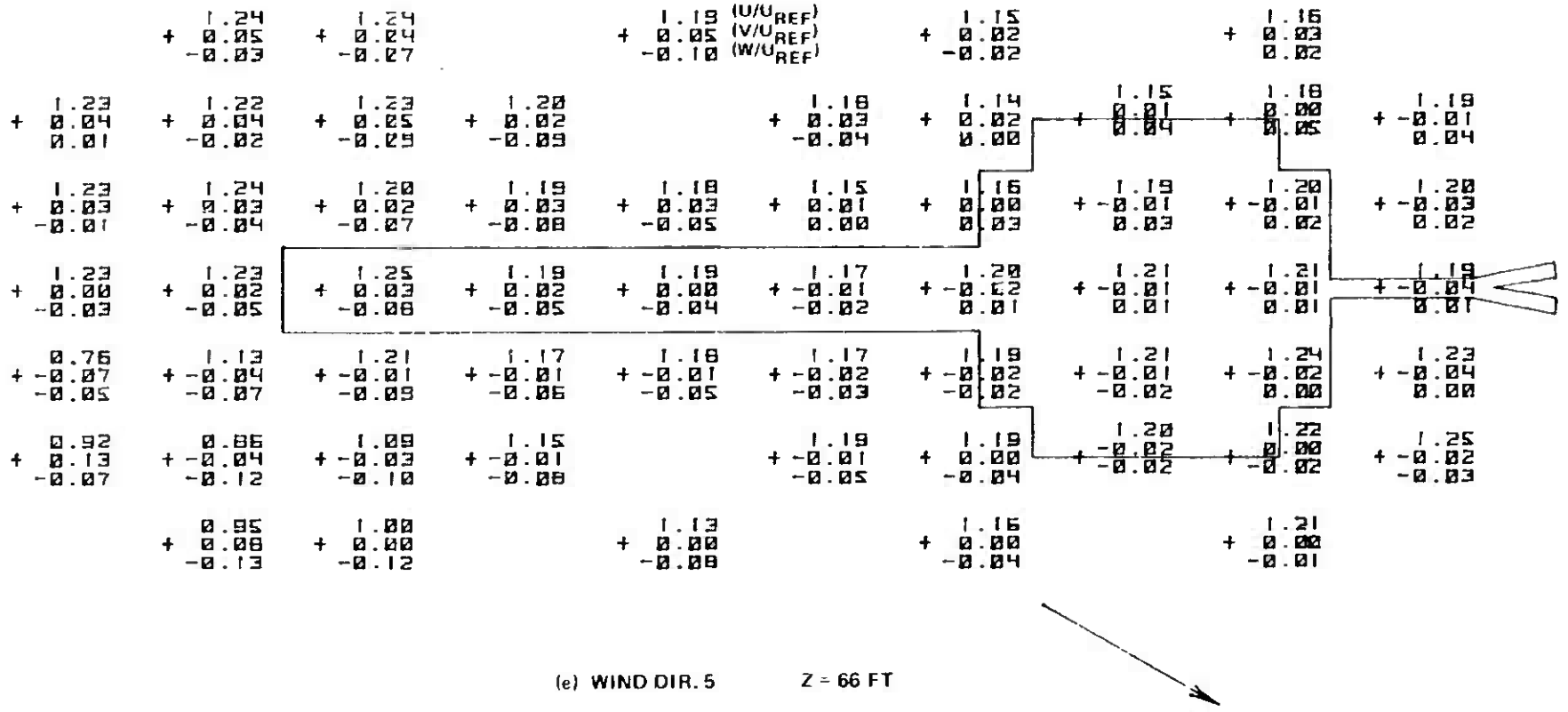

Figure B-2. Mean Velocity Components Above TRESTLE Platform (Wind Axis Coordinates)

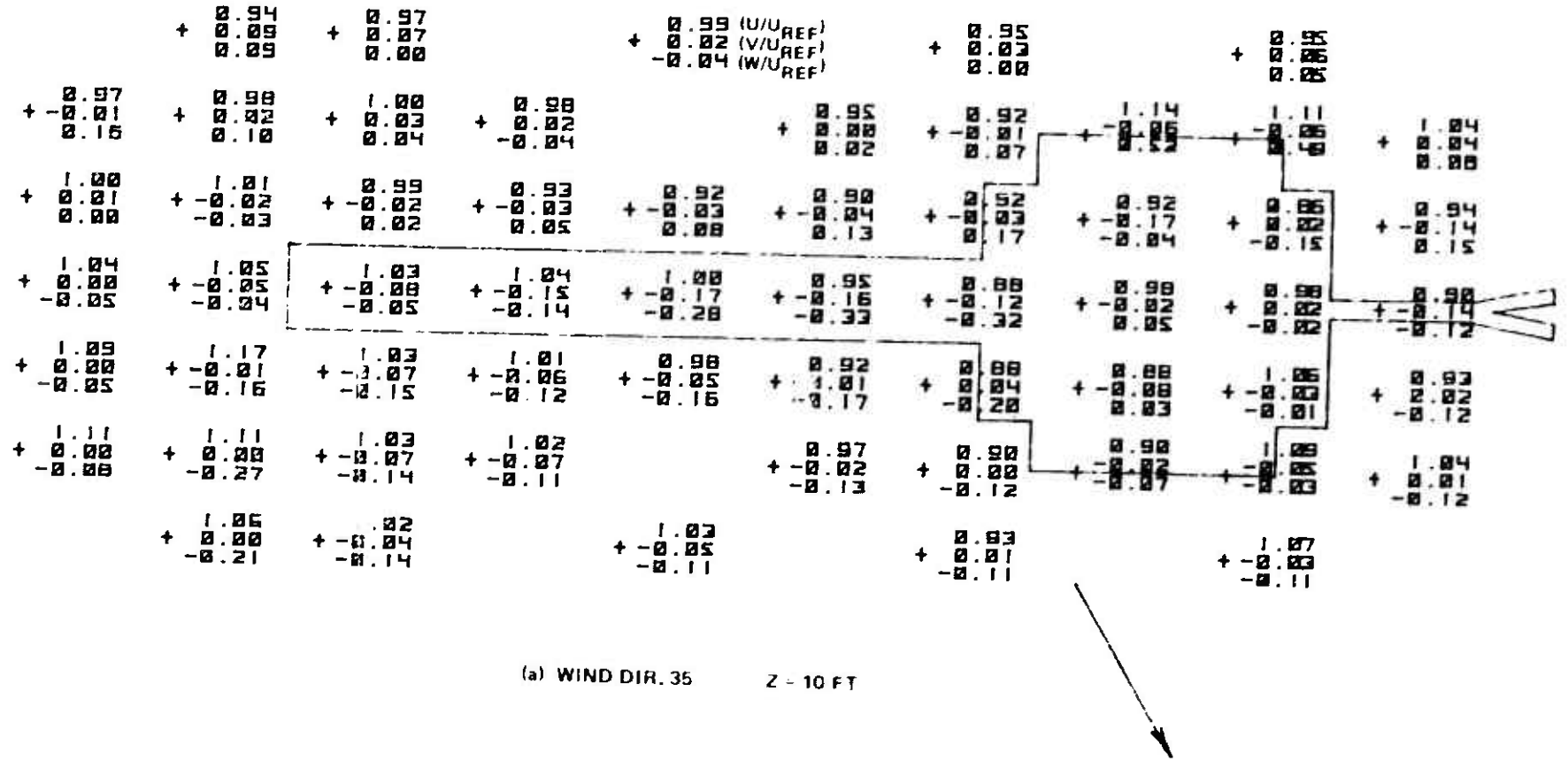

Figure B-2 (Cont.) Mean Velocity Components Above TRESTLE Platform (Wind Axis Coordinates)

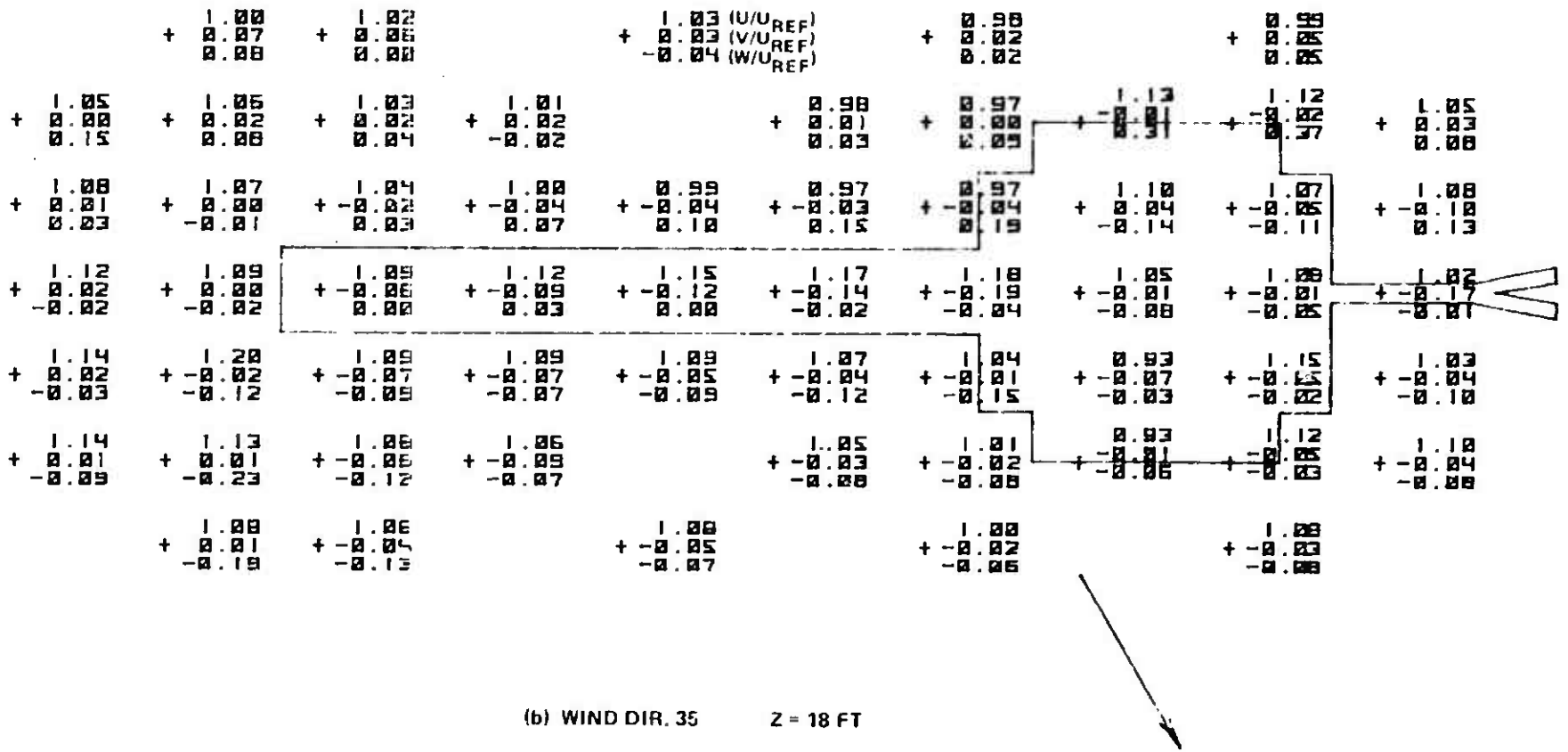

(b) WIND DIR. 35 Z = 18 FT

Figure B-2 (Cont.) Mean Velocity Components Above TRESTLE Platform (Wind Axis Coordinates)

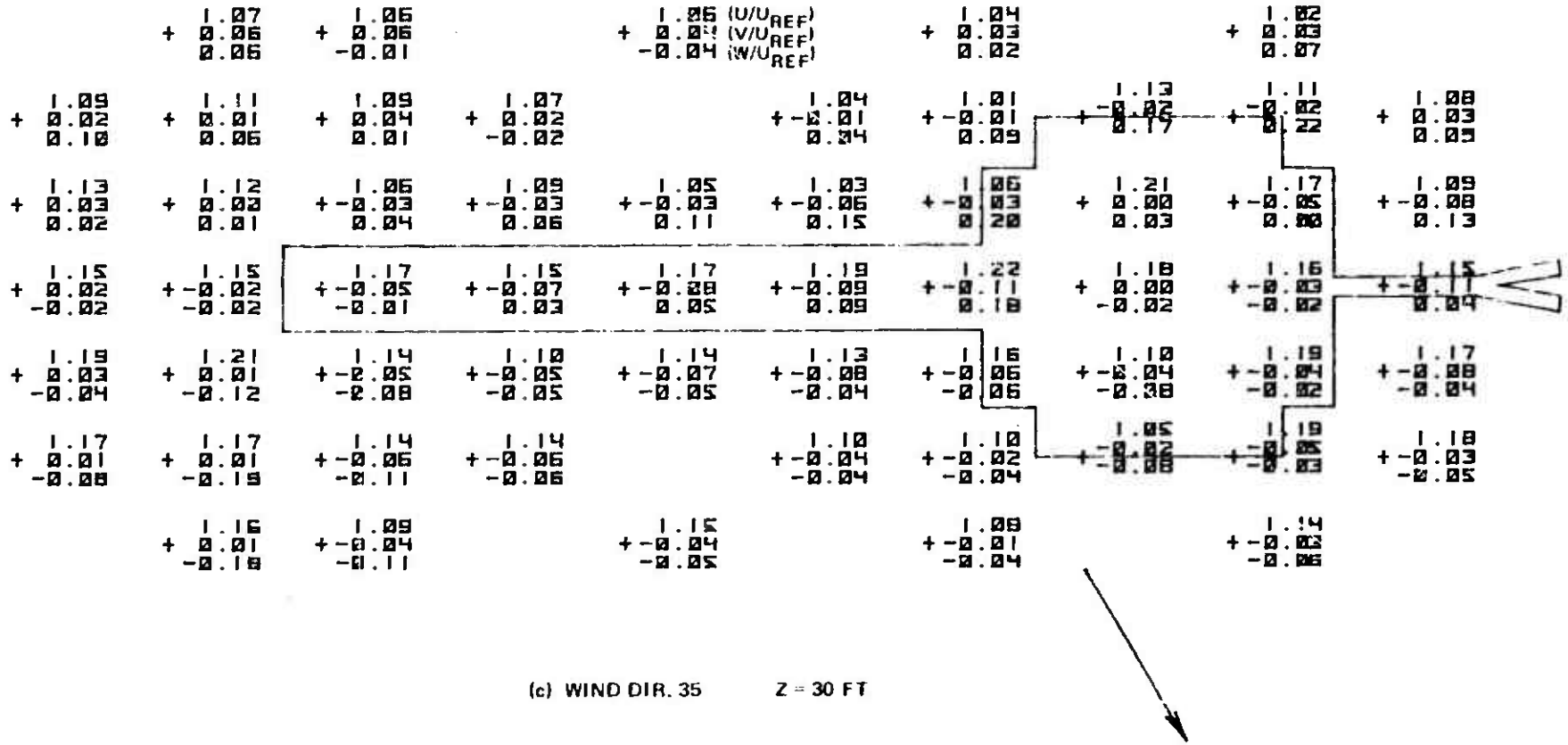

Figure B-2. (Cont.) Mean Velocity Components Above TRESTLE Platform (Wind Axis Coordinates)

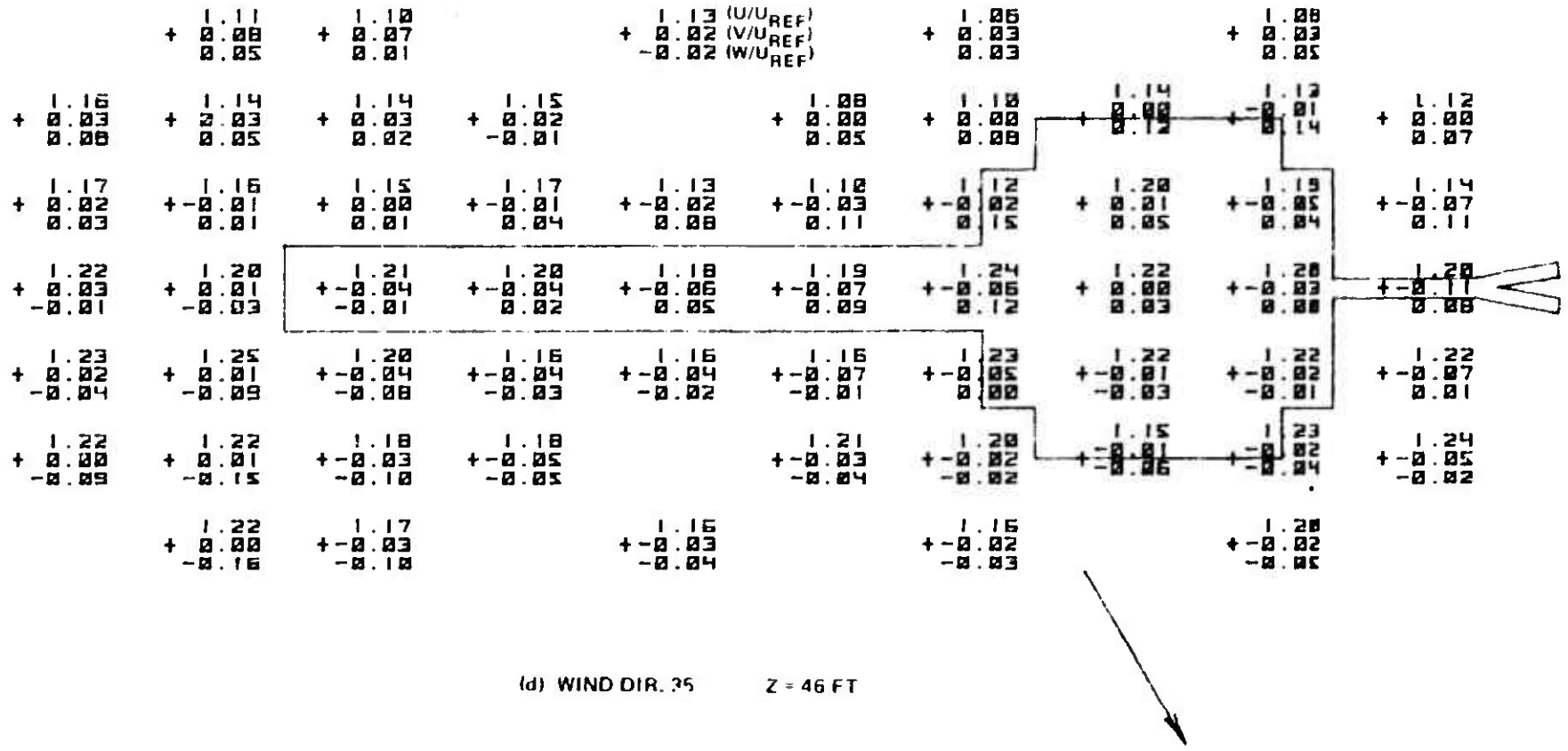

Figure B-2 (Cont.) Mean Velocity Components Above TRESTLE Platform (Wind Axis Coordinates)

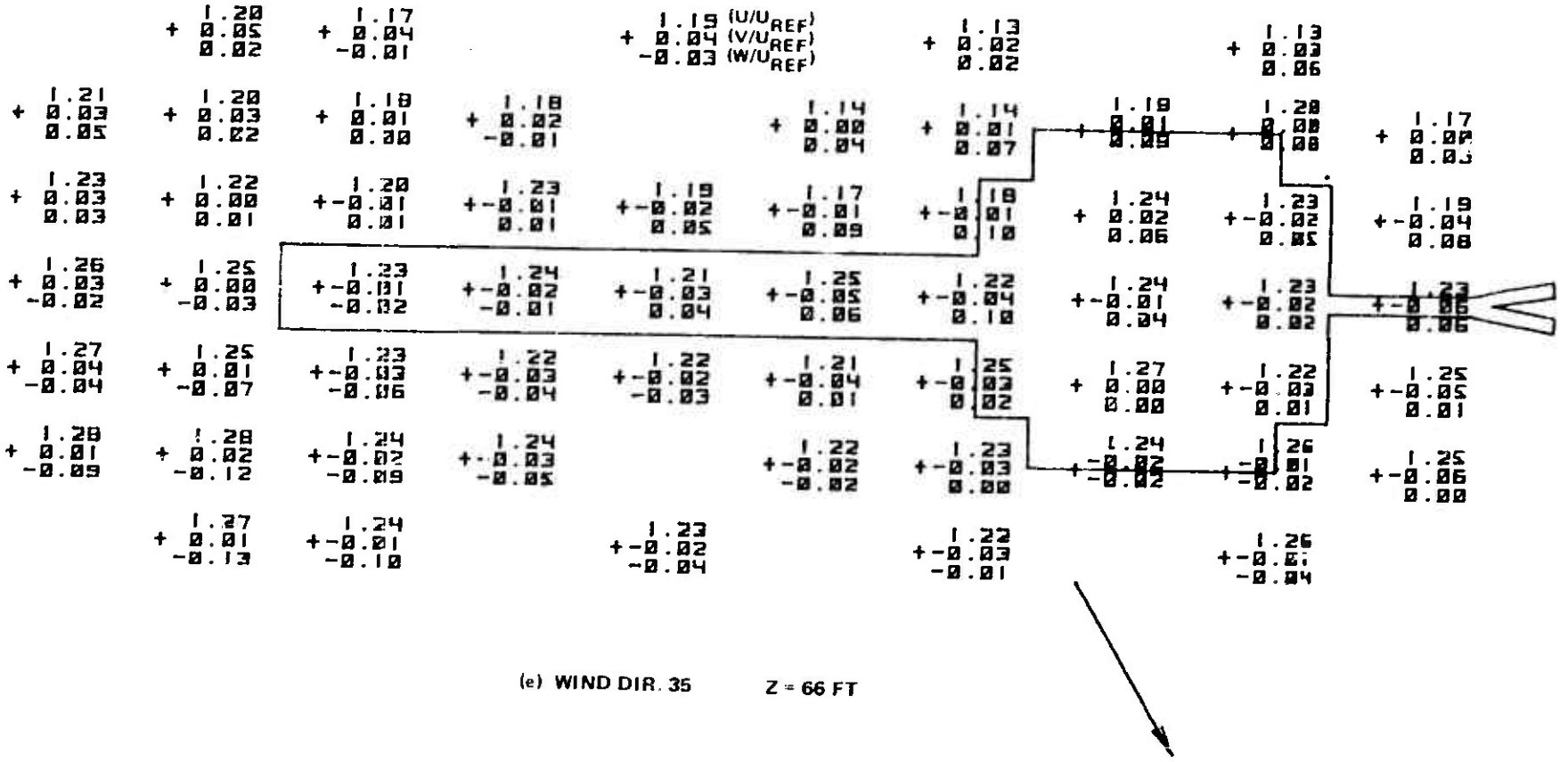

Figure B-3. Mean Velocity Components Above TRESTLE Platform (Wind Axis Coordinates)

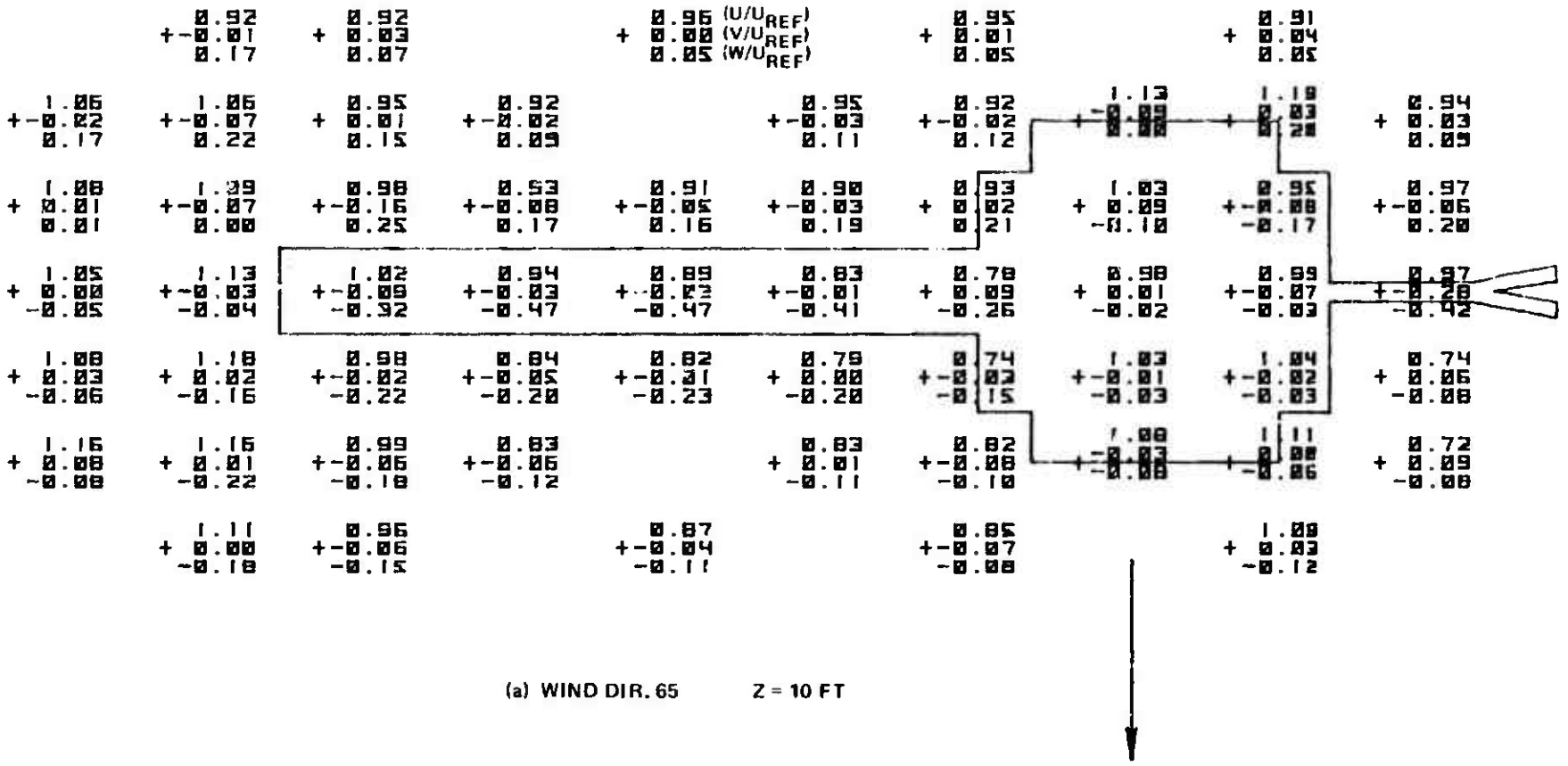

Figure B-3 (Cont.) Mean Velocity Components Above TRESTLE Platform (Wind Axis Coordinates)

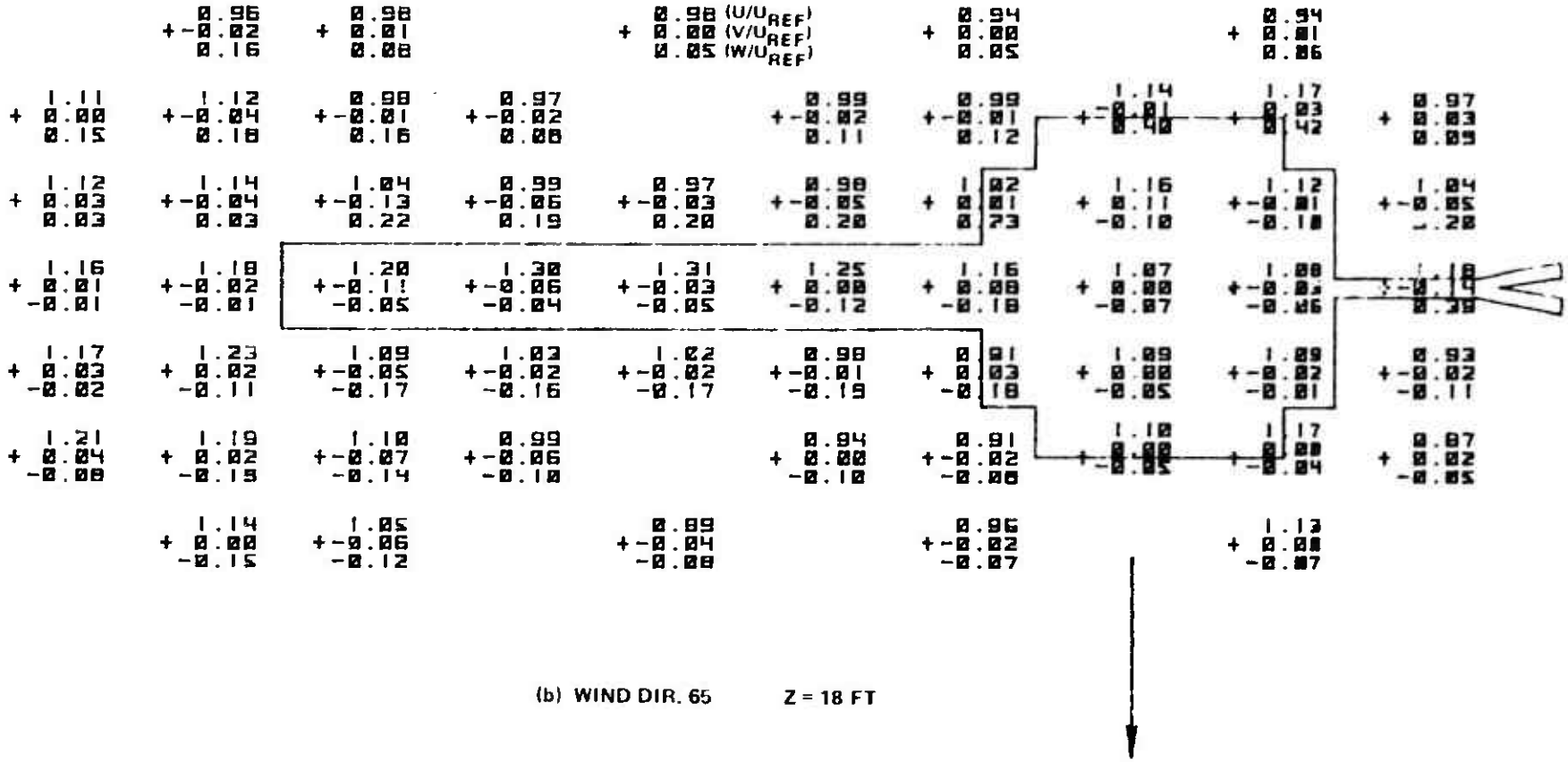

(b) WIND DIR. 65 Z = 18 FT

Figure B-3 (Cont.) Mean Velocity Components Above TRESTLE Platform (Wind Axis Coordinates)

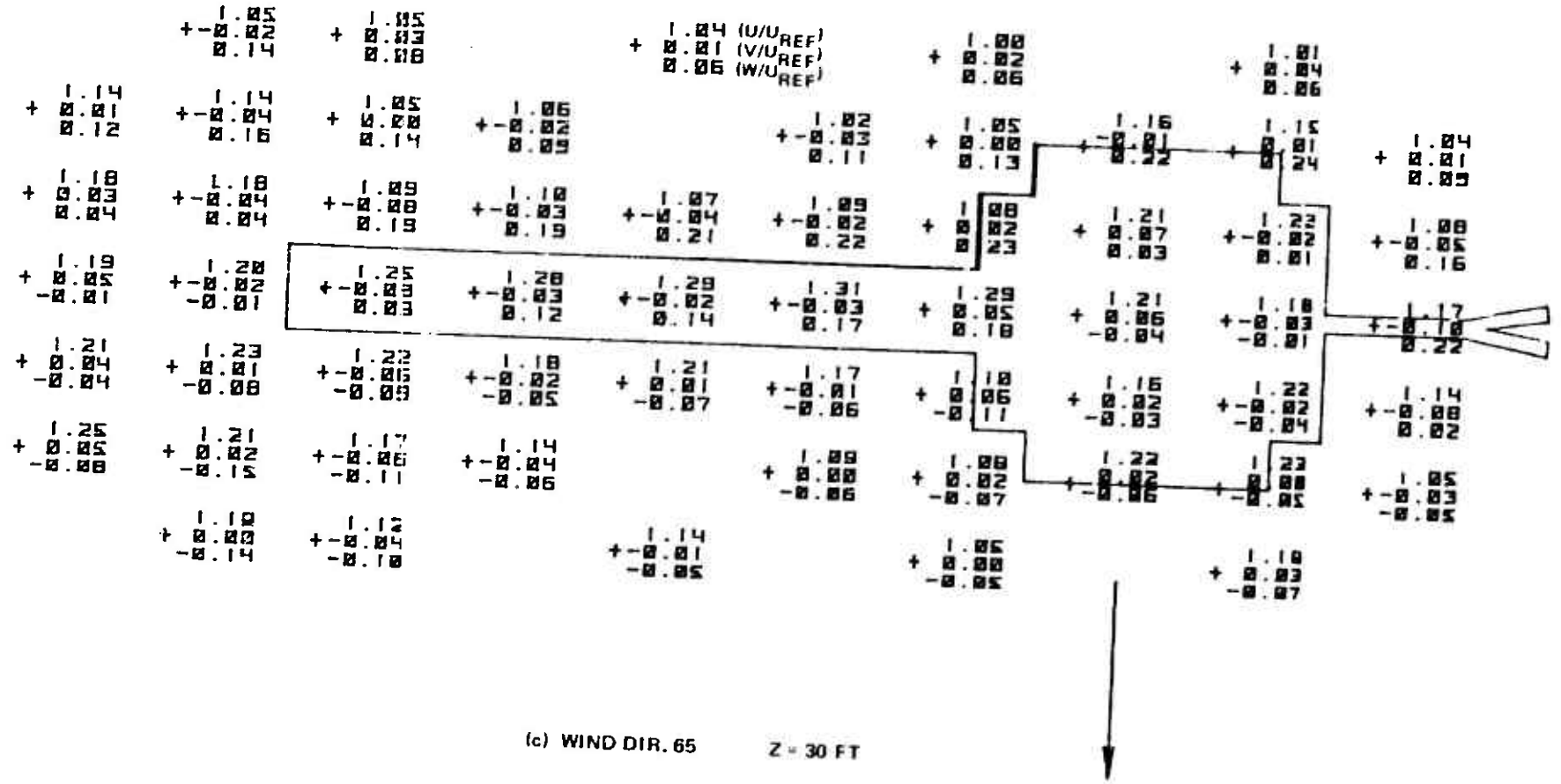

Figure B-3 (Cont.) Mean Velocity Components Above TRESTLE Platform (Wind Axis Coordinates)

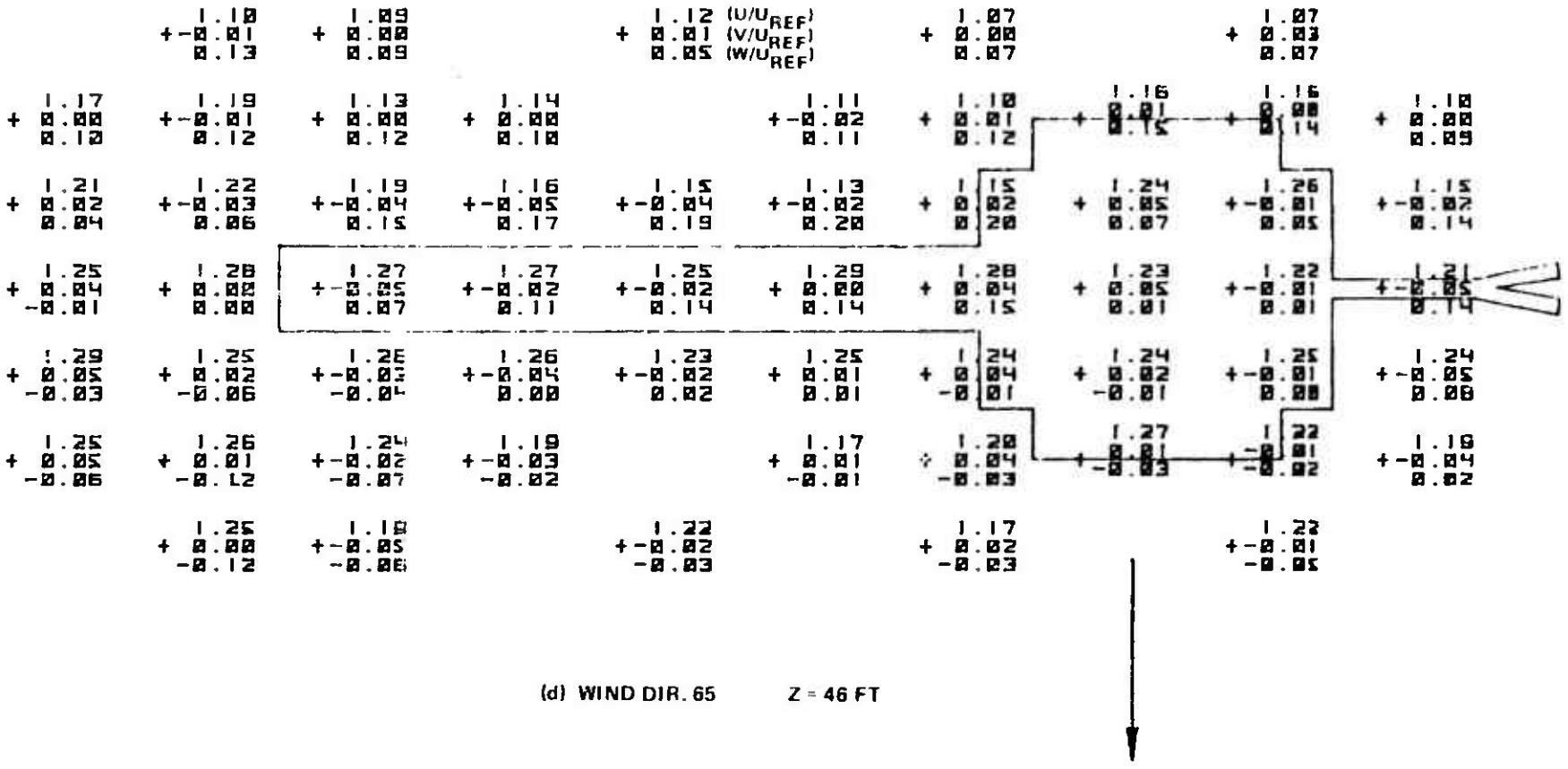

Figure B-3 (Cont.) Mean Velocity Components Above Trestle Platform (Wind Axis Coordinates)

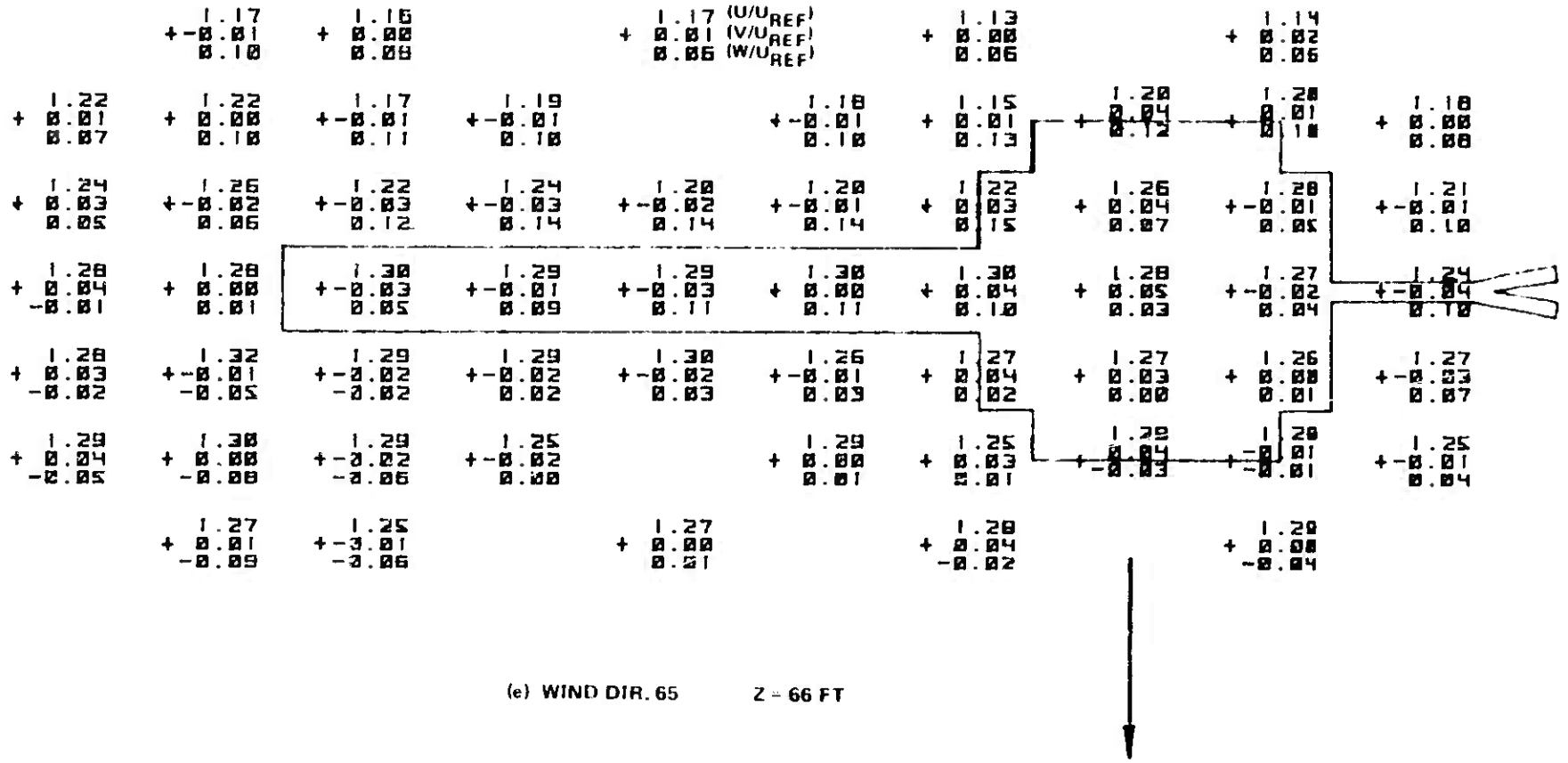

(e) WIND DIR. 65 Z = 66 FT

Figure B-3 (Cont.) Mean Velocity Components Above TRESTLE Platform (Wind Axis Coordinates)

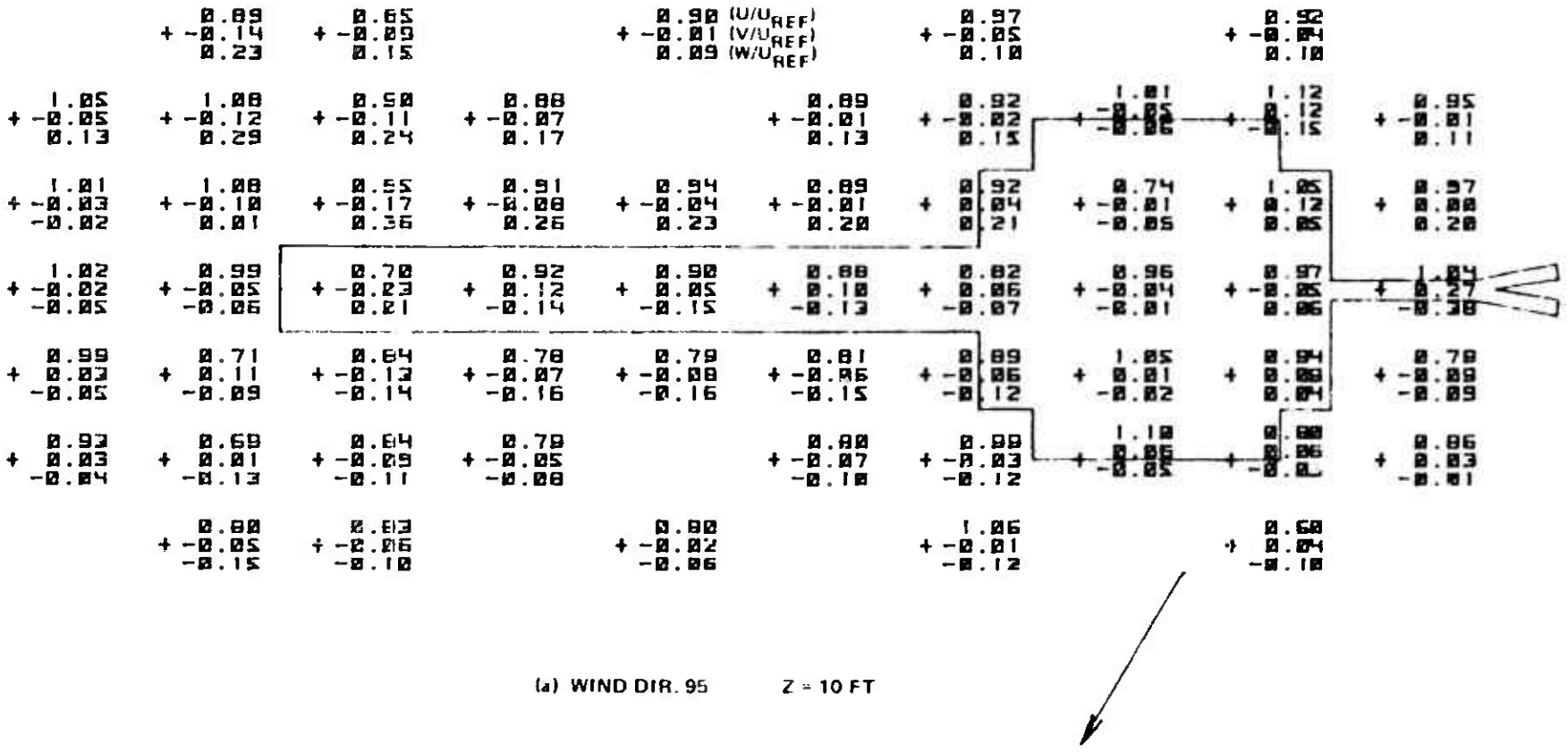

Figure B-4. Mean Velocity Components Above TRESTLE Platform (Wind Axis Coordinates)

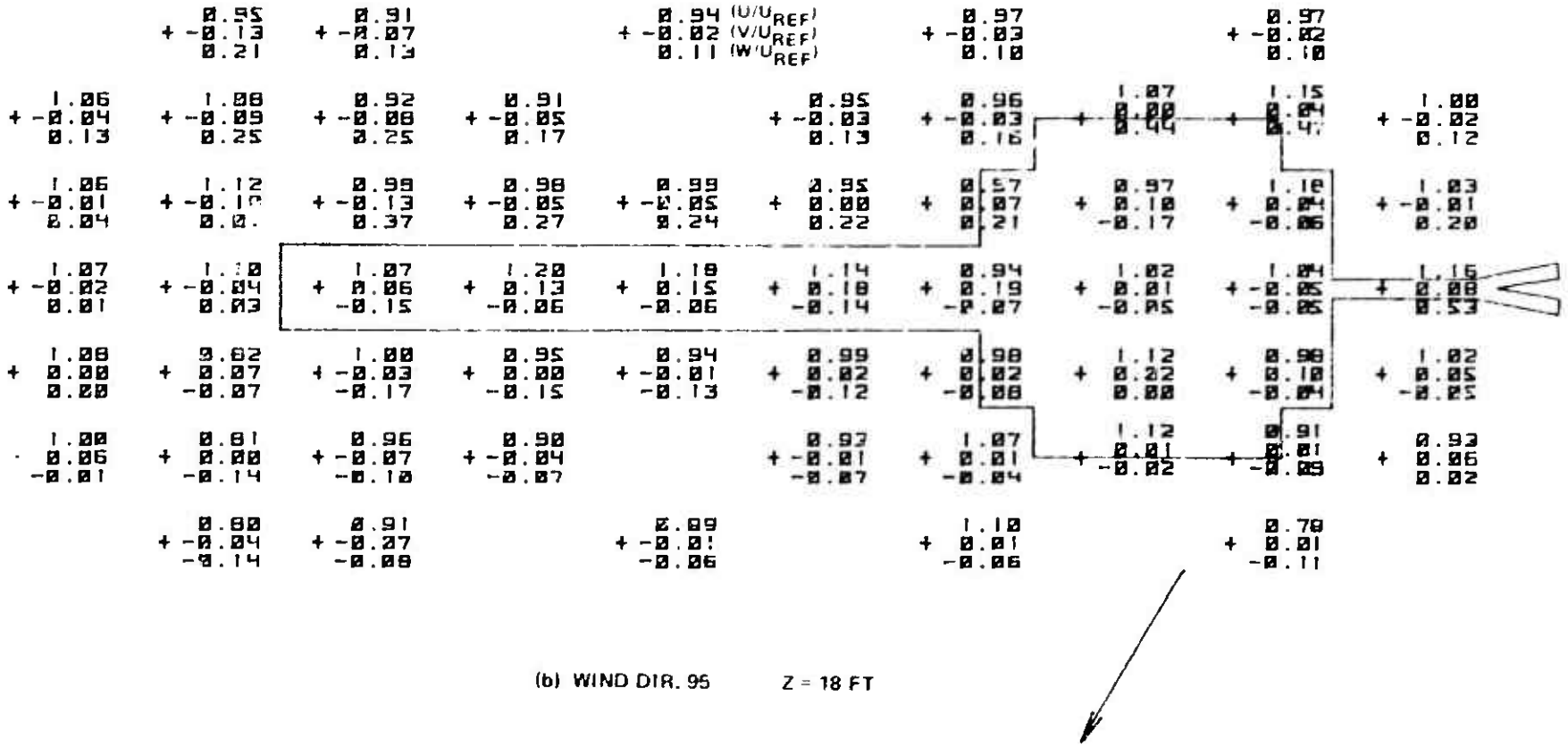

(b) WIND DIR. 95 Z = 18 FT

Figure B-4 (Cont.) Mean Velocity Components Above TRESTLE Platform (Wind Axis Coordinates)

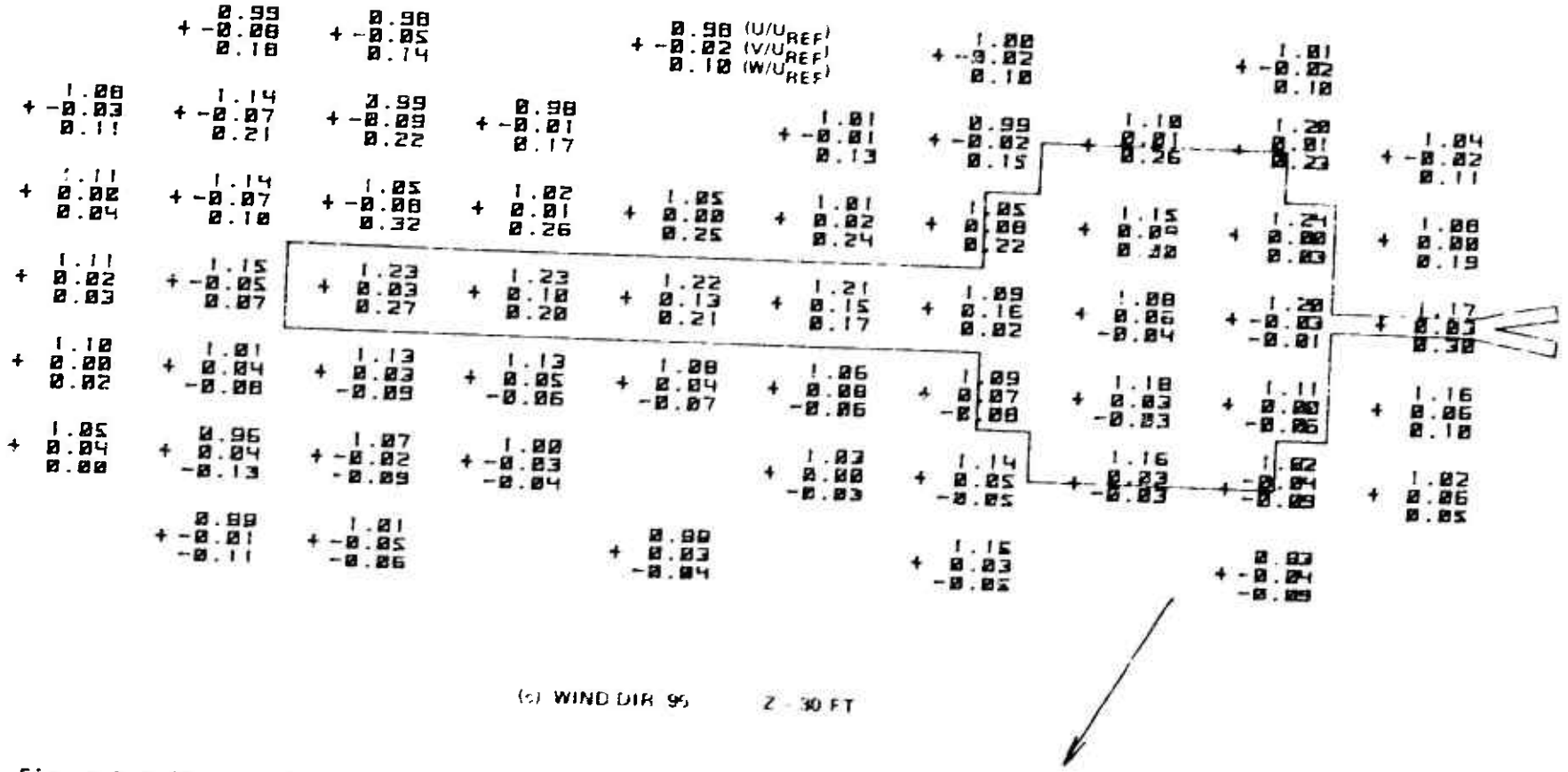

Figure B-4 (Cont.) Mean Velocity Components Above TPESTLE Platform (Wind Axis Coordinates)

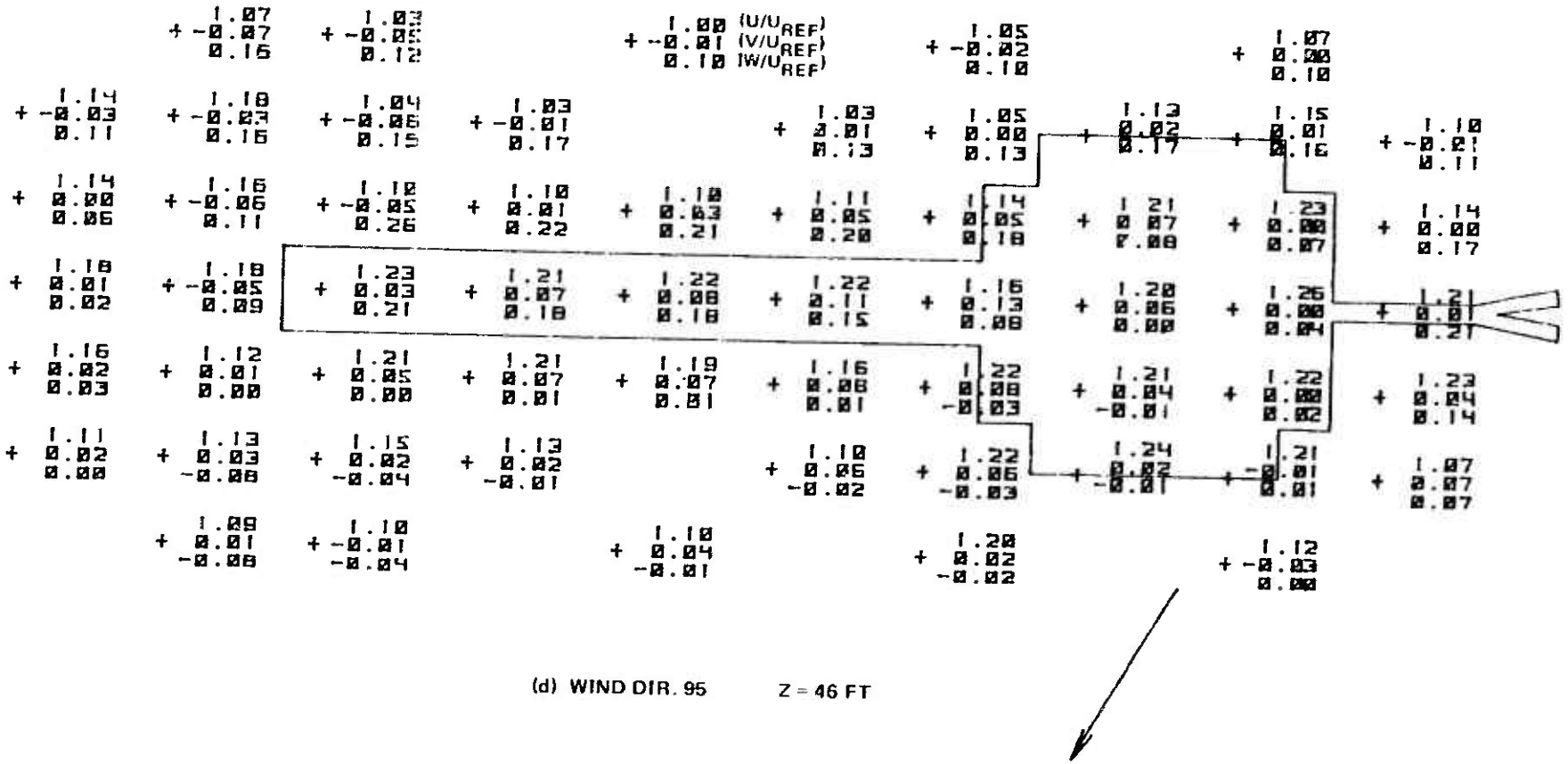

(d) WIND DIR. 95 Z = 46 FT

Figure B-4 (Cont.) Mean Velocity Components Above TRESTLE Platform (Wind Axis Coordinates)

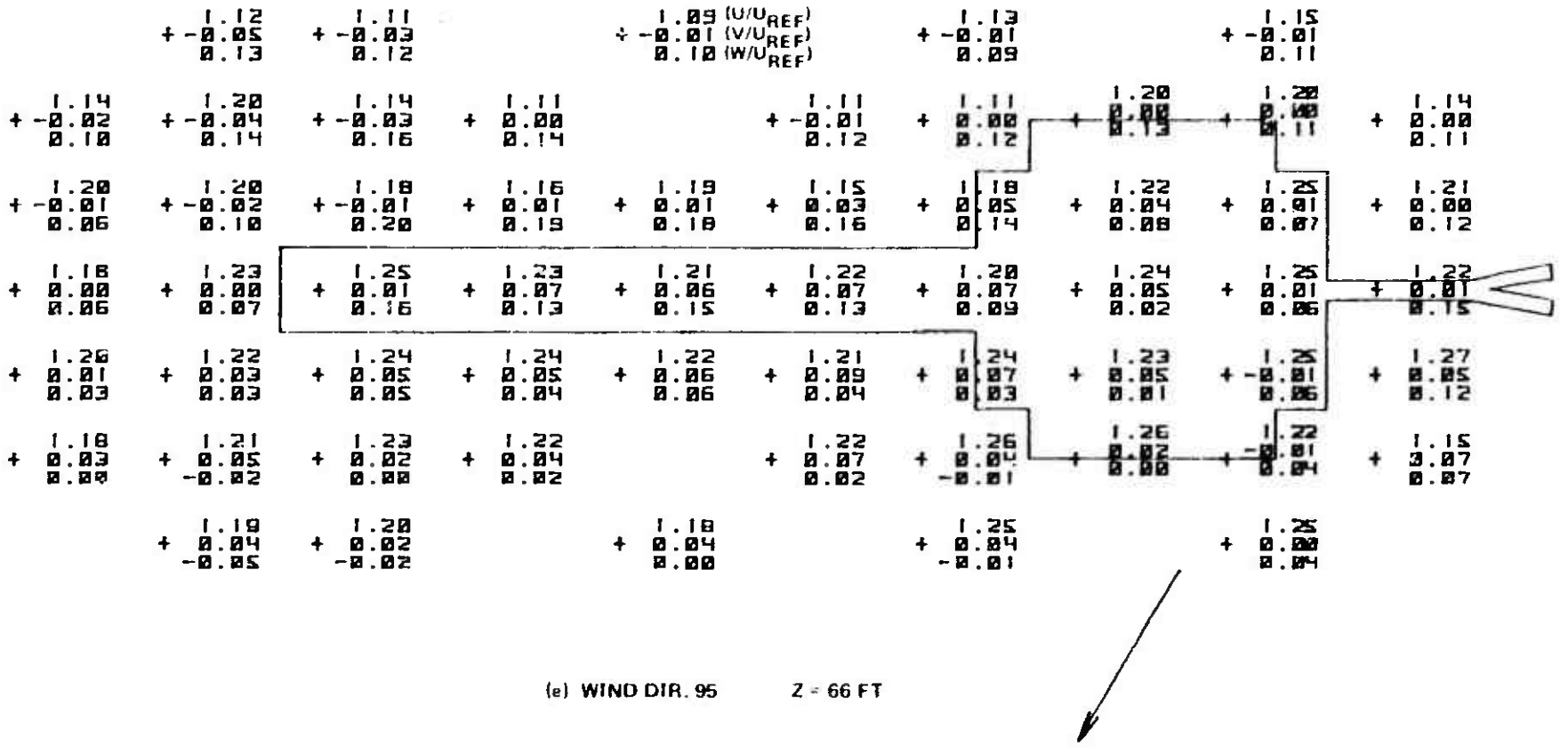

Figure B-4 (Cont.) Mean Velocity Components Above TRESTLE Platform (Wind Axis Coordinates)

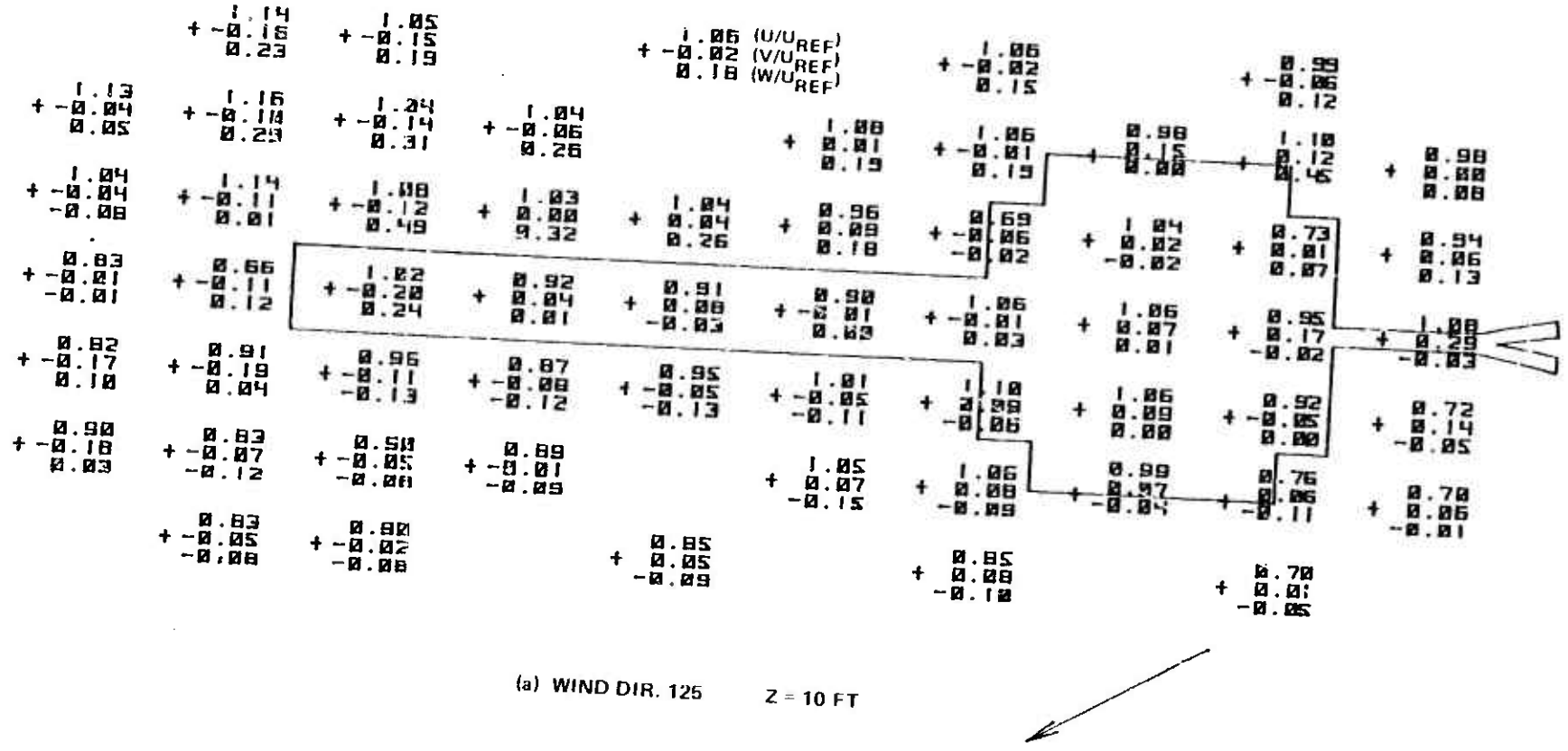

Figure B-5 Mean Velocity Components Above TRESTLE Platform (Wind Axis Coordinates)

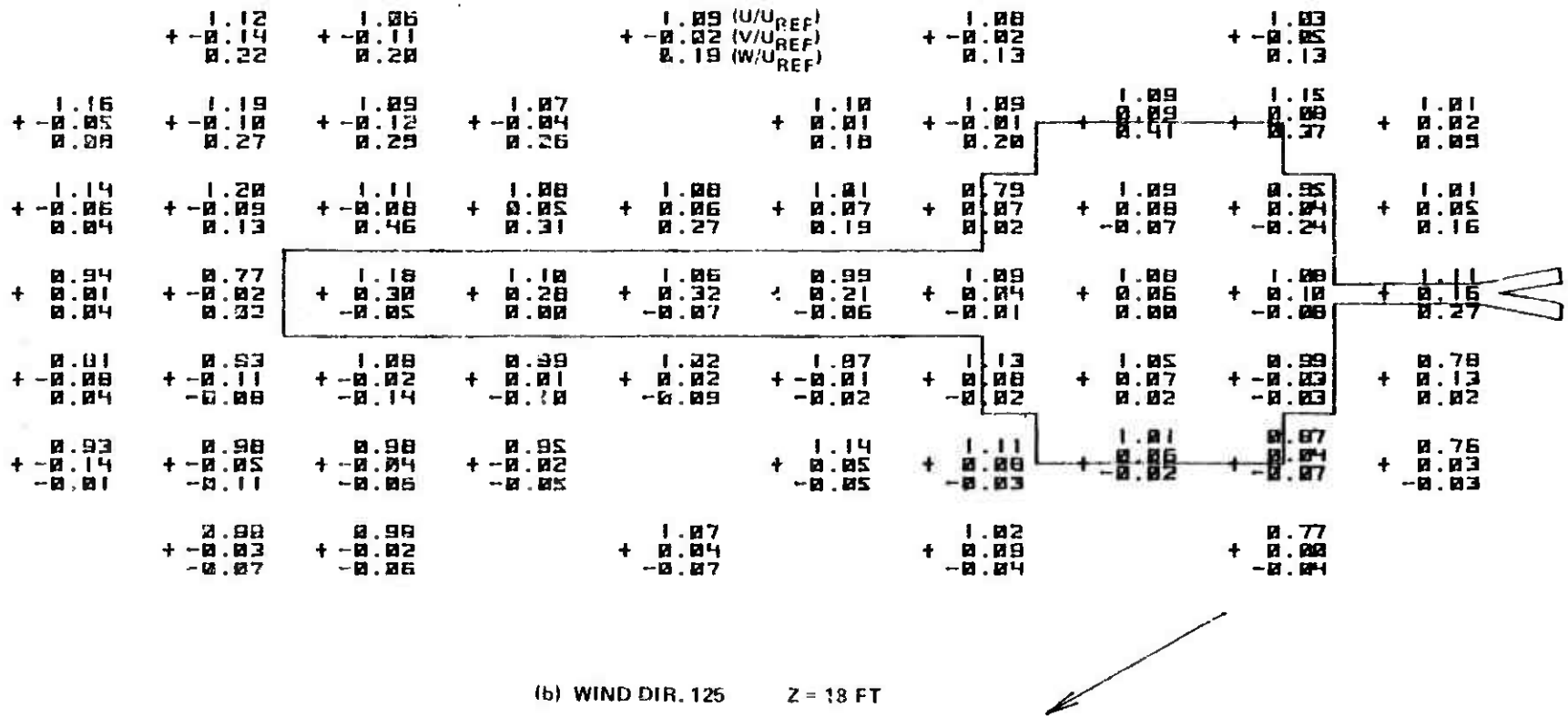

Figure B-5 (Cont.) Mean Velocity Components Above TRESTLE Platform (Wind Axis Coordinates)

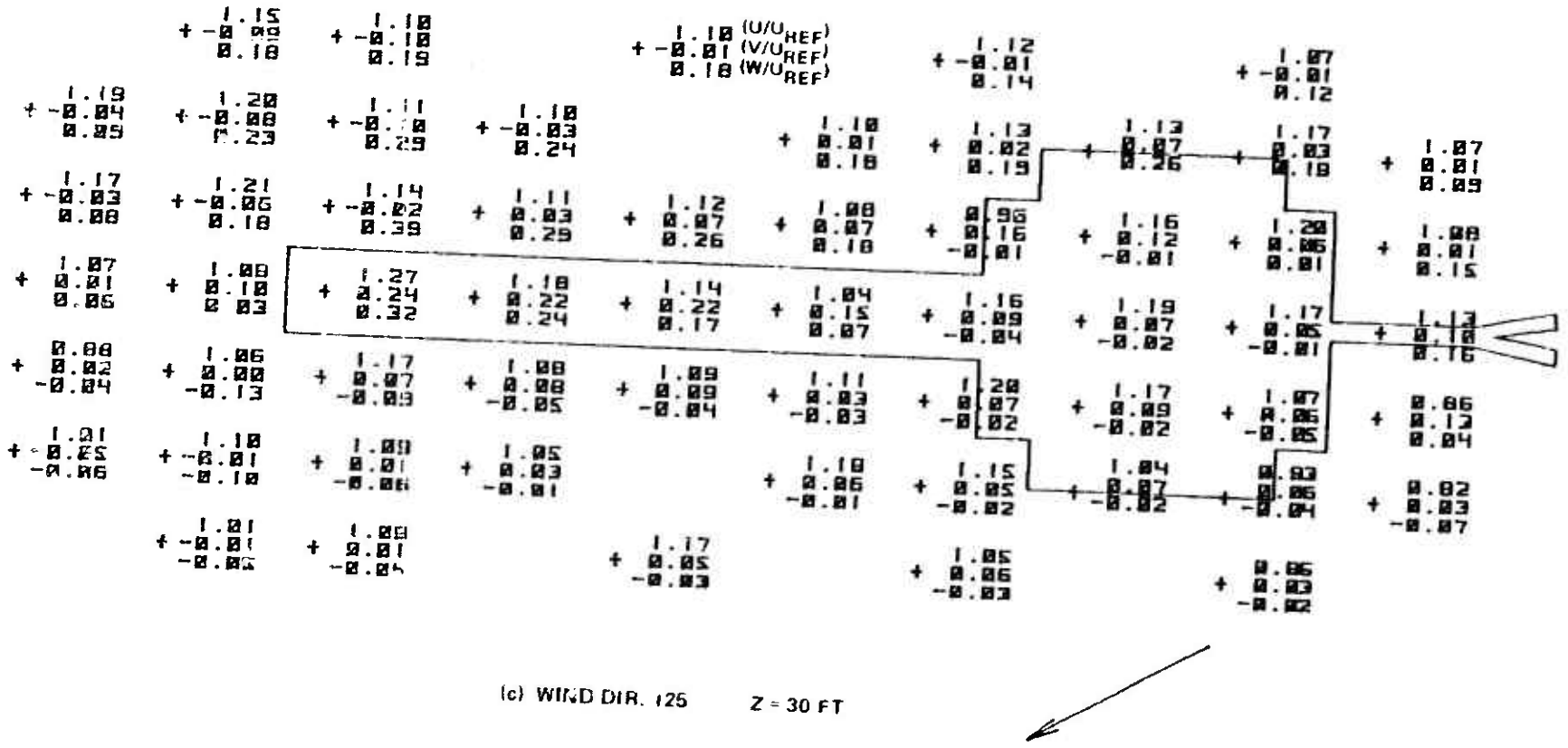

Figure B-5 (Cont.) Mean Velocity Components Above TRESTLE Platform (Wind Axis Coordinates)

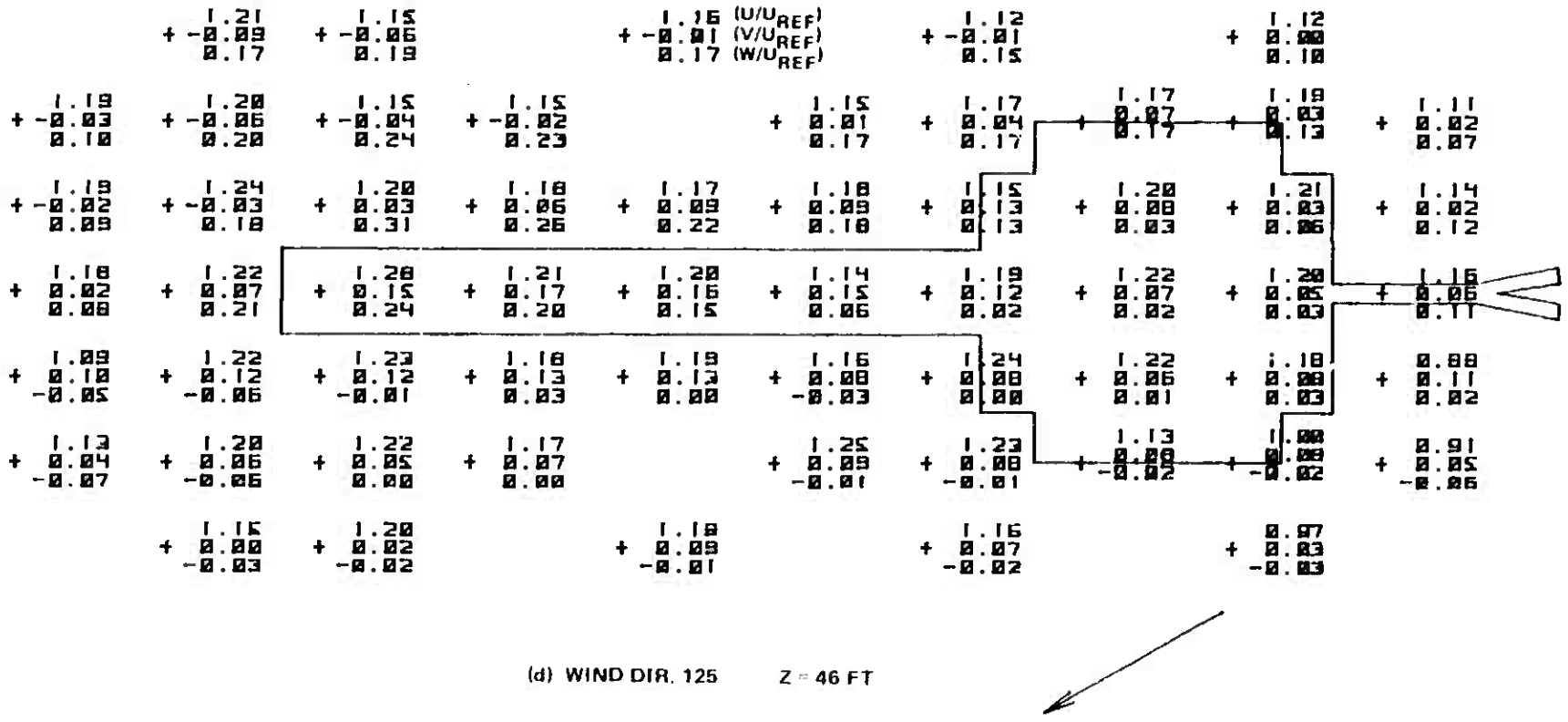

Figure B-5 (Cont.) Mean Velocity Components Above TRESTLE Platform (Wind Axis Coordinates)

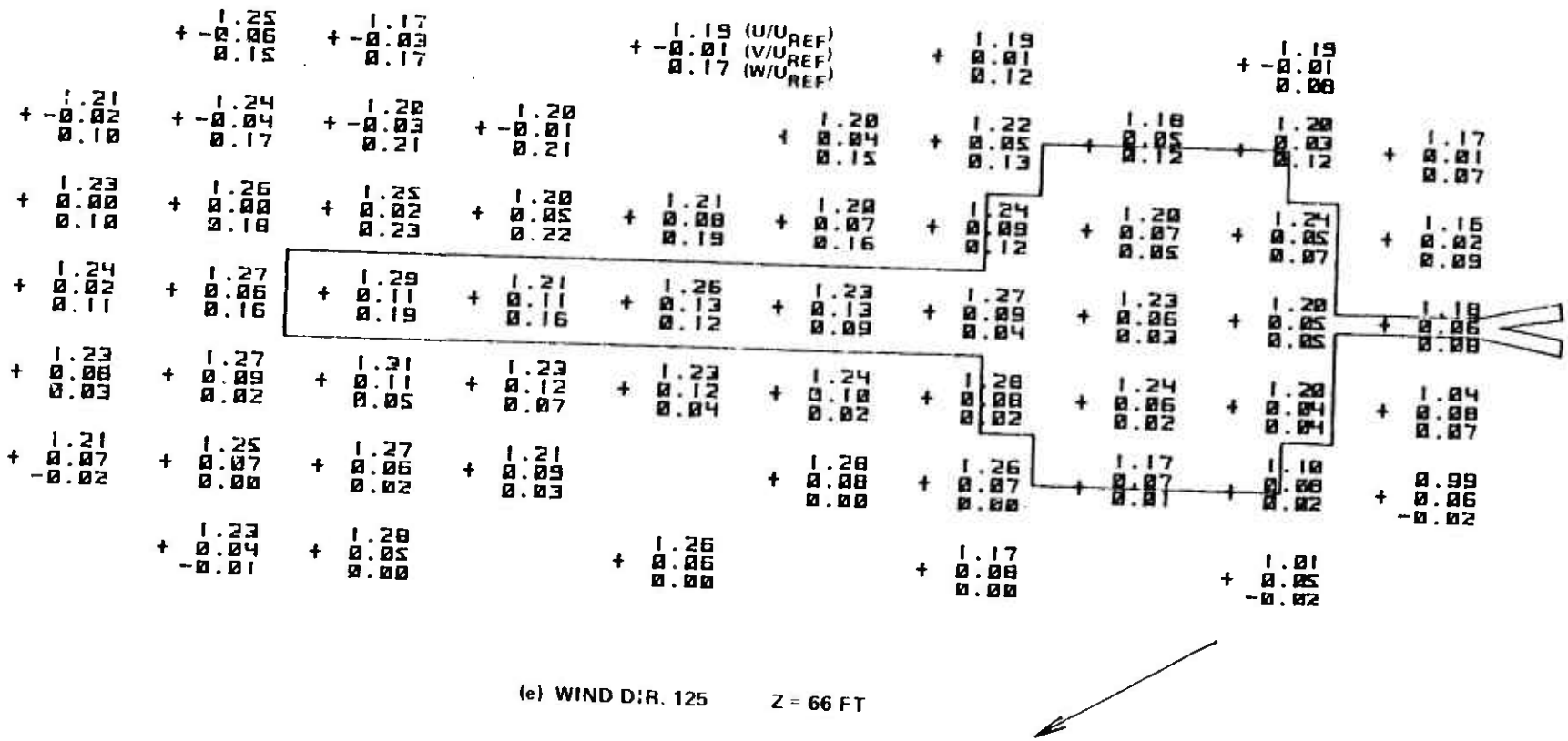

Figure B-5 (Cont.) Mean Velocity Components Above TRESTLE Platform (Wind Axis Coordinates)

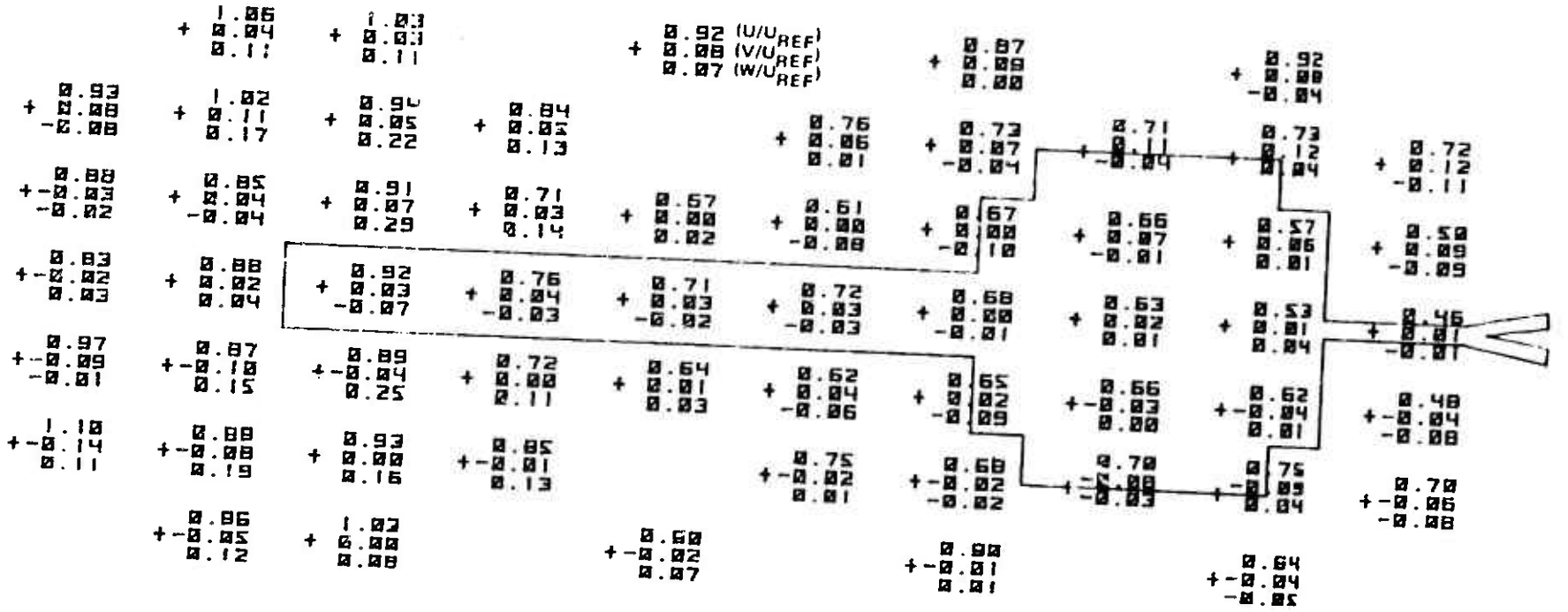

(a) WIND DIR. 155 Z = 10 FT

Figure B-6 Mean Velocity Components Above TRESTLE Platform (Wind Axis Coordinates)

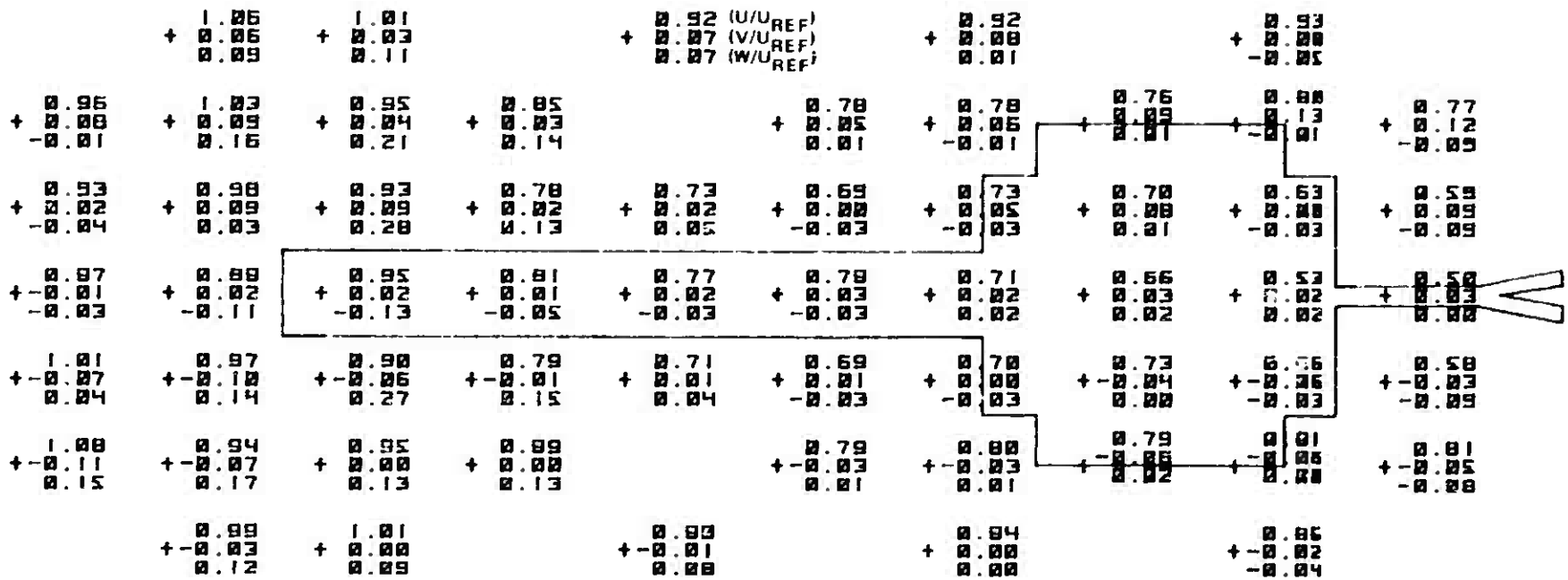

(b) WIND DIR. 155 Z - 18 FT

Figure B-6 (Cont.) Mean Velocity Components Above TRESTLE Platform (Wind Axis Coordinates)

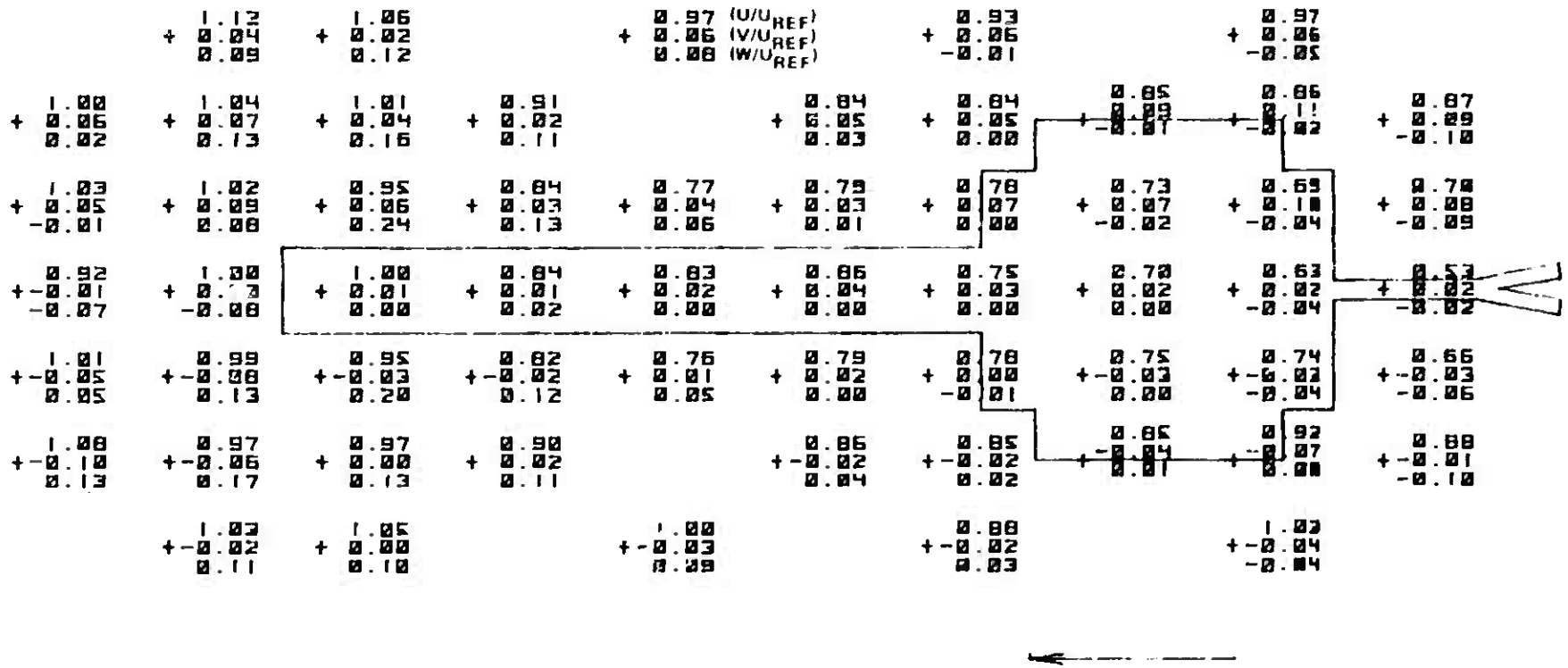

(c) WIND DIR. 155 Z 30 FT

Figure B-6 (Cont.) Mean Velocity Components Above TRESTLE Platform (Wind Axis Coordinates)

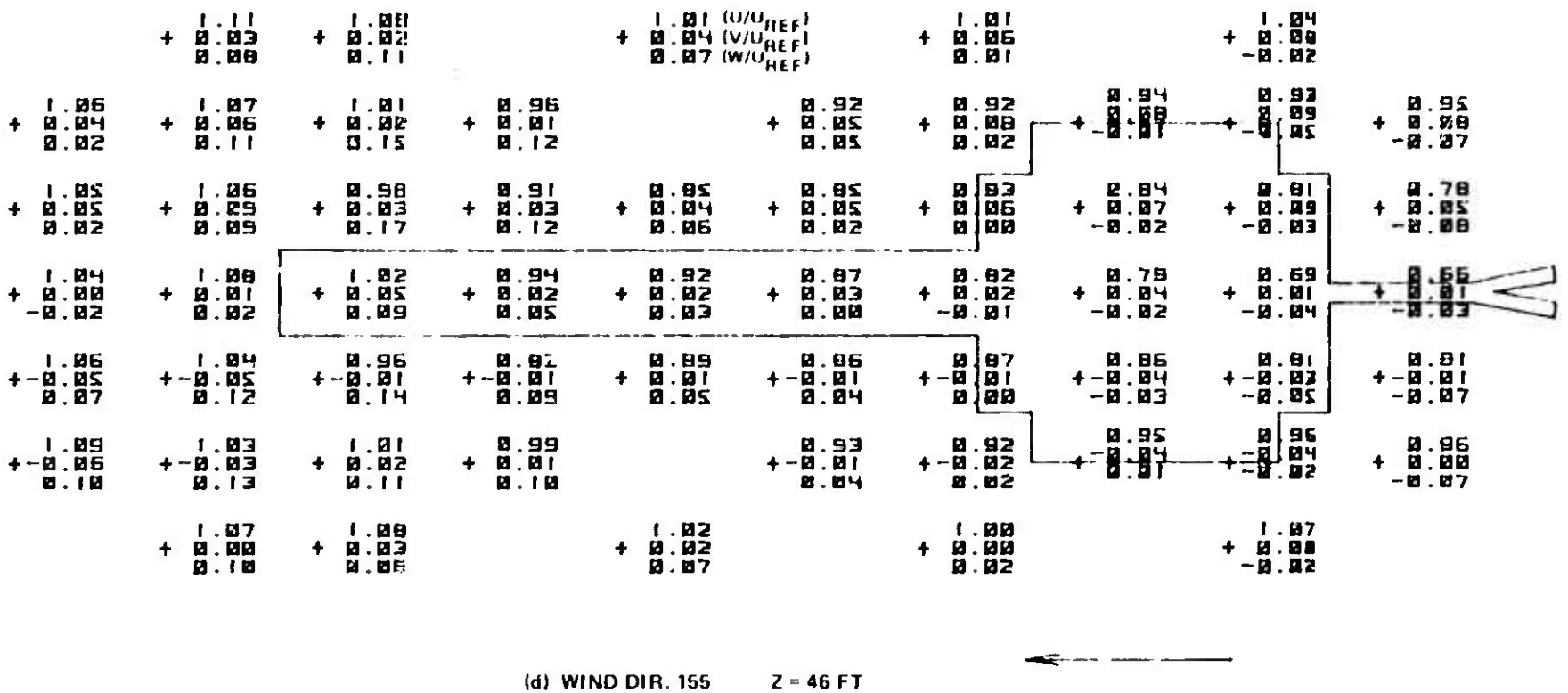

(d) WIND DIR. 155 Z = 46 FT

Figure B-6 (Cont.) Mean Velocity Components Above TRESTLE Platform (Wind Axis Coordinates)

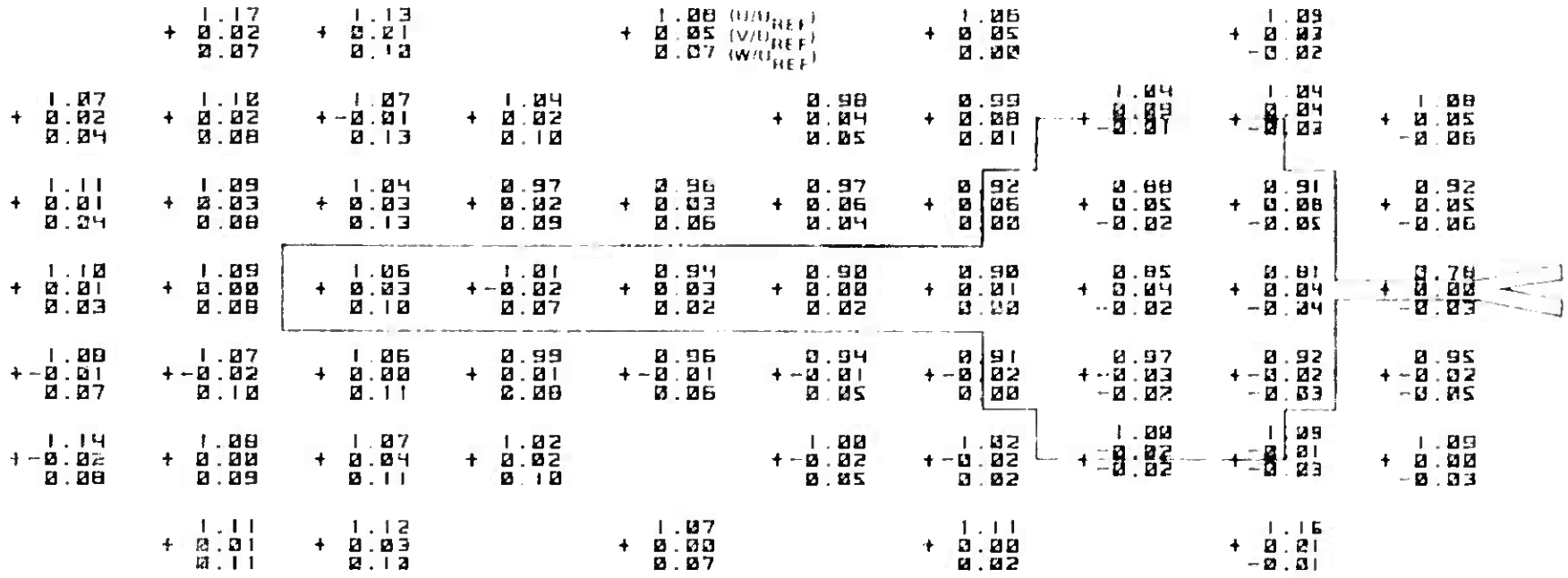

(e) WIND DIR 155 Z 66 FT

Figure B-6 (Cont.) Mean Velocity Components Above TRESTLE Platform (Wind Axis Coordinates)

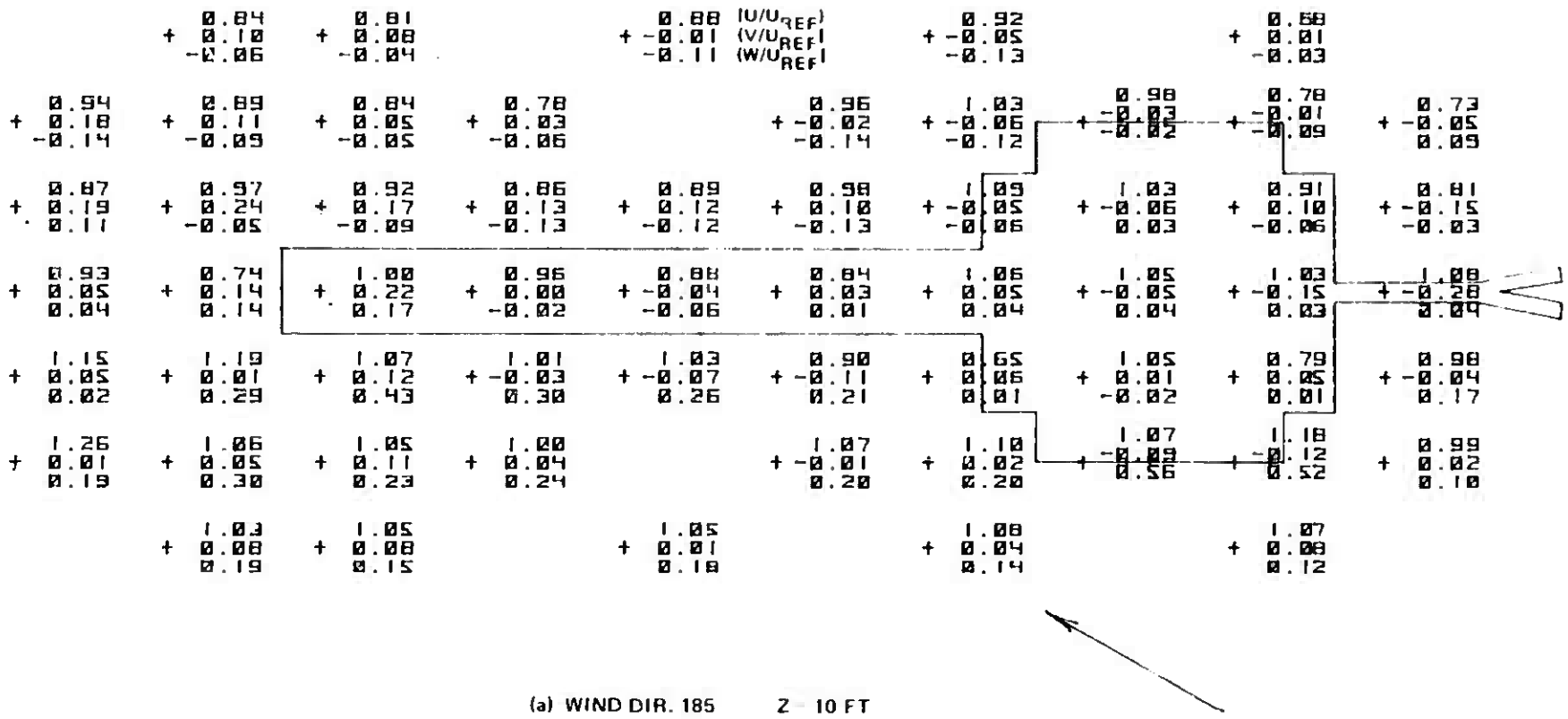

Figure B-7 Mean Velocity Components Above TRESTLE Platform (Wind Axis Coordinates)

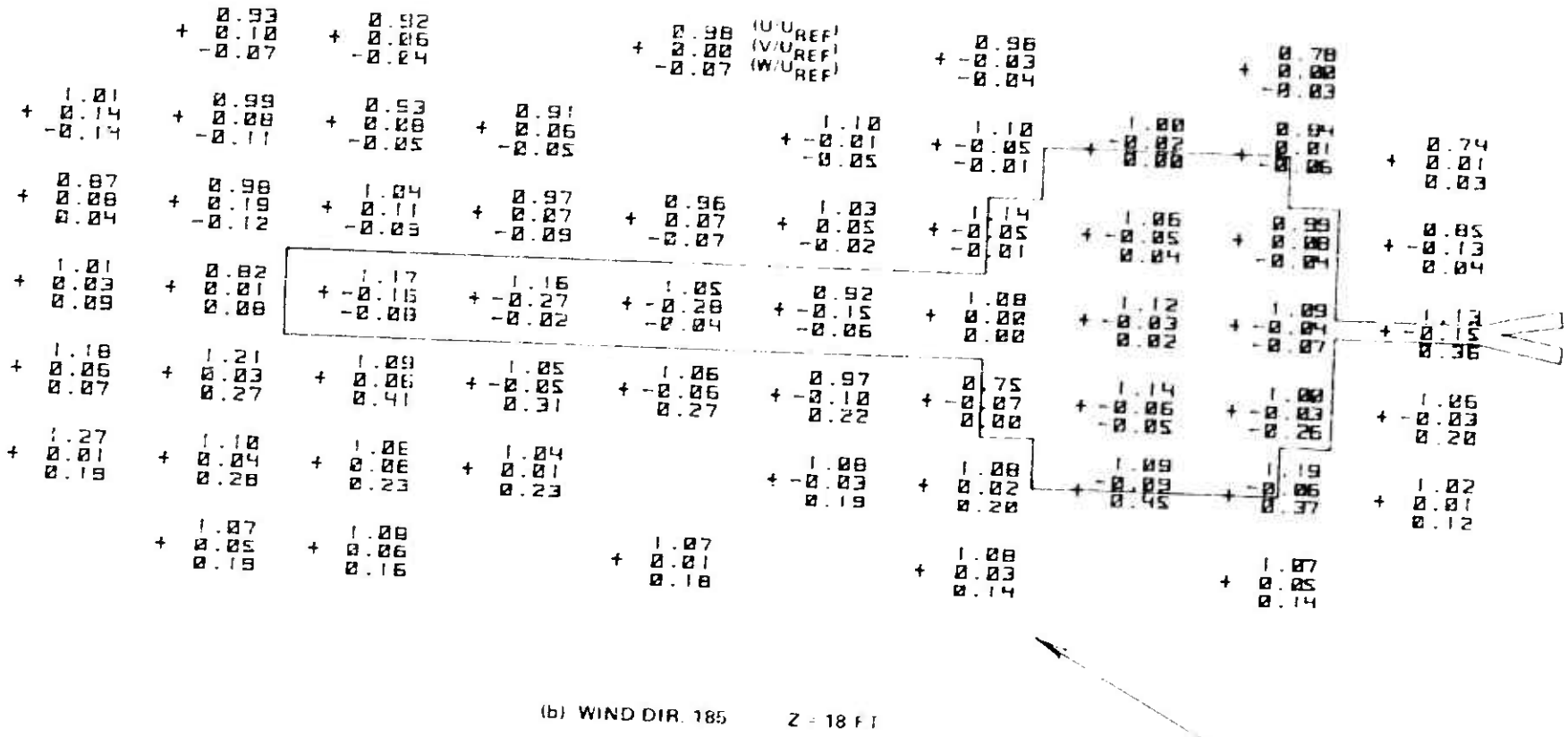

Figure B-7 (Cont.) Mean Velocity Components Above TRESTLE Platform (Wind Axis Coordinates)

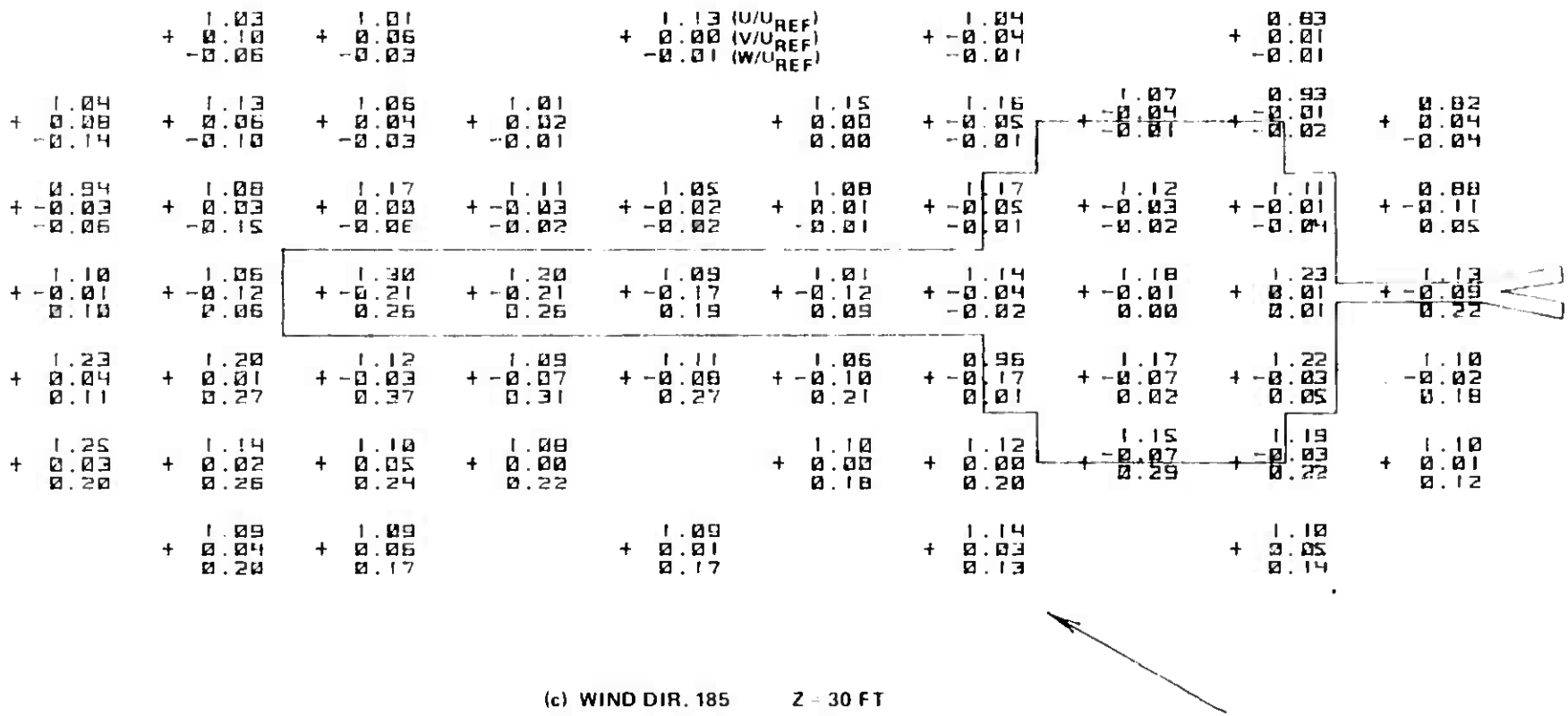

(c) WIND DIR. 185 Z = 30 FT

Figure B-7 (Cont.) Mear Velocity Components Above TRESTLE Platform (Wind Axis Coordinates)

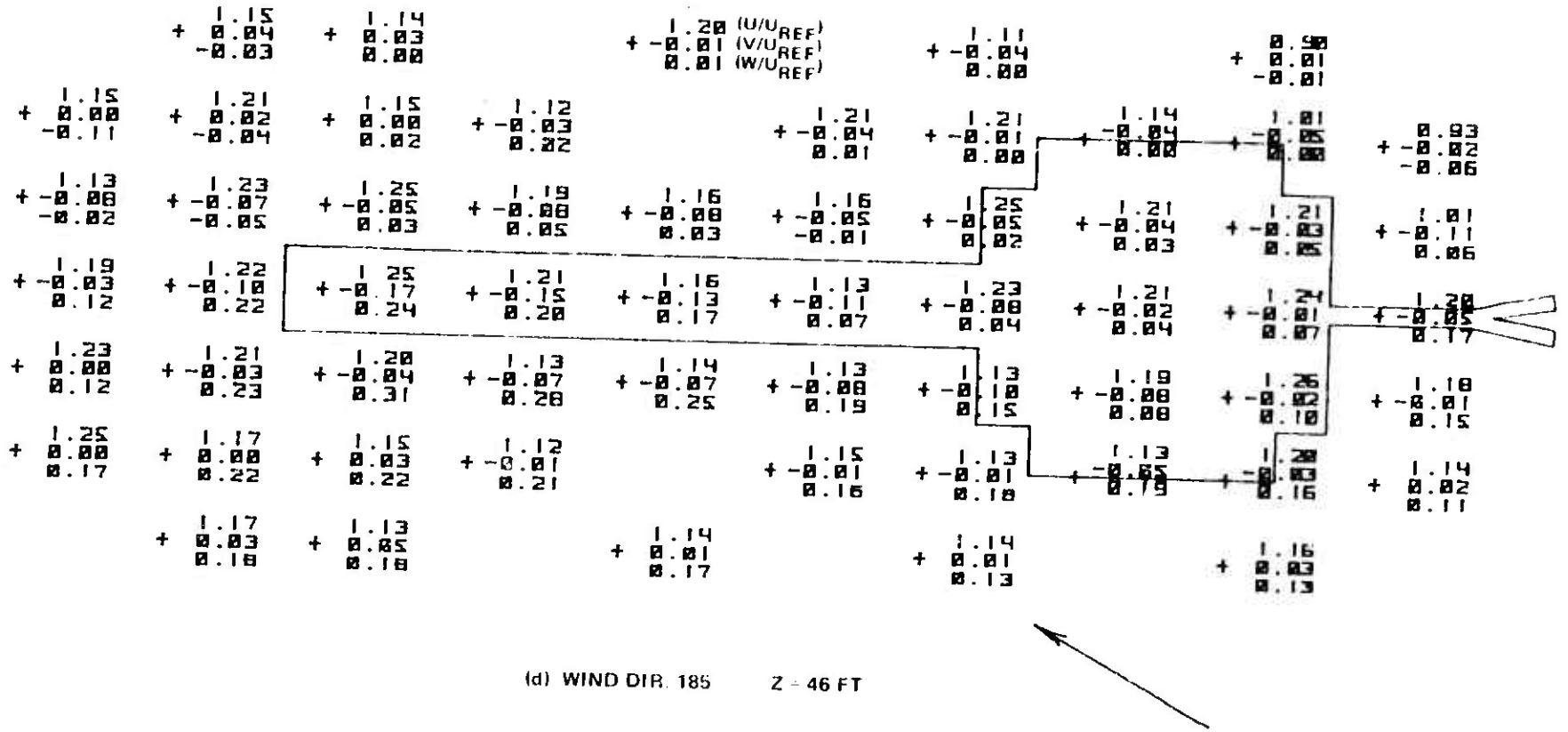

Figure B-7 (Cont.) Mean Velocity Components Above TRESTLE Platform (Wind Axis Coordinates)

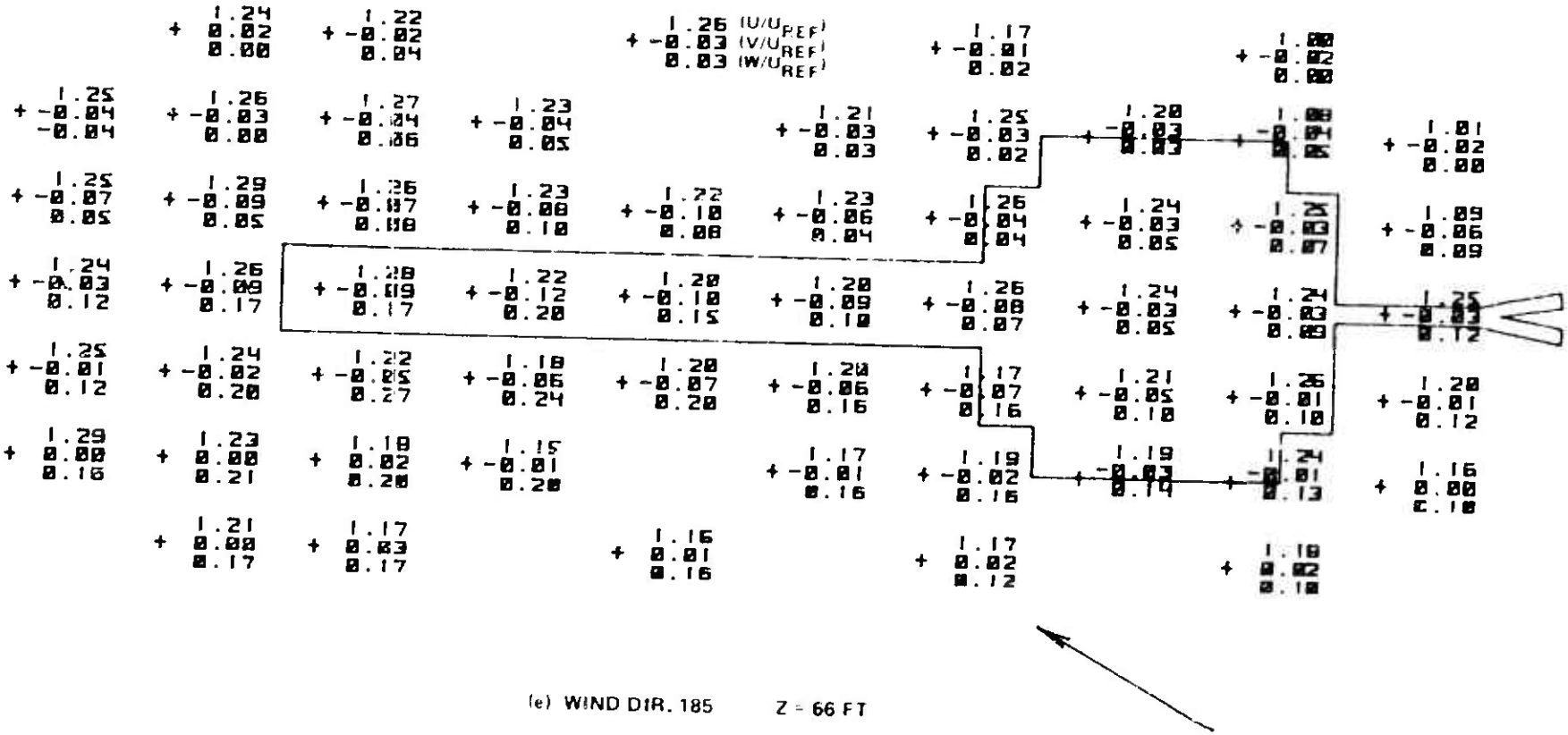

Figure B-7 (Cont.) Mean Velocity Components Above TRESTLE Platform (Wind Axis Coordinates)

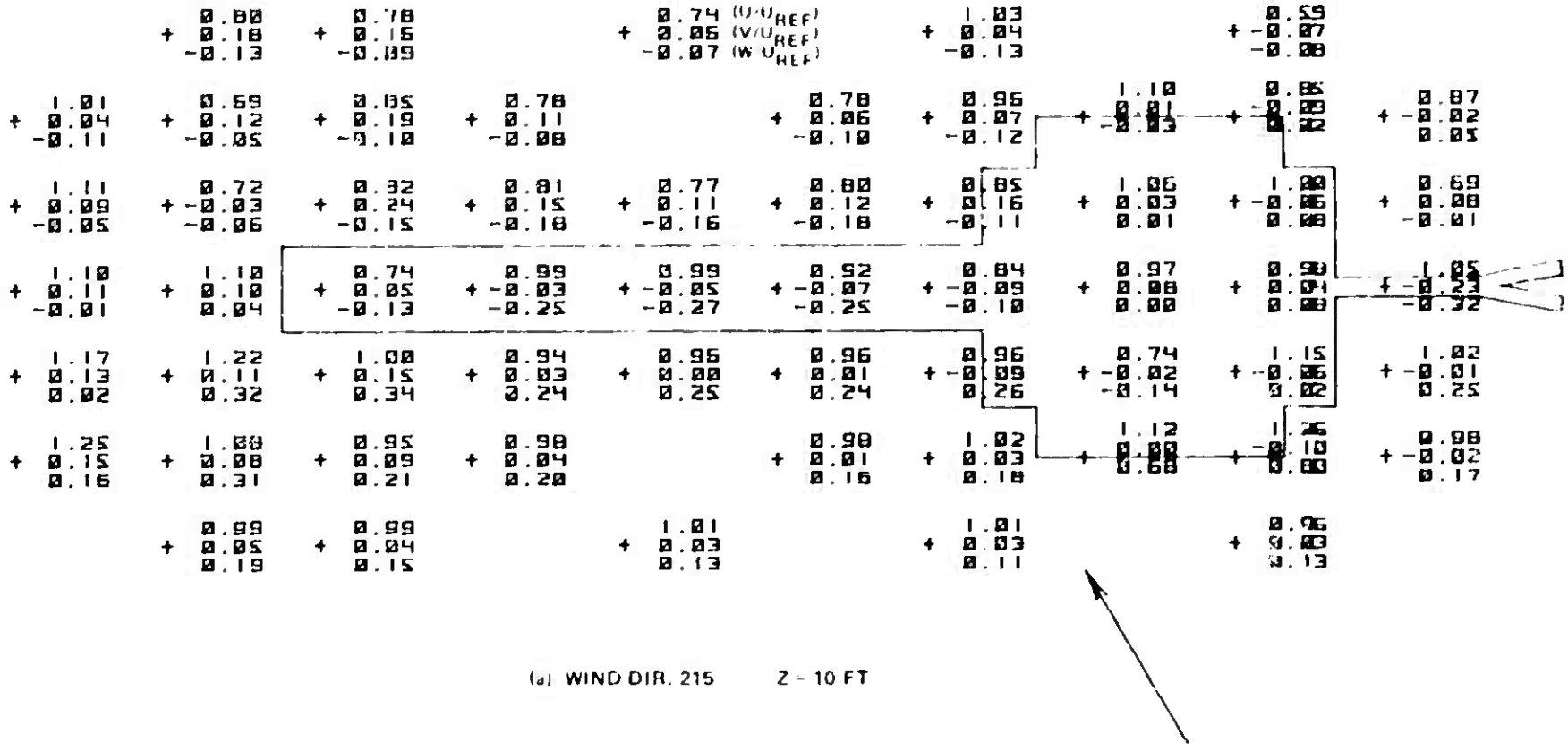

Figure B-8 Mean Velocity Components Above TPESTIE Platform (Wind Axis Coordinates)

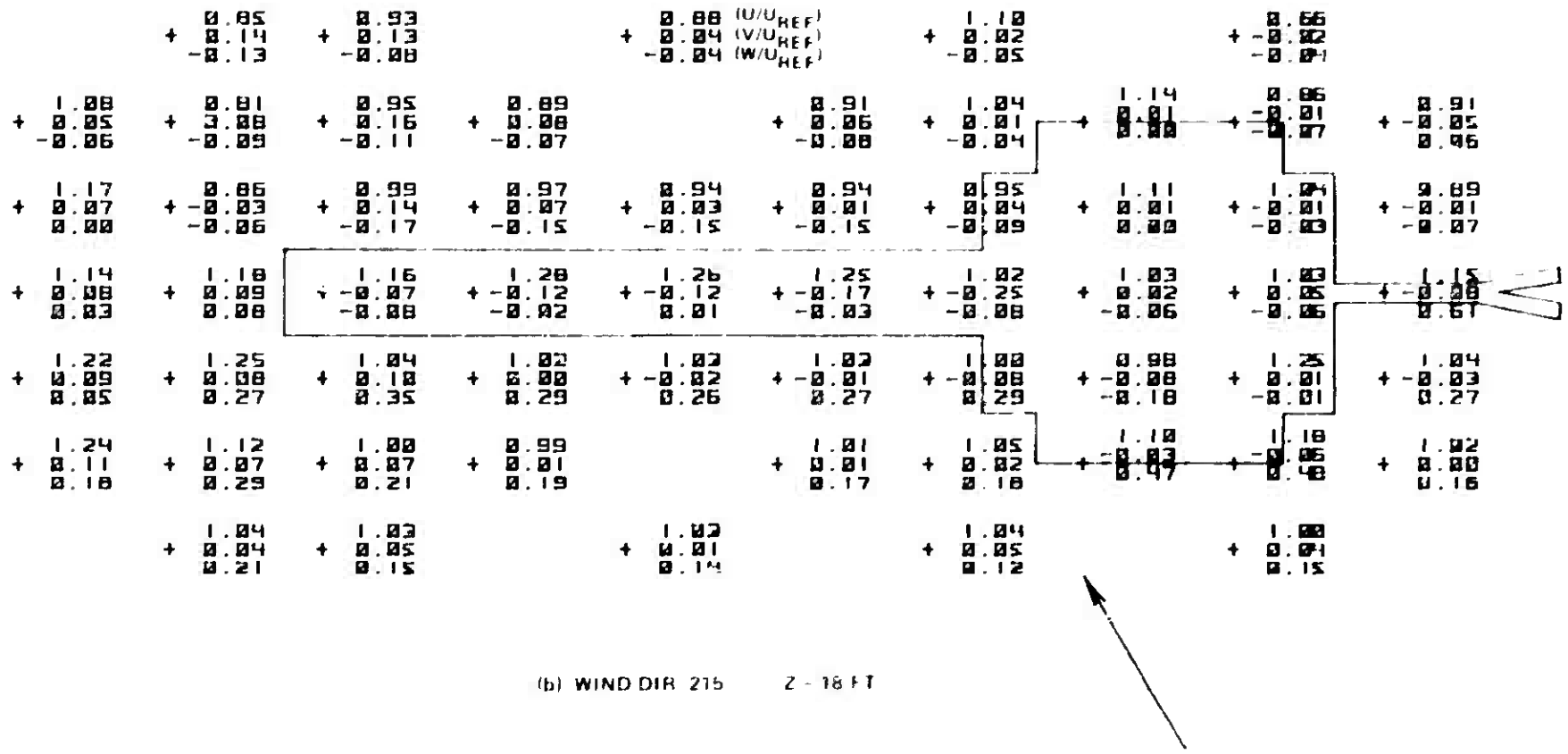

(b) WIND DIR 215 Z - 18 FT

Figure B-8 (Cont.) Mean Velocity Components Above TPESTLE Platform (Wind Axis Coordinates)

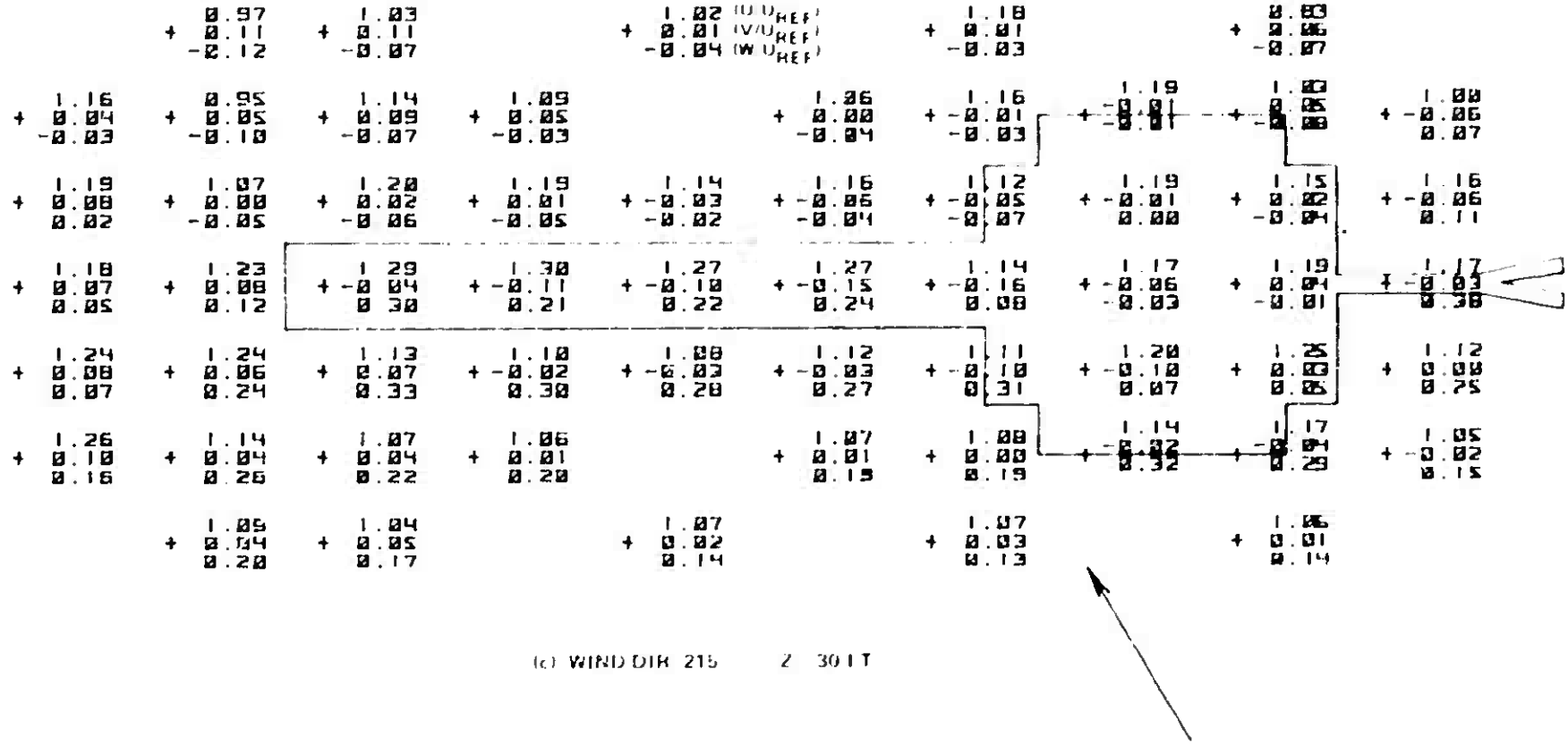

Figure B-9 (Cont.) Mean Velocity Components Above TRESTLE Platform (Wind Axis Coordinates)

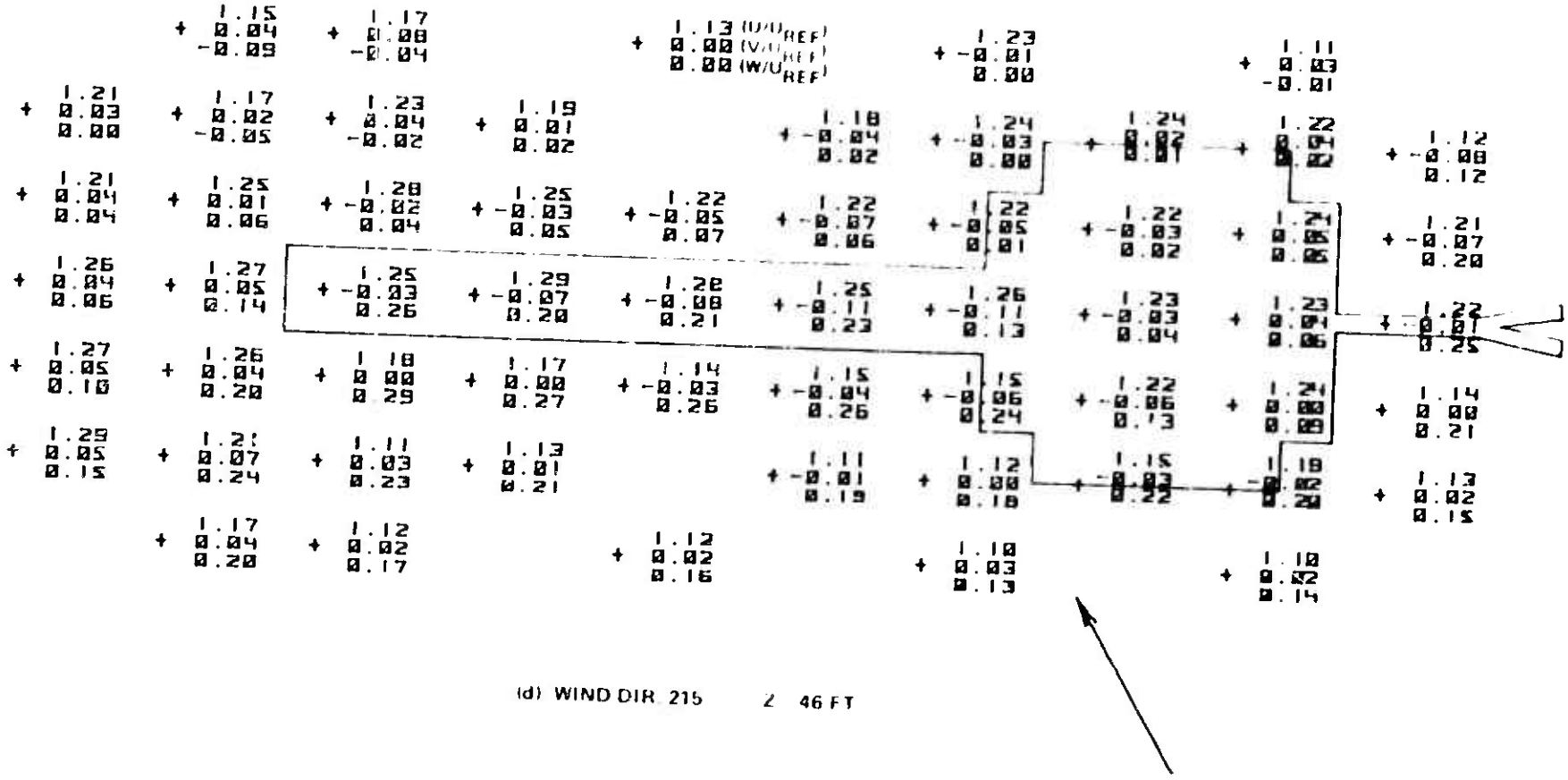

Figure B-8 (Cont.) Mean Velocity Components Above TRESTLE Platform (Wind Axis Coordinates)

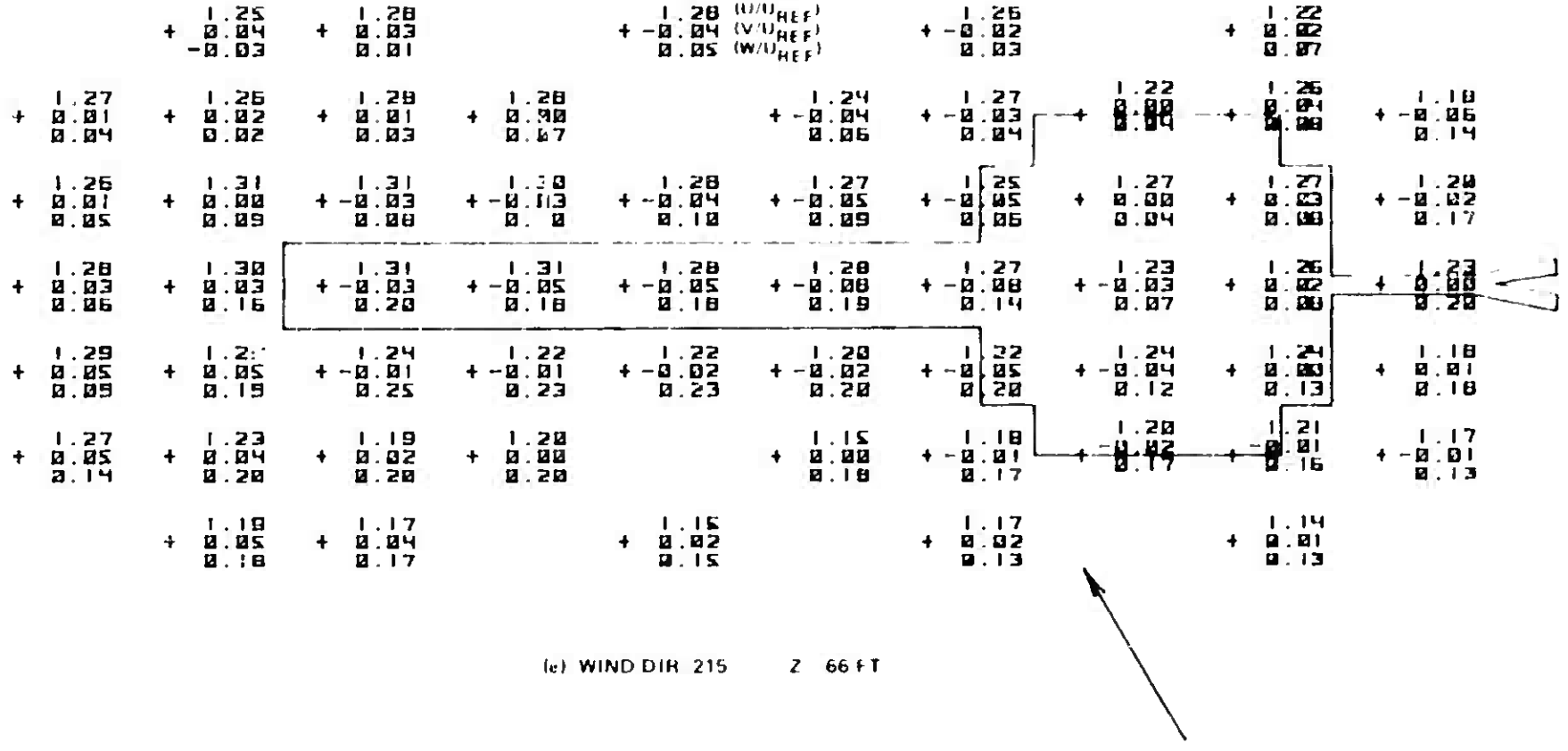

Figure B-8 (Cont.) Mean Velocity Components Above TRESTLE Platform (Wind Axis Coordinates)

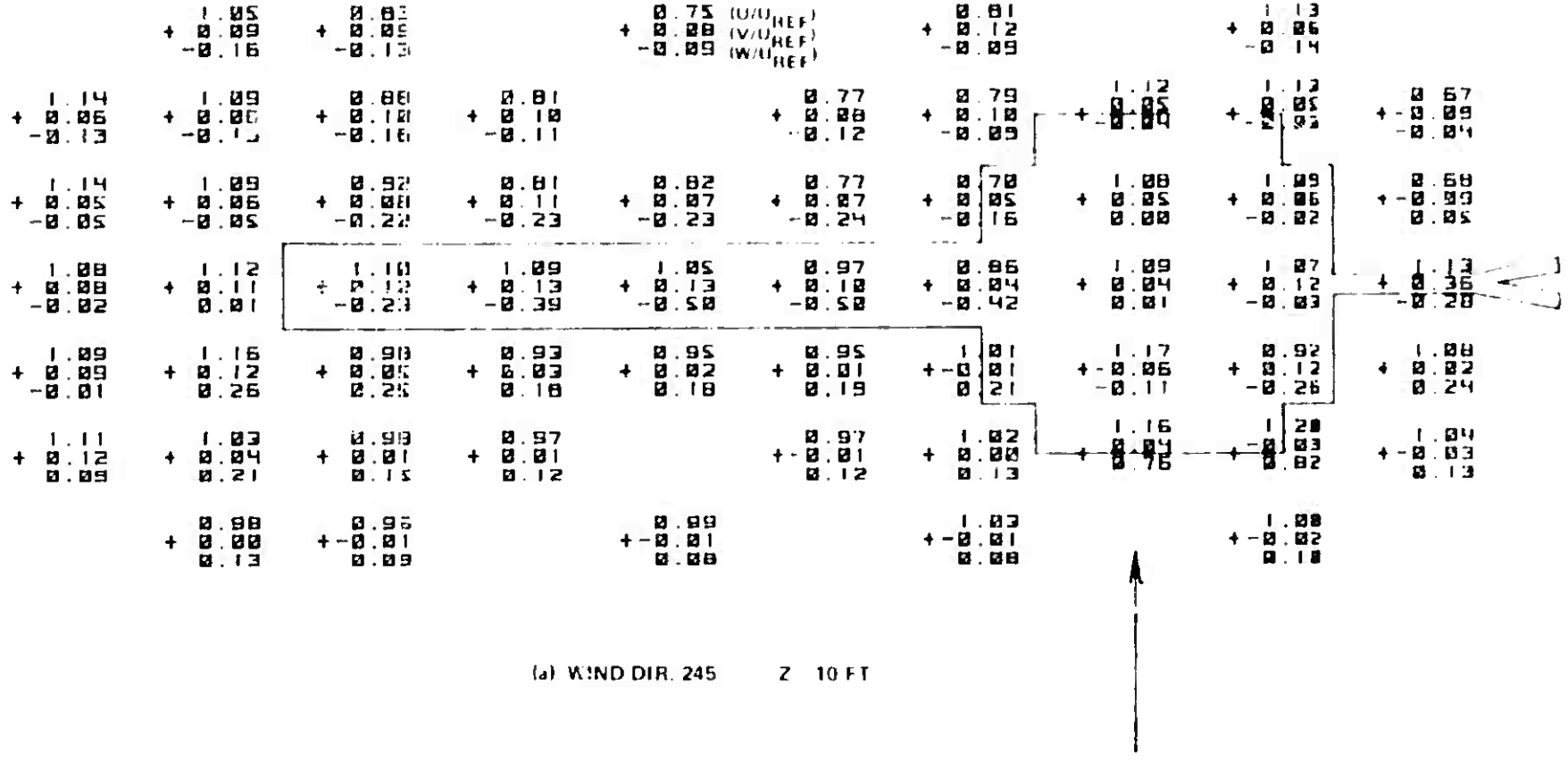

Figure B-9 Mean Velocity Components Above TRESTLE Platform (Wind Axis Coordinates)

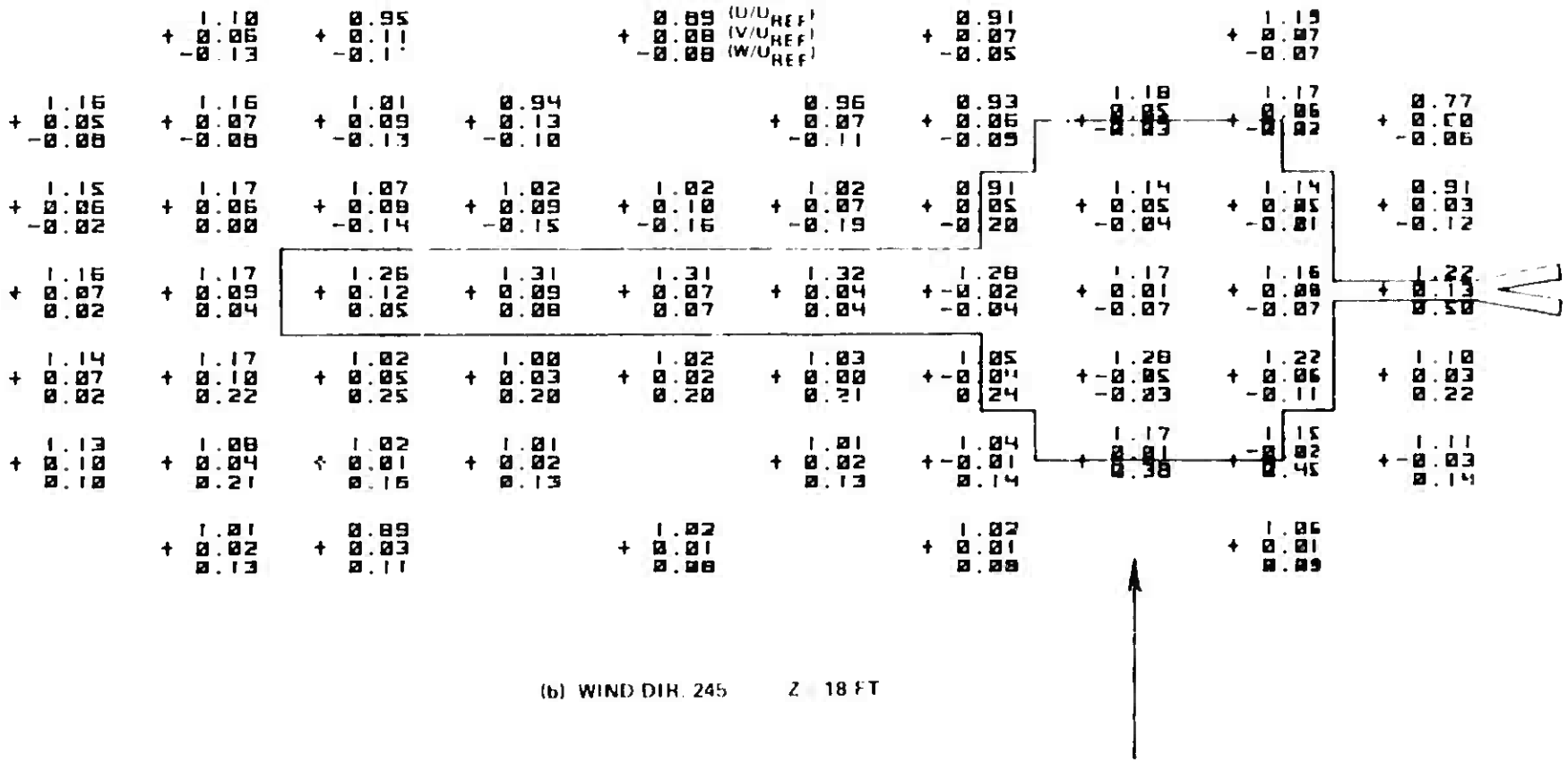

Figure B-9 (Cont.) Mean Velocity Components Above TRESTLE Platform (Wind Axis Coordinates)

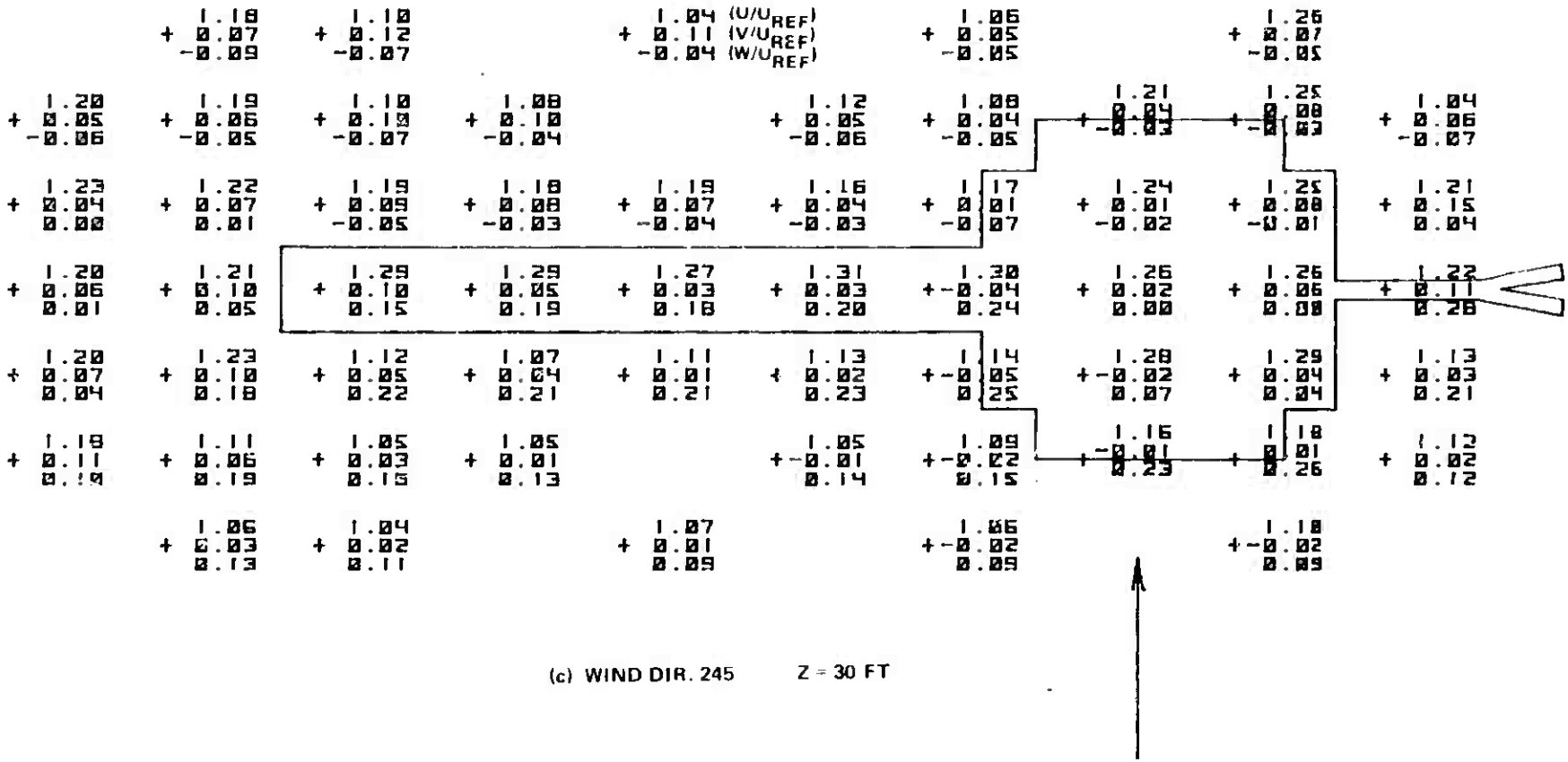

(c) WIND DIR. 245 Z = 30 FT

Figure B-9 (Cont.) Mean Velocity Components Above TRESTLE Platform (Wind Axis Coordinates)

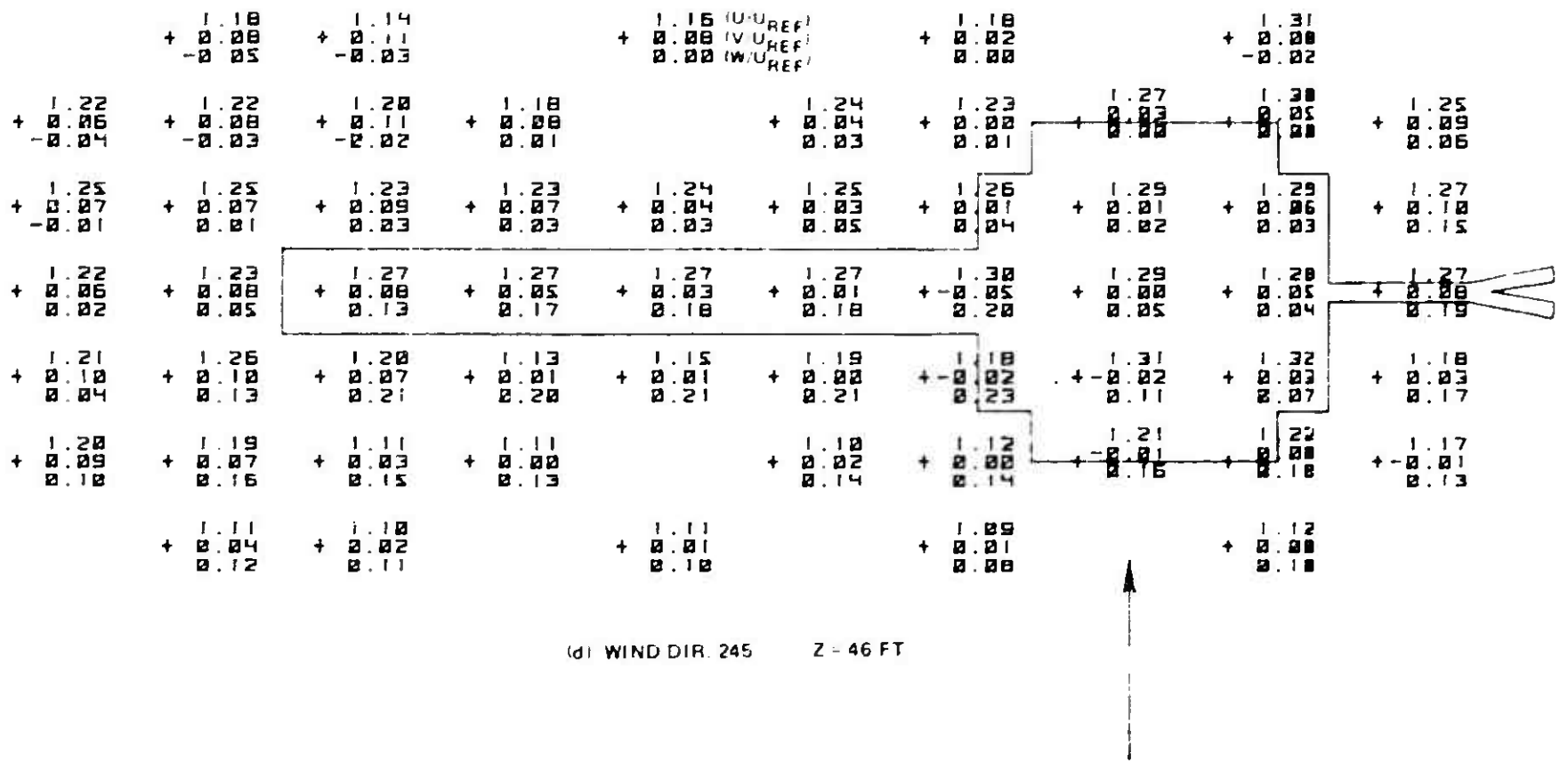

Figure B-9 (Cont.) Mean Velocity Components Above TRESTLE Platform (Wind Axis Coordinates)

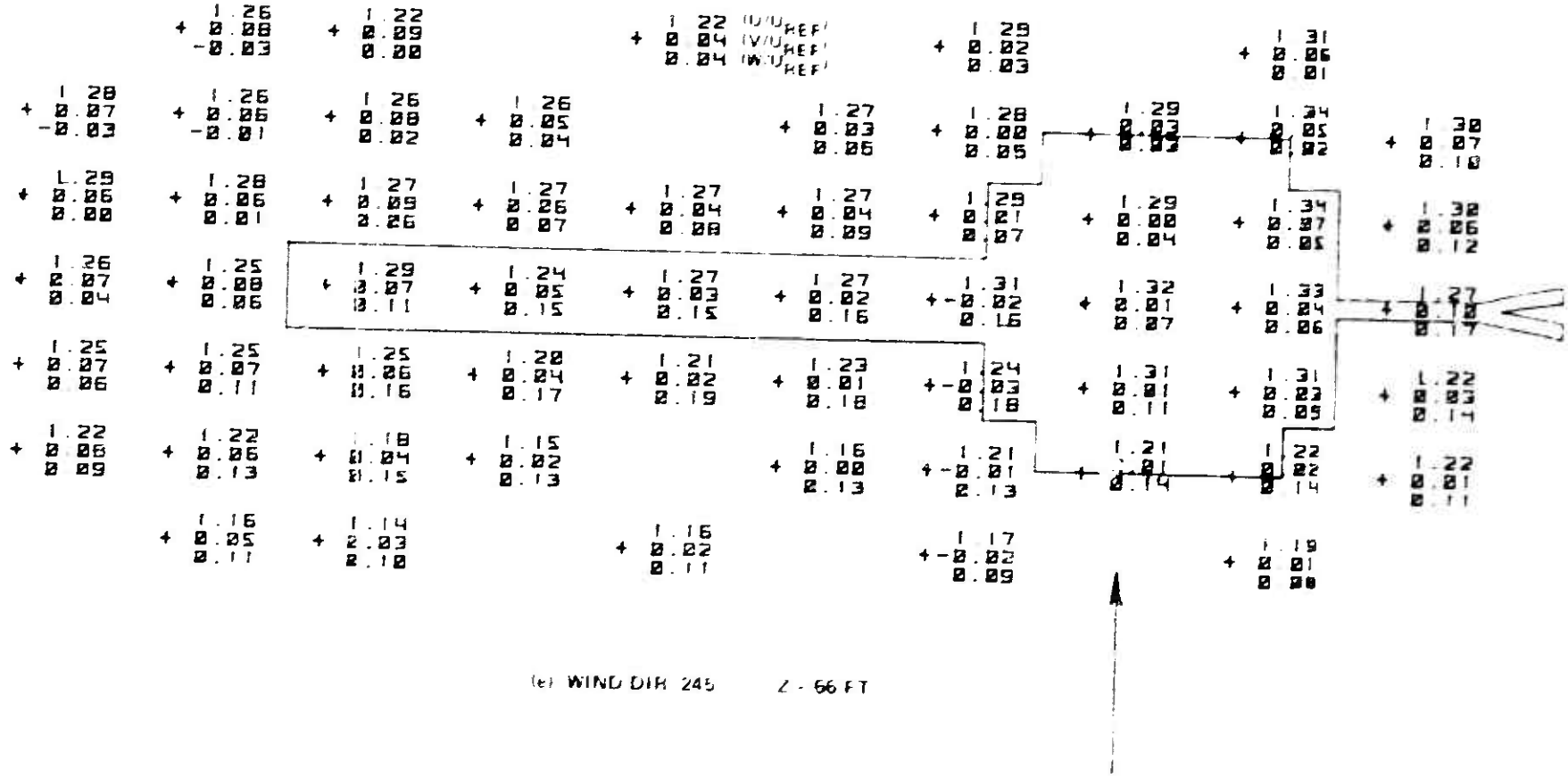

Figure B-9 (Cont.) Mean Velocity Components Above TRESTLE Platform (Wind Axis Coordinates)

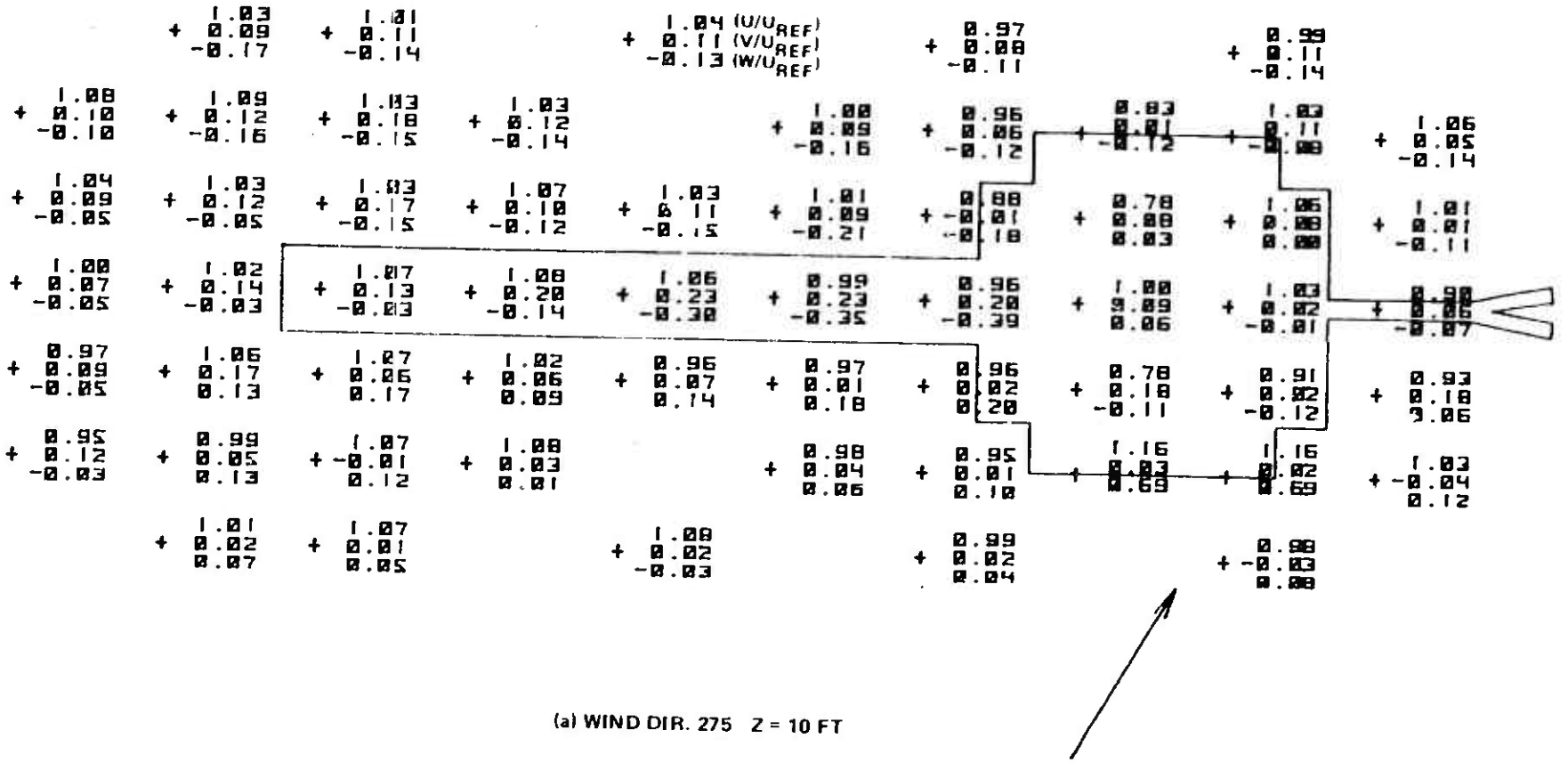

(a) WIND DIR. 275 Z = 10 FT

Figure B-10 Mean Velocity Components Above TRESTLE Platform (Wind Axis Coordinates)

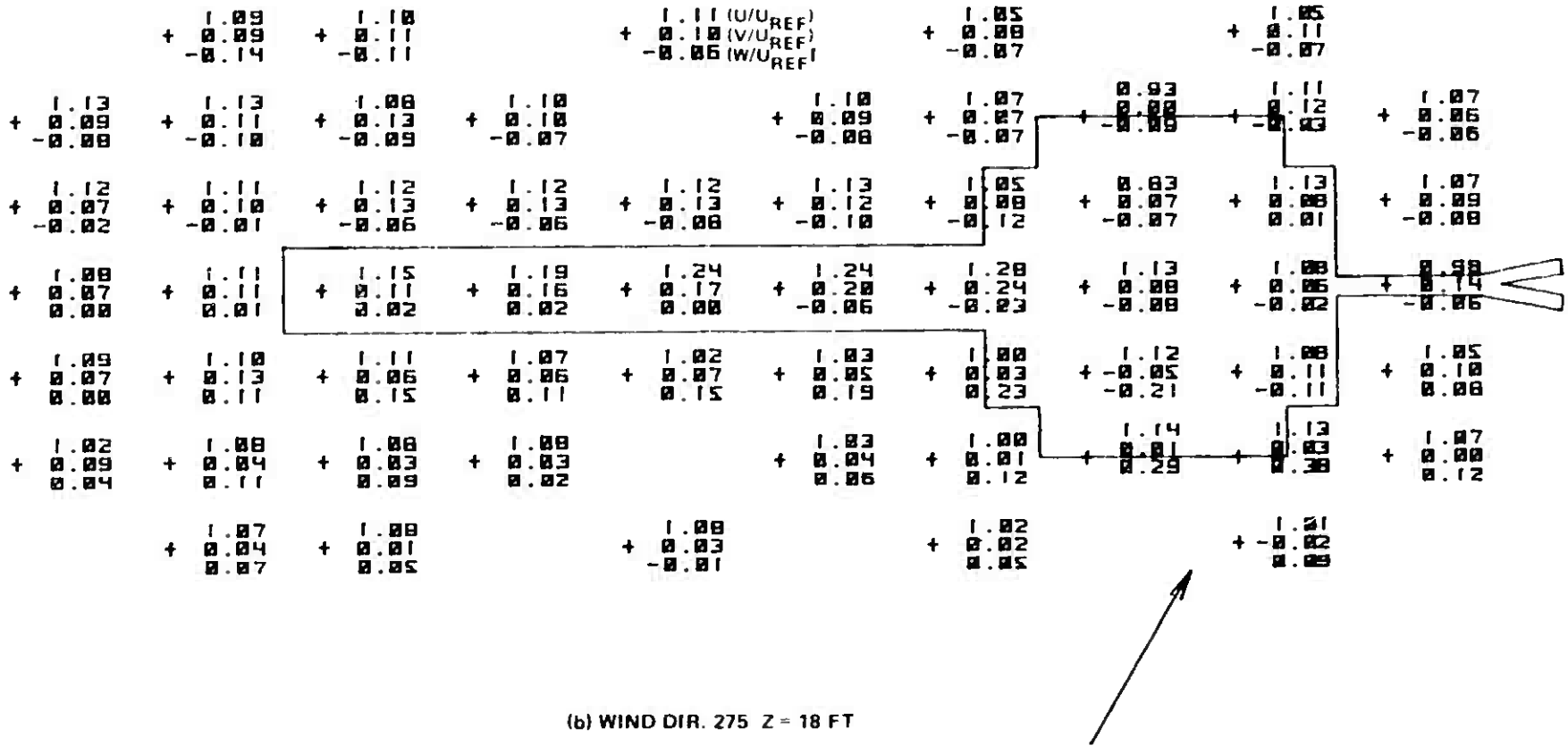

(b) WIND DIR. 275 Z = 18 FT

Figure B-10 (Cont.) Mean /elocity Components Above TRESTLE Platform (Wind Axis Coordinates)

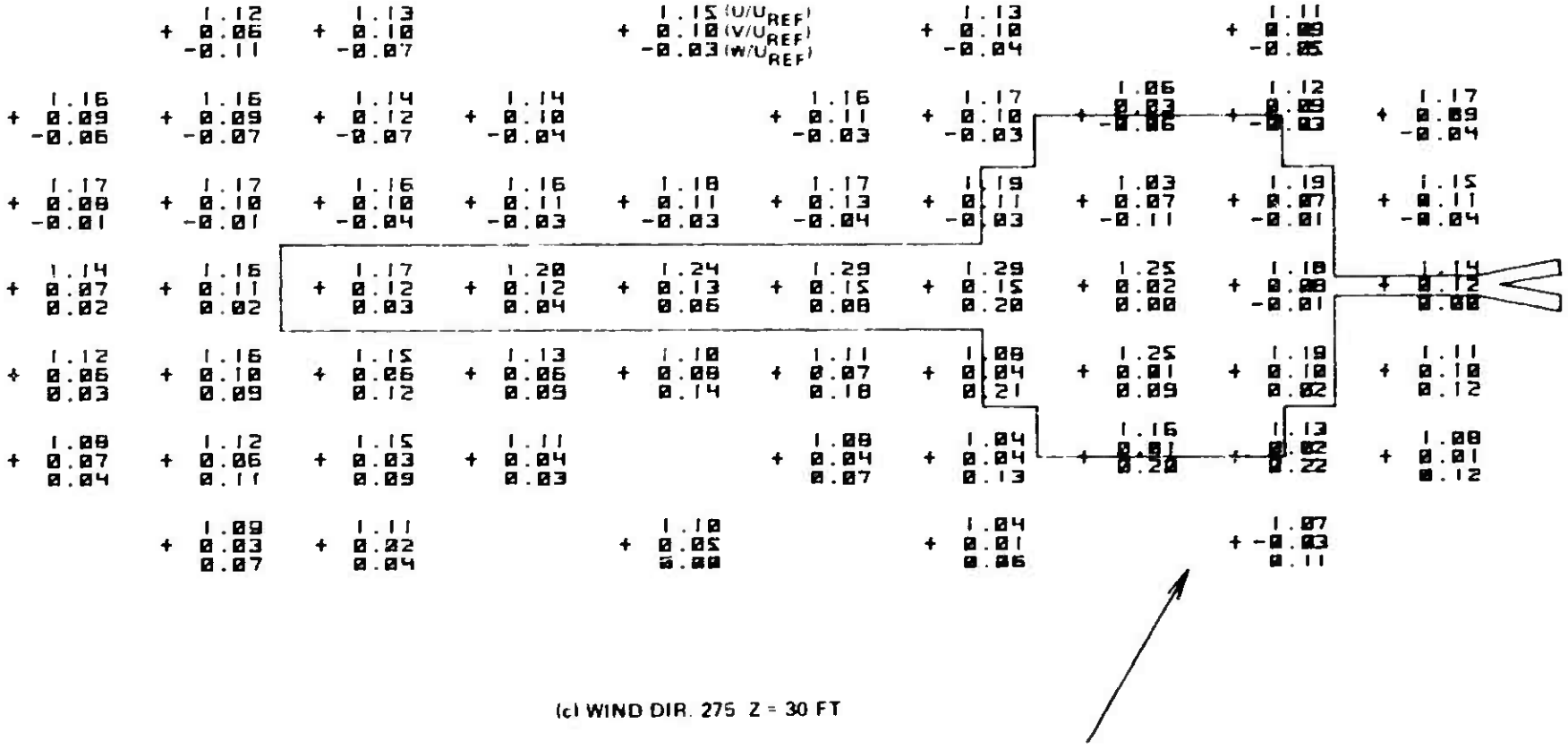

(c) WIND DIR. 275 Z = 30 FT

Figure B-10 (Cont.) Mean Velocity Components Above TRESTLE Platform (Wind Axis Coordinates)

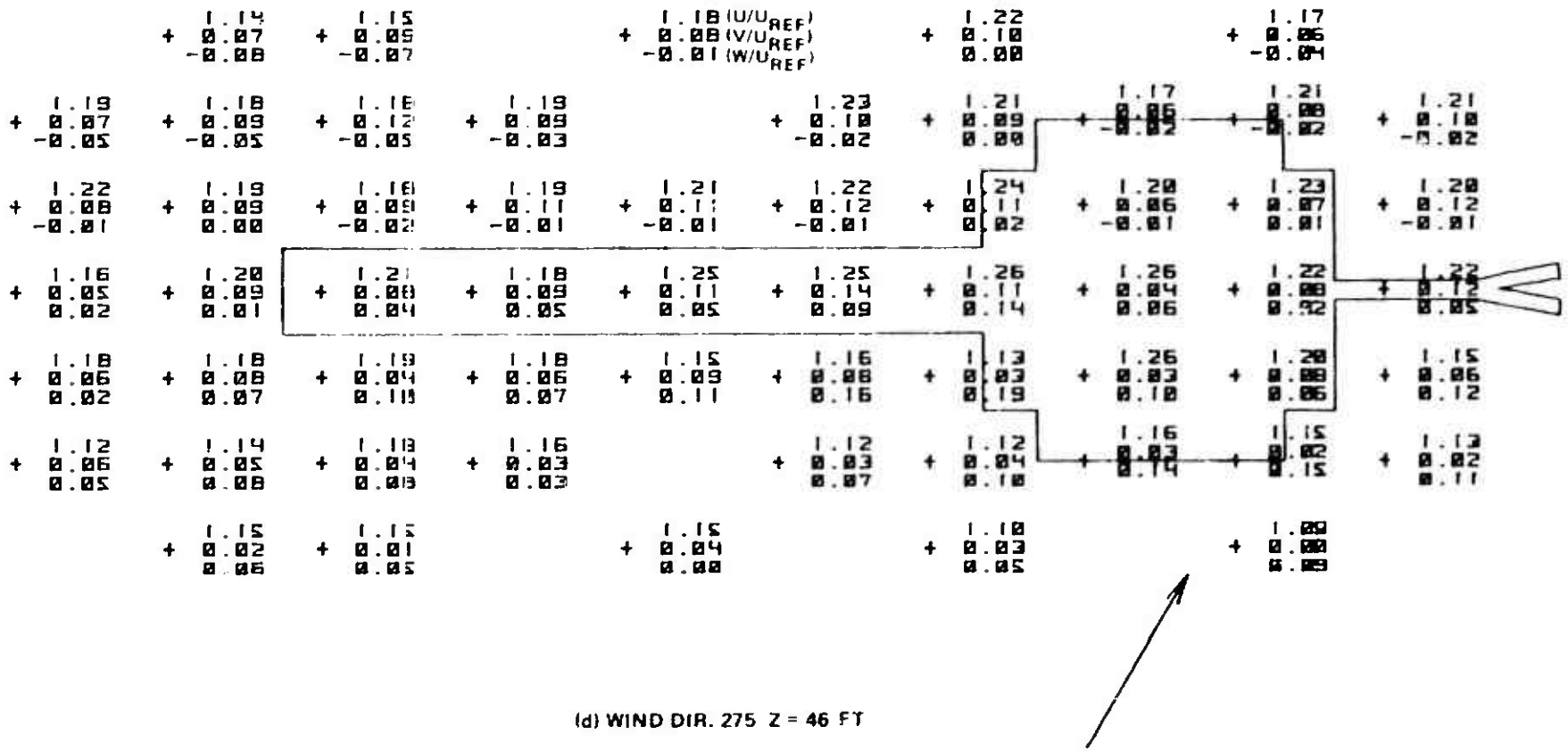

(d) WIND DIR. 275 Z = 46 FT

Figure B-10 (Cont.) Mean Velocity Components Above TRESTLE Platform (Wind Axis Coordinates)

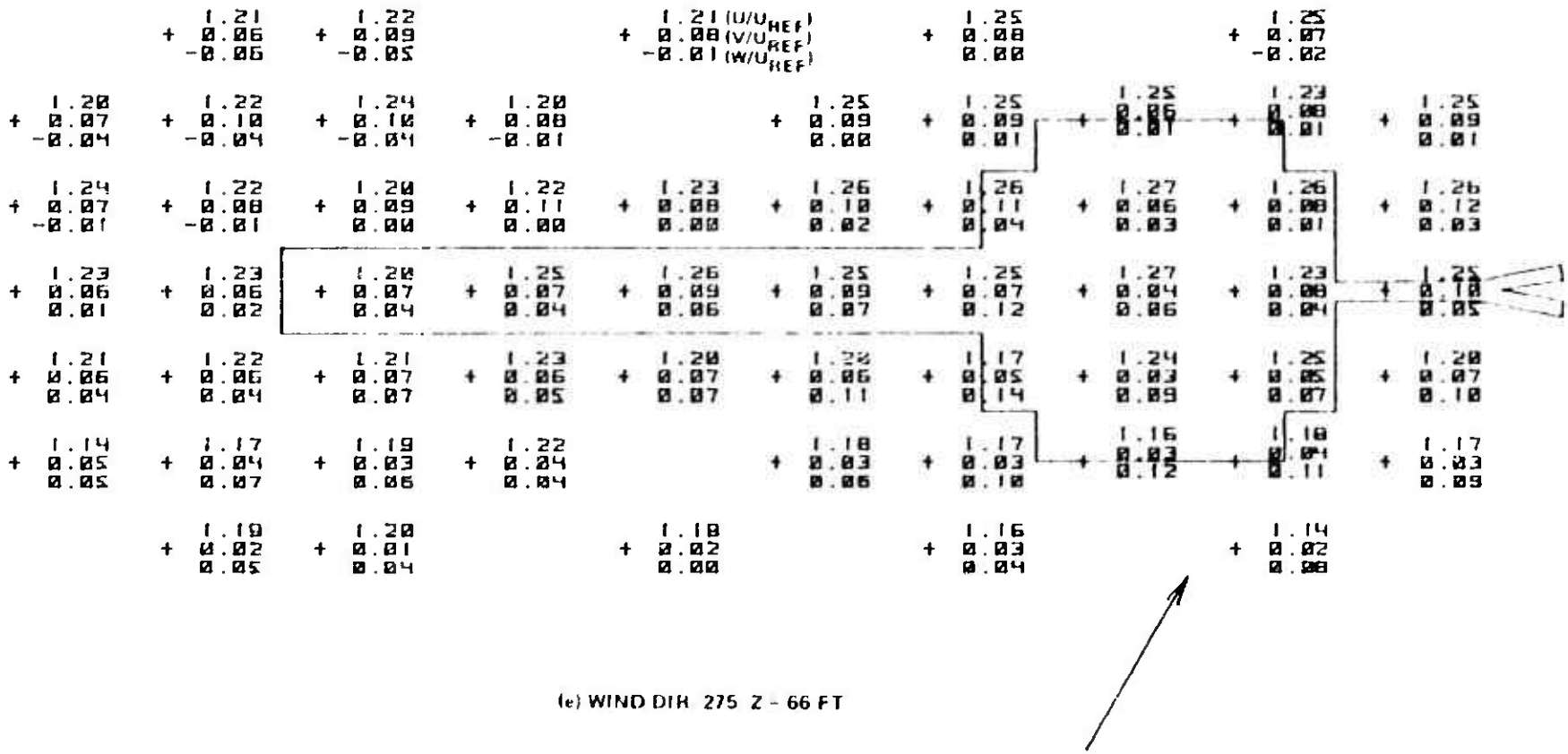

(e) WIND DIR 275 Z - 66 FT

Figure B-10 (Cont.) Mean Velocity Components Above TRESTLE Platform (Wind Axis Coordinates)

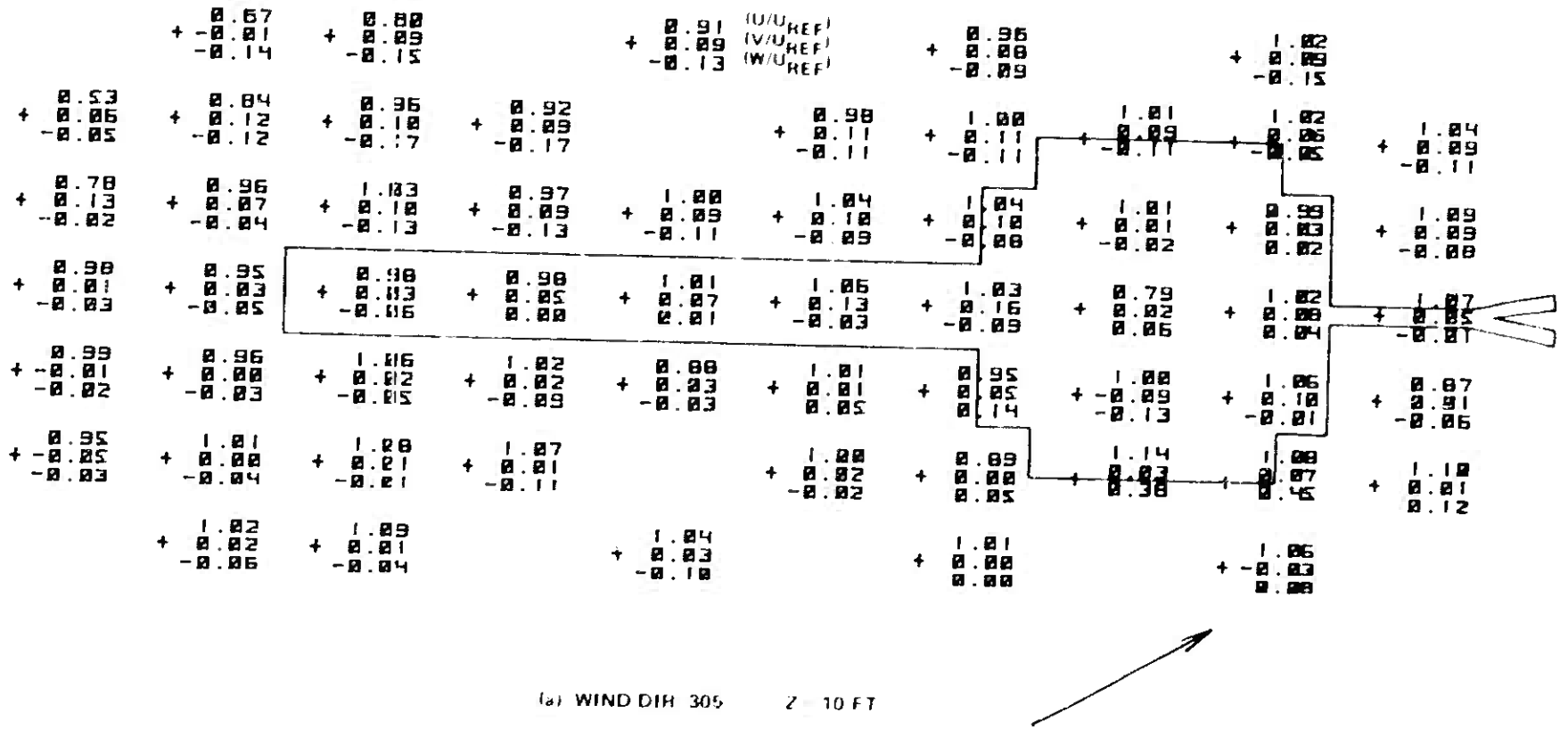

Figure B-11 Mean Velocity Components Above TRESTLE Platform (Wind Axis Coordinates)

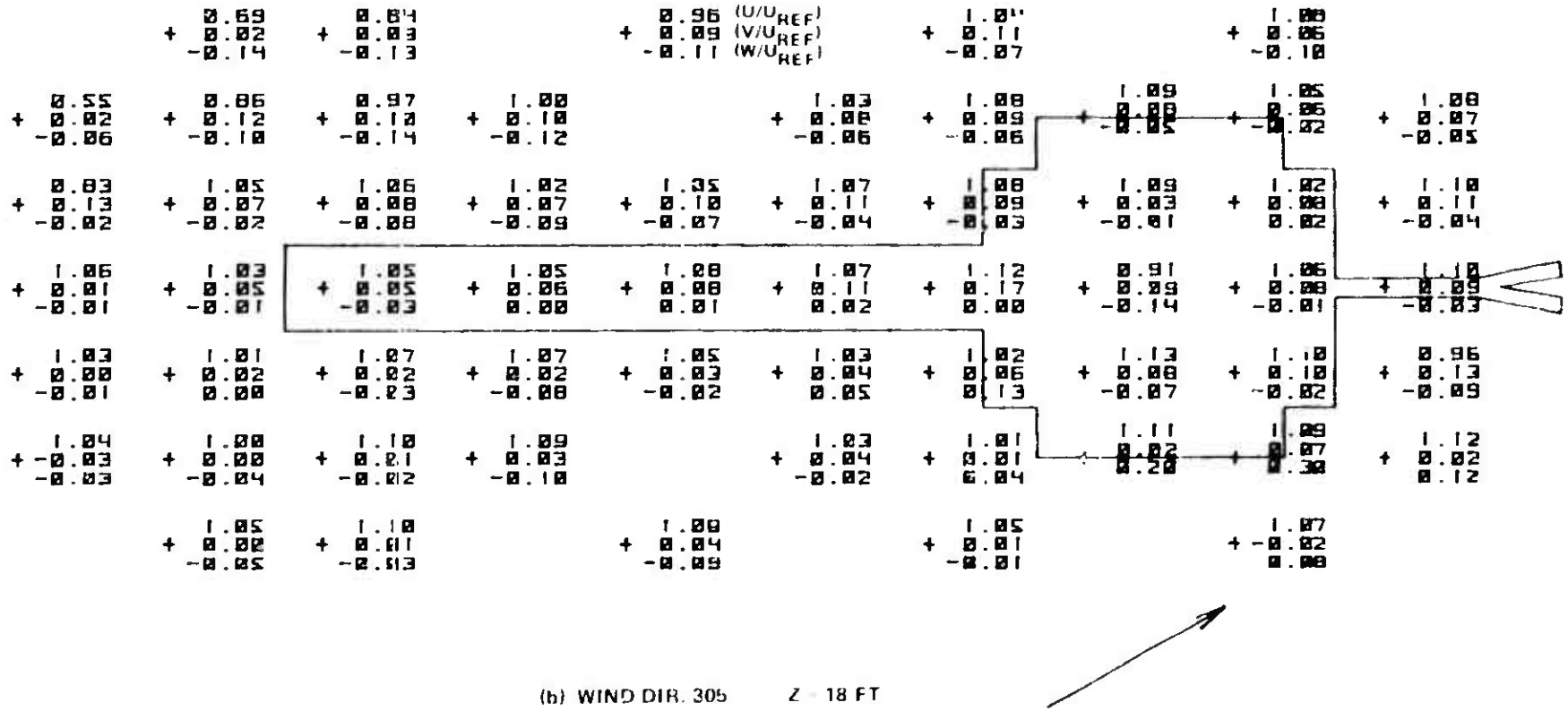

Figure B-11 (Cont.) Mean Velocity Components Above TRESTLE Platform (Wind Axis Coordinates)

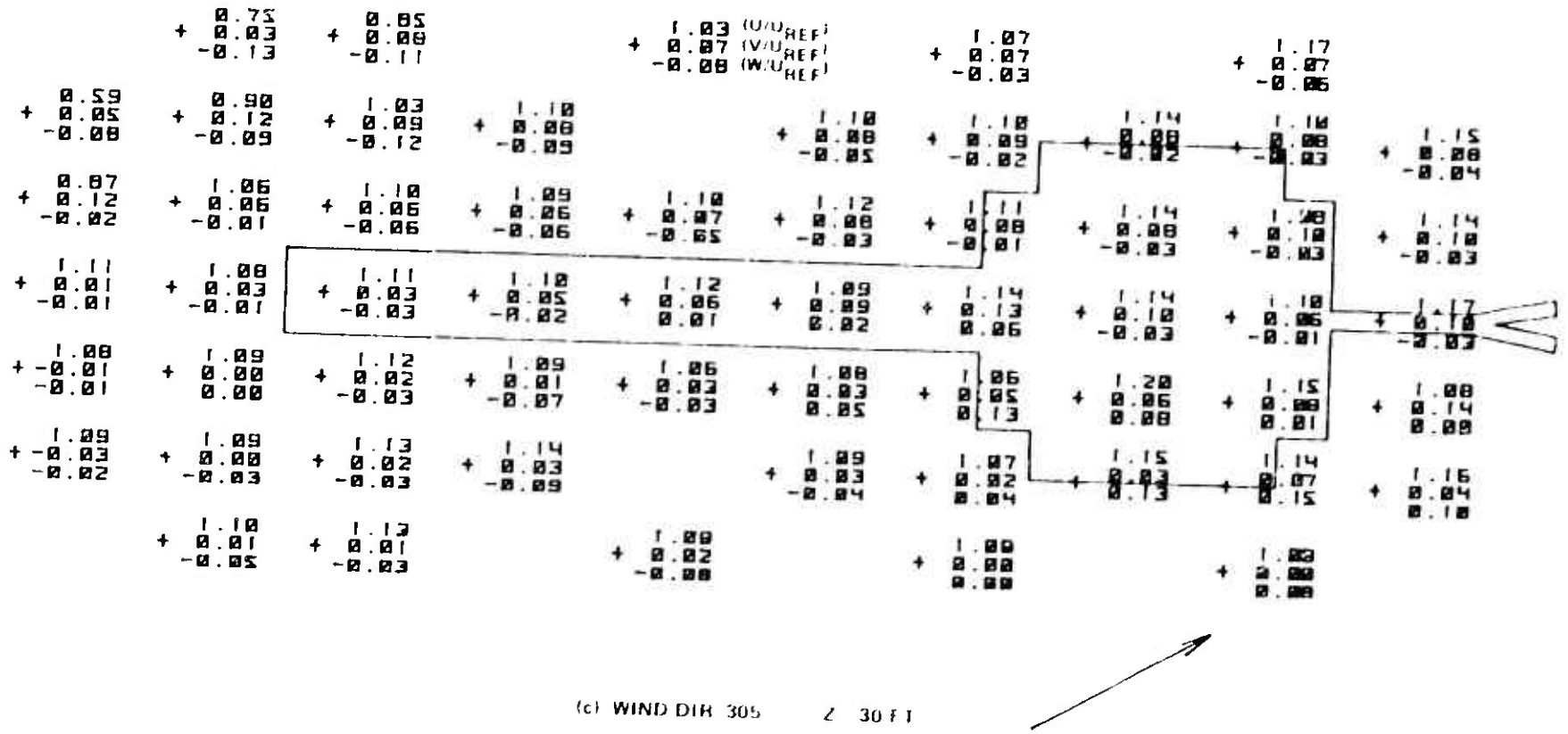

Figure B-11 (Cont.) Mean Velocity Components Above TRESTLE Platform (Wind Axis Coordinates)

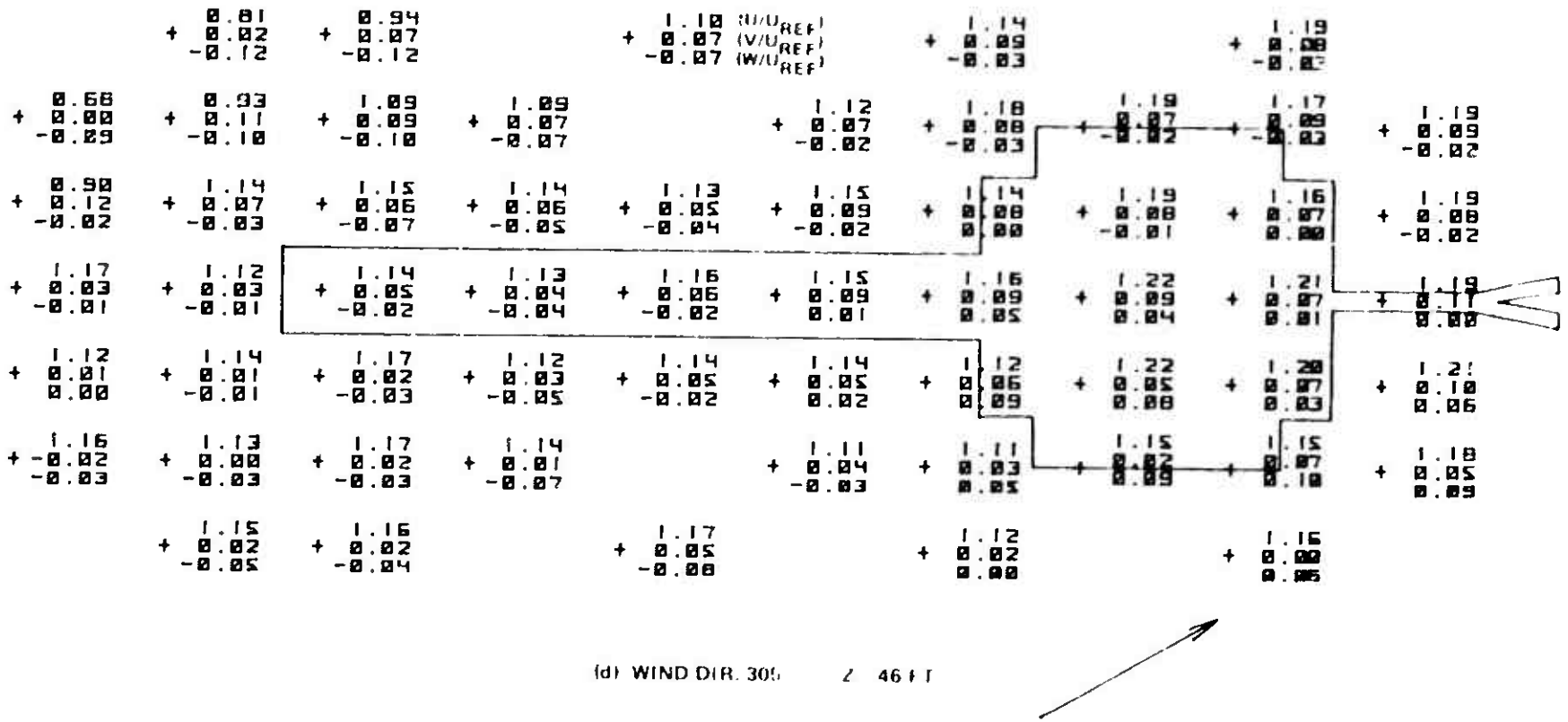

Figure B-11 (Cont.) Mean Velocity Components Above TRESTLE Platform (Wind Axis Coordinates)

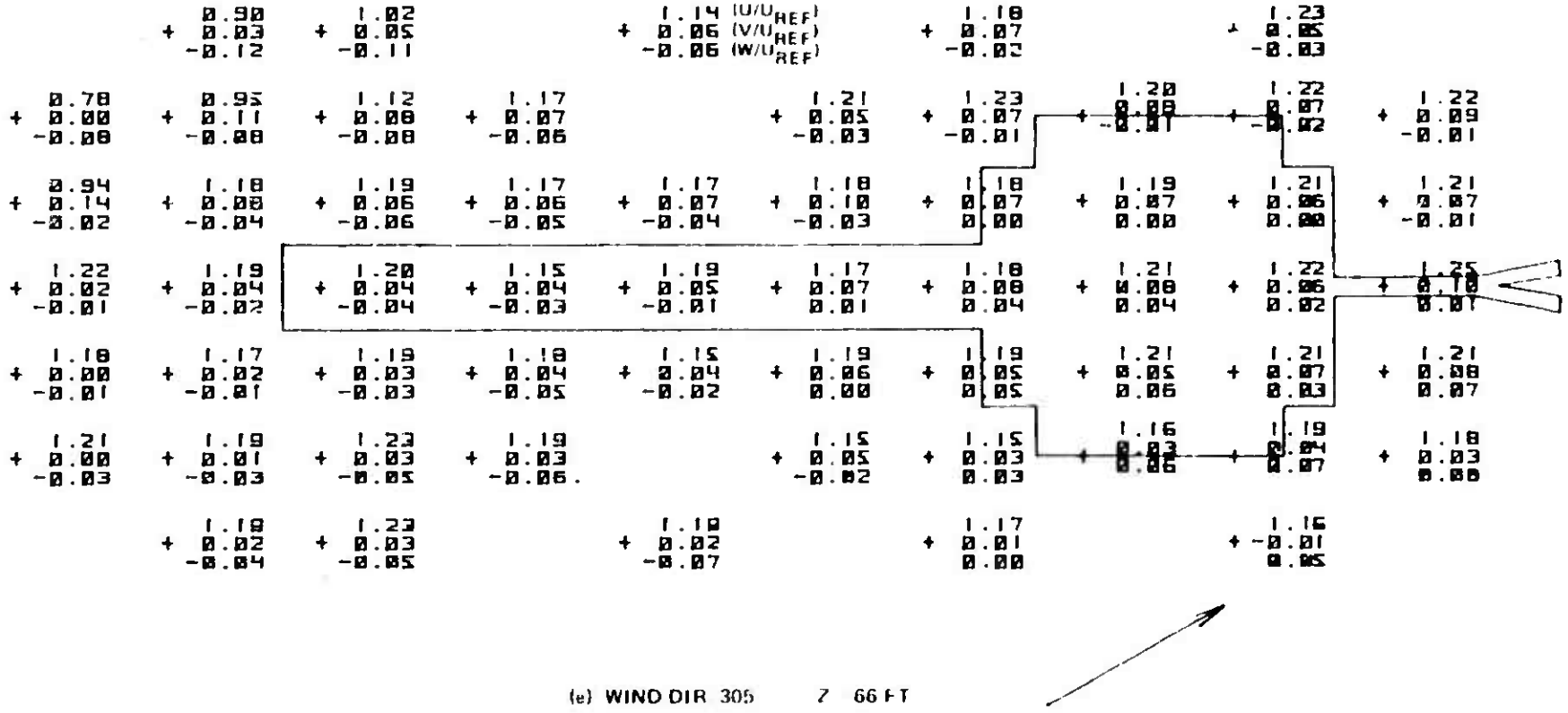

Figure B-11 (Cont.) Mean Velocity Components Above TRESTLE Platform (Wind Axis Coordinates)

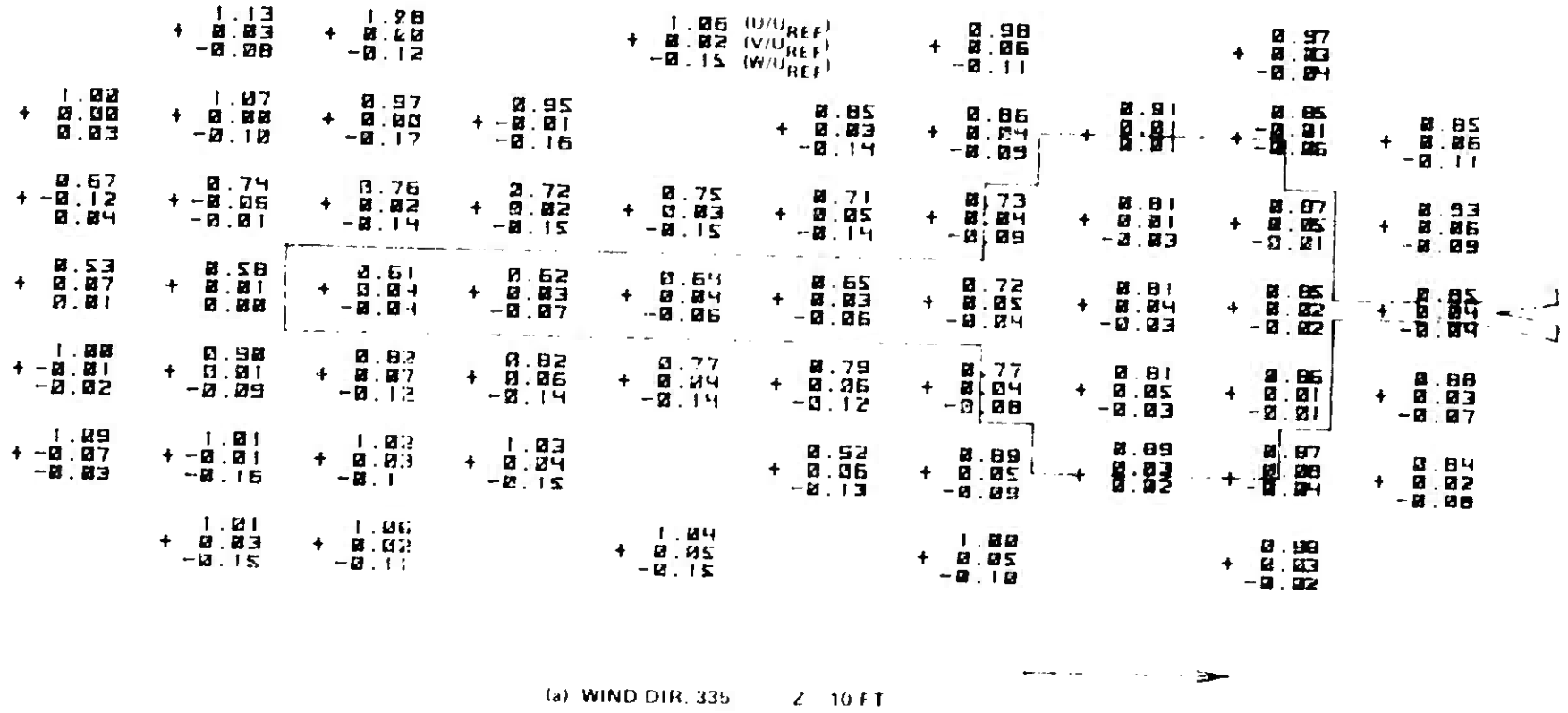

Figure B-12 Mean Velocity Components Above TRESTLE Platform (Wind Axis Coordinates)

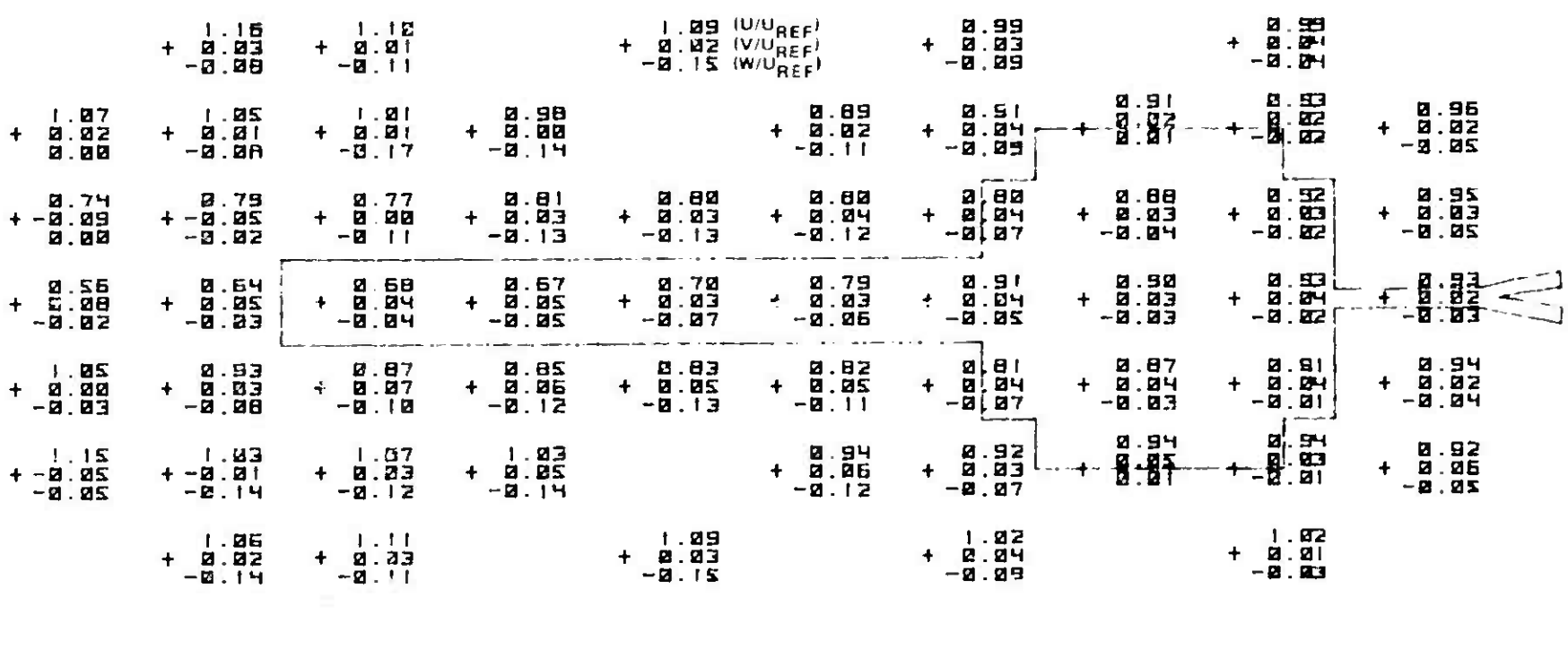

(b) WIND DIR. 335 Z = 18 FT

Figure B-12 (Cont.) Mean Velocity Components Above TRESTLE Platform (Wind Axis Coordinates)

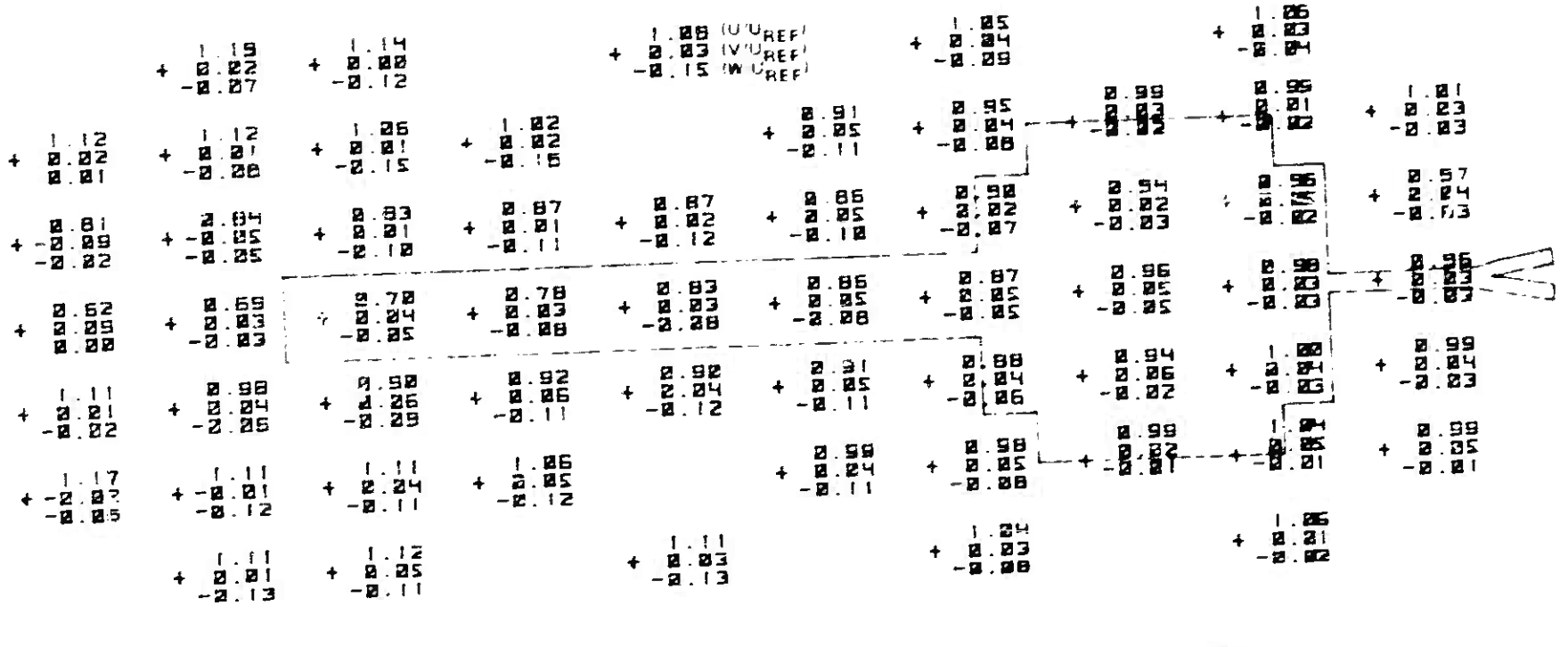

(c) WIND DIR 335 Z = 30 FT

Figure B-12 (Cont.) Mean Velocity Components Above TRESTLE Platform (Wind Axis Coordinates)

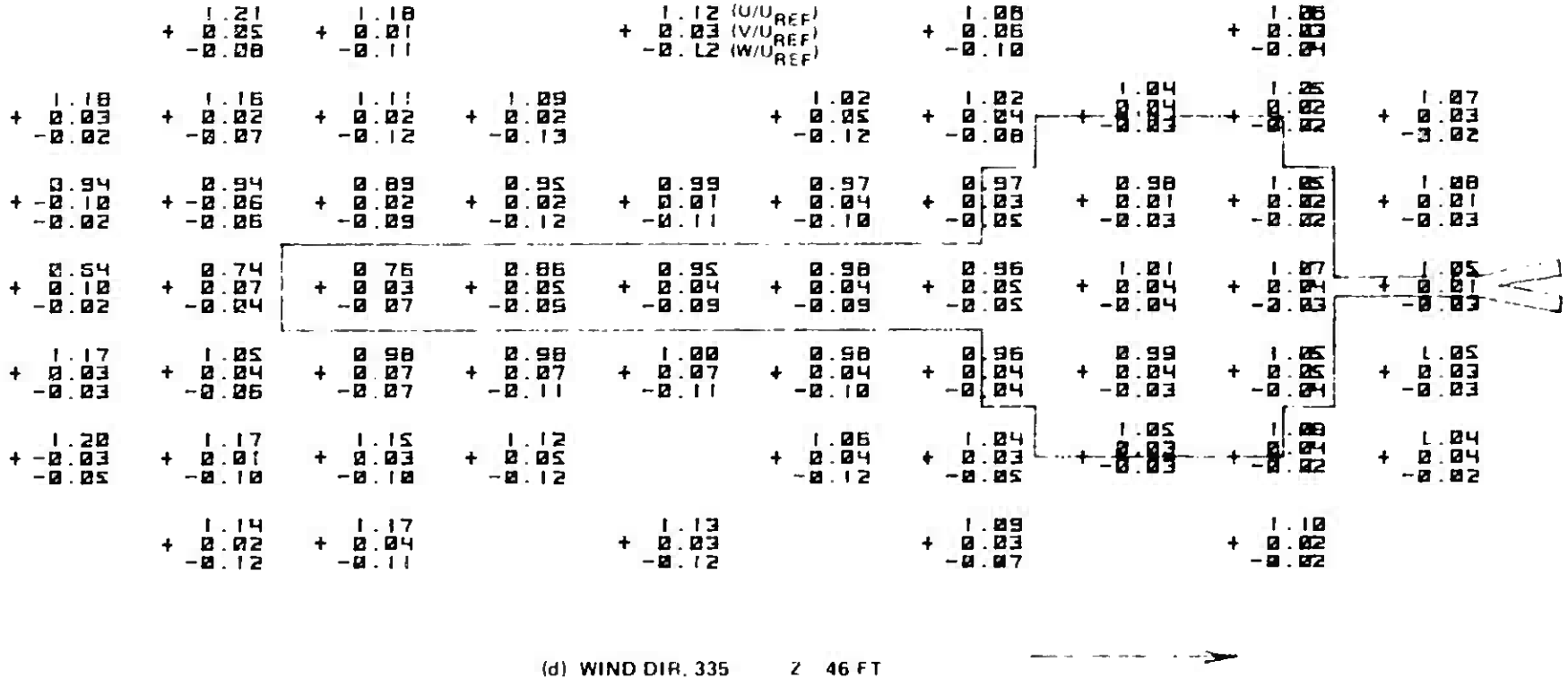

Figure B-12 (Cont.) Mean Velocity Components Above TRESTLE Platform (Wind Axis Coordinates)

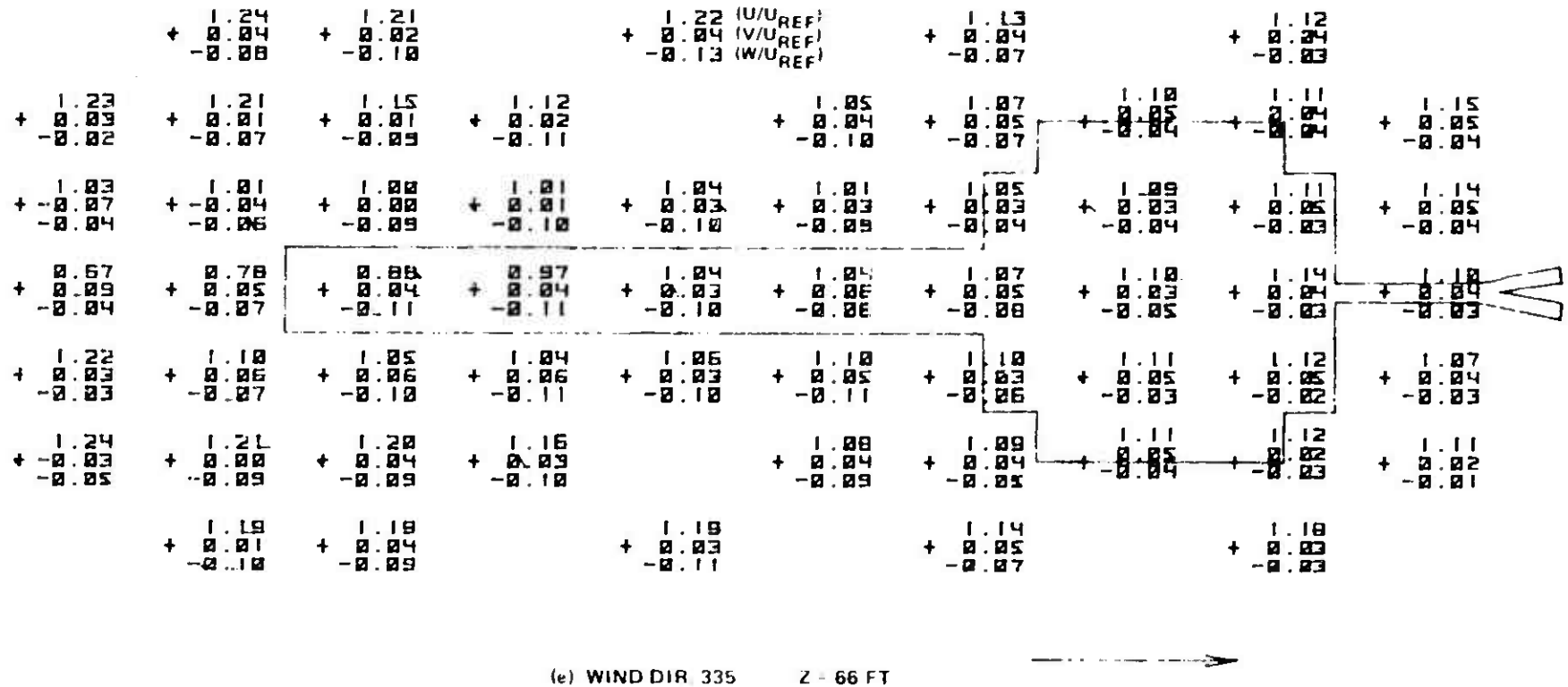

Figure B-12 (Cont.) Mean Velocity Components Above TRESTLE Platform (Wind Axis Coordinates)

APPENDIX C
CROSSFLOW VELOCITY VECTORS ABOVE TRESTLE PLATFORM

This appendix presents computer plots of crossflow velocity vectors above the TRESTLE platform. The data are presented in twelve figures (C-1 through C-12) with each figure presenting the results for a different wind direction. Each vector, $U_{y,z}$ in these figures is composed of the lateral wind velocity, U_y, and the vertical wind velocity, U_z. The axial wind component, U_x, along the TRESTLE axis is not shown in these figures. The crossflow vectors have been normalized by the mean wind velocity, U_{REF}, at the meteorological station at a height 10 meters above the ground. A velocity scale showing $U_{y,z}/U_{REF} = 1$ is provided on each figure. Note that the velocity components (U_x, U_y, U_z) are parallel to the TRESTLE axis coordinate system shown in Figure 24 in the main text. This coordinate system differs from the wind axis system used in Appendix B except for the special case of a 335 degree wind direction.

Each of Figures C-1 through C-12 contains 10 different vector plots showing the velocity vectors in vertical planes at ten axial locations, (X). The appropriate vertical cross-section of the test stand, ramp, or local ground contour is shown schematically below each plot. The wind direction is listed numerically on each figure and is also shown schematically beside each of the ten vertical planes. The full-scale coordinates for X, Y, and Z at each test point can be determined from the information listed in each figure. Data were not measured at those grid points which show only a dot without an arrowhead. A plan view of the test grid and its relation to the TRESTLE platform is shown in Figure 24 in the main text.

Figures C-1 through C-12 are foldouts and are located at the back of this document.

APPENDIX D

DESCRIPTION OF COMPUTER PROGRAM TO ANALYZE WIND EFFECTS ON AIRCRAFT

This appendix gives a brief description of the computer program that was developed to analyze the effect of the wind on aircraft on the TRESTLE facility. This appendix gives a list of the aircraft geometric parameters required as inputs to the program, a list of the major aerodynamic force and moment quantities calculated in the program and a brief description of the subroutines used in the program. A detailed listing of the computer program has been delivered to AFSWL under separate cover.

The required input geometrical data is given in the following list.

REQUIRED AIRCRAFT GEOMETRICAL DATA

Wing:

Λ	-	sweep of quarter-chord line
CR	-	root chord
CT	-	tip chord
S_1	-	body radius at wing root
S_2	-	wing half span
ZWR	-	height of root chord above ground
LQCW	-	length from nose tip to root 1/4 chord
γ_w	-	wing dihedral
β_w	-	wing incidence

Horizontal Tail:

ΛHT	-	sweep of quarter-chord line
CTR	-	root chord

CTT - tip chord

S_3 - radius to root chord

S_4 - half span of tail

ZHT - height of root chord from ground

LQCT - length from nose to 1/4 chord at root

γ_{HT} - tail dihedral

β_{HG} - tail incidence

Vertical Tail:

Λ_{VT} - sweep of quarter-chord line

CVR - root chord

CVT - tip chord

S_5 - height of root chord

S_6 - height of tip chord

LQCV - length from nose to root 1/4 chord

HVT - height of root chord from ground line

Fuselage:

LF - total length

LN - length of nose

LCC - length of cylindrical section

LAB - length of afterbody

a - width of cylindrical section

b - depth of cylindrical section

ZF - height of fuselage ℄ above ground

XN - position of a/c nose in TRESTLE axis system

Case 2: - applies to E-3

all of above plus

Circular Radome:

D	-	diameter of planform
LRD	-	distance from nose to radome 1/2 chord
ZRD	-	distance (height) from top of fuselage to radome
CS	-	strut chord
LCS	-	length from nose to 1/4 chord of strut

Landing Gear Configurations

NG = 3	XNG	-	distance of nose gear from nose
	X1G	-	distance of main gear from nose
	Y1G	-	distance of main gear from fuselage ℄
	L1G	-	length of main gear
NG = 4	X1G	-	distance of 1st main gear from nose
	X2G	-	distance of 2nd main gear from nose
	Y1G	-	distance of 1st main gear from fuselage ℄
	Y2G	-	distance of 2nd main gear from fuselage ℄
	L1G	-	length of 1st main gear
	L2G	-	length of 2nd main gear
NG = 5	XNG	-	distance of nose gear from nose
	X1G	-	distance of 1st main gear from nose
	X2G	-	distance of 2nd main gear from nose
	Y1G	-	distance of 1st main gear from fuselage ℄
	Y2G	-	distance of 2nd main gear from fuselage ℄
	L1G	-	length of 1st main gear
	L2G	-	length of 2nd main gear

The follcwing is a list of the nomenclature and quantities calculated by the Aerodynamic force and moment part of the computer program. The symbols or names of each quantity are those used in the FORTRAN listing of the program.

RWAF - axial force on right wing
LWAF - axial force on left wing
FAF - fuselage axial force
AFTR - axial force on right horizontal tail
AFTL - axial force on left horizontal tail
AFVT - axial force on vertical tail
PAF - axial force on radome pod (E-3)
BFS - axial force on radome pod strut (E-3)
RWSF - side force on right wing
LWSF - side force on left wing
WSF - sum of RWSF and LWSF
FSF - side force on fuselage
SF - side force on fuselage nose
CCSF - side force on fuselage cylindrical section
ASF - side force on fuselage afterbody
SFTR - side force on right horizontal tail
SFTL - side force on left horizontal tail
SFVT - side force on vertical tail
SFP - side force on radome pod (E-3)
SFS - side force on radome pod strut (E-3)
RWNF - normal force on right wing
LWNF - normal force on left wing
NFW - sum of RWNF and LWNF
FNF - normal force on fuselage
NL - normal force on fuselage nose
CCNF - normal force on fuselage cylindrical section
ANF - normal force on fuselage afterbody
NFTR - normal force on right horizontal tail
NFTL - normal force on left horizontal tail
PNF - normal force on radome pod
RWRM - rolling moment on right wing

LWRM - rolling moment on left wing

RMHTR - rolling moment on right horizontal tail

RMHTL - rolling moment on left horizontal tail

RMVT - rolling moment on vertical tail

PRM - rolling moment on radome pod (E-3)

RMS - rolling moment on radome pod strut (E-3)

RWPM - pitching moment on right wing

LWPM - pitching moment on left wing

WPM - sum of LWPM and RWPM

PMHTR - pitching moment on right horizontal tail

PMHTL - pitching moment on left horizontal tail

FPM - pitching moment on fuselage

PPM - pitching moment on radome pod (E-3)

RWYM - yawing moment on right wing

LWYM - yawing moment on left wing

WYM - sum of RWYM and LWYM

FYM - yawing moment on fuselage

YMHTR - yawing moment on right horizontal tail

YMHTL - yawing moment on left horizontal tail

YMVT - yawing moment on vertical tail

PYM - yawing moment on radome pod (E-3)

YMS - yawing moment on radome pod strut (E-3)

FXA - total axial force on aircraft

FYA - total side force on aircraft

FZA - total normal force on aircraft

MXA - total rolling moment on aircraft

MYA - total pitching moment on aircraft

MZA - total yawing moment on aircraft

The following is a list of the subroutines and a short description of their function, in the computer program that was used to calculate the reactions on the landing gear of each aircraft.

TRESTLE	-	Main program
INPUTS	-	Reads all input data except U_∞, ϕ and XN
GEOM	-	Computes all geometric parameters needed in the analysis
AEROFM	-	Directs the computation of the aerodynamic forces and moments on the whole aircraft
GREAC	-	Directs the computation of the gear reactions for all aircraft
PRINTS	-	Outputs all data
WING1	-	Computes forces and moments on inboard panel for both wings
WING2	-	Computes forces and moments on the middle wing panel for both wings
WING3	-	Computes forces and moments on the tip wing panel for both wings
WINGRL	-	Sums the forces and moments on all wing panels and computes the induced drag
FUNOSE	-	Computes forces and moments on fuselage nose
FUCYLN	-	Computes forces and moments on cylindrical section of fuselage
FUAFTB	-	Computes forces and moments on fuselage afterbody and sums all forces and moments on fuselage
HTPANS	-	Computes forces and moments on horizontal tail
VTFOMO	-	Computes forces and moments on vertical tail
RDOMEP	-	Computes forces and moments on radome pod (E-3)

RDOMES	-	Computes forces and moments on radome strut (E-3)
CLDVSA	-	Interpolates in tables of C_L and C_D vs. α for NACA 0012 airfoil data
WIND	-	Stores all velocity data from wind tunnel tests and interpolates as required for other subroutines
GEARS 3	-	Computes gear reactions for aircraft having 3 gears
GEARS 4	-	Computes gear reaction for aircraft having 4 gears
GEARS 5	-	Computes gear reactions for aircraft having S gears
FACKS FACSK FACSS	-	Computes special functions needed in GEARS 3, GEARS 4, GEARS S

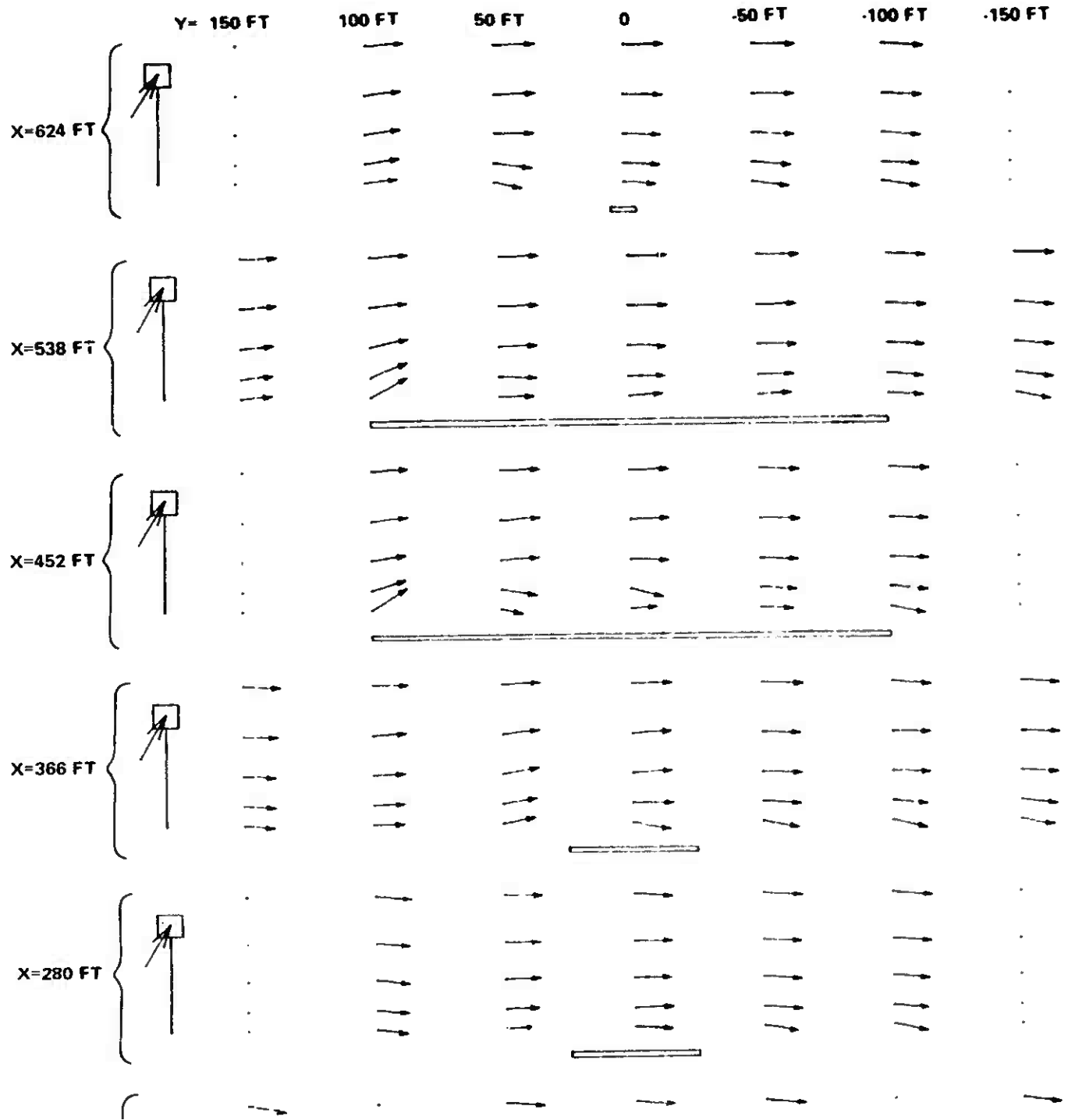
Y= 150 FT
100 FT
50 FT
0
-50 FT
-100 FT
-150 FT
X=624 FT
X=538 FT
X=452 FT
X=366 FT
X=280 FT

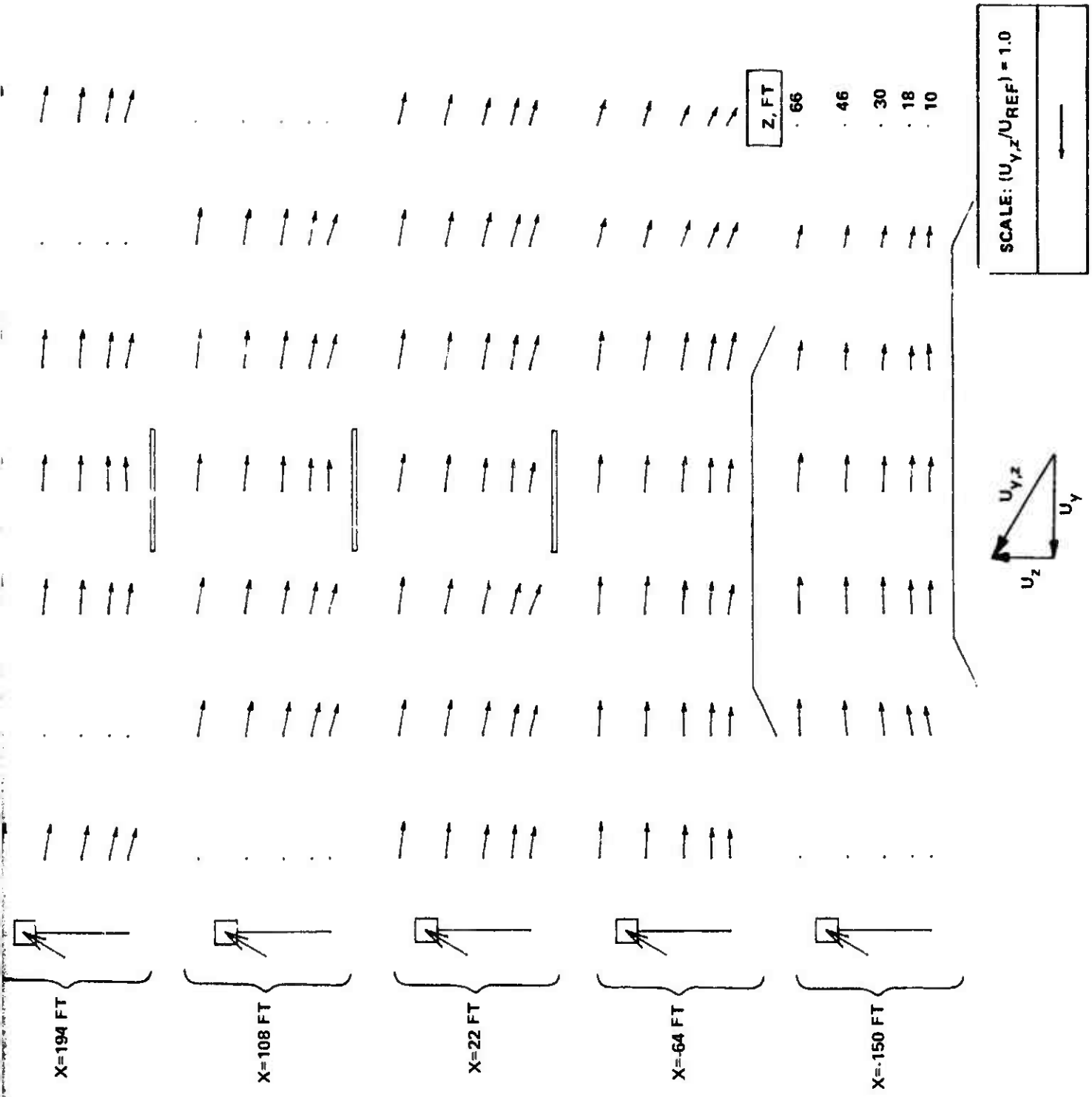

Figure C-1 Mean Crossflow Velocity Vectors, $U_{y,z}$, in Vertical Planes Above TRESTLE Platform, 005 Degree Wind

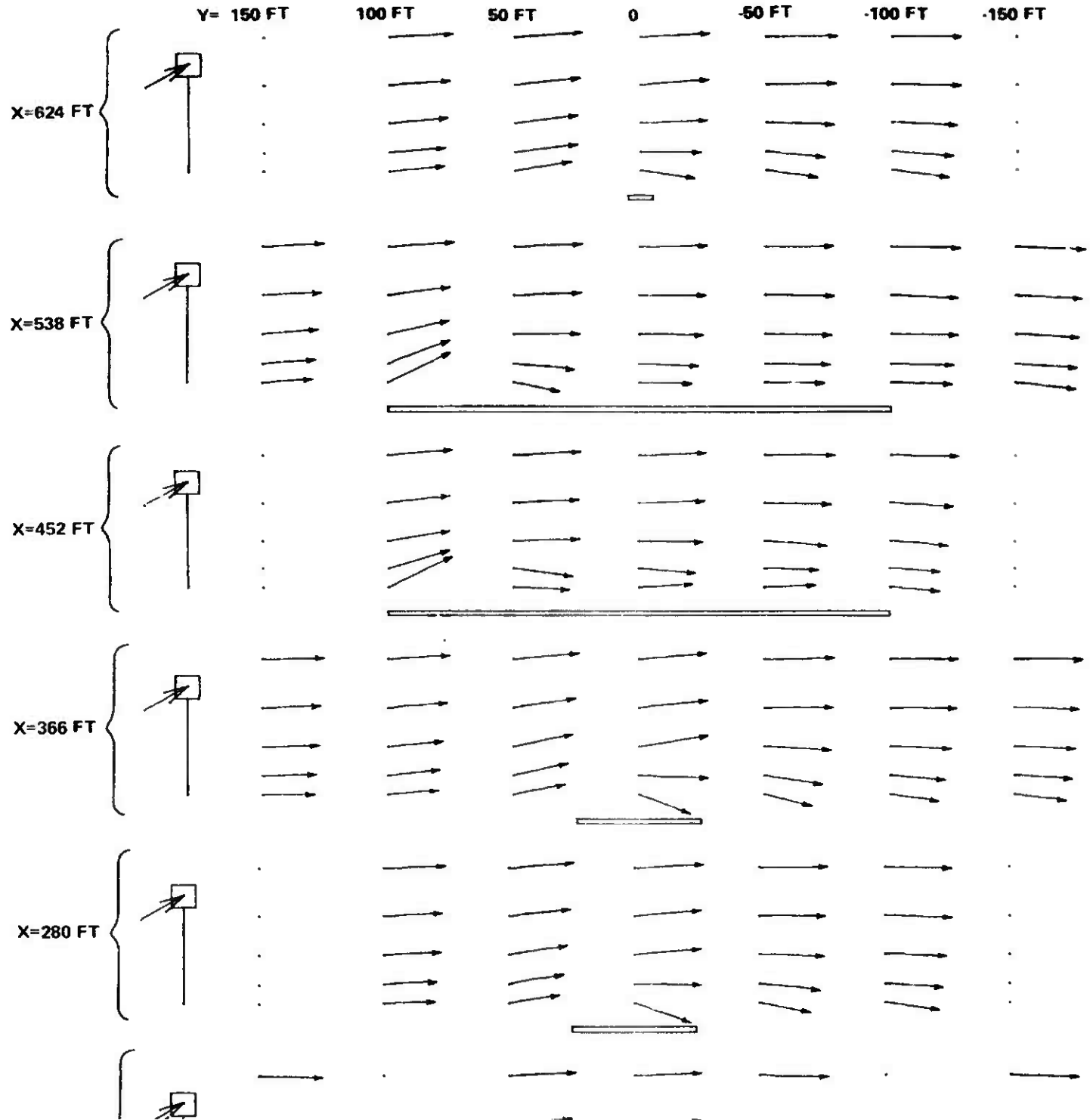
Y= 150 FT
100 FT
50 FT
0
-50 FT
-100 FT
-150 FT
X=624 FT
X=538 FT
X=452 FT
X=366 FT
X=280 FT

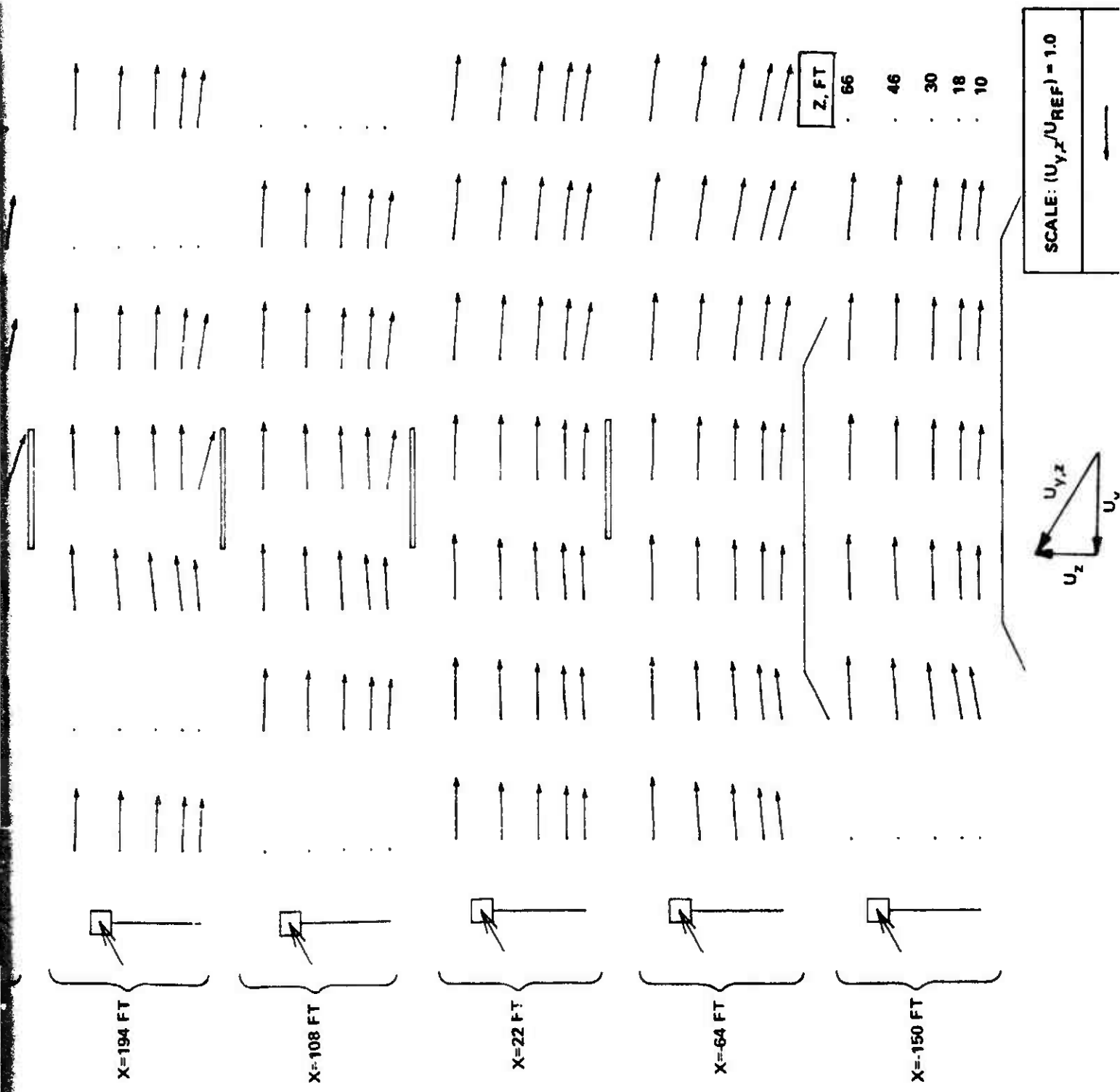

Figure C-2 Mean Crossflow Velocity Vectors, $U_{y,z}$, in Vertical Planes Abo
TRESTLE Platform, 035 Degree Wind

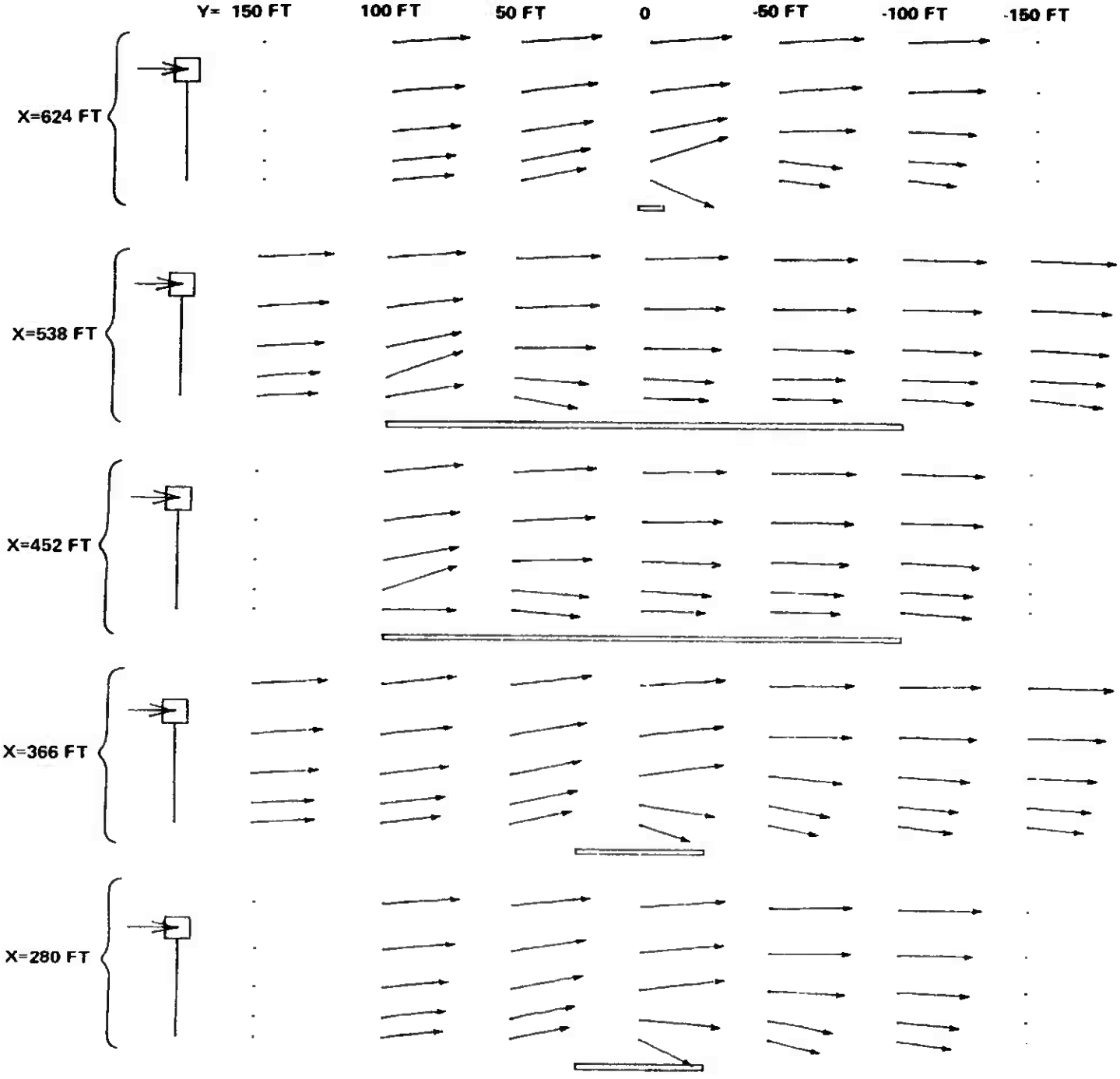
Y= 150 FT
100 FT
50 FT
0
-50 FT
-100 FT
-150 FT
X=624 FT
X=538 FT
X=452 FT
X=366 FT
X=280 FT

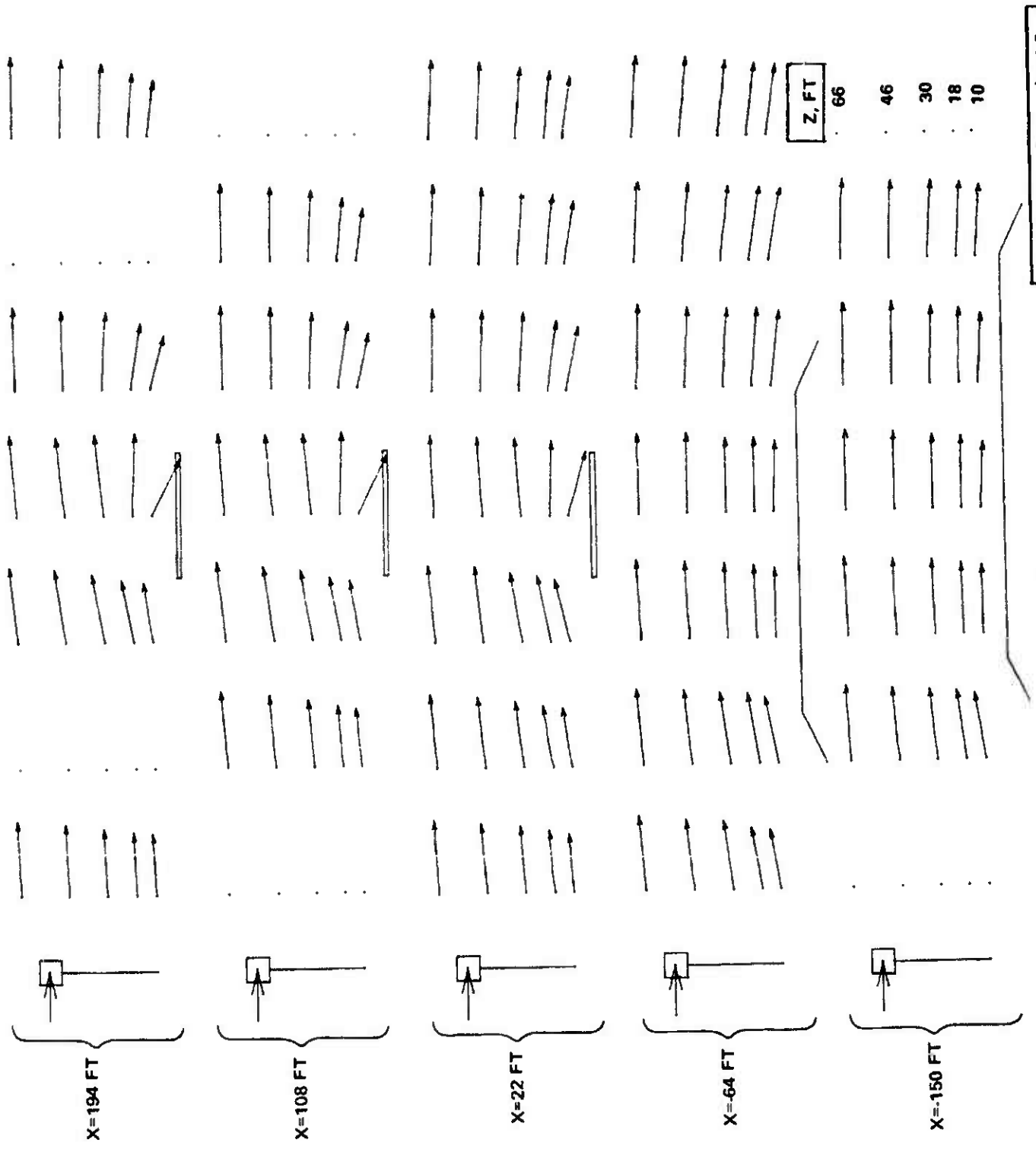

Figure C-3 Mean Crossflow Velocity Vectors, $U_{y,z}$, in Vertical Planes Above TRESTLE Platform, 065 Degree Wind

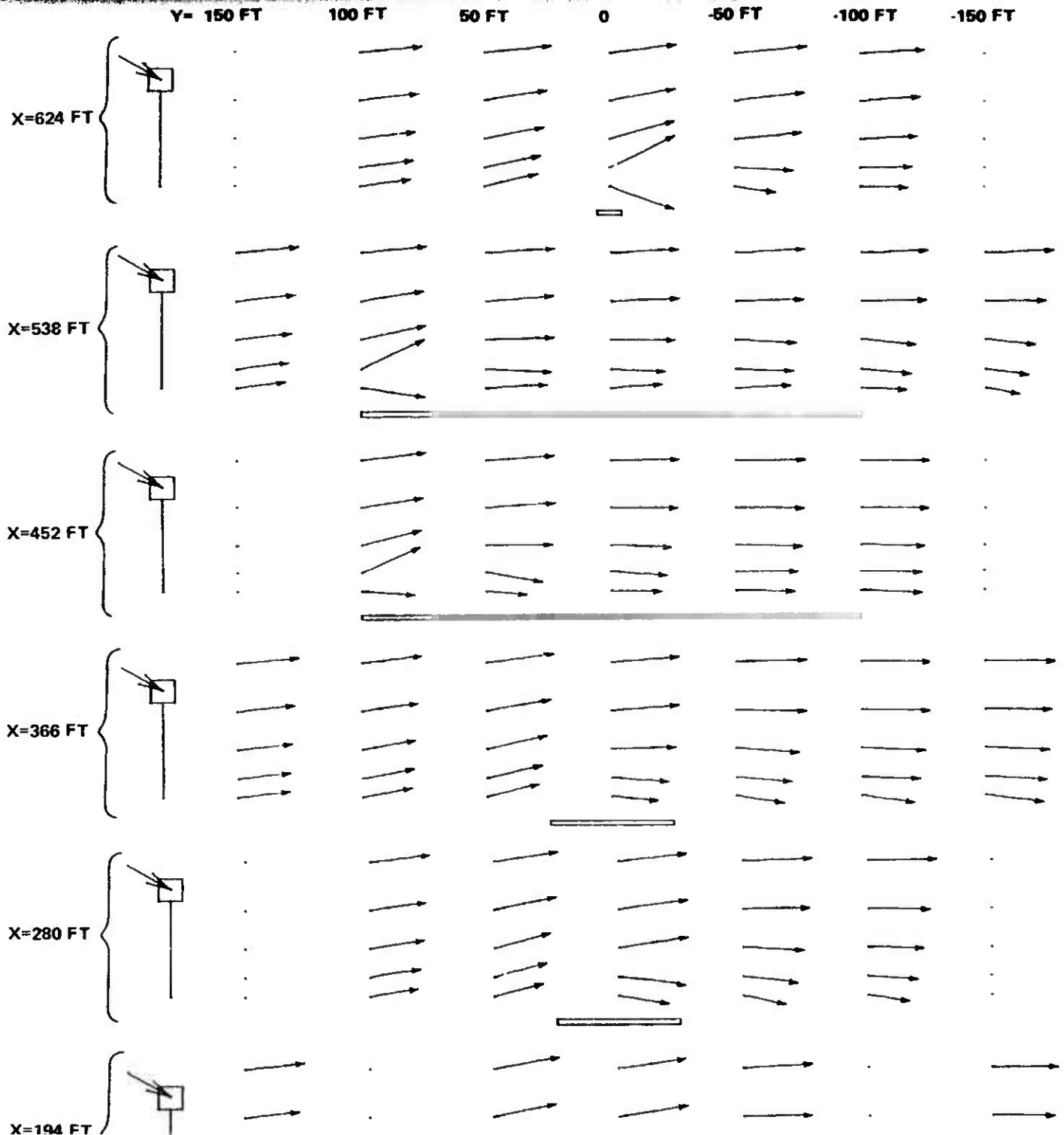
Y= 150 FT
100 FT
50 FT
0
-50 FT
-100 FT
-150 FT
X=624 FT
X=538 FT
X=452 FT
X=366 FT
X=280 FT
X=194 FT

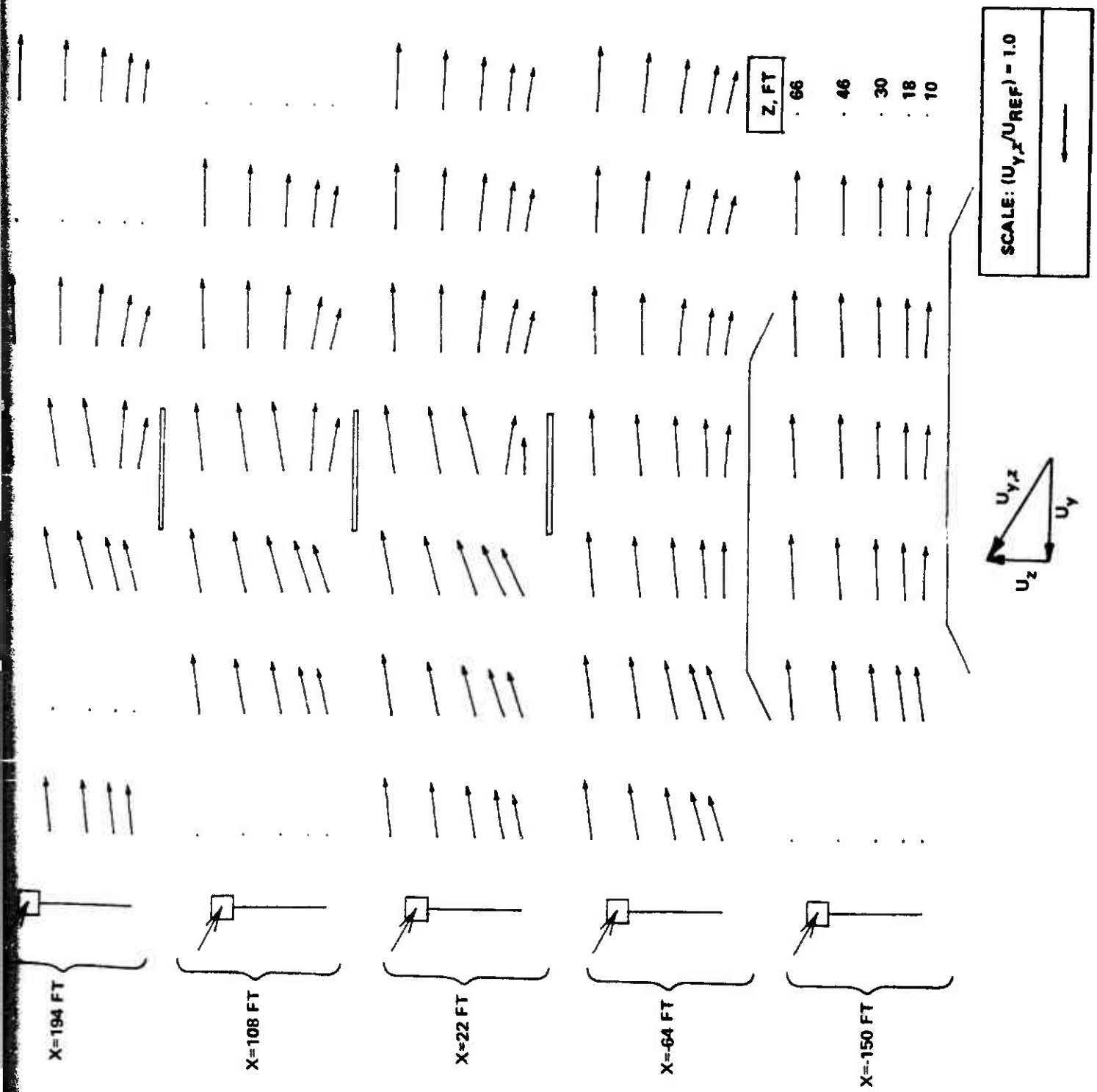

2

Figure C-4 Mean Crossflow Velocity Vectors, $U_{y,z}$, in Vertical Planes Above TRESTLE Platform, 095 Degree Wind

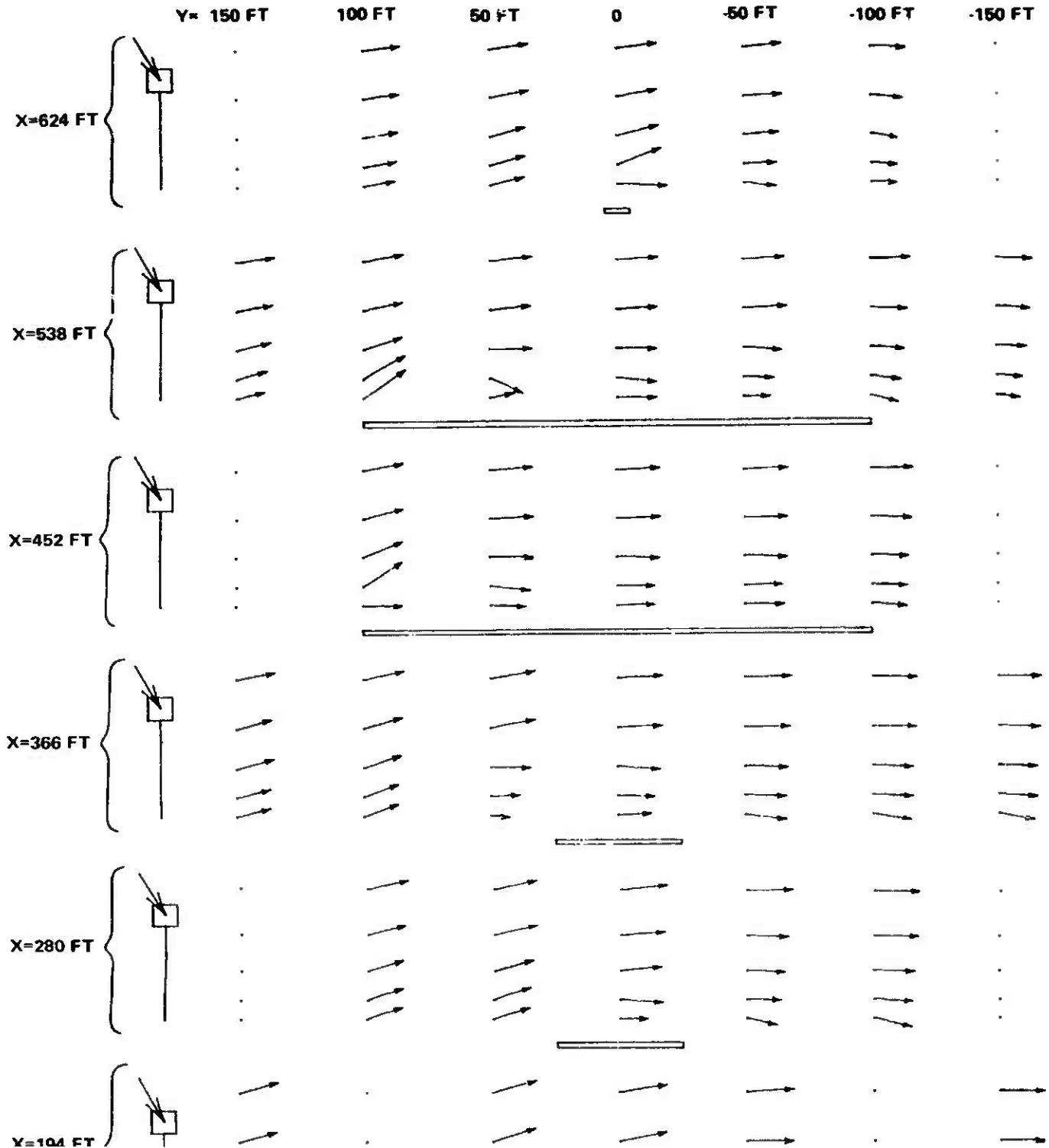
Y= 150 FT
100 FT
50 FT
0
-50 FT
-100 FT
-150 FT
X=624 FT
X=538 FT
X=452 FT
X=366 FT
X=280 FT
X=194 FT

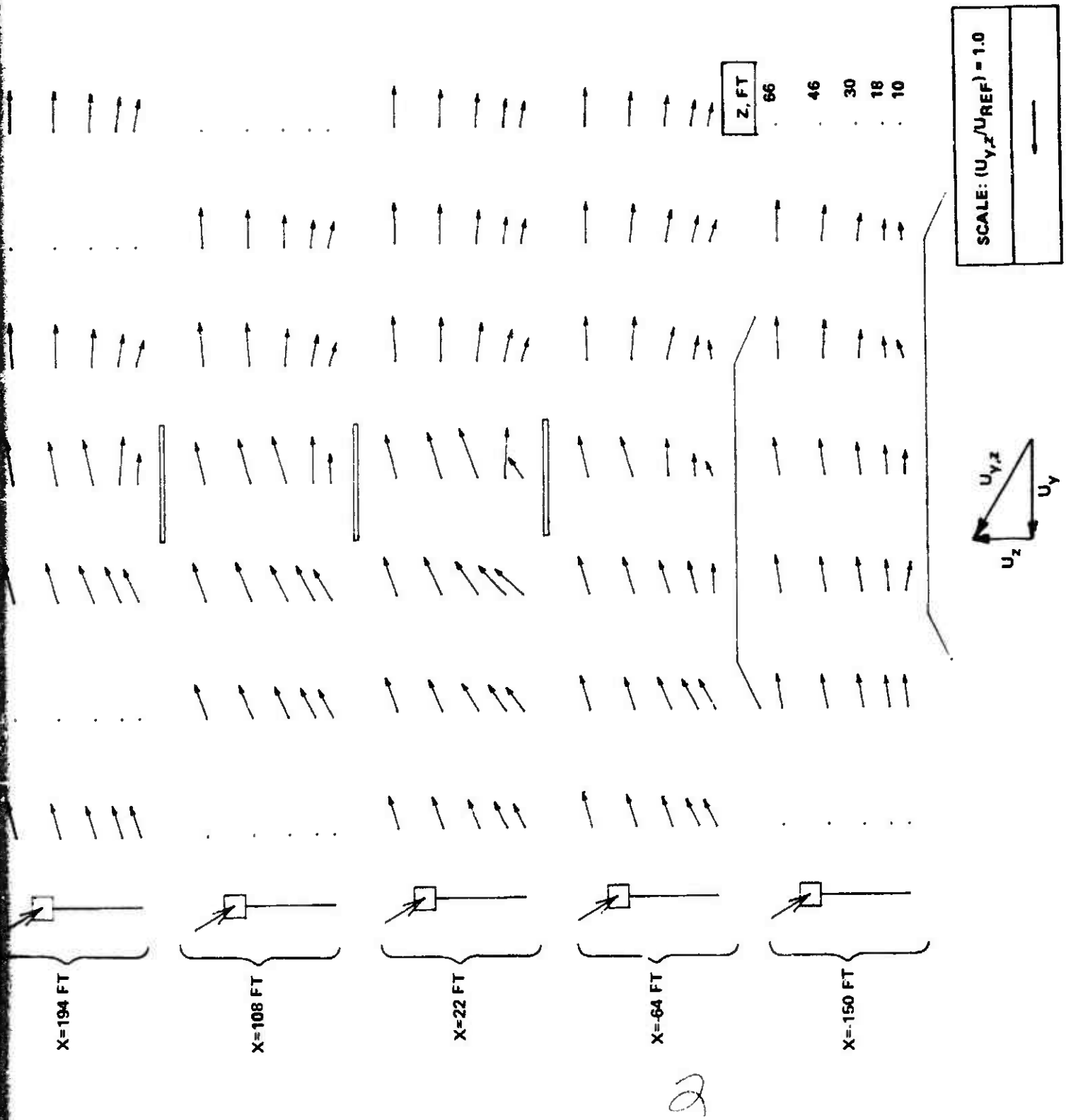

Figure C-5 Mean Crossflow Velocity Vectors, $U_{y,z}$, in Vertical Planes Above TRESTLE Platform, 125 Degree Wind

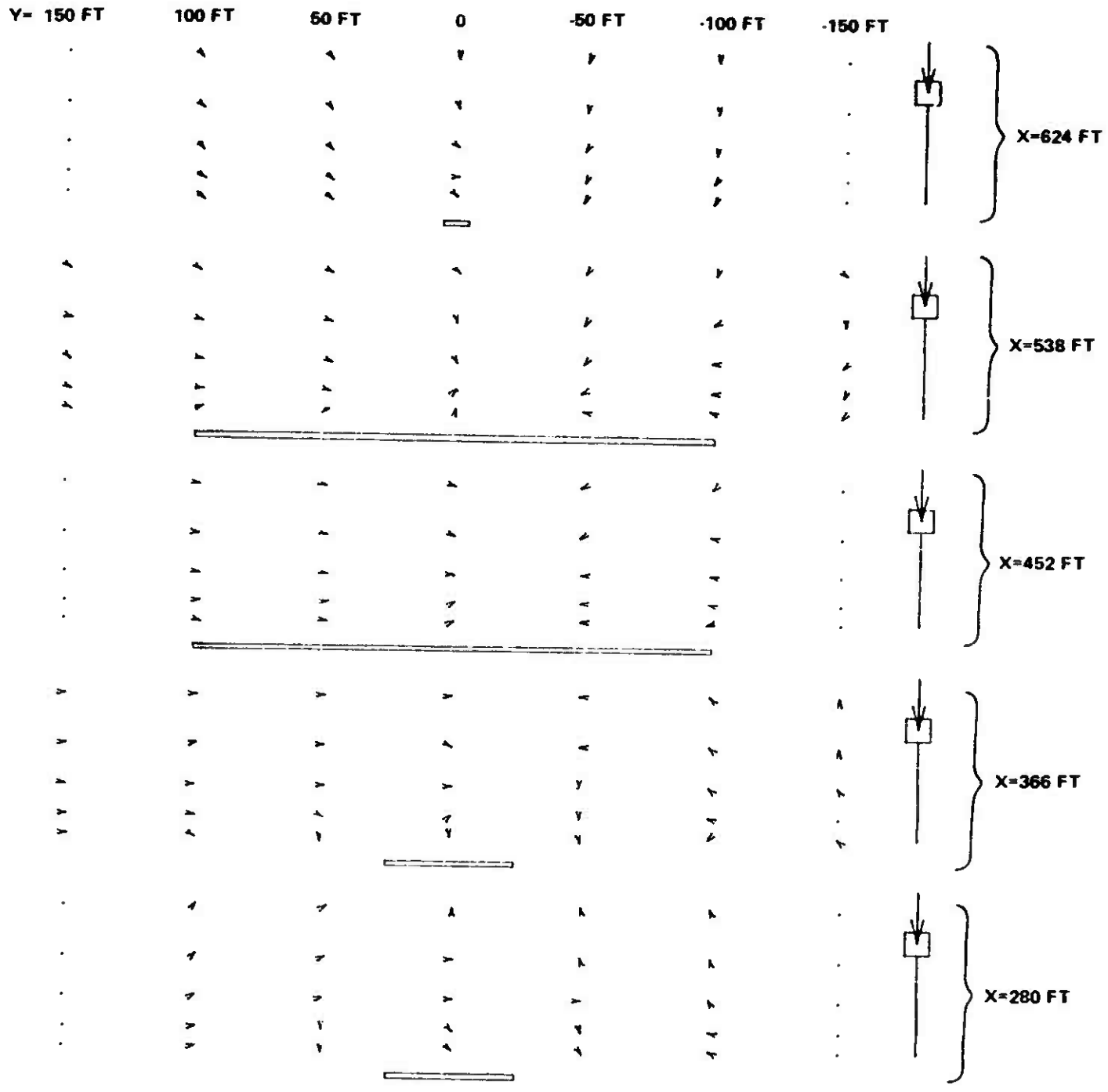
Y= 150 FT
100 FT
50 FT
0
-50 FT
-100 FT
-150 FT
X=624 FT
X=538 FT
X=452 FT
X=366 FT
X=280 FT

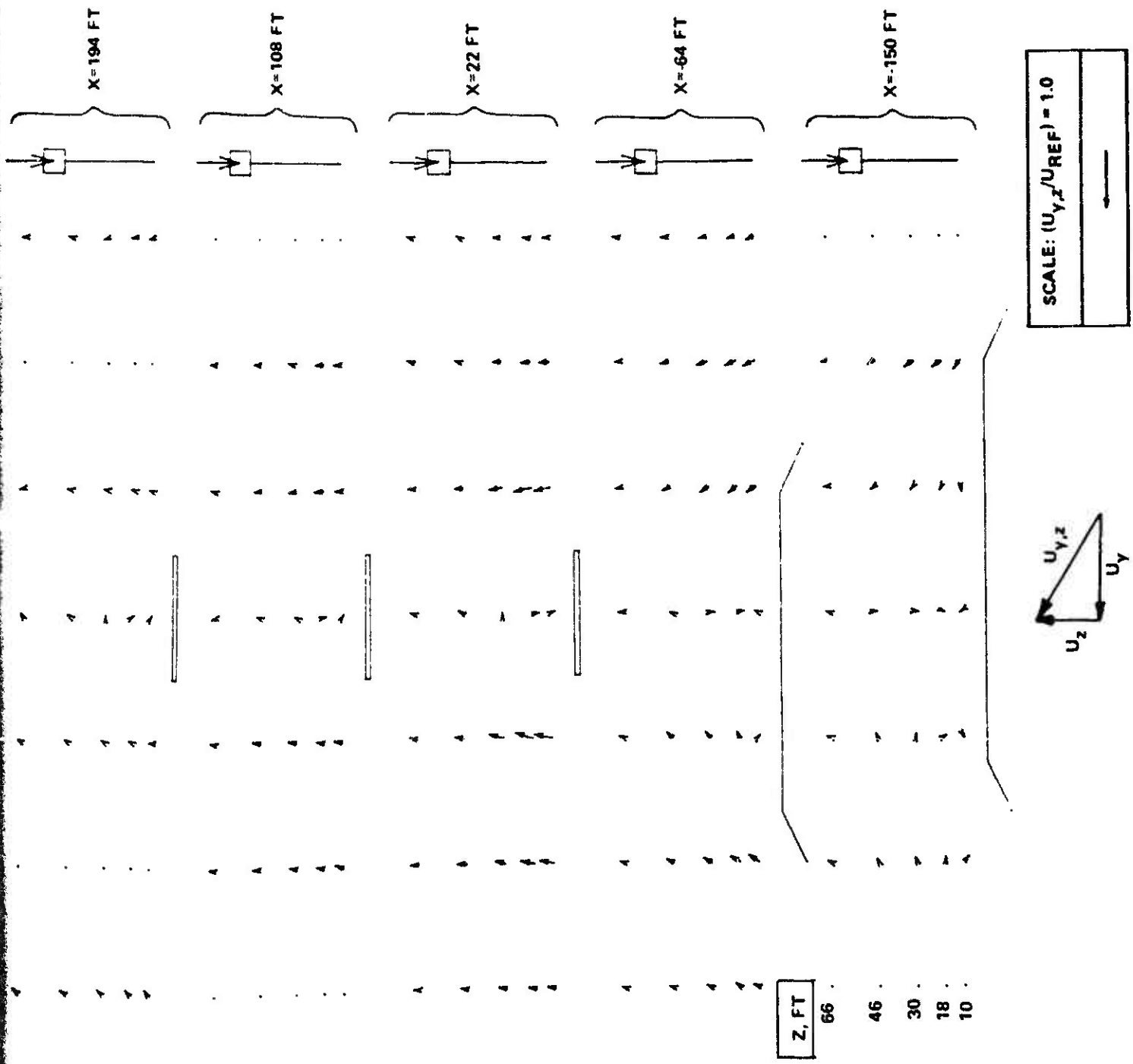

Figure C-6 Mean Crossflow Velocity Vectors, $U_{y,z}$, in Vertical Planes Above TRESTLE Platform, 155 Degree Wind

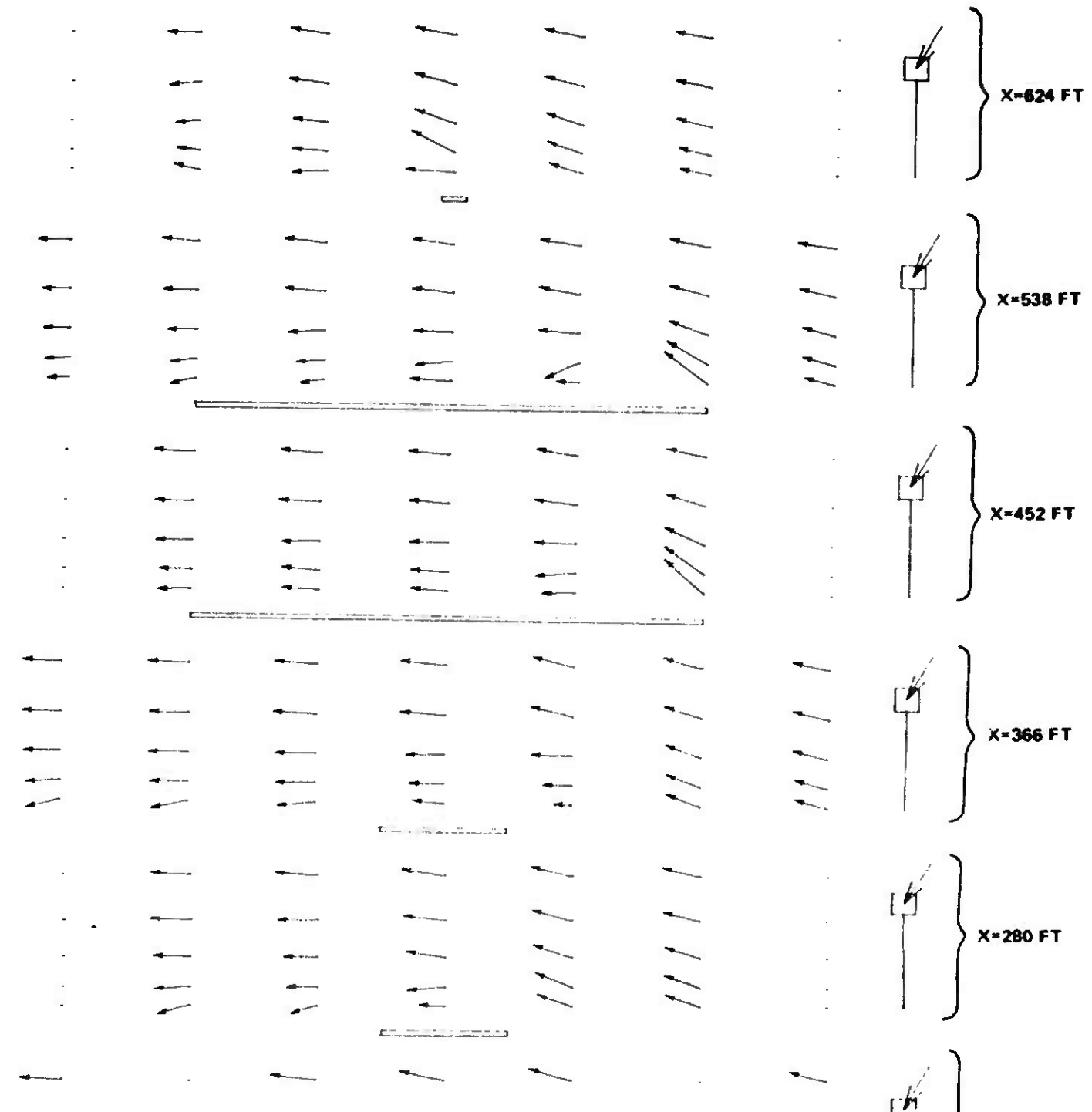
Y= 150 FT
100 FT
50 FT
0
-50 FT
-100 FT
-150 FT
X=624 FT
X=538 FT
X=452 FT
X=366 FT
X=280 FT

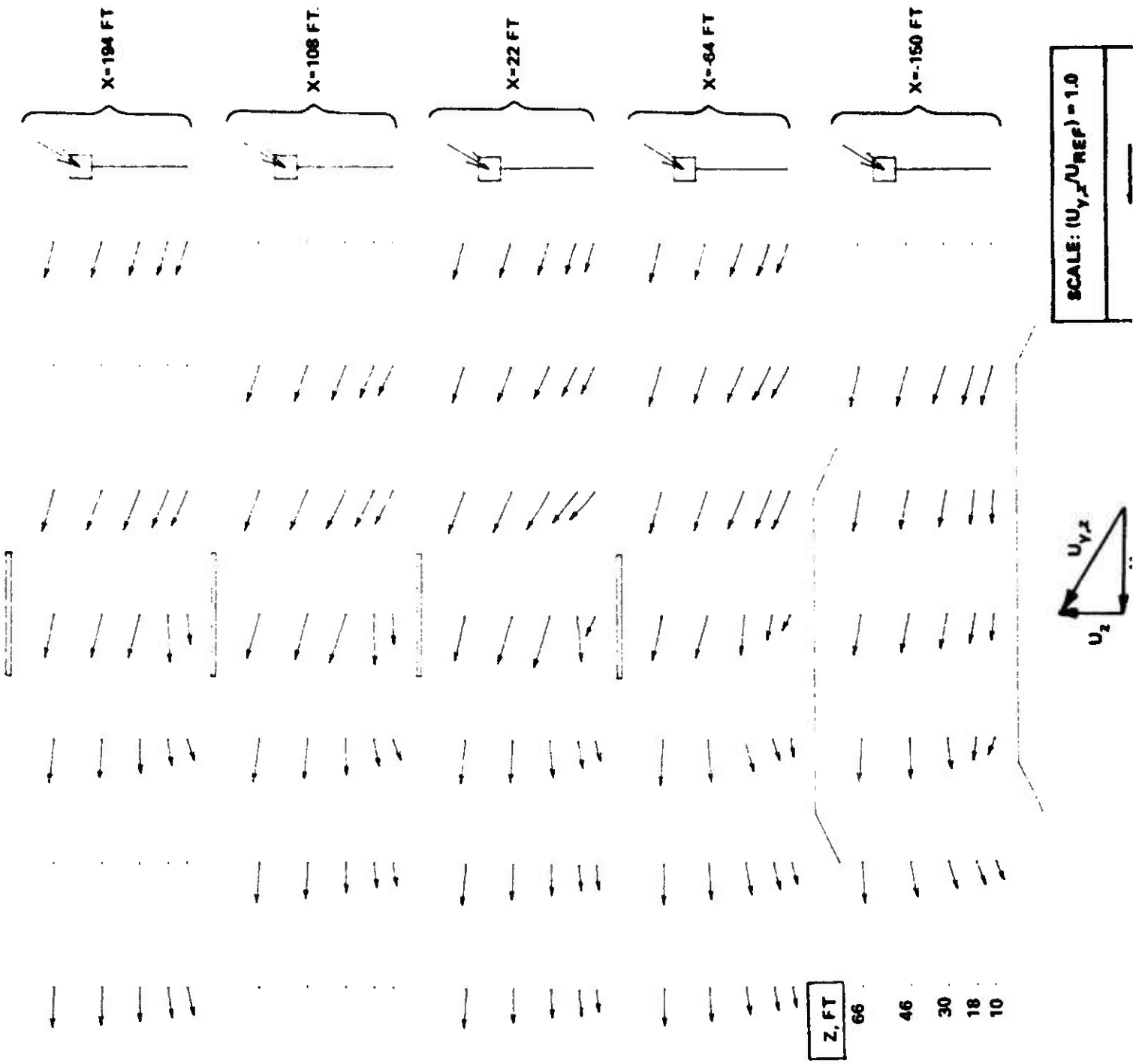

Figure C-7 Mean Crossflow Velocity Vectors, $U_{y,z}$, in Vertical Planes Above TRESTLE Platform, 185 Degree Wind

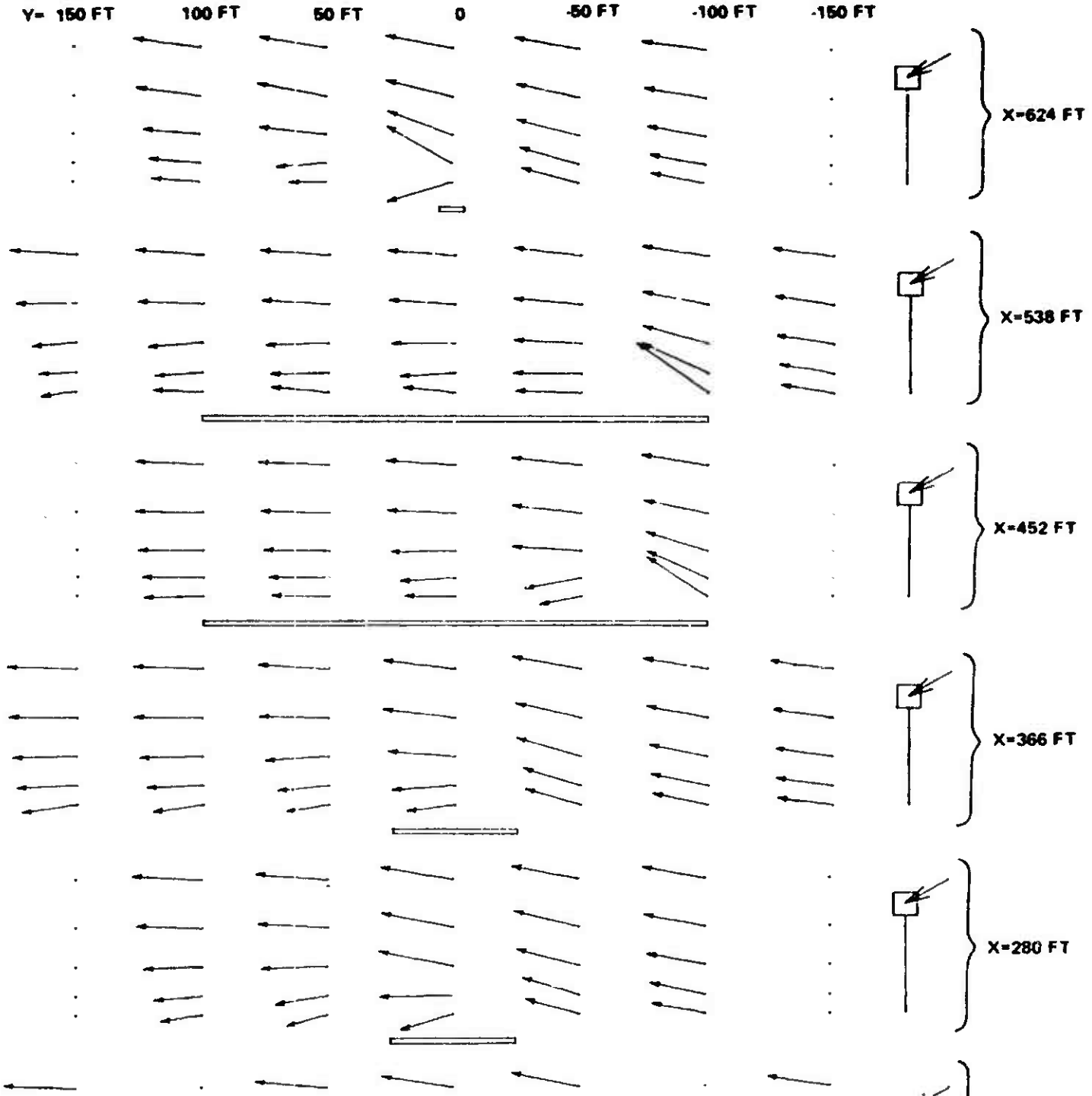
Y= 150 FT
100 FT
50 FT
0
-50 FT
-100 FT
-150 FT
X=624 FT
X=538 FT
X=452 FT
X=366 FT
X=280 FT

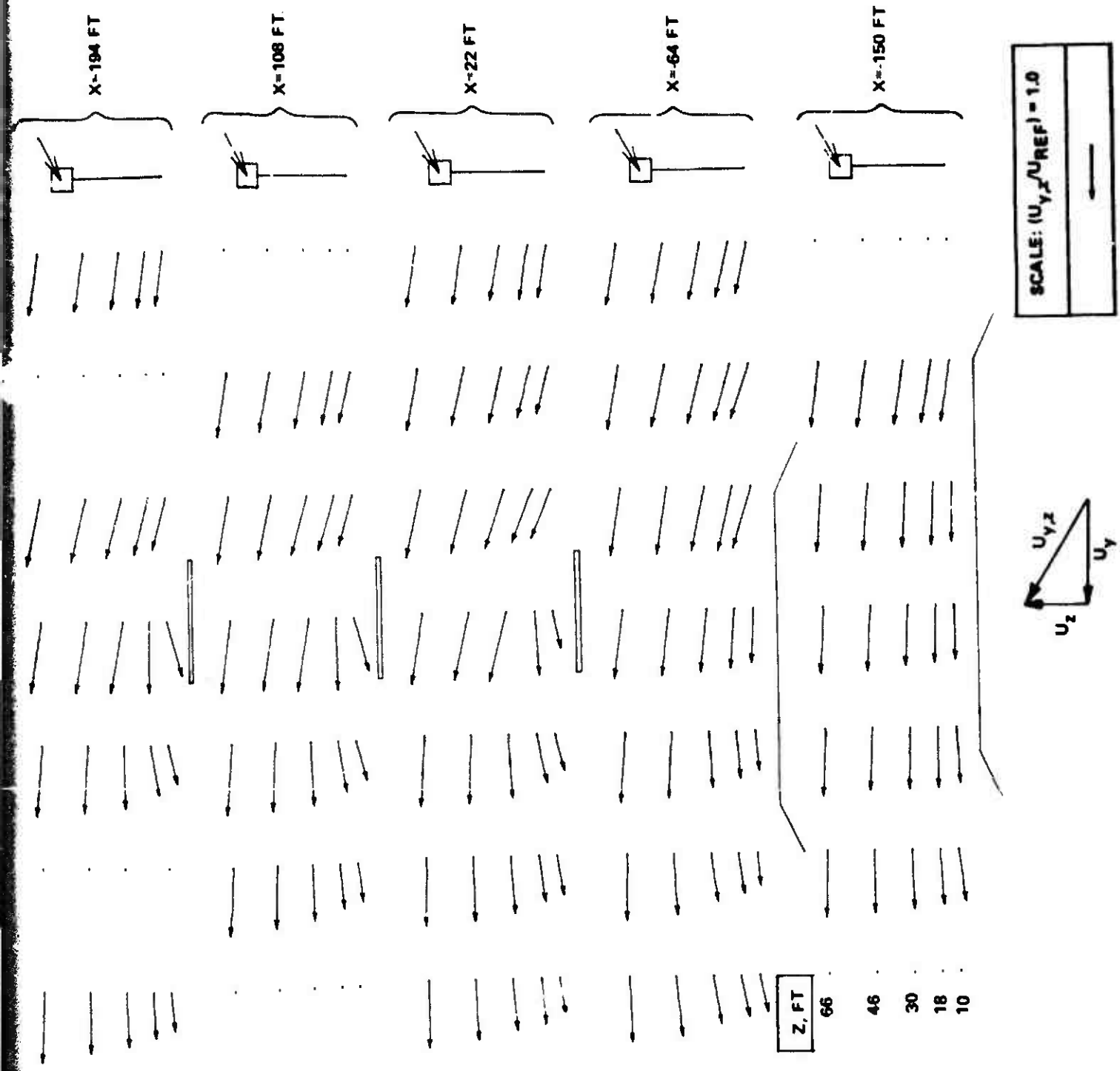

Figure C-8 Mean Crossflow Velocity Vectors, $U_{y,z}$, in Vertical Planes Above TRESTLE Platform, 215 Degree Wind

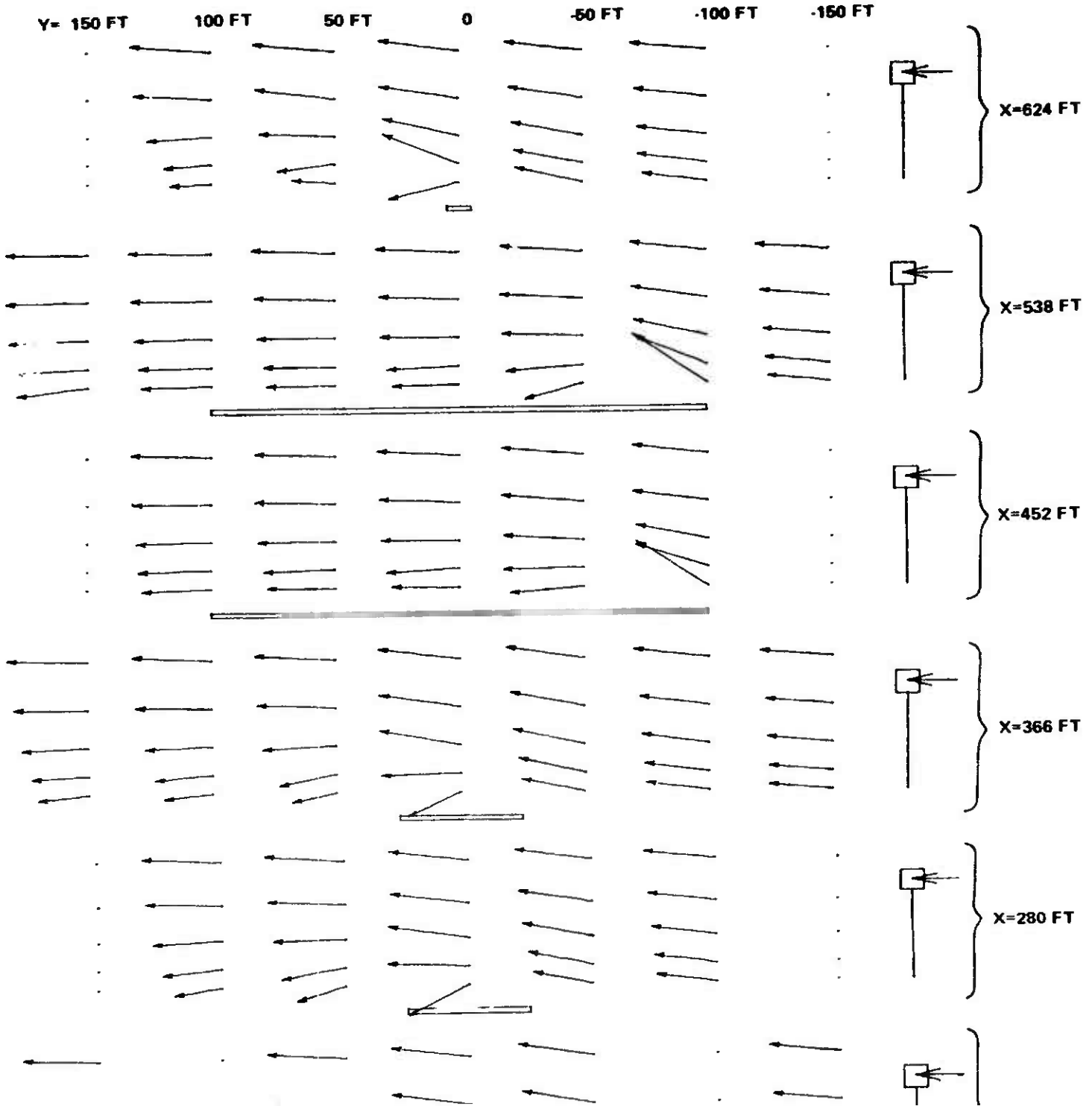
Y= 150 FT
100 FT
50 FT
0
-50 FT
-100 FT
-150 FT
X=624 FT
X=538 FT
X=452 FT
X=366 FT
X=280 FT

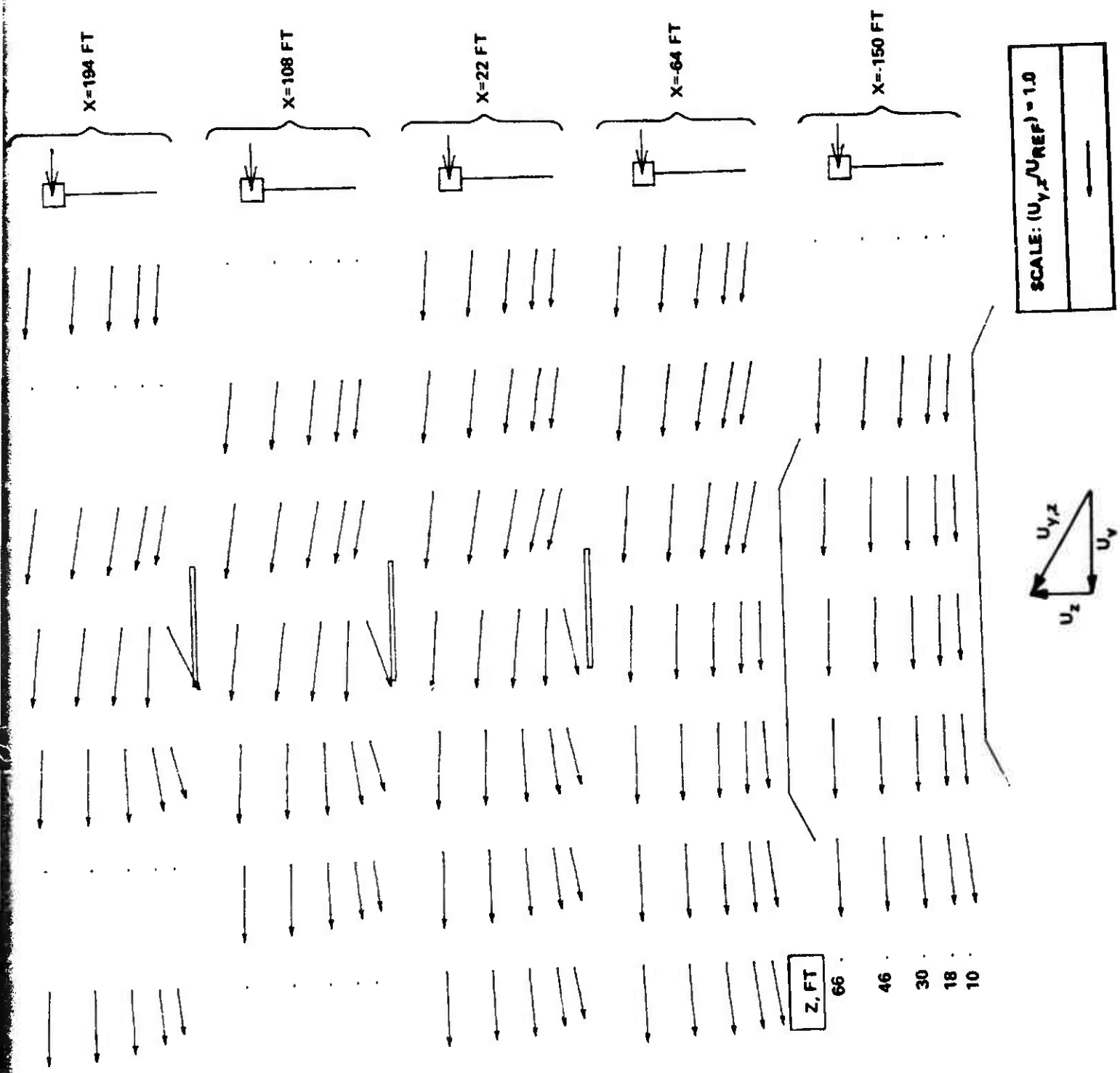

Figure C-9 Mean Crossflow Velocity Vectors, $U_{y,z}$, in Vertical Planes Above TRESTLE Platform, 245 Degree Wind

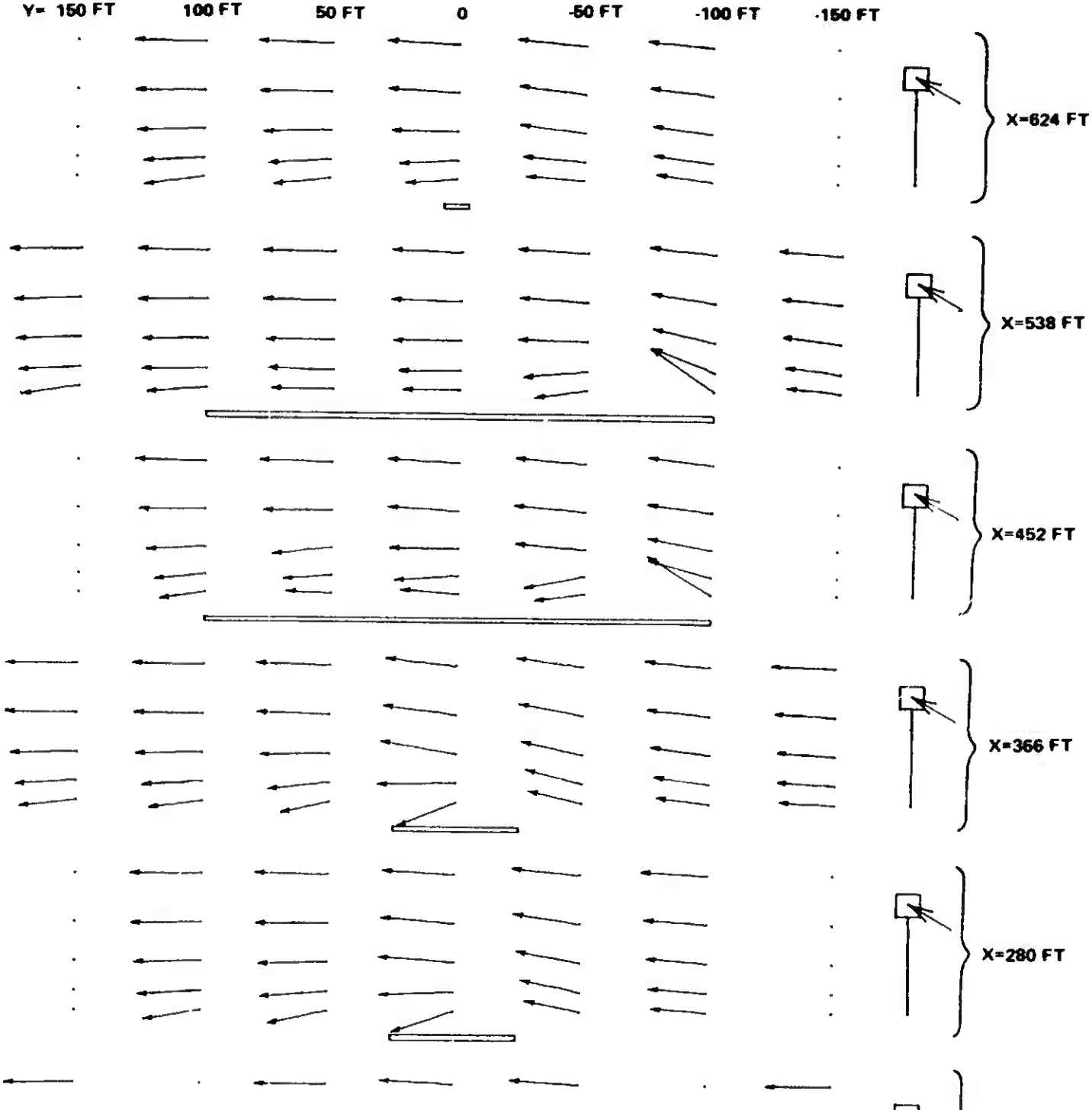
Y= 150 FT
100 FT
50 FT
0
-50 FT
-100 FT
-150 FT
X=624 FT
X=538 FT
X=452 FT
X=366 FT
X=280 FT

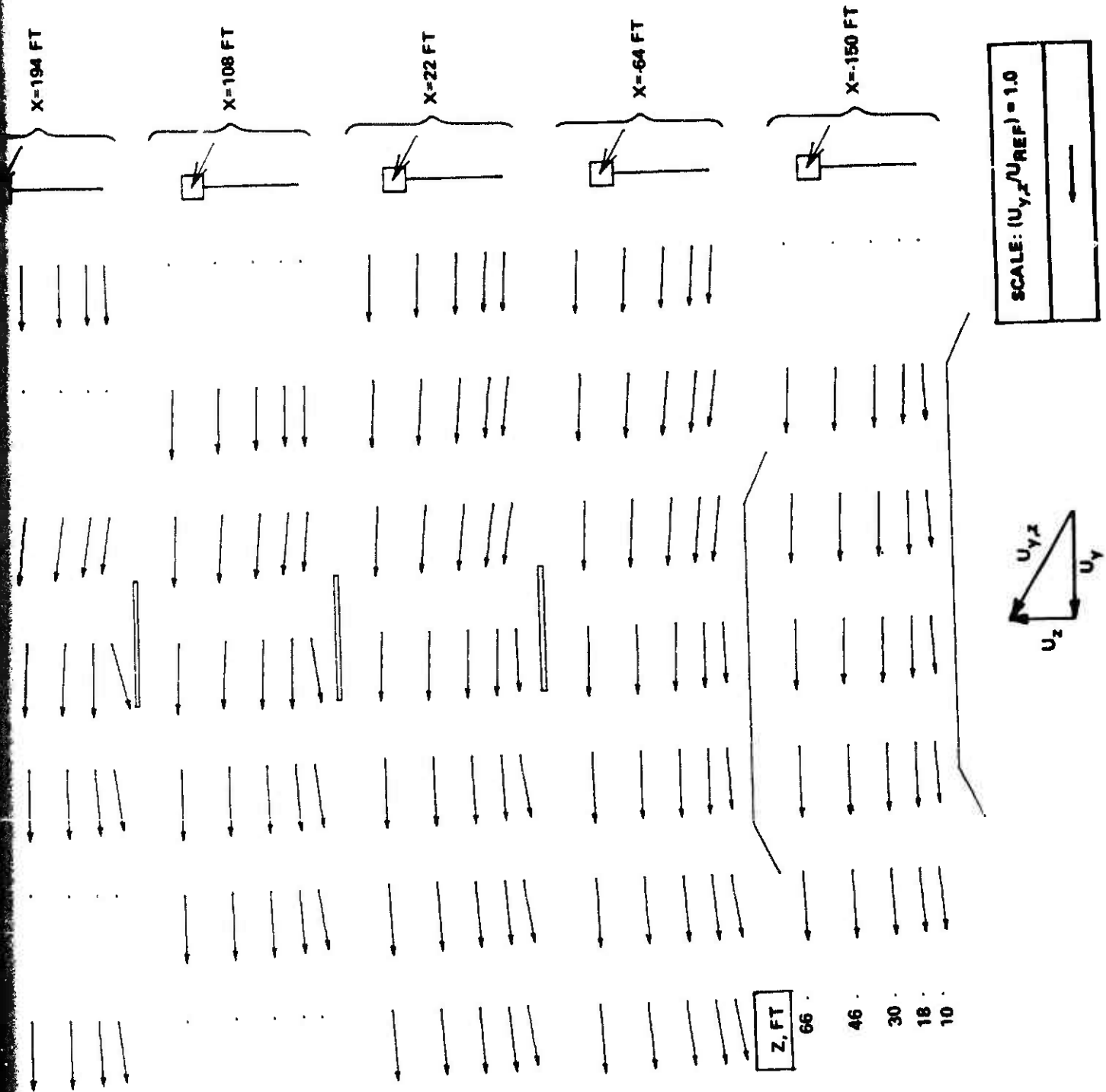

Figure C-10 Mean Crossflow Velocity Vectors, $U_{y,z}$, in Vertical Planes Above TRESTLE Platform, 275 Degree Wind

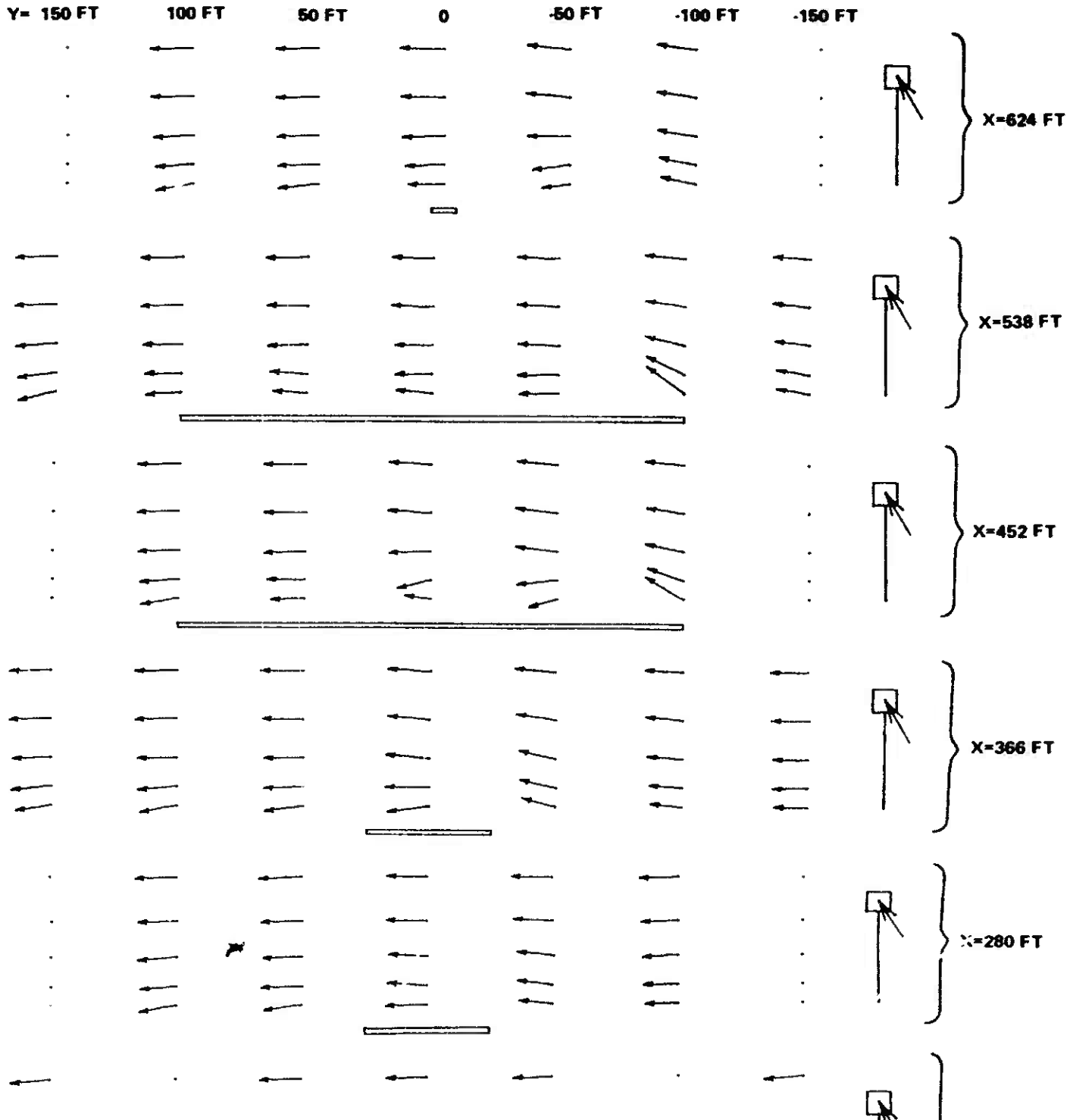
Y= 150 FT
100 FT
50 FT
0
-50 FT
-100 FT
-150 FT
X=624 FT
X=538 FT
X=452 FT
X=366 FT
X=280 FT

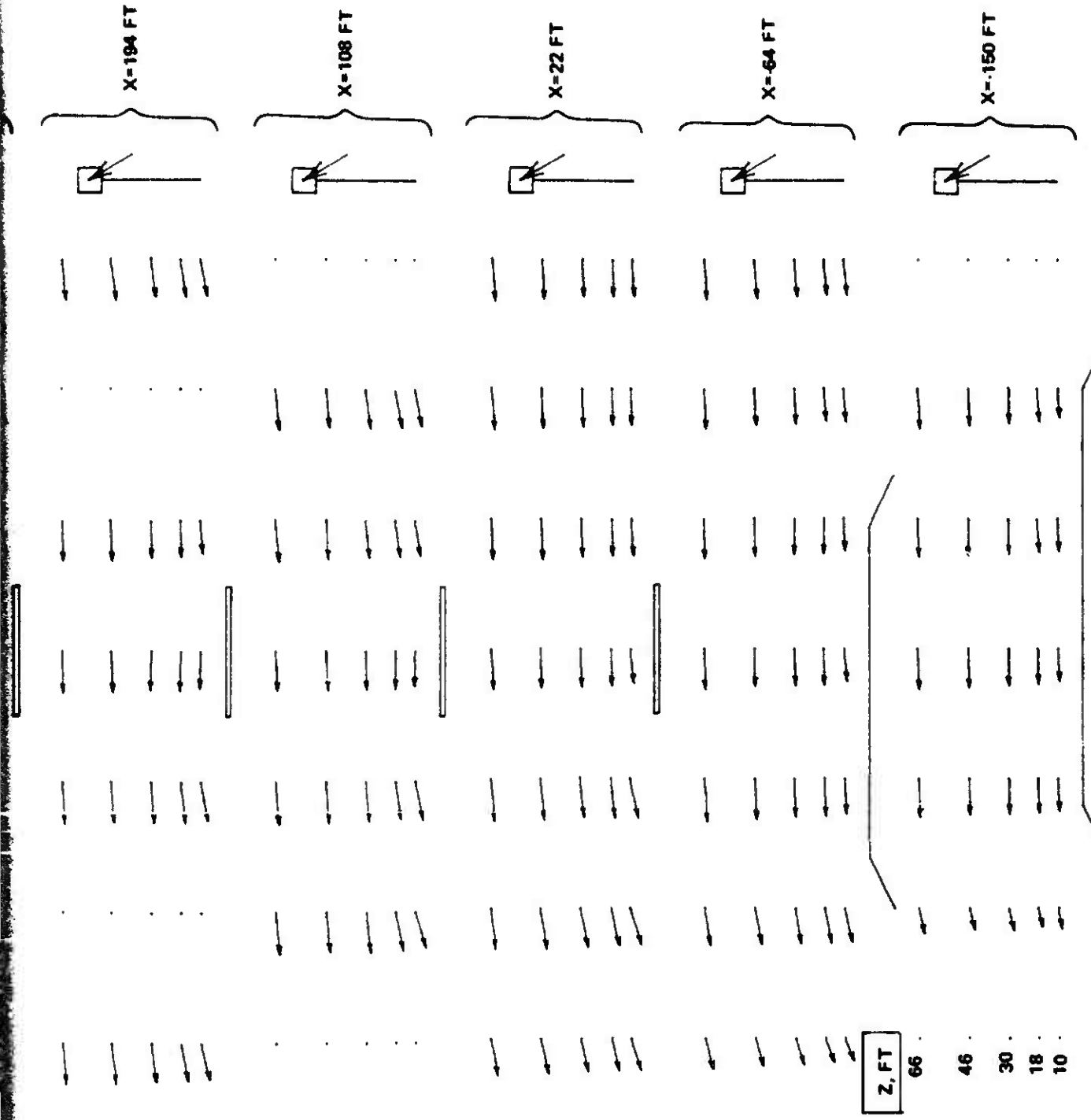

Figure C-11 Mean Crossflow Velocity Vectors, $U_{y,z}$, in Vertical Planes Above TRESTLE Platform, 305 Degree Wind

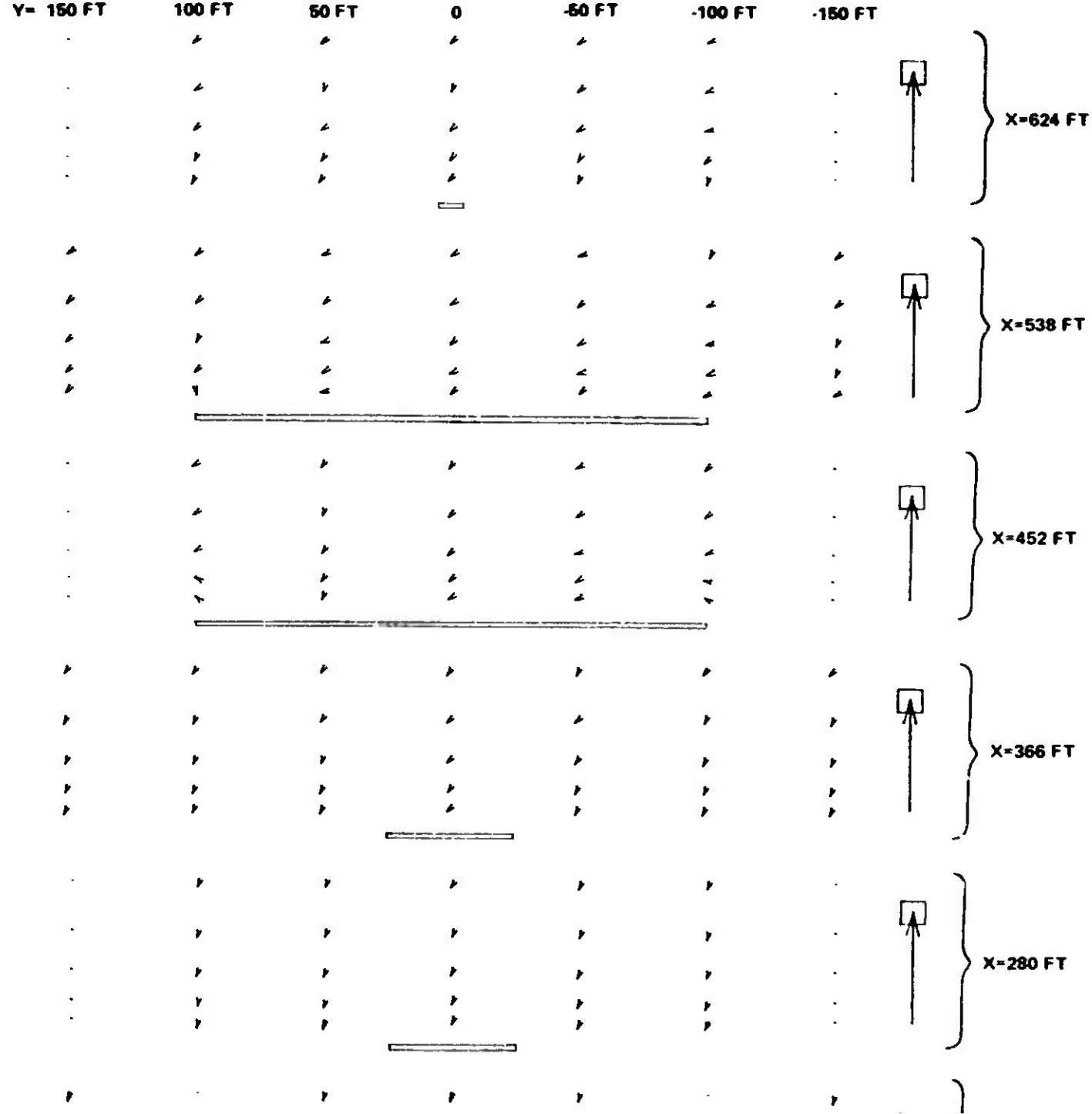
Y= 150 FT
100 FT
50 FT
0
-50 FT
-100 FT
-150 FT
X=624 FT
X=538 FT
X=452 FT
X=366 FT
X=280 FT

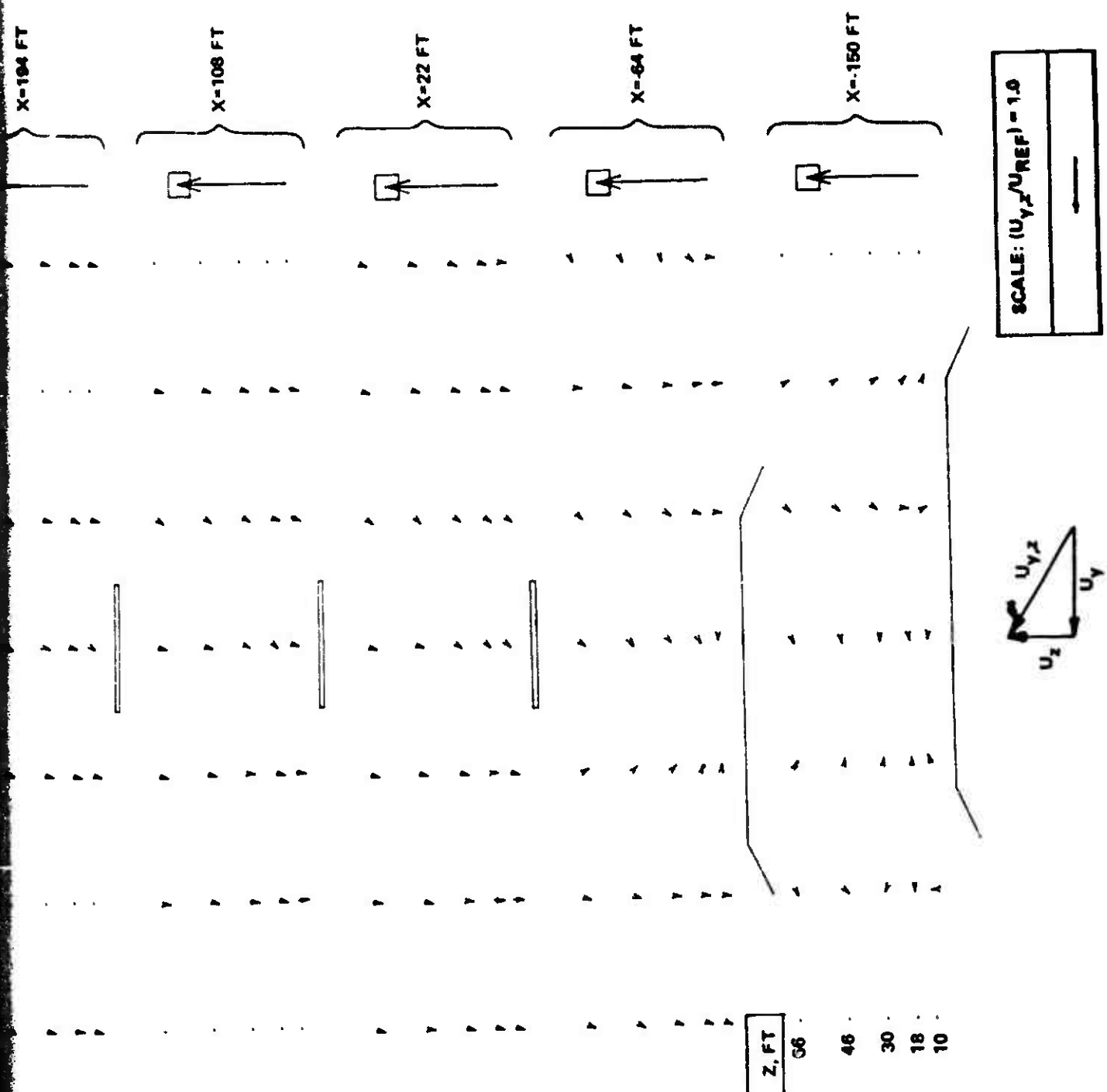

Figure C-12 Mean Crossflow Velocity Vectors, $U_{y,z}$, in Vertical Planes Above TRESTLE Platform, 335 Degree Wind